# Effects of Lignin on the Properties and Performance of Bitumen and Hot Mix Asphalt

by

Wesam AL-FALAHAT

THESIS PRESENTED TO ÉCOLE DE TECHNOLOGIE SUPÉRIEURE
IN PARTIAL FULFILLMENT FOR THE DEGREE OF
DOCTOR OF PHILOSOPHY
Ph.D.

MONTREAL, JUNE 14, 2024

ÉCOLE DE TECHNOLOGIE SUPÉRIEURE
UNIVERSITÉ DU QUÉBEC

**BOARD OF EXAMINERS**

THIS THESIS HAS BEEN EVALUATED

BY THE FOLLOWING BOARD OF EXAMINERS

Mr. Alan Carter, Thesis Supervisor
Department of construction engineering, École de technologie supérieure

Mr. Jean-Claude Carret, Thesis Co-supervisor
Department of construction engineering, École de technologie supérieure

Mr. Ricardo Zednik, President of the Board of Examiners
Department of mechanical engineering, École de technologie supérieure

Ms. Annie Levasseur, Member of the jury
Department of construction engineering, École de technologie supérieure

Mr. Jiqing Zhu, External Evaluator
Swedish National Road and Transport Research Institute (VTI)

THIS THESIS WAS PRESENTED AND DEFENDED

IN THE PRESENCE OF A BOARD OF EXAMINERS AND THE PUBLIC

ON MAY 24, 2024

AT ÉCOLE DE TECHNOLOGIE SUPÉRIEURE

## ACKNOWLEDGMENTS

I am immensely thankful to my advisors at École de technologie supérieure, Prof. Alan Carter and Prof. Jean-Claude Carret, for their unwavering dedication, mentorship, and scholarly insights. Their expertise and patience have been instrumental in shaping this research and my academic growth. I want to express my heartfelt gratitude to Sébastien Lamothe who generously shared his time, knowledge and experiences.

I would like to extend my appreciation to the members of my thesis committee for their invaluable guidance, expertise, insightful feedback and encouragement that have been instrumental in steering this project towards successful completion.

I would like to acknowledge the financial support provided from FPInnovations, which enabled me to conduct this research. Their investment in my education has made this journey possible.

I would like to express my special appreciation to Mr. Francis Bilodeau and Mr. Sylvain Bibeau for their ongoing support in conducting my experiments in the laboratory.

To my wife and family, your unwavering belief in me and your constant encouragement have been a source of strength. Your sacrifices and understanding during this time are deeply appreciated.

**Effets de la lignine sur les propriétés et les performances du bitume et des enrobés chauds à l'asphalte**

Wesam AL-FALAHAT

## RÉSUMÉ

Ce programme de recherche vise à étudier les effets de l'ajout de lignine, sous forme de poudre et de granules, sur les propriétés du bitume et les performances des enrobés (HMA). Le processus d'incorporation de différentes teneurs en lignine dans le bitume est étudié afin de sélectionner les paramètres (température, vitesse et durée) du processus d'incorporation et de montrer l'effet de chaque paramètre sur la stabilité et l'homogénéité du bitume modifié. Le processus d'incorporation est évalué en effectuant un test de stabilité au stockage et une observation au microscope. Ensuite, les propriétés rhéologiques et chimiques du bitume modifié par la lignine sont étudiées en détail à l'aide du viscosimètre rotatif Brookfield (BRV), du rhéomètre à cisaillement dynamique (DSR), de la récupération par fluage sous contraintes multiples (MSCR), du rhéomètre à flexion de poutres (BBR), du module complexe complet (G*) et des tests infrarouges à transformée de Fourier (FTIR). L'effet antioxydant de la lignine sur les propriétés de vieillissement du bitume modifié par la lignine est également discuté. Pour les enrobés, des essais de compactage par cisaillement giratoire (PCG) sont effectués pour examiner les effets de la lignine sur la compactabilité de l'enrobé modifié en utilisant le processus humide et sec. Ensuite, la performance de l'enrobé est évaluée par une série d'essais, y compris la sensibilité à l'humidité, la résistance à la traction indirecte (ITS), le module complexe (E*), l'orniérage, et l'essai de retrait thermique empêché (TSRST). Les résultats montrent que la lignine est stable dans le bitume et que la lignine est bien dispersée et répartie sur le bitume. L'effet de la température et de la durée d'incorporation sur la stabilité et l'homogénéité du bitume doit être pris en compte pour les teneurs élevées en lignine. La poudre de lignine augmente la viscosité du bitume, la rigidité à haute et basse température et la résistance à la déformation permanente. Les granules de lignine ont un comportement différent qui est dû à la présence d'huile de soja qui dilue le bitume. La lignine ne présente pas d'effet antioxydant limitant le vieillissement du bitume. Aussi, la lignine augmente la teneur en vides d'air dans les enrobés, et le processus humide produit des vides d'air plus faibles que le processus sec. Le tall oil des granules diminue la teneur en vides d'air. La lignine améliore la sensibilité à l'humidité et la résistance à l'orniérage de l'enrobé. La lignine augmente la rigidité du bitume et diminue l'angle de phase. L'ajout d'une faible teneur en lignine ne montre pas de changement significatif sur la performance à basse température, tandis qu'une teneur élevée en lignine réduit la résistance à la fissuration thermique. Globalement, il est possible de remplacer une partie du bitume par de la lignine.

**Mots-clés:** lignine, bitume, HMA, rhéologie, performances thermomécaniques

**Effects of lignin on the properties and performance of bitumen and hot mix asphalt**

Wesam AL-FALAHAT

## ABSTRACT

This research program aims to investigate the effects of lignin addition, in powder and pellet form, on the properties of bitumen and performance of HMA. The incorporation process of different lignin contents into bitumen is investigated in order to select the parameters (temperature, speed and duration) of the incorporation process and to show the effect of each parameter on the stability and homogeneity of the modified bitumen. The incorporation process is evaluated by performing storage stability test and microscope observation. Afterwards, the rheological and chemical properties of lignin-modified bitumen are studied in detail by performing Brookfield rotational viscometer (BRV), dynamic shear rheometer (DSR), multiple stress creep recovery (MSCR), bending beam rheometer (BBR), full complex modulus (G*) and Fourier-transform infrared (FTIR) tests. The anti oxidative effect of the lignin on the aging properties of the lignin modified bitumen is also discussed. For HMA, shear gyratory compaction (SGC) tests are performed to examine the lignin effects on the compactability of modified HMA by using the wet and dry process. Following, the HMA performance is evaluated through a series of tests, including moisture sensitivity, indirect tensile strength (ITS), complex modulus (E*), rutting and thermal stress restrained specimen test (TSRST). The results show that the lignin is stable in bitumen and lignin is well dispersed and distributed over bitumen. The effect of incorporation temperature and duration on the stability and homogeneity of bitumen should be considered for high lignin content. Lignin powder increases the viscosity of the bitumen, stiffness at high and low temperatures and resistance to permanent deformation, while the pellets show different behaviour which is due to the presence of soybean oil that dilutes the bitumen. Lignin does not show anti oxidative aging properties of bitumen. For the HMA compactability, lignin increases the air voids content, while the tall oil decreases it. The wet process shows lower air voids than the dry process. Lignin improves the moisture sensitivity and rutting resistance of HMA. Lignin increases the stiffness of the bitumen and decreases the phase angle. Adding low lignin content does not show a significant change on the low temperature performance, while high lignin content reduces the resistance to thermal cracking. Overall, it is possible to replace part of the bitumen by lignin.

**Keywords:** lignin, bitumen, HMA, rheology, thermomechanical performance

**TABLE OF CONTENTS**

Page

INTRODUCTION ..... 1

CHAPTER 1 PROBLEM STATEMENT AND OBJECTIVES ..... 5
1.1 Problem statement ..... 5
1.2 Objectives ..... 6
1.3 Thesis structure ..... 6

CHAPTER 2 LITERATURE REVIEW ..... 9
2.1 Introduction ..... 9
2.2 Asphalt mix design ..... 9
2.2.1 Compaction process of HMA ..... 11
2.3 Thermomechanical behaviour domains of the bituminous materials ..... 13
2.3.1 Linear viscoelastic behaviour ..... 14
2.3.2 Thermomechanical tests of the bituminous materials ..... 17
2.3.2.1 Test related to LVE behaviour ..... 18
2.3.2.2 Fatigue behaviour ..... 21
2.3.2.3 Tests related to the high temperature performance ..... 25
2.3.2.4 Tests related to the low temperature performance ..... 27
2.3.2.5 Water damage tests ..... 30
2.4 Most common bitumen and HMA modifiers ..... 31
2.4.1 Polymers ..... 31
2.4.2 Recycled plastic ..... 33
2.4.3 Fibers and crumb rubber ..... 33
2.4.4 Cement and other modifiers ..... 34
2.5 Lignin ..... 35
2.5.1 Effects of the lignin on the performance of the bitumen and HMA ..... 38
2.5.2 Incorporation process ..... 41
2.5.3 Verification of the incorporation process ..... 42
2.5.4 Antioxidation properties of lignin ..... 43
2.6 Effects of inert fillers ..... 45
2.7 Summary ..... 46

CHAPTER 3 MATERIALS CHARACTERIZATION AND TEST METHODS ..... 49
3.1 Introduction ..... 49
3.2 Materials ..... 49
3.2.1 Kraft lignin ..... 49
3.2.2 Lignin Pellets ..... 58
3.2.3 Bitumen ..... 59
3.2.4 Aggregate ..... 60
3.3 Tests methods ..... 61
3.3.1 Verification of the incorporation of lignin into the bitumen (wet process) ..... 64

3.3.1.1 Storage stability test ..... 64
3.3.1.2 Microscope observations ..... 66
3.3.2 Aging processes, rheological and chemical tests of bitumen ..... 67
3.3.2.1 Rolling Thin Film Oven (RTFO) ..... 67
3.3.2.2 Pressure Aging Vessel (PAV) ..... 68
3.3.2.3 Brookfield Rotational Viscometer (BRV) test ..... 69
3.3.2.4 Steady shear flow (SSF) method ..... 70
3.3.2.5 Dynamic Shear Rheometer (DSR) test ..... 71
3.3.2.6 Multiple Stress Creep Recovery (MSCR) test ..... 72
3.3.2.7 Bending Beam Rheometer (BBR) test ..... 72
3.3.2.8 Shear complex modulus G* ..... 73
3.3.2.9 Fourier transform infrared (FTIR) ..... 74
3.3.3 Compactability, rheological properties and thermomechanical performance tests of HMA ..... 75
3.3.3.1 Shear gyratory compaction (SGC) test ..... 76
3.3.3.2 Maximum theoretical specific gravity (Gmm) test ..... 78
3.3.3.3 Complex modulus (E*) ..... 79
3.3.3.4 Moisture sensitivity tests ..... 80
3.3.3.5 Rutting resistance test ..... 82
3.3.3.6 Thermal stress restrained specimen test (TSRST) ..... 83
3.3.3.7 Fatigue test (DGCB method) ..... 85
3.4 Field sections ..... 85

CHAPTER 4 LIGNIN INCORPORATION PROCESS IN BITUMEN ..... 87
4.1 Introduction ..... 87
4.2 Preparation of the lignin-modified bitumen ..... 88
4.2.1 Study of the incorporation lignin HT SW A 1 into the bitumen ..... 89
4.2.1.1 Storage stability tests results of the study on the incorporation process of lignin into bitumen ..... 92
4.2.2 Preparation of the modified bitumen with different types of the lignin ..... 96
4.2.2.1 Storage stability tests results of the modified bitumen PG 58S-28 with different types of the lignin ..... 97
4.2.3 Preparation of the mastic ..... 102
4.2.3.1 Storage stability tests results of the mastic ..... 103
4.2.4 Preparation of the modified bitumen with pellets ..... 104
4.2.4.1 Storage stability tests results of the modified bitumen with pellets ..... 106
4.2.5 Microscope observations ..... 107
4.3 Summary ..... 114

CHAPTER 5 ANTIOXIDATION PROPERTIES AND EFFECTS OF LIGNIN ADDITION ON THE BITUMEN PROPERTIES ..... 117
5.1 Introduction ..... 117
5.2 Effects of lignin on the rheology and oxidative aging properties of bitumen ..... 118
5.2.1 Results and analysis ..... 123

5.2.1.1 BRV tests ..... 123
5.2.1.2 DSR tests ..... 133
5.2.1.3 MSCR tests ..... 140
5.2.1.4 BBR tests ..... 145
5.2.1.5 Evolutions of the thermal range ($T_{high}$-$T_{low}$) and the performance grade (PG Hn-L) of bitumens with the lignin content ..... 153
5.2.1.6 Complex modulus G* tests ..... 155
5.2.1.7 FTIR tests ..... 162
5.3 Summary ..... 166

CHAPTER 6 EFFECTS OF THE LIGNIN ON THE COMPACTION PROCESS OF THE ASPHALT MIXTURE ..... 167
6.1 Introduction ..... 167
6.2 Effect of the lignin on the compactability of HMA ..... 168
6.2.1 Comparison between the wet and dry processes ..... 169
6.2.1.1 Results and analysis ..... 170
6.2.2 Effect of compaction temperature ..... 175
6.2.2.1 Results and analysis ..... 176
6.3 Effect of different types of lignin in powder and pellets forms on the compactability of HMA ..... 180
6.3.1 Results and analysis ..... 181
6.4 Summary ..... 187

CHAPTER 7 EFFECTS OF THE LIGNIN ON THE THERMOMECHANICAL BEHAVIOUR AND PERFORMANCE OF THE ASPHALT MIXTURE ..... 189
7.1 Introduction ..... 189
7.2 Effects of HT SW A 1 lignin on the thermomechanical performance of HMA ..... 189
7.2.1 Results and analysis ..... 190
7.2.1.1 Moisture sensitivity ..... 191
7.2.1.2 Complex modulus (E*) ..... 194
7.2.1.3 Rutting ..... 200
7.2.1.4 TSRST ..... 202
7.3 Summary ..... 205

CONCLUSION ..... 207

ANNEX I FIELD TRIAL SECTION AND LIFE CYCLE ASSESSMENT ..... 209

ANNEX II EFFECT OF TALL OIL ON THE COMPACTIBILITY OF LIGNIN MODIFIED HMA ..... 217

ANNEX III EFFECTS OF LIGNIN ON FATIGUE CRACKING RESISTANCE OF ASPHALT MIXTURE ..... 221

LIST OF REFERENCES ..... 227

## LIST OF TABLES

Page


Table 3.1 Types of lignin studied in this research program ..... 50

Table 3.2 Properties of the HT SW A 1 lignin provided by the supplier ..... 51

Table 3.3 Properties of the high and low durability index pellets provided by the supplier ..... 59

Table 3.4 Properties of the bitumen PG 58S-28 and PG 52S-34 provided by the suppliers ..... 60

Table 3.5 Properties of the aggregate used to produce HMA ..... 61

Table 3.6 Traffic level (n) class of bitumen determined with the MSCR test specifications ..... 72

Table 4.1 Summary of the prepared mixes by LSM and tests done to study the incorporation process of lignin HT SW A 1 into the bitumen PG 58S-28 ..... 91

Table 4.2 Storage stability tests results of the study on the incorporation process of the lignin HT SW A 1 into the bitumen PG 58S-28 ..... 94

Table 4.3 Summary of the prepared mixes of the modified bitumen PG 52S-34 with lignin HT SW A 1 by LSM and tests done ..... 95

Table 4.4 Storage stability tests results of the modified bitumen PG 52S-34 with the lignin HT SW A 1 ..... 96

Table 4.5 Summary of the prepared (LSM) modified bitumen PG 58S-28 with 20 % of each type of the lignin and tests done ..... 97

Table 4.6 Storage stability tests results of the modified bitumen PG 58S-28 with different types of the lignin before and after the first grinding process ..... 99

Table 4.7 Storage stability tests results of the modified bitumen PG 58S-28 with different types of the lignin after the second grinding process ..... 100

Table 4.8 Summary of the prepared mixes of mastic with the bitumen PG 58S-28 by LSM and tests done ..... 102

Table 4.9 Storage stability tests results of the modified bitumen PG 58S-28 with the inert filler ..... 103

Table 4.10 Summary of the modified bitumen with pellets prepared by LSM and HSM and tests done ..... 106

Table 4.11 Storage stability tests results of the modified bitumen PG 58S-28 with different types of the pellets incorporated by LSM and HSM ..... 107

Table 4.12 Summary of the microscope observations obtained from ImageJ for the lignin alone and modified bitumen PG 58S-28 with different contents of HT SW A 1 lignin ..... 110

Table 5.1 Summary of the experimental campaign of the tests performed on the modified bitumen with HT SW A 1 lignin (step 1) ..... 119

Table 5.2 Summary of the experimental campaign of the tests performed on the modified bitumen with different lignins (step 2) ..... 120

Table 5.3 Summary of the experimental campaign of the tests performed on the modified bitumen with HDI and LDI pellets (step 3) ..... 121

Table 5.4 Summary of the experimental campaign of the tests performed on the modified bitumen with different contents of HT SW A 1 lignin and aging levels of PAV (step 4) ..... 122

Table 5.5 Mixing ($T_{mix}$) and compaction ($T_{comp}$) temperatures for both bitumens corresponding to the targeted viscosities ..... 127

Table 5.6 Specification and DSR test results for both bitumens modified with HT SW A 1 lignin ..... 135

Table 5.7 MCSR test results, requirements and traffic level (n) class obtained for both bitumens ..... 142

Table 5.8 Specifications and BBR test results for both bitumens with different HT SW A 1 lignin contents ..... 149

Table 5.9 Summary of the high ($T_{high}$) and low ($T_{low}$) temperatures, the thermal range ($T_{high}$-$T_{low}$), the performance grade (PG Hn-L) and the thermal range of use of bitumen (H-L) for all bitumens modified with HT SW A 1 lignin ..... 154

Table 5.10 Summary of the parameters of 2S2P1D model and the constants of WLF equation for the unmodified and modified bitumens with different contents of HT SW A 1 lignin at different aging levels ..... 160

Table 6.1 Mixing ($T_{mix}$) and compaction ($T_{comp}$) temperatures measured with BRV and DSR corresponding to the targeted viscosities for the unmodified and modified bitumen with 20 % of HT SW A 1 lignin ..... 168

Table 6.2 Summary of the performed SGC tests of the unmodified and HT SW A 1 lignin-modified HMA produced by wet and dry processes with different mixing ($T_m$) and compaction ($T_c$) temperatures ..... 169

Table 6.3 Summary of the $G_{mm}$ values for each mix produced by wet and dry process ..... 170

Table 6.4 Summary of the performed SGC tests of the unmodified and modified HMA with 10 and 20 % of HT SW A 1 lignin produced at different compaction temperature ($T_c$) ..... 176

Table 6.5 Summary of the performed SGC tests of the unmodified and modified HMAs with 20 % of different types of lignin and 10 % of pellets types produced by dry process ..... 181

Table 6.6 Summary of the $G_{mm}$ values for the unmodified and modified HMAs with 20 % of each type of lignin and 10 % of pellets types produced by the dry process ..... 182

Table 7.1 Summary of the mechanical tests performed on the unmodified and modified HMA with different contents of HT SW A 1 lignin produced by using the dry process ..... 190

Table 7.2 Summary of the air voids content, parameters of the 2S2P1D model and constants of WLF equation for the unmodified and modified HMA with different contents of HT SW A 1 lignin ..... 200

Table-A I-1 Summary for the trial sections ..... 211

Table-A III-1 Summary of the air voids content and fatigue tests results for each specimen of the unmodified and lignin-modified HMAs ..... 222

Table-A III-2 Summary of $\varepsilon_6$ values obtained before and after the correction of the air voids for each lignin content ..... 226

## LIST OF FIGURES

Page


Figure 2.1 Example of the compaction curve obtained by Superpave gyratory compaction SGC test (in semi-log presentation) and its parameters ..... 13

Figure 2.2 Mechanical behaviour domains of the bituminous materials ..... 14

Figure 2.3 2S2P1D model representation for HMA ..... 16

Figure 2.4 Tension-compression test setup for complex modulus ..... 19

Figure 2.5 Example of the Cole-Cole diagram for HMA ..... 20

Figure 2.6 Example of the master curve of the norm of complex modulus |E*| for HMA ..... 20

Figure 2.7 Example of the master curve of the phase angle φ for HMA ..... 21

Figure 2.8 Evolution of the curve of |E*| as a function of N and its phases and definition of the classical criteria $N_{f50\%}$ ..... 23

Figure 2.9 Example of estimation of NfΔεax (a, top) and $N_{f\Delta\phi}$ (b, bottom) for a tension-compression fatigue test performed on a cylindrical specimen of HMA ..... 24

Figure 2.10 Evolution of the rut depth with number of loading cycles ..... 26

Figure 2.11 Stress-temperature curve of TSRST test on HMA specimen ..... 29

Figure 2.12 Extraction sources of lignin from wood cellulosic biomass: a) wood pulp, b) cotton ..... 36

Figure 2.13 Extraction sources of lignin from non-wood cellulosic biomass: a) Wheat straw, b) Pine straw, c) Flax fiber, d) Alfalfa fiber ..... 37

Figure 3.1 HT SW A 1 lignin ..... 51

Figure 3.2 Mastersizer 3000 laser granulometry apparatus and its attachments ..... 52

Figure 3.3 HT SW A 2 lignin ..... 52

Figure 3.4 HT SW B lignin: a) junk particles, b) after first grinding, c) after the second grinding process ..... 53

Figure 3.5 TB HW A lignin: a) junk particles, b) after first grinding, c) after the second grinding process ..... 54

Figure 3.6 TB HW B lignin: a) junk particles, b) after first grinding, c) after the second grinding process ..... 55

Figure 3.7 K SW A lignin: a) junk particles, b) after first grinding, c) after the second grinding process ..... 56

Figure 3.8 K SW B lignin: a) junk particles, b) after first grinding, c) after the second grinding process ..... 57

Figure 3.9 HT SW A modified lignin ..... 58

Figure 3.10 K SW A modified lignin ..... 58

Figure 3.11 High (a) and low (b) durability index pellets ..... 59

Figure 3.12 Particle size distribution of the aggregate and LC-4202 requirements for ESG-10 ..... 61

Figure 3.13 Summary of the research program ..... 63

Figure 3.14 Two mixers used in this study. a) IKA RW16 basic overhead stirrer, b) SILVERSON L4RT-W high shear mixer ..... 65

Figure 3.15 Storage stability test. a) tubes for the storage stability test, b) Softening point test ..... 65

Figure 3.16 Homogeneity tests with microscopy. a) bitumen drops on the glass plates, b) microscope apparatus ..... 67

Figure 3.17 RTFO aging. a) glass containers filled with bitumen, b) RTFO apparatus ..... 68

Figure 3.18 PAV aging. a) stainless steel pan, b) PAV apparatus ..... 69

Figure 3.19 Brookfield Rotational Viscometer (BRV) test. a) BRV mold, b) BRV apparatus ..... 70

Figure 3.20 Dynamic Shear Rheometer used for the Steady shear flow (SSF) method ..... 71

Figure 3.21 Bending Beam Rheometer (BBR) test. A) BBR apparatus, b) specimen of the beam ..... 73

Figure 3.22 Mold for the specimen preparation for G*. a) 8 mm, b) 4 mm geometry used for G* test ..... 74

Figure 3.23 Fourier transform infrared (FTIR). a) FTIR spectroscopy apparatus, b) drop of bitumen on a thin glass plate ..... 75

Figure 3.24 Mixers used in this study. a) Hobart model A200 countertop mixer, b) Thermoregulated TR (InfraTest model 30 l) mixer ..... 76

Figure 3.25 Shear gyratory compaction (SGC) test. a) scheme of the SGC test, b) gyratory shear press ..... 78

Figure 3.26 Loose HMA specimen used for $G_{mm}$ ..... 79

Figure 3.27 Marshall compaction. a) Marshall compactor, b) Marshall specimen during the test ..... 81

Figure 3.28 Marshall specimen during the indirect tensile ..... 82

Figure 3.29 Rutting resistance test. a) LPC plate, b) rut tester, c) zoom on the loaded wheel ..... 83

Figure 3.30 Thermal stress restrained specimen test (TSRST) a) specimen inside the thermal chamber, b) a broken specimen after the test ..... 84

Figure 4.1 Summary of the different steps and the objective of each step ..... 88

Figure 4.2 The bottom (left) and top (right) of the tube for the modified bitumen with K SW B lignin after the first grinding process ..... 99

Figure 4.3 Particles size based on Dx (50) value for A (including modified types) and B lignins after the first and second grinding process ..... 101

Figure 4.4 Collected filler at the bottom of the tube for storage stability test ..... 104

Figure 4.5 A photo taken during the incorporation process of the HDI pellets by LSM showing the presence of pellets ..... 106

Figure 4.6 Microscope image for HT SW A 1 lignin alone ..... 110

Figure 4.7 Microscope image for the unmodified bitumen PG 58S-28 ..... 111

Figure 4.8 Microscope image for the modified bitumen PG 58S-28 with 10 % of the HT SW A 1 lignin ..... 111

Figure 4.9 Microscope image for the modified bitumen PG 58S-28 with 20 % of the HT SW A 1 lignin ..... 112

Figure 4.10 Microscope image for the modified bitumen PG 58S-28 with 30 % of the HT SW A 1 lignin ..... 112

Figure 4.11 Microscope image for the modified bitumen PG 58S-28 with 50 % of the HT SW A 1 lignin (30 min at 140 °C) ..... 113

Figure 4.12 Microscope image for the modified bitumen PG 58S-28 with 50 % of the HT SW A 1 lignin (30 min at 165 °C) ..... 113

Figure 4.13 Microscope image for the modified bitumen PG 58S-28 with 50 % of the HT SW A 1 lignin (60 min at 165 °C) ..... 114

Figure 5.1 Summary of the four steps and the objective of each step ..... 118

Figure 5.2 Viscosities (η) of PG 58-28 with different HT SW A 1 lignin contents, 20 % of different lignins and 10 % of pellets as a function of testing temperature ($T_T$) and lignin content (% in relation to the total mass of bitumen) and targeted viscosities for mixing ($\eta_{targeted\ for\ mix}$: 170 mPa·s) and for compaction ($\eta_{targeted\ for\ comp}$: 280 mPa·s) ..... 125

Figure 5.3 Viscosities (η) of PG 52-34 with different HT SW A 1 lignin contents as a function of testing temperature ($T_T$) and lignin content (% in relation to the total mass of bitumen) and targeted viscosities for mixing ($\eta_{targeted\ for\ mix}$: 170 mPa·s) and for compaction ($\eta_{targeted\ for\ comp}$: 280 mPa·s) ..... 127

Figure 5.4 Increase of mixing ($\Delta T_{mix}$) and compaction ($\Delta T_{comp}$) temperatures of the modified bitumens compared to the unmodified bitumen (0 % of lignin) ..... 128

Figure 5.5 Viscosities (η) of the unmodified and modified bitumens with different contents of HT SW A 1 lignin at different aging levels ..... 132

Figure 5.6 Ratio of viscosity at 150 °C of the unmodified and modified bitumens with different contents of HT SW A 1 lignin referenced to unaged level ..... 132

Figure 5.7 DSR test results for PG 58-28 with different HT SW A 1 lignin contents, 20 % of different lignins and 10 % of pellets ..... 134

Figure 5.8 DSR test results for PG 52-34 with different HT SW A 1 lignin contents ..... 135

Figure 5.9 Increase of high temperature ($\Delta T_{high}$), compared to the bitumen with 0 % of lignin, according to the lignin content for both bitumens ..... 136

Figure 5.10 A photo shows the particles of HT SW A-modified lignin on the plate used for the DSR test ..... 137

Figure 5.11 G*/sin (δ) values at different temperatures for the bitumen modified with different contents of HT SW A 1 lignin at different aging levels ..... 139

Figure 5.12 Ratio of G*/sin (δ) at 58 °C of the bitumen modified with different contents of HT SW A 1 lignin referenced to unaged level ..... 139

Figure 5.13 $Jnr_{3.2}$ values at 58 °C for PG 58-28 with different HT SW A 1 lignin contents, 20 % of different lignins and 10 % of pellets ..... 141

Figure 5.14 $Jnr_{3.2}$ values at 52 °C for PG 52-34 with different HT SW A 1 lignin contents ..... 142

Figure 5.15 $Jnr_{3.2}$ values at different temperatures for the unmodified and modified bitumens with different contents of HT SW A 1 lignin at different aging levels ..... 144

Figure 5.16 Stiffness values for PG 58S-28 with different HT SW A 1 lignin contents, 20 % of different lignins and 10 % of pellets ..... 146

Figure 5.17 Slope values for PG 58S-28 with different HT SW A 1 lignin contents, 20 % of different lignins and 10 % of pellets ..... 146

Figure 5.18 Stiffness values for PG 52S-34 with different HT SW A 1 lignin contents ..... 148

Figure 5.19 Slope values for PG 52S-34 with different HT SW A 1 lignin contents ..... 148

Figure 5.20 Increase of low temperature ($\Delta T_{low}$), compared to the bitumen with 0 % of lignin, according to the lignin content for both bitumens ..... 149

Figure 5.21 Stiffness (S(60)) values at different temperatures for the unmodified and modified bitumens with different contents of HT SW A 1 lignin at different aging levels ..... 151

Figure 5.22 Slope (m(60)) values at different temperatures for the unmodified and modified bitumens with different contents of HT SW A 1 lignin at different aging levels ..... 152

Figure 5.23 High ($T_{high}$) and low ($T_{low}$) temperatures and the resulted gap ($T_{high}$-$T_{low}$: the thermal range) for both bitumens modified with HT SW A 1 lignin ..... 154

Figure 5.24 Cole-Cole diagram for the unmodified and modified bitumen with different contents of HT SW A 1 lignin at different aging levels, 2S2P1D model and its parameters ..... 156

Figure 5.25 Master curves of the norm of complex modulus (|G*|) at $T_{ref}$=22 °C for the unmodified and modified bitumens with different contents of HT SW A 1 lignin at different aging levels and 2S2P1D model ..... 157

Figure 5.26 Master curves of the phase angle (φ) at $T_{ref}$=22 °C for the unmodified and modified bitumens with different contents of HT SW A 1 lignin at different aging levels and 2S2P1D model ..... 158

Figure 5.27 Difference in percentage of the norm of complex modulus (|G*|) between the experimental data and 2S2P1D model referenced to the experimental data of |G*| for the unmodified and modified bitumens with different contents of HT SW A 1 lignin at different aging levels ..... 159

Figure 5.28 Ratio of the norm of complex modulus (|G*|) of the unmodified and modified bitumen with different contents of HT SW A 1 lignin referenced to unaged level ..... 161

Figure 5.29 Absolute difference of phase angle of the unmodified and modified bitumen with different contents of HT SW A 1 lignin referenced to unaged level ..... 162

Figure 5.30 FTIR results for the unmodified and modified bitumens with different contents of HT SW A 1 lignin at different aging levels ..... 164

Figure 5.31 Carbonyl index for the unmodified and modified bitumens with different contents of HT SW A 1 lignin at different aging levels ..... 165

Figure 5.32 Sulfoxide index for the unmodified and modified bitumens with different contents of HT SW A 1 lignin at different aging levels ..... 165

Figure 6.1 Air voids content (%) of the unmodified (0 %) and modified HMA with different contents (5 and 20 %) of HT SW A 1 lignin using wet and dry processes and LC-4202 requirements for ESG-10 formulation ..... 172

Figure 6.2 Air voids in mix at different gyrations for the unmodified and HT SW A 1 lignin-modified HMA produced by wet and dry processes ..... 174

Figure 6.3 K values for the unmodified and HT SW A 1 lignin-modified HMA produced by wet and dry processes ..... 174

Figure 6.4 Compaction energy index (CEI) values for the unmodified and HT SW A 1 lignin-modified HMA produced by wet and dry processes ..... 175

Figure 6.5 Air voids content (%) of the unmodified and modified HMA with 10 and 20 % of HT SW A 1 lignin produced at different compaction temperatures and LC-4202 requirements for ESG-10 formulation ..... 177

Figure 6.6 Air voids in mix at different gyrations for the unmodified and HT SW A 1 lignin-modified HMA produced by dry process at different compaction temperatures ..... 178

Figure 6.7 K values for the unmodified and HT SW A 1 lignin-modified HMA produced by dry process at different compaction temperatures ..... 179

Figure 6.8 Compaction energy index (CEI) values for the unmodified and HT SW A 1 lignin-modified HMA produced by dry process at different compaction temperatures ..... 179

Figure 6.9 Air voids content (%) of the unmodified, minimum and maximum air voids of the modified HMAs with 20 % of each type of lignin and 10 % of each pellets type using dry process and LC-4202 requirements for ESG-10 formulation ..... 184

Figure 6.10 Air voids in mix at different gyrations for the unmodified, minimum and maximum air voids of the modified HMAs with 20 % of each type of lignin and 10 % ..... 186

Figure 6.11 K values for the unmodified and modified HMAs with 20 % of each type of lignin (min and max) and 10 % of each pellets type using dry process ..... 186

Figure 6.12 Compaction energy index (CEI) values for the unmodified and modified HMAs with 20 % of each lignin type (min and max) and 10 % of each pellets type using dry process ..... 187

Figure 7.1 Moisture sensitivity test results for the non-soaked (N) and soaked (S) specimens of the unmodified and modified HMA with different contents of HT SW A 1 lignin: Marshall stability at 60 °C, water resistance (WR) and air voids content (underlined value in %) ..... 193

Figure 7.2 Indirect tensile strength (ITS) test results for the dry (D) and conditioned (C) specimens of the unmodified and modified HMA with different contents of HT SW A 1 lignin: ITS at 25 °C, ITS ratio (ITSR) and air voids content (underlined value in %)..... 193

Figure 7.3 Cole-Cole diagram for the unmodified and modified HMA with different contents of HT SW A 1 lignin and 2S2P1D model parameters (E00, E0, h, k and δ)..... 194

Figure 7.4 Master curves of the norm of complex modulus (|E*|) at $T_{ref}$=10 °C for the unmodified and modified HMA with different contents of HT SW A 1 lignin and 2S2P1D model..... 195

Figure 7.5 Normalized Cole-Cole diagram for the unmodified and modified HMA with different contents of HT SW A 1 lignin ..... 196

Figure 7.6 Ratio of the norm of complex modulus (|E*|) for the modified HMA with different contents of HT SW A 1 lignin referenced to the unmodified HMA..... 197

Figure 7.7 Master curves of the phase angle (φ) at $T_{ref}$=10 °C for the unmodified and modified HMA with different contents of HT SW A 1 lignin and 2S2P1D model..... 198

Figure 7.8 Difference in percentage of the norm of complex modulus (|E*|) between the experimental data and 2S2P1D model referenced to the experimental data of |E*| for the unmodified and modified HMA with different contents of HT SW A 1 lignin ..... 199

Figure 7.9 Rut depth at 58 °C for the unmodified and modified HMA with different contents of HT SW A 1 lignin, air voids (Av) and requirements of LC 26-410..... 201

Figure 7.10 Evolution of the thermal stress versus the decrease in the temperature for each specimen of the unmodified and lignin-modified HMAs with different contents ..... 204

Figure 7.11 Fracture and glass-transition temperatures and fracture strength for the unmodified and lignin-modified HMAs with different contents (average of 3 results) ..... 204

Figure-A I-1 Alberta's trial ..... 212

Figure-A I-2 Ontario's trial ..... 213

Figure-A I-3 Quebec city's trial ..... 214

Figure-A I-4 Laval University's trial ..... 214

Figure-A II-1 SGC tests results for the lignin-modified HMA with and without tall oil ..... 219

Figure-A III-1 Wöhler curves ($N_{f\,50\%}$ criterion) of the uniaxial tension-compression tests results of the unmodified and lignin-modified HMAs tested at 10 °C and 10 Hz and different strain levels ..... 223

Figure-A III-2 Wöhler curves ($N_{f\,50\%}$ criterion) of the uniaxial tension-compression tests results based on the corrected air voids content of the unmodified and lignin-modified HMAs tested at 10 °C and 10 Hz and different strain levels ..... 225

## LIST OF ABBREVIATIONS

| | |
|---|---|
| AASHTO | American Association of State Highway and Transportation |
| APT | Accelerated Pavement Testing |
| ASTM | American society for testing and materials |
| BBR | Bending Beam Rheometer |
| BRV | Brookfield Rotational Viscometer |
| CDW | Construction and Demolition Waste |
| CEI | Compaction Energy Index |
| CMA | Cold Mix Asphalt |
| COV | Coefficient of Variation |
| CR | Chloroprene Rubber |
| DGCB | Département de Génie civil et bâtiment |
| DPA | Date Palm Ash |
| DSR | Dynamic Shear Rheometer |
| DTT | Direct Tension Tests |
| ENTPE | École Nationale de Travaux Publics de l'État |
| ESG | Enrobé Semi-Grenu |
| EVA | Ethylene-Vinyl Acetate |
| FLRT | French Laboratory Rut Tester |
| FP | Flash Point |
| FTIR | Fourier-Transform Infrared |
| FWTT | French Wheel Tracking Tester |
| GHG | Green-House Gases |

| | |
|---|---|
| GTR | Grounded Tire Rubber |
| HDI | High Durability Index |
| HDPE | High Density Polyethylene |
| HMA | Hot Mix Asphalt |
| HSM | High Shear Mixer |
| HWTD | Hamburg Wheel Tracking Device |
| ITS | Indirect Tensile Strength |
| ITSR | Indirect Tensile Strength Ratio |
| LC | Laboratoire des Chaussées |
| LCA | Life Cycle Assessment |
| LCMB | Laboratoire sur les Chaussées et les Matériaux Bitumineux |
| LPC | Laboratoire des Ponts et Chaussées |
| LDI | Low Durability Index |
| LDPE | Low Density Polyethylene |
| LSM | Low Shear Mixer |
| LVE | Linear Viscoelastic |
| MSCR | Multiple Stress Creep Recovery |
| MTQ | Ministère des Transports du Québec |
| MTS | Material Testing System |
| PAV | Pressure Aging Vessel |
| PG | Performance Grade |
| PmB | Polymer-modified Bitumen |

| | |
|---|---|
| PP | Polypropylene |
| PPA | Polyphosphoric Acid |
| RAP | Reclaimed Asphalt Pavement |
| RPWA | Recycled Plastic Waste Aggregate |
| RTFO | Rolling Thin Film Oven |
| SBR | Styrene Butadiene Rubber |
| SBS | Styrene Butadiene Styrene |
| SEBS | Styrene-Ethylene–Butylene-Styrene |
| SGC | Shear Gyratory Compactor |
| SHRP | Strategic Highway Research Program |
| SMA | Stone Matrix Asphalt |
| SP | Softening point |
| SSF | Steady Shear Flow |
| ST | Separation Tube |
| TGA | Thermo-Gravimetric Analysis |
| TSRST | Thermal Stress Restrained Specimen Test |
| TTSP | Time Temperature superposition principle |
| WR | Water Resistance |
| WLF | Williams, Landell and Ferry |
| WMA | Warm Mix Asphalt |
| WTT | Wheel-Tracking Tests |

# INTRODUCTION

Asphalt pavement is considered one of the main components of road networks worldwide. Constructed from a composite material termed asphalt mix which consists of mainly mineral aggregates such as crushed stone, gravel and sand bound together by a petroleum-derived binding agent known as bitumen. Mixing aggregates with bitumen, forming asphalt mixture, produces a flexible road surface capable of withstanding, to some extent, heavy vehicular loads, traffic stresses and environmental conditions. Asphalt mixes are the first layers of a flexible pavement structure. Other than flexible pavements, you can find rigid pavement, made with concrete, but this research program focuses on only the flexible pavement.

Flexible pavement is typically built with three to four layers. These layers are asphalt mix layers (1 to 3 layers), granular base course, and sometimes granular subbase course constructed over a compacted natural soil subgrade (Jenks et al., 2011). Usually, asphalt mix layer comprises interconnected sublayers, collectively responsible for bearing the loads applied by traffic. These layers are surface course and then base course. There can be a third layer, in between, that is called the binder course. Since the asphalt mix layer is in direct touch with traffic, high quality (better properties) is needed for the materials of its composition. The layer positioned below is the granular base course. This layer provides the thickness essential for the pavement's enduring quality against both traffic and environmental effects. Many researches stated that great care should be taken when designing the granular base course layer and care even more rigorously than the asphalt mix layer to ensure the durability and lifespan of asphalt pavement (Maupin & Diefenderfer, 2006; Olard, 2012; Theyse et al., 1996). In regions characterized by notably weak subgrade soils, a subbase layer is used. In Canada, for high traffic loads, there is always a granular subbase, regardless of the conditions of the subgrade layer. It is used for frost protection purposes. This layer functions like the granular base course layer, but the material specifications for the subbase layer are relatively less stringent compared to those for the granular base course layer. This is justified by the fact that the load subjected to the subbase layer is lower than that for the base course layer. The subbase layer composes of compacted or stabilized granular materials, fulfills its function (Huang, 2004). Lastly, the

subgrade layer is the natural soil beneath the pavement structure. Usually, the top of this layer is graded and compacted, aiming to address inconsistencies and improve load-bearing capability.

Constructing this sequence of layers in accordance with the defined specifications, thereby constituting a flexible pavement system, provides safe roadways that effectively cater to driver needs. However, asphalt pavement is not impervious to challenges. Over time, temperature fluctuations, water infiltration and freeze-haw cycles can result in deterioration of asphalt pavement. To this end, improving the properties and the performance of the asphalt pavement is necessary.

Asphalt mixes can be classified into four types according to their corresponding mixing temperatures (Alossta & Zeiada, 2011). These types are cold mix asphalt (CMA), warm mix asphalt (WMA), half WMA and hot mix asphalt (HMA). The research is concentrated on HMA. HMA is a blend of heated aggregate and bitumen. The mixing temperature for HMA is typically at a range of approximately 150 to 180 °C. In Quebec, the maximum mixing temperature of polymer-modified bitumen is 170 °C (LC 26-003). Dense-graded mix, stone matrix asphalt (SMA) and open-graded mix are the subcategories of HMA (Alossta & Zeiada, 2011). The dense-graded mix is used in constructing roadways with high traffic volumes due to its durability. However, dense-graded mix can also be used in rural very low volume roads. In Canada, the dense-graded mix is the predominant choice for paving applications whereas the SMA and open-graded mixes are limited instances. Generally speaking, the performance of HMA is mainly affected by the aggregate type and gradation, grade of base bitumen and additives. Some researchers stated that the aggregate skeleton should be considered in the analysis of test results for better evaluation of HMA performance since it carries most of the loads (Sefimazgi et al., 2012). Regarding the full-scale production of HMA, it can be done by using one of the two HMA plants: dryer drum mixer and batch plants (Olard et al., 2008). The data obtained from the field section can be used to help pavement designers improving and developing the design methods.

This research program focuses on improving the performance and sustainability of the HMA. Using modifiers within this layer can increase the durability, sustainability and service life of the asphalt pavement (Robert & Suckhong, 1996; Mirabdolazimi & Shafabakhsh, 2017). Different modifiers and their corresponding effects on the asphalt mix are presented in chapter 2. In this research program, lignin, as a modifier, is used due to its demonstrated efficacy in improving the performance of the asphalt mix (Batista et al., 2018; Gao et al., 2020; Norgbey et al., 2020). Using lignin presents a promising opportunity to revolutionize the asphalt industry. Traditional asphalt production process requires a lot of energy and emits a huge amount of greenhouse gases (GHG). In this context, lignin, derived from renewable sources such as wood pulp, aligns with the sustainability goals since incorporating it into the bitumen reduces the dependence on fossil fuels (Khandelwal, 2019). So, considering lignin as an eco-friendly alternative and a green solution for asphalt production is standing. In conclusion, the integration of lignin into the asphalt industry is a forward-thinking choice that combines improved performance with environmental benefits.

However, due to a shortage in the information provided in the literature review, questionable findings and the limitations stated by the researchers, further investigation is needed to develop the utilization of lignin within the asphalt mix. In particular, several critical gaps such as long-term performance hinder the understanding of how lignin-modified bitumen holds up under different conditions like environment and traffic loads. In addition, there is a need for standardized testing protocols in order to guarantee consistent evaluation of the properties and performance of lignin-modified bitumen across different regions and research studies. In summary, addressing these research gaps will promote the widespread adoption and acceptance of lignin-modified bitumen in sustainable infrastructure projects. Overall, the use of lignin in HMA is not common. The work done in this research program answers many questions and provides new information into the field of asphalt industry. During this research, several lignins were tested, and with the active participation of the industrial partner, significant changes were made to the initial planning throughout the project.

# CHAPTER 1

# PROBLEM STATEMENT AND OBJECTIVES

## 1.1 Problem statement

For more than a century, asphalt mixtures have been utilized in the construction of paved road networks in Canada and worldwide. Nonetheless, significant challenges are still existing in the realm of asphalt pavement, involving various forms of damage such as rutting, fatigue, thermal cracking and potholes. These forms of damage stem primarily from a growth of traffic loads and adverse environmental conditions that decrease the performance, quality and the service life of the asphalt pavements. Particularly in frigid climates like Canada, the performance of asphalt pavements under low temperatures proves unsatisfactory. As a result, the incorporation of additives becomes imperative to improve the efficacy of asphalt pavement and boost its overall quality and lifespan. Herein, the incorporation of lignin into the bitumen is possible. Lignin, among the potential bitumen modifiers, is selected owing to its abundant presence in Canada's forested landscapes where lignin can be found. Consequently, a significant amount of unused lignin exists, since it is a waste product of the paper and wood industry. However, the literature review did not show the methodology of the incorporation wet process of lignin into the bitumen and its limitations. Furthermore, limited studies have been conducted concerning the incorporation of lignin into HMA. Therefore, the effects of lignin on the properties and performance of the bitumen and HMA remain relatively unexplored, leaving the optimum lignin dosage undetermined. This knowledge gap has consequently hindered the development of pavement designs for asphalt pavements modified with lignin, as the ramifications of introducing lignin into the complex modulus of HMA have not been comprehensively assessed. Moreover, the sparse research undertaken on lignin has not been followed up with extensive implementations, such as trial sections. This deficiency in practical application has left the thorough evaluation of full-scale production for lignin-modified HMA incomplete. As known, bitumen, being a non-renewable resource, has notable adverse environmental consequences arising from its extraction and production. Regrettably, the potential environmental benefits of substituting bitumen with lignin have not undergone a

thorough evaluation. To this end, this research offers innovative insights and a fresh perspective on the utilization of lignin in HMA.

## 1.2 Objectives

The main objective of this research program is to develop the modified hot mix asphalt (HMA) with Kraft lignin for Canada. The following are the specific objectives to achieve the main objective:

- To establish a methodology of incorporating lignin into bitumen;
- To evaluate the effects of lignin on the bitumen properties and performance;
- To evaluate the effects of lignin on the oxidation of the bitumen;
- To evaluate the effects of lignin on the compaction of the HMA;
- To evaluate the effects of lignin on the rheological properties and thermomechanical performance of the HMA.

## 1.3 Thesis structure

The research is divided into seven chapters, overall conclusion, three annexes and a list of references. In Chapter 1, the foundation is laid by discussing asphalt pavements and mixtures, outlining the research objectives, elucidating the problem statement, and providing an overview of the thesis structure. Chapter 2 delves into previous researches that present the performance of HMA and the effects of modifiers on the properties and behaviour of modified bitumen and HMA. In Chapter 3, the focus shifts to the types of lignin used in this research, detailing the research methodology, and providing descriptions of the different tests performed on both, bitumen and HMA. Chapter 4 centers on the incorporation of lignin into bitumen through the wet process. Specifically, this chapter presents results from storage stability tests, morphological analysis of microscope observations and shows a summary outlining the parameters selected for the incorporation process. Chapter 5 investigates the effects of adding lignin in both forms, powder and pellets, on the rheological properties of bitumen and its behaviour, along with assessing the antioxidative aging properties of the lignin-modified

bitumen. Chapter 6 presents how lignin, in powder and pellets forms, affects the compactability of HMA. In Chapter 7, the focus shifts to the effects of lignin on the thermomechanical behaviour and performance of HMA at high and low temperatures. Subsequently, a summary of the main findings of this research is presented in the conclusion. Following this, Annex I shows the trial sections conducted in different provinces in Canada. The impact of the addition of tall oil on HMA compactability is presented in Annex II. The effect of lignin on fatigue cracking resistance of HMA is presented in Annex III. Lastly, the list of references used in this research is provided.

# CHAPTER 2

# LITERATURE REVIEW

## 2.1 Introduction

This chapter presents the previous studies that were conducted on the use of the modifiers with bitumen and hot mix asphalt (HMA). In particular, the effects of these modifiers on the performance of bitumen and HMA at high, intermediate and low temperatures are discussed. This research focuses on the lignin in both forms, powder and pellets. First, the asphalt mix design and compactability of HMA are presented. Afterwards, the thermomechanical behaviour of bituminous materials is presented. Then, modifiers such as polymers, recycled plastic, crumb rubber and cement are discussed briefly. Following, the incorporation process of lignin into bitumen and the verification of the lignin-modified bitumen in terms of the stability and homogeneity are presented. Afterwards, the effects of the lignin on the behaviour of the bitumen, including oxidation process, and HMA at high, intermediate and low temperatures are shown. Since the lignin is a powder, the effects of the inert filler on the bitumen and HMA are presented. Finally, a summary presents the advantages of the integration of lignin with the asphalt industry in comparison with the other modifiers.

## 2.2 Asphalt mix design

Asphalt mix design is an important and critical process to construct a durable flexible pavement that can carry the traffic loads and the environmental conditions. This process aims to determine the optimal combination of asphalt binder and aggregate, forming asphalt mix, that leads to the desired performance (Leandro et al., 2017). In addition, the materials selection stage should be done carefully. More specifically, aggregates with good gradation, surface, shape and texture are usually required, and for the bitumen, the selection process is influenced by many factors such as climate and traffic.

The volumetric properties of asphalt mix play a crucial role in the design process of asphalt mix. In particular, the air voids, voids filled with asphalt (VFA) and voids in mineral aggregate (VMA). The percentage of the total volume of air inside a compacted HMA specimen represents the air voids. Excessive air voids within an asphalt mix can result in a reduction of durability due to permeability issues, while insufficient air voids can lead to potential moisture damage and permanent deformation (rutting). For VFA, it represents the voids in percent that are filled with asphalt binder. It is an important property for the evaluation of the asphalt mix durability and moisture damage resistance. The VMA property represents the percentage of the volume of voids within the aggregate particles in HMA specimens.

As mentioned previously, the mix design process aims to determine the optimal asphalt binder content that leads to the desired volumetric properties and performance characteristics (Wang et al., 2019). In this context, a range of asphalt binder contents is typically tested in order to determine the optimum one that meets specific requirements. To this end, the above-mentioned volumetric properties (air voids, VFA and VMA) of an asphalt mix are affected by the volume of asphalt binder, particularly the effective volume, and absorbed asphalt binder. An adequate effective volume of asphalt binder leads to adequate air voids within asphalt mix. Regarding the workability and compactability of an asphalt mix, they are affected by the effective volume and absorbed asphalt binder. Finally, the volumetric properties of an asphalt mix can be studied after conducting the compaction process on this asphalt mix.

In this research program, the Laboratoire des Chaussées (LC) method from Ministère des Transports du Québec (MTQ) is used. The principle of LC mix design is to reach a specific effective volume of bitumen which differs according to the mix type (12.2 % for the ESG-10 used in this research program), and then verify the compaction, moisture sensitivity and rutting performance of the produced HMA. It should be noted that VMA and VFA are not used in the LC method.

### 2.2.1 Compaction process of HMA

The air voids content within the HMA is considered one of the main factors that influence the thermomechanical performance of HMA (Bell et al., 1984; Linden et al., 1989; Harvey et al., 1994; Roque et al., 1995; Harrigan, 2002). In other words, the air voids content is considered as a key parameter influencing the resistance of HMA to the fatigue cracking, moisture damage, rutting and low temperature cracking (Monismith, 1992). Determining the evolution of the air voids content during the compaction process is an efficient method to evaluate HMA compactability (Kassem et al., 2011). The Marshall and shear gyratory compactor (SGC) are the most common methods that can be employed for the HMA compaction in the laboratory (Guler et al., 2000). Yue et al. (1995) stated that the SGC, a laboratory compaction method, can simulate the field compaction method since both methods showed uniform orientation and distribution of coarse aggregate through the HMA. Consuegra et al. (1988) demonstrated that the SGC method, among other methods, produced HMA specimens with properties closest to those determined from the field HMA cores. Wang et al. (2019) stated that the particle rotation and movement pattern in SGC, due to particle close proximity to the nearby particle in a confined particulate structure, is very similar to that in the rollers used in field compaction, especially pneumatic rollers. This can be explained by the fact that SGC applies both shear and compression simultaneously to the HMA. The shear force can well simulate the kneading process by pneumatic roller.

As a prior step for the compaction process, it is necessary to measure the viscosity of the asphalt binder. Many methods can be employed to measure the viscosity such as equiviscous and steady shear flow (SSF) methods (Almusawi et al., 2019). In equiviscous method, the Brookfield rotational viscometer (BRV) is used. In this method, a spindle rotates inside a cylindrical mold at a certain speed which is 20 rpm to measure the viscosity of the unaged bitumen at specific temperatures, usually 135 and 165 °C. Whereas in the SSF method (Reinke method), the DSR is utilized. In this method, the unaged bitumen specimen is placed between two parallel plates of a specific gap, usually 0.5 mm, and different shear stress levels, from 0.3 to 500 Pa (or 1000 Pa), are applied. Therefore, the behaviour of the bitumen in this method is

shear-dependent (Reinke, 2003). The targeted viscosity of the mixing temperature Tm for the BRV and DSR is the same, 170 ± 20 mPa·s. Whereas this viscosity is different for the compaction temperature Tc, 280 ± 30 mPa·s for the BRV and 350 ± 30 mPa·s for the DSR. According to these targeted viscosities, the Tm and Tc temperatures can be determined for the HMA. However, Raschia et al. (2020) stated that Tc plays a major role for the evaluation of the compactability of HMA, while Tm did not show significant effect.

In order to evaluate the compaction process of the HMA, three parameters can be discussed, namely workability, compactability and compaction energy index (CEI). Figure 2.1 shows an example of the compaction curve and its parameters. The air voids content in the mix after 10 gyrations is called workability parameter and it is denoted by Vm (10). A low value corresponds to a better workability. The compactability parameter (K) represents the slope of the curve. A high value of (K) corresponds to a better compactability. The CEI, in general, is the area under the compaction curve from the 8th gyration to the number of gyrations associated with 92 % of the maximum theoretical specific gravity (Gmm) (Raschia et al., 2020; Jamshidi et al., 2022). It represents the work applied by a roller to reach the target compaction degree during the construction phase. Low value means improved constructability, but very low value should be avoided since it indicates a tender mix which makes it difficult to handle the traffic loads at the opening stage without causing distresses or at least early problems for the asphalt pavement.

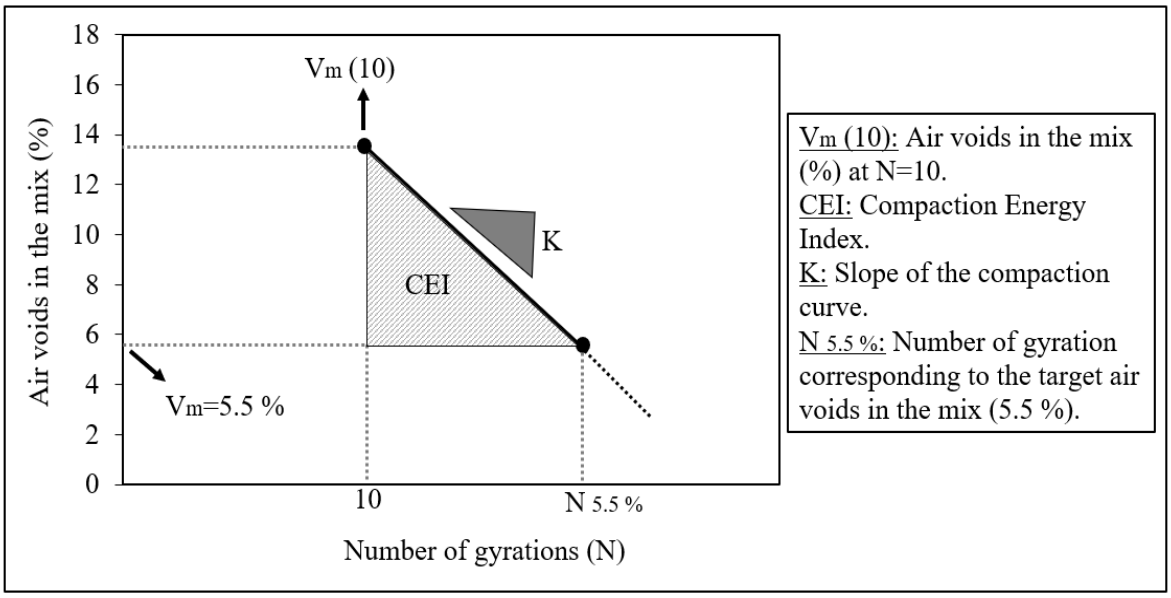


Figure 2.1 Example of the compaction curve obtained by Superpave gyratory compaction SGC test (in semi-log presentation) and its parameters
Taken from Raschia et al. (2020)

## 2.3 Thermomechanical behaviour domains of the bituminous materials

The behaviour of the bituminous materials depends on several factors such as the temperature (T), the loading frequency, the strain amplitude (ε) and the number of the load repetitions(N) (Mangiafico, 2014; Di Benedetto et al., 2007b; Olard et al., 2005). As indicated in Figure 2.2, the behaviour can be considered as a linear viscoelastic (LVE) (section 2.2.1), if a small ε is applied for a relatively low N on the bituminous material. The fatigue can occur if a small ε is applied for a relatively high N on the bituminous material. However, the mechanical behaviour of the bituminous material becomes non-linear if it is subjected to high ε. For the rutting domain (repeated cyclic stress loading not centered on zero), the bituminous material can experience a permanent deformation if it is subjected to a combination of high N and ε. The highest the strain is, the less repetition is needed for a permanent deformation. More details about these mechanical behaviours are shown in section 2.3.2.

The threshold value is called “linear viscoelastic limit” (Mangiafico, 2014). This strain value depends on the temperature of the test and the material, and it is approximately 100

microstrains for bituminous material (Airey et al., 2003). Anyway, the threshold value of each mechanical behaviour domain is displayed as only an indication of the order of magnitude. In the field, the transition process from a mechanical behaviour domain to another is not abrupt (Mangiafico, 2014).

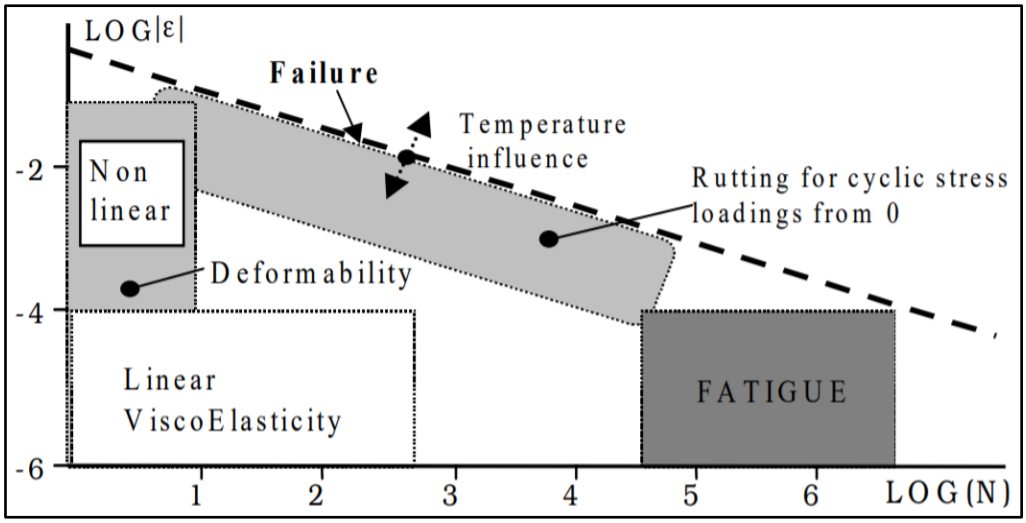


Figure 2.2 Mechanical behaviour domains of the bituminous materials
Taken from Olard & Di Benedetto (2005b)

### 2.3.1 Linear viscoelastic behaviour

Materials can exhibit different behaviours under various conditions. Materials can behave as purely elastic (solid) or purely viscous (liquid) or both (viscoelastic). For the LVE domain, the temperature (weather conditions) and frequency (loading rate) are the main factors that govern the mechanical behaviour of the bituminous materials (El-Hakim and Tighe, 2014). In addition, different aspects of the mechanical behaviour, depending on the test performed, can be defined based on the rheology of the material which is the study of the response of a material subjected to a load.

The elastic behaviour can be considered if the material returns instantaneously to its original shape when the applied load is removed (Lundstrom, 2002). In particular, at low temperatures

and/or high frequencies (short loading times), the material exhibits elastic behaviour. Hook's law describes the linear elastic behaviour of the material (Pellinen, 2001).

In a similar pattern, Newton's law describes the viscous behaviour of the material (Lundstrom, 2002). This law indicates that the viscous behaviour can be considered if the applied shear stress on the material is directly proportional to the resultant strain rate. However, based on Hook's and Newton's laws, a linear relationship between the stress and strain is obtained as long as the strain rate is low (Lundstrom, 2002; Young, 1998). With the increase of the strain rate, deviation is expected to occur. In general, at high temperatures and/or low frequencies (long loading times), the material exhibits viscous behaviour.

However, most materials exhibit behaviour that is neither purely elastic nor purely viscous, but behaviour in between that can be defined as viscoelastic behaviour (Lundstrom, 2002). This behaviour can be seen at intermediate temperatures and frequencies. Bituminous materials exhibit linear viscoelastic (LVE) mechanical behaviour (Di Benedetto and Corte, 2005). LVE materials obey the Boltzmann superposition principle (Boltzmann, 1876). Therefore, the total response of a material to a superposition of different loads is equal to the superposition of individual responses to each load (Salençon, 2009).

Recalling the effect of temperature and frequency factors on LVE behaviour, the equivalence effect of both factors on the material behaviour allows applying Time-Temperature Superposition Principle TTSP (Basueny, 2016). TTSP allows using the isothermal curves (plot in logarithmic scale between the norm of the complex modulus ($|E^*|$) and the corresponding test frequencies, for each test temperature of the complex modulus to obtain unique $|E^*|$ and phase angle ($\varphi$) curves at an arbitrarily chosen reference temperature $T_{ref}$. This curve is called master curve. This procedure consists of shifting the isothermal curves along the horizontal frequency axis to superpose all points having the same ordinate. Simply, the shifting of the isothermal curves is operated by multiplying the frequencies of all points of each curve by the so-called shift factor $a_T$ which depends on the temperature of the curve to shift.

Many rheological models can be used to express the viscoelastic behaviour of the bituminous materials such as Maxwell, Kelvin-Voigt and 2S2P1D model. These rheological models can be described as a combination of basic elements like elastic spring and viscous dashpot that obey Hook's and Newton's law, respectively. These elements can be linked in series (Maxwell model) or parallel (Kelvin-Voigt model). The two models, Maxwell and Kelvin-Voigt, are considered as the simplest models. From a practical perspective, these models cannot express correctly the complex behaviour of bitumen, mastic and HMA in the LVE domain (Orald and Di Benedetto, 2003). The 2S2P1D model is frequently selected to describe the LVE behaviour of the bituminous materials since it translates this behaviour correctly (Orald and Di Benedetto, 2003; Delaporte et al., 2007). Figure 2.3 shows the representation of the 2S2P1D model for the HMA.

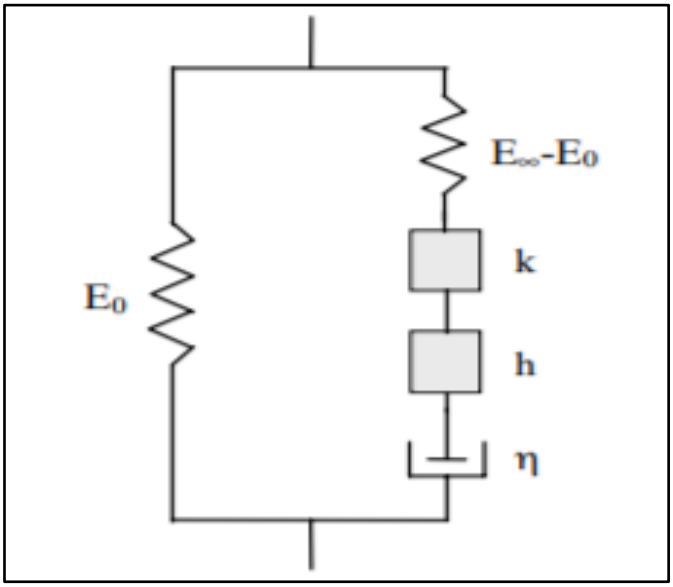


Figure 2.3 2S2P1D model representation for HMA
Taken from Di Benedetto et al. (2004)

At a given temperature, the complex modulus of the 2S2P1D model can be expressed by the following equation (Olard et al. 2003):

$$E^*_{2S2P1D}(\omega) = E_0 + \frac{E_{00} - E_0}{1 + \delta(i\omega\tau_E)^{-k} + (i\omega\tau_E)^{-h} + (i\omega\beta\tau_E)^{-1}} \quad (2.1)$$

where i is complex number defined by $i^2$ = -1, $E_0$ is the glassy modulus when ( $\omega \rightarrow 0$), $E_{00}$ is the static modulus when ( $\omega \rightarrow \infty$), ω is the pulsation (equal to $2\pi f_r$ ), $f_r$ is frequency, δ (delta) is constant, β is dimension constant linked with the Newtonian viscosity η ($\eta = (E_0 - E_{00}) * \beta * \tau_E$), and h and k are the parameters of the parabolic elements of the model ($0 < k < h < 1$). $\tau_E$is characteristic time, which varies only with the temperature. The changing of $\tau_E$ by the temperature can be explained by means of the $a_T$ if the TTSP holds as shown in Eq. 2.2.

$$\tau_E(T) = a_T(T) * \tau_{0E} \tag{2.2}$$

where $a_T$ (T) is the shift factor at temperature T and $\tau_{0E} = \tau(T_{ref})$ at reference temperature $T_{ref}$. Only seven parameters ($E_{00}$, $E_0$, δ, k, h, β, and $\tau_E$) of the 2S2P1D formula are needed to analyze the linear viscoelastic behaviour of the tested material at a given temperature. The progression of $\tau_E$ was determined by the William-Landel-Ferry (WLF) equation (Olard & Di Benedetto, 2003). When the temperature effect is determined, the number of the parameters becomes nine, including the two WLF constants (C1 and C2) which are determined at the $T_{ref}$ (Eq. 2.3).

$$log(a_T) = \frac{-C1\ (T - T_{ref})}{C2 + (T - T_{ref})} \tag{2.3}$$

where C1 and C2 are constants varying with the material and $T_{ref}$. T, $T_{ref}$ and $a_T$ are explained above.

### 2.3.2 Thermomechanical tests of the bituminous materials

This section presents the thermomechanical tests that are related to the different behaviours and performance of HMA and bitumen (Figure 2.2). In particular, tests to describe the LVE behaviour, fatigue cracking resistance, high and low temperature performance and water damage tests.

#### 2.3.2.1 Test related to LVE behaviour

The evaluation of the mechanical behaviour of bitumen and HMA, bituminous materials, in the LVE domain can be done by performing the shear complex modulus (G*) and complex modulus (E*) tests, respectively. The main concept of these two tests is similar. In general, from the measurement of a dynamic oscillation, G* or E* are defined as the ratio calculated by dividing the stress (absolute value of the peak-to-peak) by the strain (absolute value of the peak-to-peak). This ratio represents the stiffness of the bituminous materials. These tests allow determining the rheological properties of the bituminous materials at a wide range of temperatures and frequencies.

Different types of tests exist to evaluate the LVE behaviour of bituminous materials. This research program focuses on tension-compression test for HMA. Figure 2.4 shows the setup of tension-compression test on a cylindrical specimen for complex modulus. During this test, a sinusoidal oscillating axial load is applied on the specimen. The axial deformation is measured by three on-specimen extensometers spaced 120° apart and connected by springs around the middle of the specimen. The sequence of temperatures starts from the lowest to the highest. A 4-hour conditioning period is mandated to ensure uniform temperature within the specimen whenever the testing temperature is altered. At each temperature, in order to reach constant variation of strain, stress is applied to the different target frequencies starting from the fastest to the slowest. Rest period, approximately 120 seconds, is considered each time the frequency is changed (Basueny, 2016).

The data collected from the test is employed to study the properties of the tested specimen. The force, axial deformation from each extensometer and the temperature recorded by the probe are collected at each data acquisition (two consecutive cycles). Herein, it is important to check the quality of the signal during the test. The quality index (QI) that represents the gap between the experimental points and the sinusoidal function can be used. According to QI values, the test is considered ideal (QI is less than 10 %) or acceptable (QI is less than 15 %) (Basueny,

2016). Particularly, this applies to stress and strain signals measured by the extensometers which are the equipment used to control the test.

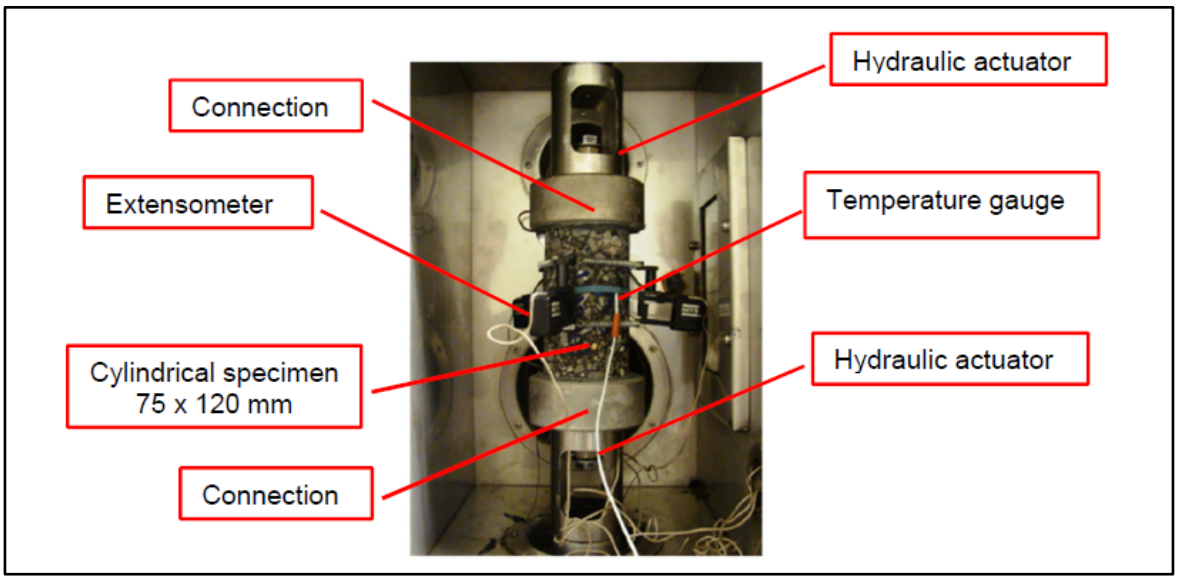


Figure 2.4 Tension-compression test setup for complex modulus
Taken from Basueny (2016)

The collected data from the test is processed and results presented to be analyzed, leading to the evaluation of the bituminous materials behaviour within the LVE domain. Many graphical representations of complex modulus test results can be displayed such as Cole-Cole diagram (Figure 2.5), master curves of the norm of complex modulus |E*| (Figure 2.6) and phase angle φ (Figure 2.7). The Cole-Cole plot is a graph obtained between the storage modulus E1 (real axis, X-axis), which represents the elastic aspect of the E*, and the loss modulus E2 (imaginary axis, Y-axis), which represents the viscous aspect of the E*.

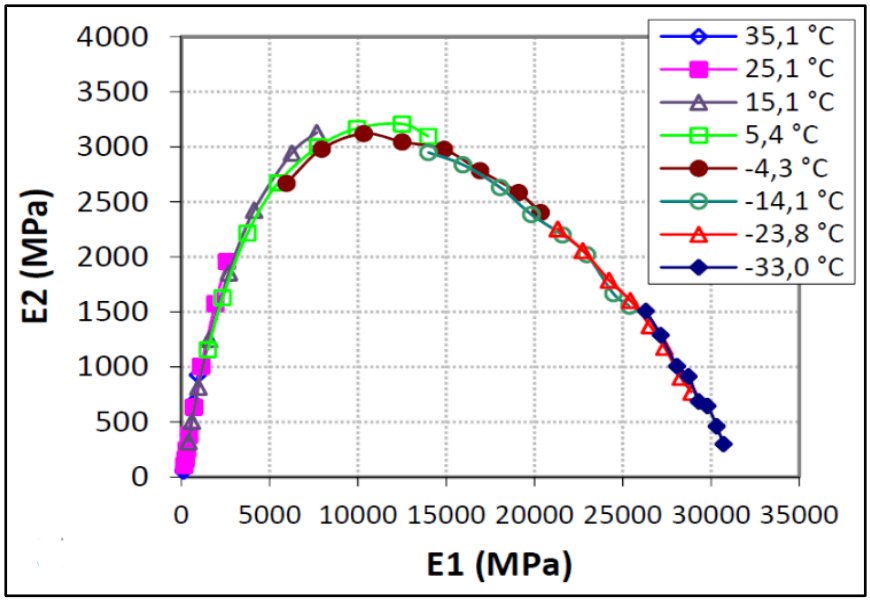


Figure 2.5 Example of the Cole-Cole diagram for HMA
Taken from Basueny (2016)

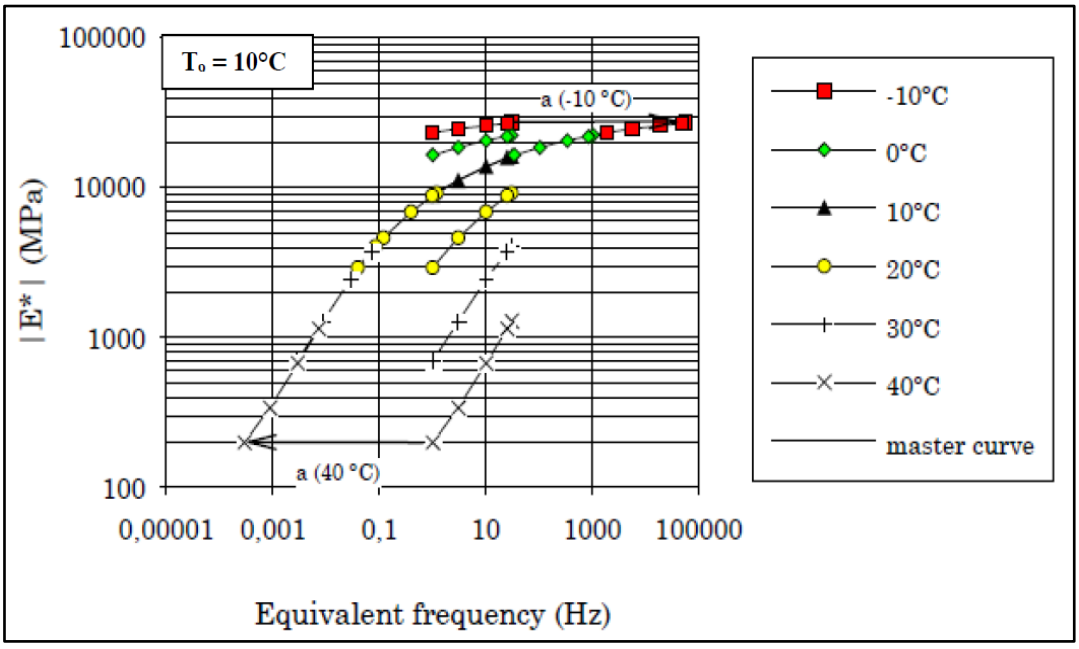


Figure 2.6 Example of the master curve of the norm of complex modulus |E*| for HMA
Taken from Di Benedetto & De La Roche (1998)

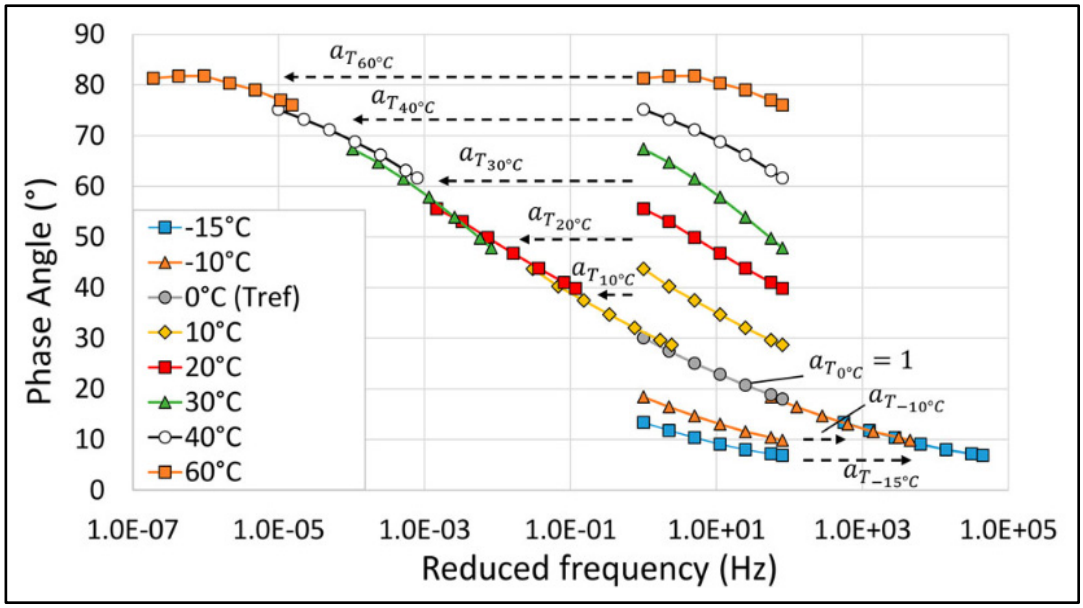


Figure 2.7 Example of the master curve of the phase angle φ for HMA
Taken from Siroma et al. (2021)

The complex modulus represents the stiffness of the tested materials at a given temperature and frequency. When the asphalt material is loaded a high number of times, this stiffness will change. Because of that, it is common to use the change of complex modulus as a measure of the fatigue resistance of the materials.

#### 2.3.2.2 Fatigue behaviour

The fatigue phenomenon is defined as a reduction in the strength and/or stiffness (material properties) of the HMA, eventually leading to failure, caused by the repetition of small strain loads with (Lundstrom, 2002; Iliuta et al., 2004; Di Benedetto & Corté, 2005; Moghaddam et al., 2011; Mangiafico et al., 2014). Also, the fatigue of HMA leads to the appearance of surface fatigue cracking (Al-Qadi & Nassar, 2003).

For the evaluation of the fatigue behaviour of HMA, a fatigue test is performed at one temperature and one frequency, usually around 10 °C and 10 Hz (Basueny, 2016). Different strain amplitudes should be chosen in order to develop the Wöhler curve which is a plot with a linear regression in log-log scale that represents values of fatigue life (number of loading

cycles) and corresponding strain amplitude obtained for each tested specimen (Wöhler, 1870; Di Benedetto et al., 2004; Mangiafico, 2014). The fatigue behaviour of HMA can be evaluated by performing bending tests (two-, three- and four-points), indirect tensile test) and cyclic tension-compression test (Di Benedetto et al., 2004). The main advantage of cyclic tension-compression test is that it is a homogeneous test. So, the modulus at each loading cycle can be directly determined (Mangiafico et al., 2014).

A uniaxial tension-compression test can be considered as a suitable way to predict the design life of the pavement structure in terms of $\varepsilon_6$ (strain amplitude at one million cycles). During the fatigue test, the material properties undergo a progressive deterioration which is considered as the effect of the repeated loading (number of cycles). In fatigue tests, the evolution of the |E*| as a function of the number of cycles (N) can be observed and three phases (Figure 2.8) can be distinguished (Lamothe, 2014; Mangiafico, 2014; Basueny, 2016):

- Phase I (adaption phase): |E*| decreases rapidly due to mostly the biasing effects: the non-linearity of the behaviour of the mix, the self-heating of the material and the thixotropy of the bitumen. Because of the internal structure of the asphalt mixture, the binder located within inter-aggregate voids can be subjected to higher strain amplitudes than the overall strain of the mix. Thus, the mix can exhibit non-linear behaviour. The self-heating bias effect is due to the increase of the temperature when the repeated loading is subjected to the mix. The recovery of the original viscosity is called thixotropy. Applying a finite shear to a material system after a long time of rest may cause a viscosity reduction. During this phase, fatigue damage does not seem to have a major role in the evolution of the material properties;

- Phase II (quasi-stationary): |E*| shows a slow and quasi-linear decrease. The fatigue damage contributes to the deterioration of the material properties. Besides the fatigue damage, the biasing effects (self-heating and thixotropy) are still present and need to be considered despite the fact that their influence is less important compared to phase II;

- Phase III (failure): |E*| decreases rapidly and the material shows a failure due to the propagation of the microcracks and their transformation to the macro-cracks. Therefore, the use of the continuum mechanics assumption (quantifying the damage of the material by fatigue from the measurement of the stiffness of the material) is not valid anymore and the test can no longer be interpreted. In addition, the LVE properties cannot be determined.

The two most commonly criteria that are employed to develop the Wöhler curve are classical ($N_{f50\%}$) and local ($N_{fII\text{-}III}$) criteria (Di Benedetto et al., 2004). $N_{f50\%}$ is the number of cycles corresponding to the loss of 50 % of the initial norm of complex modulus $|E^*_0|$ (Figure 2.8). $N_{f50\%}$ criterion is criticized by the majority of the researchers and the choice of the reduction percentage (50 %) of the |E*| is arbitrary (Di Benedetto et al., 2004; Di Benedetto et al., 1996; Kim et al., 1997).

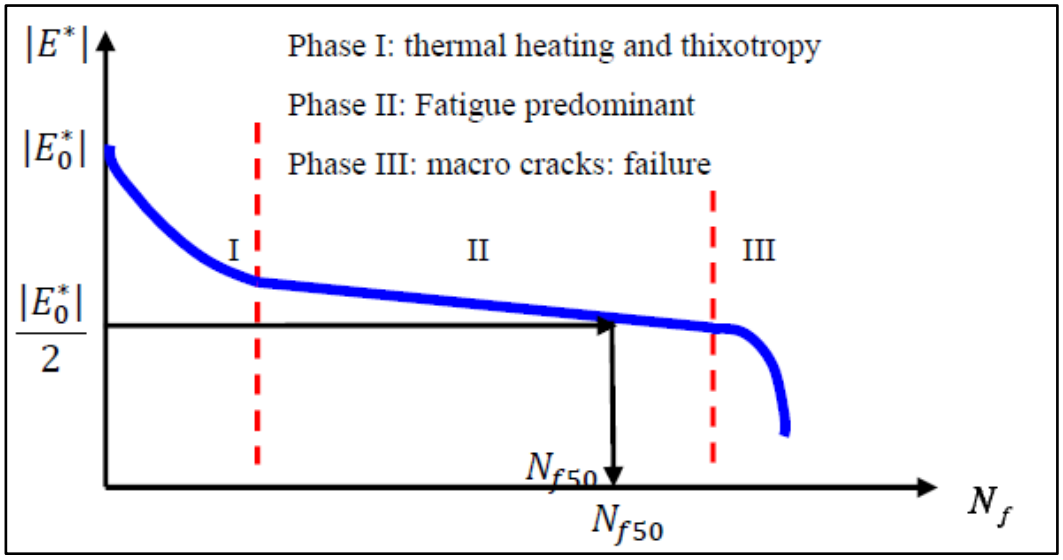


Figure 2.8 Evolution of the curve of |E*| as a function of N and its phases and definition of the classical criteria $N_{f50\%}$
Taken from Basueny (2016)

$N_{fII\text{-}III}$ is the number of cycles corresponding to the transition between phase II and III. $N_{fII\text{-}III}$ is considered as a representative specimen failure since it is the propagation of the microcracks and, therefore, disturbing the homogeneity of the strain field of the specimen (Ashayer Soltani, 1998; Baaj, 2002). $N_{fII\text{-}III}$ can be determined based on the average of many values such as $N_{f\Delta\varepsilon ax}$

and $N_{f\Delta\phi}$ (Mangiafico, 2014). $N_{f\Delta\varepsilon ax}$ (Figure 2.9 a) is the number of cycles that indicates a difference of more than 25 % between the deformation (non-homogeneous test) of one of the extensometers compared to the average value of the three extensometers. $N_{f\Delta\phi}$ (Figure 2.9 b) is the number of cycles that indicates a deviation of more than 5° of the phase angle (non-homogeneous test) for one of the extensometers compared to the average value of the three extensometers.

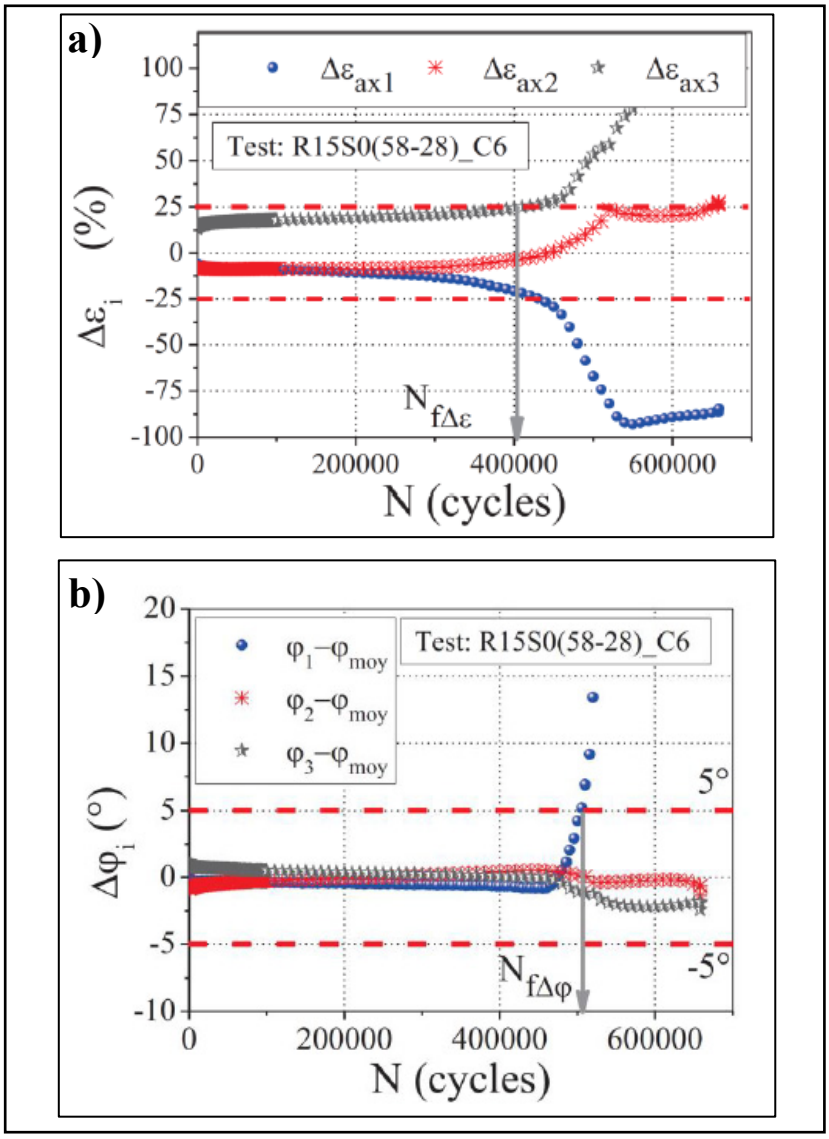


Figure 2.9 Example of estimation of NfΔεax (a, top) and $N_{f\Delta\phi}$ (b, bottom) for a tension-compression fatigue test performed on a cylindrical specimen of HMA
Taken from Mangiafico (2014)

#### 2.3.2.3 Tests related to the high temperature performance

The bituminous materials undergo softening at high temperature, leading to reduced stiffness and increased flowability. This can contribute to the permanent deformation of the asphalt pavement under repeated cycles of the traffic loading. More specifically, at high temperature, bituminous materials become more viscous, and their elastic properties diminish. Consequently, bituminous materials become more susceptible to deformation with the repetition of traffic loading. The combination of both effects, high temperature and repeated loading, can cause the bituminous materials to undergo cumulative permanent deformation, leading to rutting over time. Accordingly, rutting (permanent deformation) is defined as a progressive accumulation of the permanent viscoplastic deformation in the wheel path which is caused by the repetition of the traffic loading (Abdulshafi, 1988; Tayfur et al., 2007). The thermomechanical performance of bituminous materials at high temperature is evaluated by the resistance to the permanent deformation (rutting). Many factors affect the rut depth such as speed and axle load of vehicles, HMA thickness and properties and temperature. Therefore, it is difficult to find a specific equation that evaluates the rutting performance (Moghaddam et al., 2011). However, the Esso model that was developed for Hamburg wheel tracking device (HWTD) can be employed in the evaluation of the rutting performance (Romero & Stuart, 1998). Figure 2.10 Shows the evolution of the rut depth with the number of loading cycles that is obtained by using French laboratory rut tester (FLRT). In the first phase, the beginning of pavement life, the relationship between the rut depth and number of loading cycles is non-linear, as illustrated in Figure 2.10. This trend alters into a linear relationship, representing the second phase. For the conventional HMA, the rut depth increases remarkably with number of loading cycles (first phase) which can refer to the compaction process due to the axle load of vehicles. Following, second phase, the rate of the rut depth decreases.

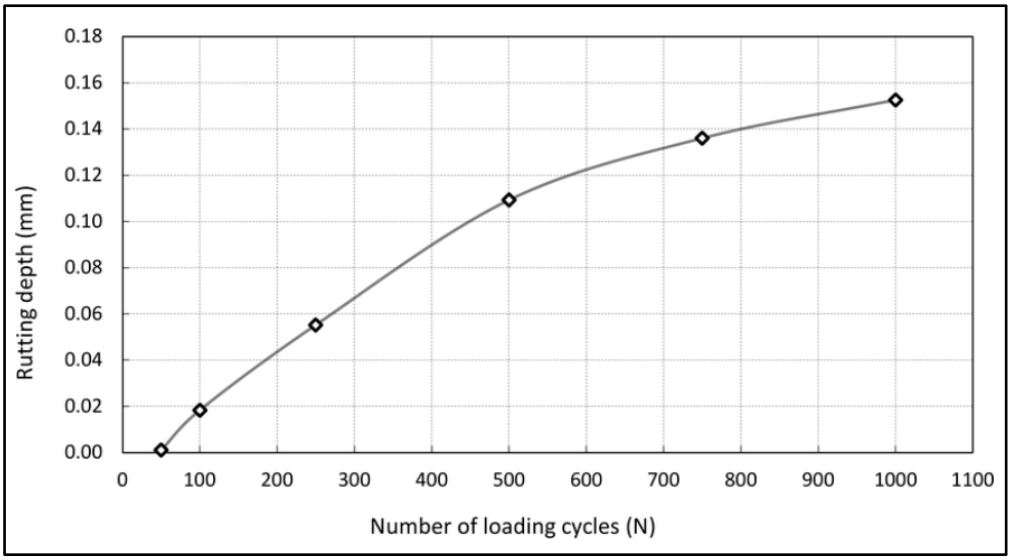


Figure 2.10 Evolution of the rut depth with number of loading cycles
Taken from Leonardi (2015)

However, the permanent deformation of the asphalt pavement is not only linked to the deformation of the HMA layer, but also to the granular and subgrade layers. Accordingly, three different types of rutting can be generally considered (Emery, 2005). These are wear rutting, viscoplastic deformation and structural rutting. The wear rutting of the HMA layer is a result of wear in the wheel path. The viscoplastic deformation is associated with the densification (compaction) and/or shear of the HMA in the wheel path. This deformation is directly linked to the mix design of HMA and it causes either dilatation or densification of HMA (Dongmo-Engeland, 2005; Olard & Di Benedetto, 2005a; Ossa & Collop, 2006; Di Benedetto et al., 2007a). The structural rutting is accompanied with a general subsidence of the bottom layers, granular and subgrade, of the asphalt pavement (Dongmo-Engeland, 2005).

In general, wheel-tracking tests (WTT) can be employed to evaluate the rutting performance of HMA. The French wheel tracking tester (FWTT), accelerated pavement testing (APT) and HWTD are some of the different types of tests that have been developed to measure the rut depth at the surface of the HMA layer (Olard & Di Benedetto, 2005a; Ossa & Collop, 2006).

For the bitumen, the dynamic shear rheometer (DSR) and multiple stress creep recovery (MSCR) tests can be employed to evaluate the performance at high temperature (rutting performance). However, these bitumen tests results are just indicators of the rutting performance, so it is still important to perform tests on mixtures in order to obtain the full evaluation of the rutting performance. From the DSR test, the norm of the shear complex modulus (|G*|), stiffness, and phase angle (δ) values can be obtained. According to strategic highway research program (SHRP), the |G*|/sin(δ) is considered as a rutting parameter (Xu et al., 2017). Performing the MSCR test allows evaluating the elasticity of the bitumen by applying a series of loading and relaxation cycles. In particular, this test shows the non-recoverable part of the deformation which is so-called permanent deformation. The DSR and MSCR tests can also be used for the classification of the high temperature performance grade (PG) and traffic level, respectively. For PG classification, the high temperature of the bitumen class is determined as the temperature at which |G*|/sin(δ) is greater than 1.0 kPa for unaged bitumen and greater than 2.2 kPa for aged bitumen. This parameter indicates the material's rheological behaviour at high temperature and assesses the ability to resist rutting. Also, it provides insights into the viscoelastic nature of the material and how it performs under high-temperature loading conditions.

#### 2.3.2.4 Tests related to the low temperature performance

Bituminous materials undergo significant changes in their properties at low temperature. The behaviour of bituminous materials at low temperature is crucial for the asphalt pavement performance. More specifically, the ability of bituminous materials to resist cracking and maintain their structural integrity is affected. Particularly, the bituminous materials tend to become less ductile at low temperature, making them more prone to cracking. As temperature decreases, these materials become increasingly brittle. The transition from a ductile to a brittle state is characterized by an increase in the likelihood of cracking and a reduction in flexibility. In this regard, bituminous materials must have sufficient flexibility to resist the tensile stresses induced by the temperature fluctuations. If these materials become too brittle, they may crack

under these stresses. To this end, the performance at low temperature is evaluated by the resistance to the thermal cracking (Jung & Vinson, 1994).

The TSRST is used to evaluate the low temperature performance of HMA (Tapsoba et al., 2016). This test involves placing a cylindrical specimen of HMA in an enclosure at which the temperature is controlled. The specimen should be well glued with two fixed ends. At the beginning of the test, the temperature inside the thermal chamber starts to decrease at a constant rate and the HMA specimen tries to shrink while it is prohibited from the longitudinal contraction. At this point, the thermal stresses start to increase within the HMA specimen and these stresses intensify with the progression of the cooling process. When the induced thermal stress due to the restrained longitudinal contraction exceeds the tensile strength of the HMA, the specimen breaks. Figure 2.11 shows an example of the stress-temperature curve of TSRST test on HMA specimen that represents the evolution of the thermal stress with temperature. It can be seen that the corresponding value of the failure point (breakage of the specimen) on x-axis is called failure temperature which is associated with the failure strength, the corresponding value on y-axis. The failure strength is defined as the maximum thermal stress that can be carried by the specimen, and the obtained temperature at the maximum stress is defined as the failure temperature (Carter & Paradis, 2010). Another important output of the test is the glass transition temperature (Tg). It represents the end of the stress relaxation domain and the beginning of a linear relationship between the thermal stress and temperature (Badeli et al., 2018). During the relaxation stress phase, the slope of the stress-temperature curve maintains relatively consistent until a certain temperature at which point the slope increases remarkably and the stress-temperature curve becomes linear. In most of the analysis, Tg can be assumed the temperature that corresponds to the determined stress at 50 % of the failure strength (Tapsoba et al., 2016). Therefore, Tg corresponds to the temperature that describes the change in the behaviour of the material, from brittle to ductile or vice versa. Also, it can be used to characterize the rheological behaviour of HMA at low temperatures and in the evaluation of the repeatability of the TSRST test (Jung & Vinson, 1994).

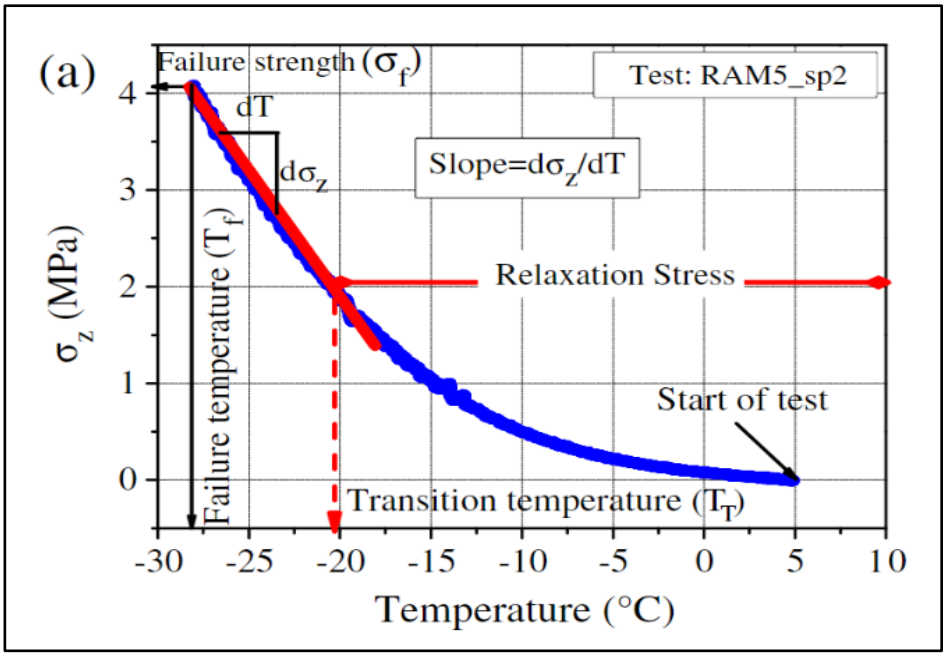


Figure 2.11 Stress-temperature curve of TSRST test on HMA specimen
Taken from Tapsoba et al. (2016)

For the bitumen, the bending beam rheometer (BBR) test can be employed to evaluate the performance at low temperature. Through the outputs of this test, the low temperature performance of HMA can be predicted. The stiffness and relaxation (slope) parameters, outputs of the test, are used to describe the resistance of the bitumen to the thermal cracking. In this test, a load is applied to the center of a rectangular beam of bitumen. Based on the measured deflection against time, the stiffness is calculated, and the relaxation properties describe how the bitumen dissipates the induced thermal stresses. However, this test can also be used for the low temperature PG classification.

The presence of low temperature cracks on the surface of the HMA layer allows water to penetrate the asphalt pavement layers. In cold regions (e.g. Canada), due to the temperature oscillation, the freeze and thaw cycles of the water can cause serious damage to the asphalt pavement system (Badeli et al., 2018).

#### 2.3.2.5 Water damage tests

The resistance of HMA to the moisture damage can be evaluated by the moisture sensitivity and moisture-induced damage tests (Shatnawi et al., 1995; Pinzón & Such, 2004; Júnior et al., 2019; Soenen et al., 2020). The chemistry of the asphalt binder, aggregate mineralogy and texture and the interaction between both components are the main factors that affect the moisture damage of HMA (Solaimanian et al., 2006). Two main mechanisms are responsible for the degradation of HMA through the moisture damage: loss of adhesion bond between the aggregate and asphalt binder and loss of cohesion within the asphalt binder (Terrel & Al-Swailmi, 1992). In particular, the loss of adhesion mechanism refers to the degradation of the asphalt binder-aggregate bond which occurs due to the very thin film of mastic, asphalt binder and filler, and the presence of the moisture that enters the pore structure (i.e. air voids) of HMA (Lytton, 2004; Copeland, 2007). On the other hand, the loss of cohesion mechanism refers to the infiltration and the action of the moisture within the mastic or bitumen, and the very thick film of mastic helps this mechanism to occur (Kennedy et al., 1984; Lytton, 2004). However, Caro et al. (2008) stated that the loss of adhesion is more responsible, compared to the cohesion loss, for the moisture distress of an asphalt pavement. To this end, these two mechanisms can lead to the loss of strength and reduction in the durability of HMA.

Many reasons can cause the loss of the adhesion and cohesion such as weather conditions, aggregate gradation, water absorption, heavy traffic loads and aggregate-mastic compatibility (Goh & You, 2012). Bausano et al. (2006), reported four theories that can explain the characteristics of adhesion in HMA, namely mechanical adhesion, surface energy, molecular orientation and chemical reaction. Also, the mechanical interlock is reported as one of the main concepts that contribute to the adhesion mechanism, as stated by Stuart, (1990). However, there is no correlation between moisture damage of HMA and the properties of aggregate (Hicks, 1991; Yoon & Tarrer, 1988).

During the moisture sensitivity and moisture-induced damage tests, the HMA specimen is subjected to different moist conditions that accelerate the deterioration of the HMA properties.

More precisely, these conditions work on weakening the ability of the bitumen to agglutinate to the aggregate surface, leading to stripping. Generally, stripping is defined as the reduction in the bonding strength that occurs due to the water infiltration into the HMA, including asphalt binder-aggregate separation (Chen & Huang, 2008; Omar et al., 2020). Following the applied moist conditions on the HMA specimens, Marshall stability and indirect tensile strength (ITS) are measured for the moisture sensitivity and moisture-induced damage tests, respectively. Accordingly, these tests can be used as indicators for the durability of the asphalt pavement (Solaimanian et al., 2003; Shamshuddin et al., 2010).

## 2.4 Most common bitumen and HMA modifiers

In general, different bitumen and HMA modifiers have been widely used to enhance the high, intermediate and low temperature performance of the bitumen and HMA while reducing the environmental impact of the pavement industry (Li et al., 2020a). In this section, the effects of the modifiers, lignin not included, will be presented. The most common modifiers are polymers. There are other modifiers such as recycled plastic, fibers, crumb rubber and cement. Despite the fact that lignin is a polymer, it is presented in a specific section (section 2.5).

### 2.4.1 Polymers

The performance of the polymer-modified bitumen (PmB) depends on the properties of the polymer and the micro-structure of PmB (Topal, 2010). The polymers are usually incorporated to the preheated base bitumen at 160-180 °C for 2-4 hours with a speed of 4000-5000 rpm by using high shear mixer (HSM) (Zoorob et al., 2018; Jelčić et al., 2017). The principle of the HSM is to create flow and shear by rotating a high-speed rotor. This rotor is powered by an electric motor. The rotation of the rotor draws upwards movement of the liquid (bitumen) and solid materials (additive) from the bottom of the vessel into the workhead center of the incorporation zone. Because of this movement, a generated centrifugal force drives the materials towards the workhead where a milling action is applied on these materials. This milling process occurs between the inner wall of the stator and the ends of the rotor. Moreover, the speed of the materials (bitumen and lignin powder or pellets) at the inner wall of the stator

and the ends of the rotor is different. This difference in the speed creates shear. At this point, the intensive shear and movement force the materials, at high speed, to go out of the stator through the perforations and then circulated into the incorporation high-shear zone (within the stator). Keeping the same pattern, many cycles are required to obtain well-incorporated materials. However, many key design factors govern the incorporation process such as the time in the mixer, the rotational speed of the rotor and its diameter and the distance between the stator and the rotor. The opening width of the perforations, their angle and the number of rows that contain the perforations, are considered as variables (Banaszek, 2009; IKA laboratory equipment, 2009; Czerwinski & Birsan, 2017).

Different types of polymers can be incorporated into the bitumen such as styrene-butadiene-styrene (SBS), the most common one (Lu & Isacsson, 1997), styrene-butadiene rubber (SBR), ethylene-vinyl acetate (EVA), and polyphosphoric acid (PPA) (Behnood and Olek, 2017). As long as the polymer content is low (less than 3 %), a continuous phase of bitumen with dispersed particles of polymer can be seen, leading to stable and homogeneous PmB (Topal, 2010). While the use of higher polymer content (5-7 %) leads to a continuous matrix of polymer with dispersed globules of bitumen which negatively affects the storage stability and homogeneity of PmB (Lu & Isacsson, 2000). In other words, the compatibility of the polymer with bitumen is poor and the modification of the bitumen is futile (Zhu et al., 2014). Increasing the incorporation temperature is not beneficial to get stable modified bitumen with high polymer contents (Topal, 2010). Adding PPA could improve the compatibility of bitumen with polymers by changing the bitumen structure from sol (low viscosity) to gel (high viscosity).

Modified bitumen with 2-4 % of SBS, 4-8 % of SBR, 3-7 % of EVA, and 0.3-1.2 % of PPA showed an improvement on the resistance to the permanent deformation (rutting) at high temperature (Behnood and Olek, 2017; Mostafa and Mahmoud, 2018; Zoorob et al., 2018). For the performance at the intermediate and low temperatures, it was stated that the effect is not significant (Zoorob et al., 2018). While the modified bitumen with 8-16 % of grounded tire rubber GTR showed a significant decrease of the stiffness of the bitumen. By performing DSR and MSCR tests, adding 6 % of SBR latex and styrene-ethylene–butylene-styrene SEBS

copolymer and 8 % of chloroprene rubber CR latex improved the rutting performance at high temperature (Jiang et al., 2018). Generally speaking, the use of polymers increased the high and low temperatures of the bitumen PG, including improvement on the temperature susceptibility of the bitumen (Jelčić et al., 2017). In addition, according to the MSCR tests results, PmB showed higher elasticity than the unmodified bitumen, including better performance at high temperature, which encourages the use of polymers with the bitumen (Mostafa and Mahmoud, 2018).

### 2.4.2 Recycled plastic

Using 1.5-4.5 % of low-density polyethylene (LDPE) and 1-3 % of high-density polyethylene (HDPE) and Polypropylene (PP) improved the moisture sensitivity, fracture toughness, indirect tensile strength (ITS) and compressive strength of HMA, and they also enhanced the physical characteristics by reducing the penetration and ductility accompanied with an increase in the softening point and viscosity (Othman, 2010; Prasad, 2012; Nasir et al., 2014). In addition, they increased the rutting resistance, creep and resilient modulus at high temperature. At low temperature (below -10 °C), the stiffness of HMA was increased (Attaelmanan et al., 2011; Prasad, 2012; Abdullah et al., 2017). For the performance at intermediate temperature, it was stated that the cross-linked polyethylene PEX improved the fatigue cracking resistance (Costa et al., 2017). Azam et al., 2019 and Liu et al., 2019 stated that the use of polymer products and wax improved the Marshall stability, cohesion and freeze-thaw resistance of HMA in cold weather. Moreover, the overall performance of modified HMA with Recycled Plastic Waste Aggregate (RPWA) was improved (Abas and Abass, 2014).

### 2.4.3 Fibers and crumb rubber

Rubberized HMA can be produced using a wet or dry mixing process. In the wet process, tire rubber is added to a heated virgin bitumen before mixing with the aggregates, while in the dry process tire rubber is added directly with the aggregates in the mixing step of HMA production (Bairgi, 2015). Crumb rubber of 2.0 to 6.3 mm is mixed with the aggregates (usually within a range of 1 to 3 % by the total weight of the mix) before adding the asphalt binder (Cheriet et

al., 2021). Tire rubber can be considered as a part of the bitumen or the aggregates. The gradation of the tire rubber used in the dry process is coarser than the gradation of the tire rubber used in the wet process. In this case, the tire rubber is considered as aggregates in HMA (Bairgi, 2015).

The modified HMA with fibers and 5-20 % of crumb rubber improved the performance by increasing Marshall stability, tensile strength and the resistance to the permanent deformation and abrasion (Ziari et al., 2016; Kumar and Mahendran, 2014; Ferrotti et al., 2014; Al Qudah et al., 2018; Al-Azawee and Qasim, 2018; Irfan et al., 2018; Msallam and Asi, 2018; Bakheit and Xiaoming, 2019). Using fibers as a bitumen modifier in the production of cold mix asphalt (CMA) has demonstrated its efficacy when compared to HMA (Shanbara et al., 2018). It improved the indirect tensile stiffness, moisture damage and the resistance to the cracking and permanent deformation. Merging of fibers and crumb rubber in the asphalt mixtures containing Reclaimed Asphalt Pavement (RAP) showed higher Indirect Tensile Strength (ITS). Also, merging of crumb rubber, epolene EE-2 and date palm ash DPA improved the rheological characteristics and the performance of the asphalt pavement at high temperature and under heavy traffic loading (Khan et al., 2019). However, it was found that and the HMA modified with SBS and PmB showed higher Marshall stability in comparison with the modified HMA with fibres (Eskandarsefat et al., 2019). This means that these HMAs are less likely to lose their structural integrity when exposed to water.

### 2.4.4 Cement and other modifiers

Iwański and Chomicz-Kowalska, 2013 indicated that the addition of Portland cement to HMA materials increased the Marshall stability, ITS, MR and improved the resistance to the water damage. On the other hand, only 1-2 % cement content is recommended in HMA due to the increase in the brittleness of HMA and its strong negative impact on the environment (Fang, 2016). Moreover, some researchers stated that the addition of cement is critical for the development of the strength of emulsion asphalt since it accelerates the breaking of the emulsion and it behaves as a secondary binder after the hydration process (Fang et al., 2016).

In addition, using cement with lime showed an improvement on the volumetric properties of the HMA (Babagoli et al., 2016). Also, they increased the resistance to permanent deformation. Anyway, using other modifiers such as nano-clay and nano-lime highlighted the effects on the performance grade PG of the bitumen and increased the stiffness of the HMA, especially at high temperatures (Ghanoon et al., 2020). Regarding the stiffness parameter, using Construction and Demolition Waste (CDW), as recycled waste materials, instead of the natural aggregates increased the stiffness of the HMA (Gómez-Meijide et al., 2016).

## 2.5 Lignin

The researchers are concerned about improving the performance and sustainability of HMA. This can be achieved by using additives. These additives change the HMA properties and enhance its durability. Bio-derived materials, such as lignin, can be used with HMA. In general, lignin has a complex chemical structure and its properties depend on the extraction process (Kun and Pukánszky, 2017). In particular, lignin is a three-dimensional, highly cross-linked macromolecule that is composed of three kinds of substituted phenols: sinapyl, coniferyl, and p-coumaryl alcohols (Watkins et al., 2015). This structure is formed by the enzymatic polymerization process which allows producing huge number of functional groups and linkages. One of the factors that affect the lignin properties is the raw material (original source).

There are different types of lignin such as lignosulfonate, soda-anthraquinone, organosolv, ethanol process, and Kraft lignins. These lignins can be characterized by a functional group's analysis, elemental analysis, Mannich reactivity, molecular weight distribution and other techniques (El Mansouri and Salvadó, 2006). However, the chemical and physical behaviour of the lignin vary according to the extraction method used and the original source of the lignin. Lignin is the second most abundant natural polymer, while cellulose is ranked first (Watkins et al., 2015). Lignin makes up to 10–25% of lignocellulosic biomass (Watkins et al., 2015). In addition, lignocellulosic biomass was acknowledged for potential use in the production of chemicals and biomaterials due to its reaction with the component of these materials and products.

There are many different sources of lignin extracted from wood cellulosic biomass such as wood pulp and cotton (Figure 2.12). Also, lignin can be extracted from non-wood cellulosic biomass (wheat straw, pine straw, flax fiber and alfalfa fiber) by formic acid treatment followed by peroxyformic acid treatment (Figure 2.13). These kinds of treatment affect the chemical composition and the thermal properties of the produced lignin (Watkins et al., 2015). Using of Fourier transform infrared spectroscopy (FTIR) and thermogravimetric analysis (TGA), respectively, can be used to determine the effects of the treatment process of each source of lignin (Watkins et al., 2015). For example, the lignin extracted from the wheat straw and flax fiber shows the greatest thermal stability among the other sources.

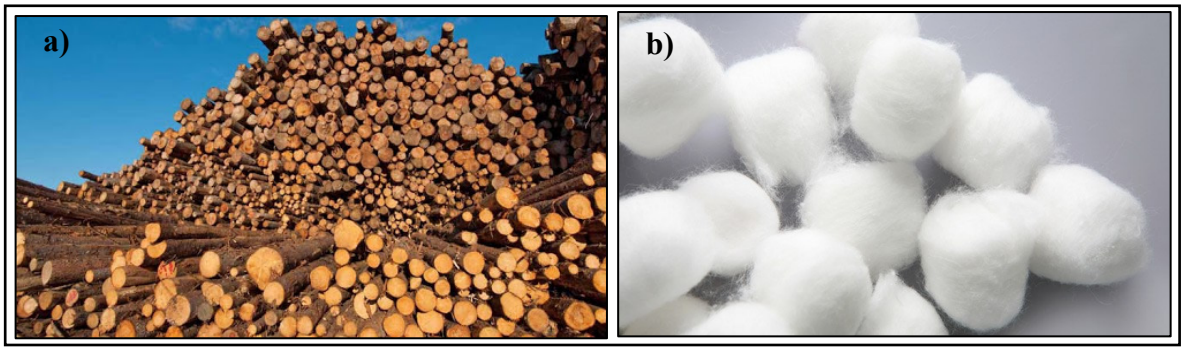


Figure 2.12 Extraction sources of lignin from wood cellulosic biomass: a) wood pulp, b) cotton
Taken from Watkins et al. (2015)


Figure 2.13 Extraction sources of lignin from non-wood cellulosic biomass:
a) Wheat straw, b) Pine straw, c) Flax fiber, d) Alfalfa fiber
Taken from Watkins et al. (2015)

The produced lignin from the presented extraction sources, wood and non-wood cellulosic biomass, are in the powder form. Accordingly, many problems are expected to appear such as safety issues, health risks and air pollution due to the dust and emissions to the atmosphere. Nowadays, many organizations are concerned with the environmental problems. Therefore, the attention is directed towards mitigating the impacts of these problems on the environment by searching for alternative solutions. One of these alternatives is the use of the biomass (García, 2012; Nunes et al., 2014). In addition to the environmental benefits, substantial socio-economic ones can be obtained from the use of the biomass (Miranda et al., 2015). More precisely, the biomass that is used as an energy source can be utilized to compress the raw materials with homogeneous properties and size.

Pelletizing technique is the most common one among the other available techniques that are used to compress the raw materials (Poddar et al., 2014). In this technique, different types of oil or bark can be used to compress the raw materials of certain industries (Filbakk et al., 2011). Many factors govern the properties of the pellets, especially the durability, such as the proportions of the raw material and oil or back, moisture content and treatment conditions. However, this thesis focuses only on the Kraft lignin in both forms, powder and pellets. More details about these materials are presented in chapter 3 (section 3.2.1 and 3.2.2).

### 2.5.1 Effects of the lignin on the performance of the bitumen and HMA

The use of lignin with bitumen is possible (Al-falahat et al., 2023), and lignin can be introduced as a bitumen modifier, extender or replacement (Gaudenzi et al., 2023). Thus, it is expected that lignin could become a common renewable source to be used in asphalt mixture production. It is worth mentioning that the chemical structure of the bitumen and lignin is similar since both are primarily carbon-based materials (Watkins et al., 2015; Boeriu et al., 2014). According to the literature (Wu et al., 2021; Yu et al., 2021; Xie et al., 2019), it is possible to have a stable lignin-modified bitumen and the lignin can be well dispersed. As well, the storage stability test can be employed to check the stability of the modified bitumen. Anyway, if some segregation is noticed, a simple mixing is sufficient to put the lignin back in suspension (Pérez et al., 2019; Norgbey et al., 2020). To this end, it is very important to check the stability of lignin-modified bitumen in order to obtain representative results.

At very high temperatures, using lignin increases the viscosity (η) of bitumen, mainly at 135 °C (Batista et al., 2018). However, Norgbey et al. (2020) mentioned that the effect of lignin on the viscosity of bitumen is limited when used in small amounts (up to 10 %). Nonetheless, according to Wu et al. (2021), the mixing and compaction temperatures that are required for the Superpave gyratory compaction (SGC) test for HMA need to be increased by over 10 °C. However, bio-oils such as soybean oil or tall oil can be used in order to reduce the viscosity of HMA (Fini et al., 2010; You et al., 2011; Fini et al., 2013; Mills-Beale et al., 2014; Guduru et

al., 2021). Li et al. (2020b) showed the effectiveness of the use of waste cooking oil as a rejuvenator to restore the properties of the HMA.

At high temperatures, the addition of Kraft lignin tends to improve the performance of the bitumen. In particular, lignin improved the rutting resistance of the bitumen (Ren et al., 2021; Zhang et al., 2022). Nevertheless, according to Fu et al. (2021), incorporating an appropriate percentage of lignin (12 %) will reduce the softening point (SP) of the bitumen. It should be noted that the pH value of the lignin used in this study is 6.9-8.0 which means base lignin and this might explain this finding. Others have shown a significant improvement on the elastic recovery due to the addition of organosolv lignin and bio-oil to the bitumen, while the creep compliance was decreased (Zhang et al., 2022). Lignin also improved the resistance of bitumen to permanent deformation (Gordobil et al., 2015; Xie et al., 2017; Batista et al., 2018; Zarei et al., 2018; Luo et al., 2019; Yue et al., 2019; Gao et al., 2020; Norgbey et al., 2020).

At intermediate temperatures, Yu et al. (2021) showed that the lignin powder (up to 10 %) improved significantly the fatigue performance of bitumen. However, Ren et al. (2021), Zhang et al. (2022), Xu et al. (2017) and Gao et al. (2020) mention the adverse effects on the fatigue performance of bitumen due to the weakness of the molecular interaction and internal friction. At low temperatures, the addition of Kraft lignin tends to reduce the resistance of bitumen and HMA to thermal cracking (Batista et al., 2018; Norgbey et al., 2020; Arafat et al., 2019; Fakhri and Norouzi, 2022). Yu et al. (2021) showed a slight reduction in the low-temperature cracking was observed with high incorporation percentage (15 % and 20 %). However, Xu et al. (2021) showed that adding 5 % of lignin to the bitumen enhanced the low temperature performance. While, Wang and Derewecki (2013) and Gao et al. (2020) stated that adding up to 10 % of lignin did not significantly affect the susceptibility of the bitumen to the low temperature thermal cracking. According to Xie et al. (2017), using 6 % of lignin in HMA improved the low temperature performance. Overall, Batista et al. (2018) and Wu et al. (2021) explained that the incorporation of lignin increased the stiffness (S) of bitumen, while the temperature susceptibility was reduced resulting in a wider thermal range of use of bitumen (difference between high and low temperature performance grade PG of bitumen).

Regarding the damage due to the presence of water, lignin increased the Marshall stability and the indirect tensile strength (ITS) for HMA. Therefore, the lignin-modified HMA has better resistance to cracking and less likely to absorb water and lose its structural integrity. Maintaining a good structural integrity can be due to a good adhesion bond between aggregates which will help to prevent or at least retard the stripping distress of HMA, leading to longer service life of the asphalt pavement (Fayzrakhmanova et al., 2016; Zarei et al., 2018; Luo et al., 2019; Pérez et al., 2019). This includes that the resistance to the water damage was improved by adding lignin to HMA (Yue et al., 2019; Pérez et al., 2020; Zhang et al., 2020). However, many agents can be utilized in order to obtain superior resistance to the water damage resulting in longer-lasting pavements. One of these agents is Morlife 5000 (Badry et al., 2021). Morlife 5000 works on the improvement of the retained strength of HMA by increasing the bond between the bitumen and aggregates.

Besides, it is important to note that from the previous studies mentioned, and according to Xu et al. (2021), the lignin does change the viscoelastic behaviour of the modified bitumen. Because of this, it can be stated that at least part of the lignin plays the role of a binder and a bitumen modifier. In this context, Hobson (2017) has shown an increase in the content of extracted binder from lignin modified mixes compared with non-modified mixes, considering lignin as a bitumen extender.

Globally, according to Pérez et al. (2019 and 2020), up to 20 % of the bitumen could be successfully replaced with lignin. The effects of the lignin addition to the bitumen are different, and they depend on many factors (for example, but not limited to, the chemical and physical properties of the lignin).

Since the production of lignin-modified HMA on the laboratory scale is possible, there is no doubt that it is also possible on the large scale, field trial section. Constructing trial sections provides substantial data to the municipalities and transportation agencies. These data can be used to improve pavement designs and material selections (Hesp et al., 2007; Hesp et al., 2009a; Rigg et al., 2017). In addition, the test methods and acceptance criteria for the bitumen

and HMA can be developed and validated (Iliuta et al., 2004; Bodley et al., 2007; Hesp et al., 2009b; Hesp et al., 2009c; Evans et al., 2011; Wright et al., 2011; Erskine et al., 2012; Paul Togunde and Hesp, 2012; Freeston et al., 2015; Holt et al., 2015). Modified asphalt pavements showed better performance at high, intermediate and low temperatures and higher resistance to the water damage (Ma et al., 2022). Moreover, the use of the modifiers reduced the maintenance cost of the asphalt pavements. In particular, the partial replacement of bitumen by lignin improved the performance of the asphalt pavements at very high, high and intermediate temperatures (Lamothe et al., 2022). Regarding the low temperature performance, no negative effects can be observed as long as the content of lignin is low.

Following the implementation of the field trial section, it is worth investigating the environmental impact of using modifiers by performing life cycle assessments (LCA). The production process of the bitumen requires a lot of energy and fuel, which causes a large amount of greenhouse gas (GHG) emissions (Gao et al., 2020). This confirms that fully or partially replacement of bitumen with greener and sustainable products is needed (Al-Hadidy, 2023). Khandelwal (2019) showed GHG emissions between 53 and 65 kg CO2 eq. for lignin-modified asphalt pavement and 72 kg CO2 eq. for the unmodified asphalt pavement. Also, Lamothe et al. (2022) indicated that the use of lignin in the asphalt pavement industry is promising in terms of the GHG emissions to the atmosphere. To this end, besides using of lignin as a binder or bitumen modifier in HMA, it can be used as a greener product which will open a market for the use of lignin in the asphalt pavement industry.

### 2.5.2 Incorporation process

Lignin, powder and pellets forms, can be incorporated into the bitumen by using the low shear mixer (LSM) and HSM. Xu et al. (2017) used LSM to incorporate 5 % and 10 % of lignin powder with two different types of bitumen, unmodified and SBS-modified bitumen. The incorporation temperature and speed were 163 °C and 1500 rpm, respectively. At the beginning of the incorporation process, a volumetric expansion was observed in addition to floated air bubbles on the bitumen surface. The incorporation process continued for 30 minutes until the

air bubbles disappeared. These observations might be due to the moisture content within the added lignin which made the bitumen foam. Accordingly, it is necessary to make sure that the added lignin is completely dry before being incorporated into the bitumen. Pérez et al. (2019) incorporated 5, 10, 20 and 40 % of lignin powder into the bitumen by employing LSM. The incorporation temperature and speed were 160 °C and 300 rpm. The incorporation process continued for 60 minutes. Herein, it may be concluded that the incorporation time can be increased due to the addition of high lignin content, 40 % in this study.

HSM was used in many studies in order to prepare lignin-modified bitumen. Different contents of lignin powder, from 1 % to 12 %, were incorporated into different types of bitumen (Batista et al., 2018; Zhang et al., 2019; Gao, et al. 2020; Norgbey et al., 2020; Zahedi et al., 2020). The incorporation temperature, speed and time were 150-160 °C, 5000-6000 rpm and 30-60 minutes, respectively.

### 2.5.3 Verification of the incorporation process

The performance of asphalt pavements is strongly influenced by the performance of the bitumen. The modification of the bitumen resulted in chemical and physical changes in the bitumen composition (Almusawi et al., 2019). In most cases, these changes appear as an increase in the viscosity and stiffness of the modified bitumen. However, when something is added to bitumen, it is necessary to verify the stability and homogeneity of the modified bitumen. This verification process can be done by performing the storage stability test and taking microscope images (Diebold, 1999; Batista et al., 2018; Norgbey et al., 2020). In the storage stability test, upon the completion of the conditioning, the softening point of the lower and upper part of a filled tube of bitumen is measured. Simply, the absolute difference value of the two softening points represents the storage stability of the modified bitumen. According to the laboratoire des chaussées (LC 25-003) and the American society for testing and materials (ASTM D 5892) standards, the absolute difference value should be less than 2.0 and 2.2 °C, respectively, to consider the modified bitumen as stable. Pérez et al. (2019) reported that the maximum difference is 5.0 °C.

For the microscope images, they have become a hotspot in many researches, especially for the quantifying of particles morphology (Koohmishi & Palassi, 2017). Although it is difficult to link the observation of these images with a successful incorporation process, many morphological indices can be used as indicators to describe the particles of a filler or additive such as surface texture, shape and angularity (Liu et al., 2017; Rajan & Singh, 2017; Xie et al., 2017). For example, the formation of rough edges of an additive may result in stiff and viscous bitumen. However, these morphological indices are independent of each other (Xing et al., 2022). In other words, if one of these indices undergoes a change, the other indices will not be affected. Also, the dispersion of the particles of an additive throughout the bitumen can be used to describe the homogeneity (Norgbey et al., 2020). The uniform dispersion of the particles leads to a homogeneous modified bitumen (Zhang et al., 2018). This may result in a better overall performance of HMA. As the content of an additive increases, the small particles start to coalesce and form big ones which will affect negatively the stability and homogeneity of the modified bitumen (Pérez et al., 2019). However, the content of the aromatics and asphaltenes plays a significant role in the compatibility of the lignin with the bitumen (Dong et al., 2014). In particular, high aromatics content and low asphaltenes content lead to well-dispersed particles throughout the bitumen, including stable and homogeneous modified bitumen. On the other hand, although high aromatics content shows better performed bitumen, but low asphaltenes content leads to less performed bitumen at high temperature (Dong et al., 2014).

### 2.5.4 Antioxidation properties of lignin

As time progresses, the bitumen stiffens, becomes brittle and eventually cracks. This occurs due to the reaction of bitumen with air, including oxidized bitumen. The oxidation mechanism leads to the deterioration of the properties of bituminous material, which identifies by aging (Read and Whiteoak, 2003). For this purpose, using of antioxidants, lignin included, can be utilized to delay the aging of bitumen and, thus, extend the service life of the road asphalt pavements (Zhang et al., 2019). In order to simulate the oxidative aging process, the bitumen must be subjected to the regimes of accelerated oxidative aging (Oliviero Rossi et al., 2018). In particular, the short-term aging process according to the rolling thin film oven RTFO

(AASHTO T 240-13) and long-term aging process according to the pressure aging vessel PAV (AASHTO R 28-12) methods can be employed.

The addition of lignin improved the long-term aging index of the bitumen (Arafat et al., 2019). Zhang et al. (2019) pointed out that the microstructure of the aged lignin-modified bitumen, compared to the unaged one, was not affected. In addition, as obtained from FTIR tests results, different functional groups of lignin did not change significantly. Moreover, in order to evaluate the aging state of lignin-modified bitumen, the sulfoxide and carbonyl indices could still be employed. Regarding the viscoelastic properties, lignin showed a little effect on the aged bitumen, as revealed by DSR tests. Oliviero Rossi et al. (2018) studied three antioxidant agents: phospholipids, ascorbic acid and lignin. Lignin, among the other agents, showed minor effect on the resistance to the oxidative aging in addition to the highest age-hardening effect.

A global interlaboratory study was carried out on seven different types of bitumen from different geographical places in the world in order to evaluate the effectiveness of using antioxidant agents with bitumen (Adwani et al., 2023). Four different agents were studied, including lignin. For the majority of the tested bitumens, lignin did not highlight a high degree of effectiveness in terms of oxidative aging. Luz et al. (2021) stated that the use of lignin delayed the stiffening of bitumen which was subjected to the short-term aging process (RTFO method).

On the other hand, Su et al. (2023) and Lu et al. (2022) pointed out that lignin-modified bitumen has better resistance to the oxidative aging than the unmodified bitumen. This was due to changes of the indices of some of the functional groups. However, this result proved that the state of the oxidative aging mechanism was the decomposition of the lignin itself, which inhibited the bitumen from being aged.

## 2.6 Effects of inert fillers

Since lignin is a powder form, it could be just a filler. Herein, it is worth investigating the effects of fillers on the properties and performance of bitumen and HMA. This helps to distinguish between inert fillers and lignin. Different types of filler are used in the asphalt pavement industry such as lime, stone dust and cement (Kavussi & Hicks, 1997; Little & Petersen, 2005; Lesueur et al., 2013). In general, fillers represent the particles that passed sieve no. 200, smaller than 75 μm in diameter (Sharma et al., 2010; Zulkati et al., 2012; Csanyi, 1962; Muniandy et al., 2012). Due to the significant difference of density between fillers, some researchers suggested using volume proportioning while using fillers in HMA (Tapkın, 2008; Xue et al., 2009; Uzun & Terzi, 2012). For example, using low-density filler leads to the use of higher quantity in HMA than what is desirable (Chen et al., 2011a). However, the use of fillers in HMA weakens the adhesion bonding between the asphalt binder and aggregates, which is due to the acidic nature of fillers and the presence of silica (Kütük-Sert & Kütük, 2013; Kuity et al., 2014). In addition, fillers showed a negative effect on the ITS of HMA, which might be due to the high clay content for some types (White et al., 2006). Also, the use of filler increases the density and stiffness modulus of HMA (Sengoz & Topal, 2005; Kütük-Sert & Kütük, 2013; Barra et al., 2014). Wong et al. (2007) indicated that the resilient modulus of a control mix was comparable with a mix that has 6 % of recycled concrete. A study was conducted on the use of 4 % of recycled brick powder and limestone filler by the weight of aggregate in HMA (Chen et al., 2011b). It was reported that the water sensitivity, ITS, rutting and fatigue were improved. The incinerator ash filler can be used in HMA for up to 15 % to improve the stability (Hassan, 2005). However, this type of filler is recommended for roads with low traffic volume.

Generally speaking, some studies showed positive effects of using fillers in HMA and others presented negative effects. However, the difference of the HMA performance depends on the physical and chemical properties of the used filler and its interaction with the HMA, including asphalt binder. Moreover, the particle size of the filler plays a major role in the rheological properties of the asphalt binder (Chen & Peng, 1998). To this end, particle size and surface

area of the filler are considered as the main factors that are responsible for the interfacial interaction between filler and asphalt binder, while the chemical composition of filler did not show a significant effect on the interfacial interaction (Antunes et al., 2015; Antunes et al., 2016). Herein, it is necessary to quantify the morphology of the filler particles. For different types of fillers, it was found that the filler particles tend to form clusters (Feng et al., 2020; Su et al., 2020). This observation indicates that it is difficult for filler particles to disperse into a single particle (Kuang et al., 2017). Therefore, according to the morphological quantifying of filler particles by microscope images, it is expected to observe negative effects on the performance of HMA that has been treated by adding fillers.

Robati et al. (2015) studied the effect of the inert filler on the asphalt binder. They stated that the effect is governed by the properties of the filler and its concentration. Optimum concentration of the inert filler in the asphalt binder gives optimum interaction between the particles of the filler, forming a mastic. In other words, low filler concentration leads to minimal interaction of the mastic due to the presence of high amount of free asphalt binder, while high filler concentration results in a reduction of the capability of the mastic to adhere and then to bond the aggregates together. They also showed that in case of the high filler concentration, the increase rate in the stiffness of the mastic is sharp. Michel et al. (2023) showed that the stiffness of the mastic was significantly affected by another parameter which is the effective volume of the inert filler. The effective volume is the virtual volume fraction of the filler for a given volume of filler when its fractional voids, also known as Rigden voids, are added. High value of this parameter prevented the dispersion of the filler particles in the asphalt binder matrix and coating issue was observed, including difficulties in the preparation of the mastic.

## 2.7 Summary

Based on the findings from the literature, lignin can be incorporated into the bitumen as a partial replacement. Although it increases the viscosity of the bitumen which will negatively impact the workability of HMA and results in higher air voids content within HMA (very high

temperature), it shows an improvement on the performance of bitumen at intermediate and high temperatures, including fatigue cracking and rutting resistance respectively. Regarding the low temperature performance, lignin does not show negative effects as long as its content is low. Moreover, lignin increased the HMA resistance to the water damage. Besides, lignin can be integrated with the HMA production on the large scale. Therefore, it is possible to open a market for the use of lignin in the modification of road asphalt pavements. Following, lignin is distinguished from the other modifiers as a greener and sustainable product, in addition to its abundance in the nature, especially in Canada.

Despite the amount of work conducted on lignin-based asphalt, more work is required not only to better understand its behaviour, but also to address the non-completed or unknown aspects. For example, there is no clear methodology for how lignin is added to the bitumen (wet process) or HMA (dry process). In addition, the effects of the incorporation process parameters (temperature, time and speed) are not discussed. Also, it is not reported if there is a need for using specific mixer (LSM or HSM) or even the effects of these mixers on the incorporation process. In other words, the methodology for the incorporation process that is used in each cited study is often based from previous studies without any further discussion. In addition, the evaluation of the effects of adding lignin to the bitumen is still incomplete. For example, the combination of the BBR and DSR tests results is not shown and discussed in the literature review. In general, combining and linking the results of the performed tests can help to understand the behaviour of the lignin as a powder (filler or binder or both).

Regarding the anti-oxidation process of lignin-modified bitumen, the studies reported that the lignin can be considered as an antioxidant agent despite the non-remarkable effects on the oxidative aging. However, this conclusion was drawn based on test results that had been performed on the residue of RTFO or after 10 hours of PAV (one completed cycle of PAV is equal to 20 hours). In other words, lignin-modified bitumen was not aged aggressively. Therefore, the real long-term of oxidative aging process should be further investigated.

Regarding the fatigue cracking resistance and rheological properties (E*) of lignin-modified HMA, there is a strong need to perform the related tests since it is not possible, through the research in the literature review, to find a study that presents these behaviours. In addition, the evaluation of the high and low temperatures performance of lignin-modified HMA should be further developed in order to better characterize the thermomechanical behaviour in different domains.

# CHAPTER 3

# MATERIALS CHARACTERIZATION AND TEST METHODS

## 3.1 Introduction

This chapter explains the materials and tests employed in this research program. The experimental tests of the research program were carried out on both bitumen and hot mix asphalt (HMA). The shown tests in this research were chosen to evaluate the effects of bitumen substitution by lignin on the properties and performance of the bitumen and HMA at high, intermediate and low temperatures. The different tests of the research program were selected in order to reach the different objectives. To that end, the tests are separated into two main parts. The first part covers the procedure used to add lignin in bitumen and the related tests where the second part covers the work done on the addition of lignin directly in HMA. More specifically, the experimental program begins with the study of the lignin incorporation process, followed by the evaluation of the impact of the replacement of part of the bitumen with lignin on the properties of the resulting binder. This is followed by the study of the impact of the addition of lignin by the dry process on the preparation of mixes before studying the properties of the asphalt mixes modified with lignin by the wet or dry process. Before showing the methodology, the different materials used are presented.

## 3.2 Materials

This section presents the materials used in this research program and their properties. These materials are: Kraft lignin in powder and pellet forms, bitumen and the aggregate used to produce the HMA.

### 3.2.1 Kraft lignin

In this research, eight various types of Kraft lignin were studied, each with different sizes. Each is a biopolymer and waste product of the Canadian wood industry, which is derived from soft

or hard wood and has acid (A) form or basic (B) form which is the pH. Some were received as junk particles and they were grinded twice at the provider's facility in order to have fine powder. Each lignin has a brown color, light or dark, and can be described as a sticky powder material, especially after being grinded. These lignins were produced by different lignin producers in Canada. Table 3.1 shows each type of lignin and the details about the abbreviation of the name. It should be noted that the lignins HT SW A 1 and HT SW A 2 are basically the same, but the conditions during the manufacturing process are different. As shown in Table 3.1, with the 8 initial lignins, 19 lignins were studied since they have been modified from their original version.

Table 3.1 Types of lignin studied in this research program

| No. | Type of lignin | Details of the type |
|---|---|---|
| 1 | HT SW A 1 | Hinton soft wood, acid form |
| 2 | HT SW A 2 | |
| 3 | HT SW B [a] | Hinton soft wood, base form |
| 4 | HT SW B 1st [b] | |
| 5 | HT SW B 2nd [c] | |
| 6 | TB HW A [a] | Thunder Bay-hard wood, acid form |
| 7 | TB HW A 1st [b] | |
| 8 | TB HW A 2nd [c] | |
| 9 | TB HW B [a] | Thunder Bay-hard wood, base form |
| 10 | TB HW B 1st [b] | |
| 11 | TB HW B 2nd [c] | |
| 12 | K SW A [a] | Kruger soft wood, acid form |
| 13 | K SW A 1st [b] | |
| 14 | K SW A 2nd [c] | |
| 15 | K SW B [a] | Kruger soft wood, base form |
| 16 | K SW B 1st [b] | |
| 17 | K SW B 2nd [c] | |
| 18 | HT SW A-modified | Hinton soft wood, acid form (modified) |
| 19 | K SW A-modified | Kruger soft wood, acid form (modified) |

[a] The lignin is not grinded (junk particles);
[b] The lignin is grinded once (smaller size of solid particles);
[c] The lignin is grinded twice (fine powder).

Figure 3.1 and Table 3.2 show the photo and the main properties of the first type of lignin (HT SW A 1). For the other types, there is no available information from the supplier. However, the potential hydrogen (pH) test was done at ÉTS in addition to the laser granulation, which was done with Mastersizer 3000 laser granulometry device (Figure 3.2). Figures 3.3 to 3.10 show the other types of lignin in different sizes: junk particles and after the first and second grinding process.


Figure 3.1 HT SW A 1 lignin

Table 3.2 Properties of the HT SW A 1 lignin provided by the supplier

| Property | Value * |
|---|---|
| Passing of 100 mesh or 149 µm (%) | 99.3 |
| Passing of 200 mesh or 74 µm (%) | 97.6 |
| Density, ρ (g/cm3) | 1.2-1.3 |
| Potential hydrogen (pH) | 3-4 |
| Moisture content, w (% mass) | 1.0 |
| Decomposition temperature (°C) | 160-170 |
| Glass transition temperature, Tg (°C) | 150-160 |
| Purity (%) | 95 |
| * The values are provided by the supplier: no specific standards. | |

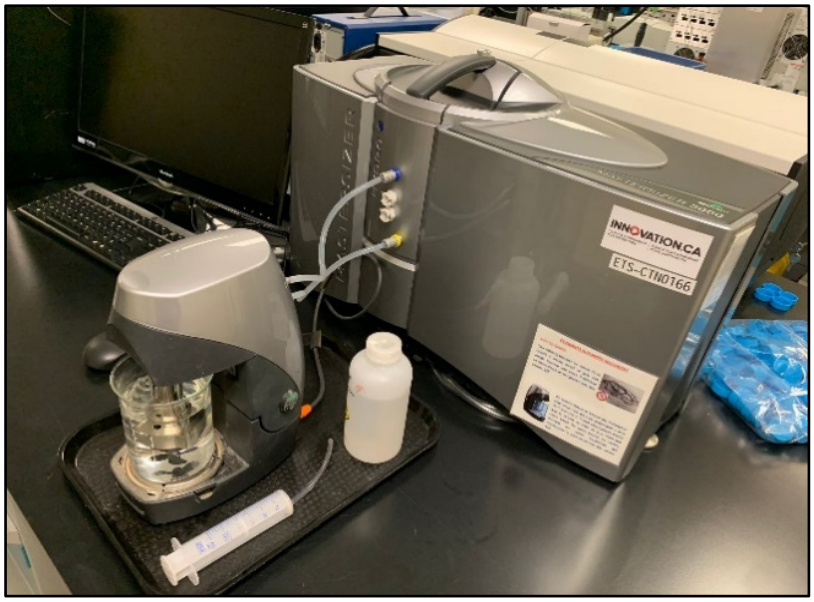


Figure 3.2 Mastersizer 3000 laser granulometry apparatus and its attachments


Figure 3.3 HT SW A 2 lignin

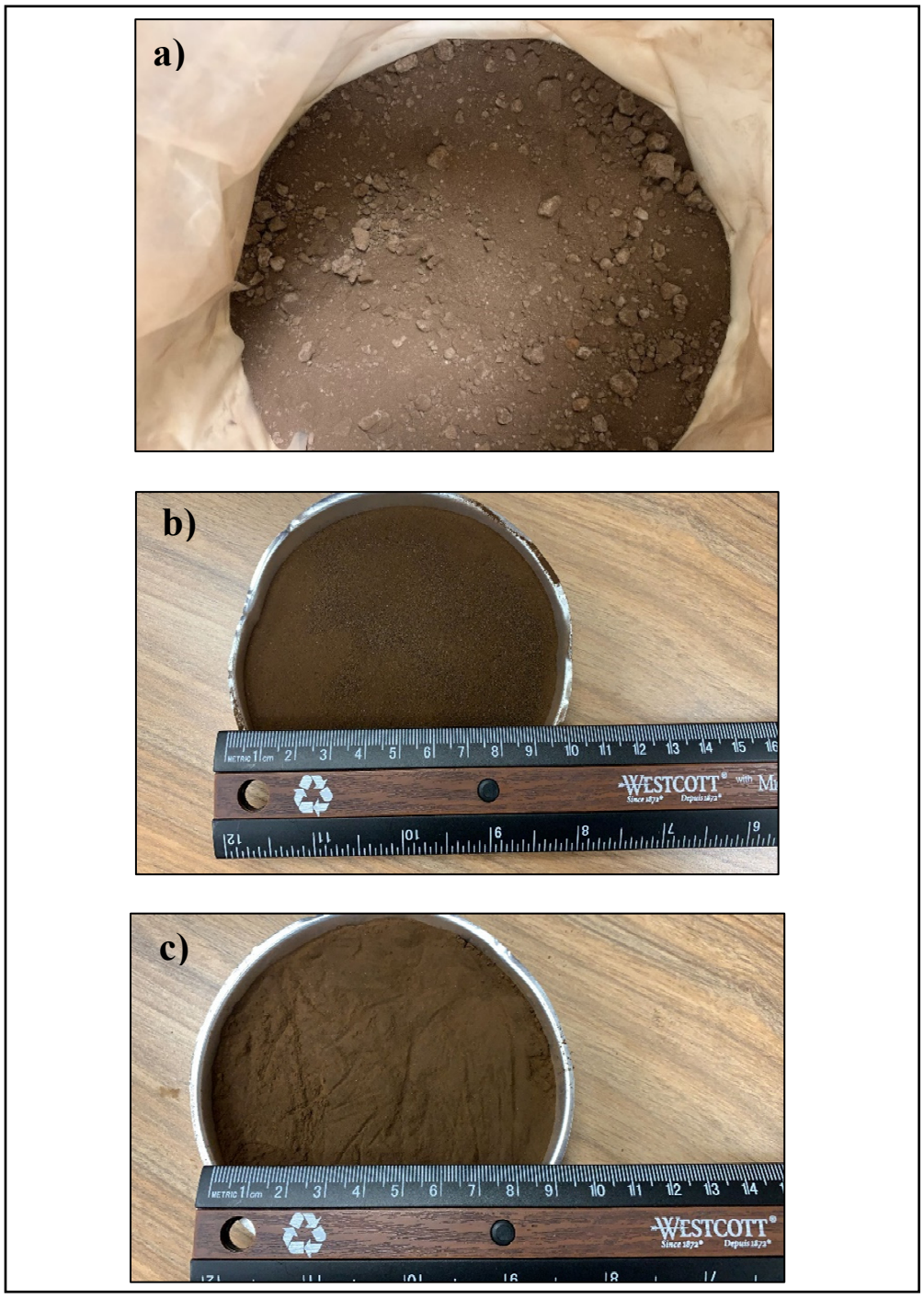


Figure 3.4 HT SW B lignin: a) junk particles, b) after first grinding, c) after the second grinding process

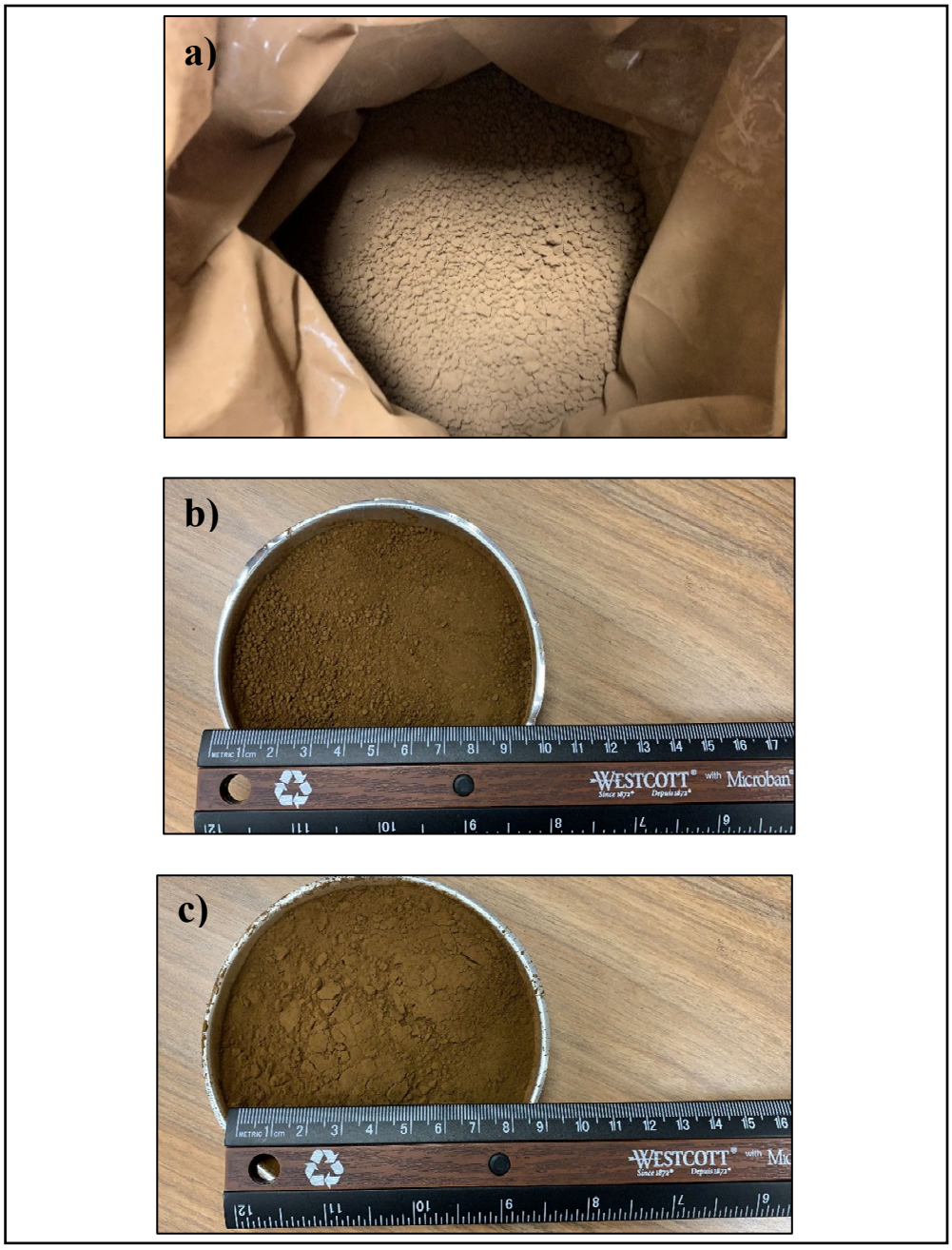


Figure 3.5 TB HW A lignin: a) junk particles, b) after first grinding, c) after the second grinding process

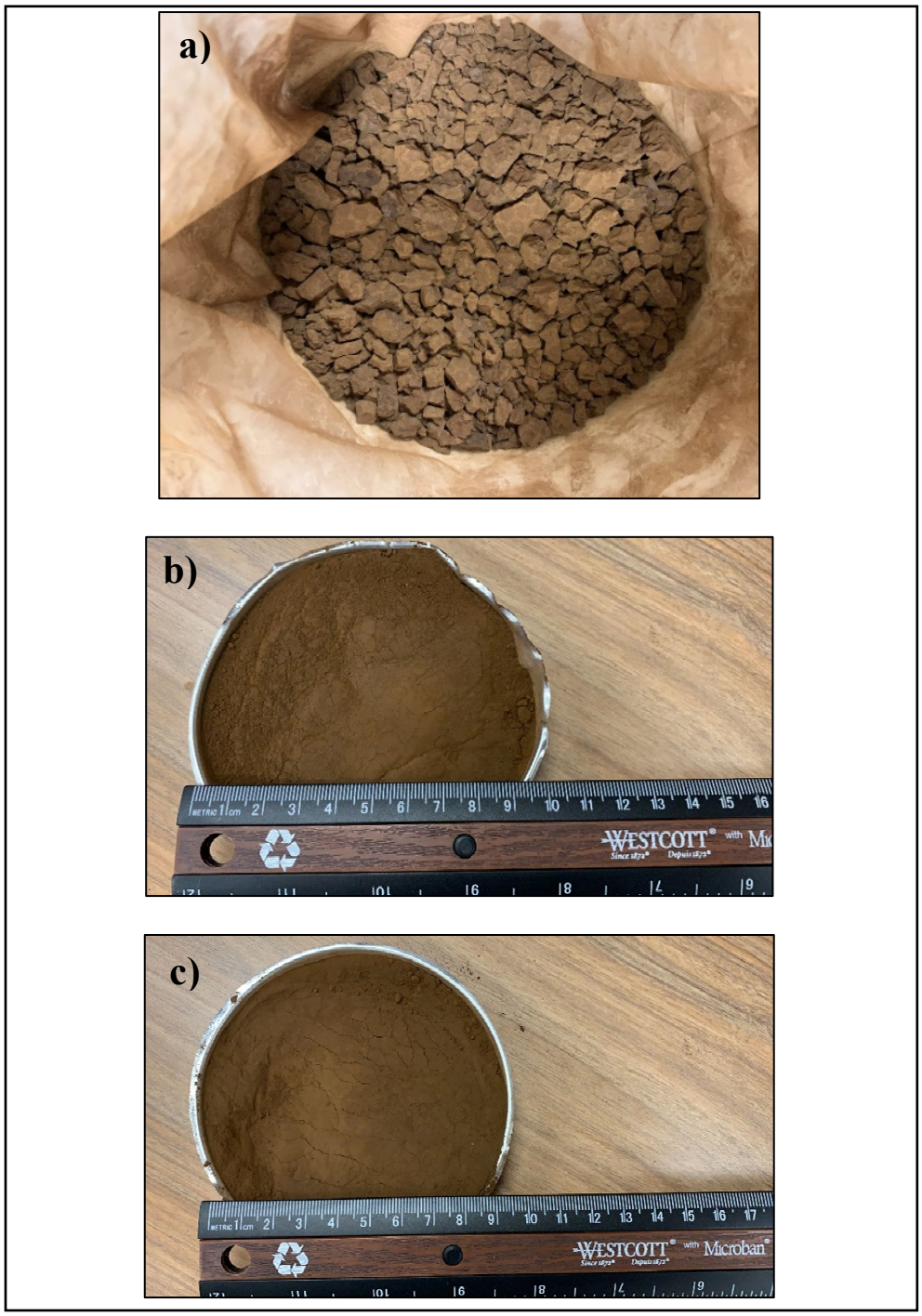


Figure 3.6 TB HW B lignin: a) junk particles, b) after first grinding, c) after the second grinding process

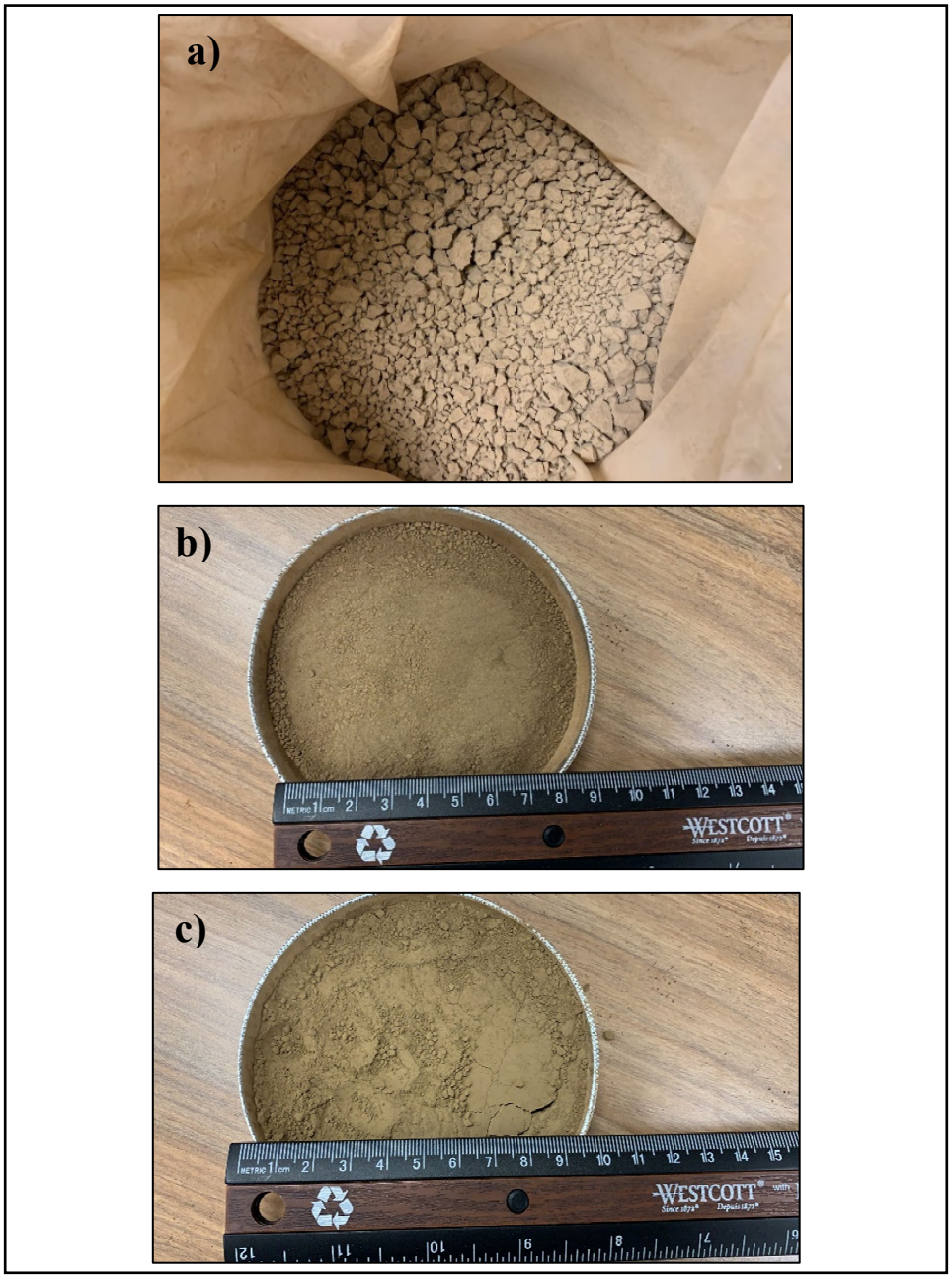


Figure 3.7 K SW A lignin: a) junk particles, b) after first grinding, c) after the second grinding process

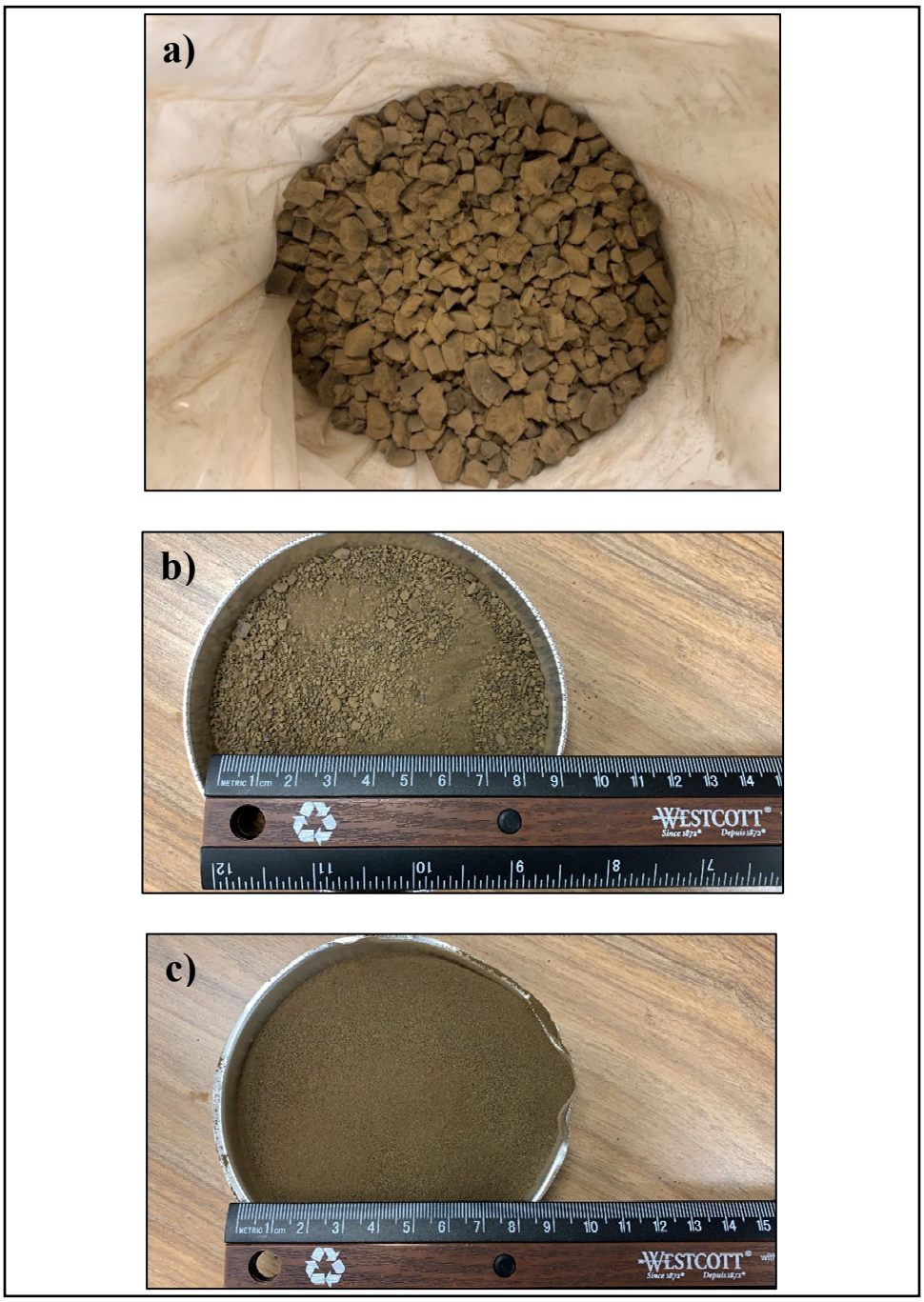


Figure 3.8 K SW B lignin: a) junk particles, b) after first grinding, c) after the second grinding process


Figure 3.9 HT SW A modified lignin


Figure 3.10 K SW A modified lignin

### 3.2.2 Lignin Pellets

In order to limit the potential health and environmental problem of working with a fine powder, lignin pellets were produced for us. Simply, the pelletizing process of the Kraft lignin consisted in mixing lignin with soybean oil in different percentages and at different moisture before being compressed into pellets. Two types of the pellets were tested in this research: high durability index (HDI) and low durability index (LDI) pellets. The durability index represents the resistance of pellets to degradation, heat, aging and environmental influences. In this research program, the pellets that have a durability index of 79.2 is considered as HDI, while a durability index of 43.4 is considered as LDI. However, from the properties of the pellets (Table 3.3), the

acquired durability could be obtained mostly by adding more soybean oil in addition to the moisture condition. For example, 10 % soybean oil and 0 % added moisture are needed for the HDI, while for LDI, 5 % soybean oil and 5 % added moisture are needed. Figure 3.11 shows the HDI and LDI pellets tested in this research. The pellets were produced by CPM, a company located in Iowa, USA, specifically for this research program. The soybean oil content was decided by CPM based on their experience in producing pellets.

Table 3.3 Properties of the high and low durability index pellets provided by the supplier

| Property | High durability index pellets HDI * | Low durability index pellets LDI * |
|---|---|---|
| Soybean oil content (%) | 10 | 5 |
| Moisture content (%) | > 1 | 2.1 |
| Density, ρ (g/cm$^3$) | 0.42 | 0.34 |
| Pellets Durability Index PDI | 79.2 | 43.4 |
| * The values are provided by the supplier: no specific standards. | | |

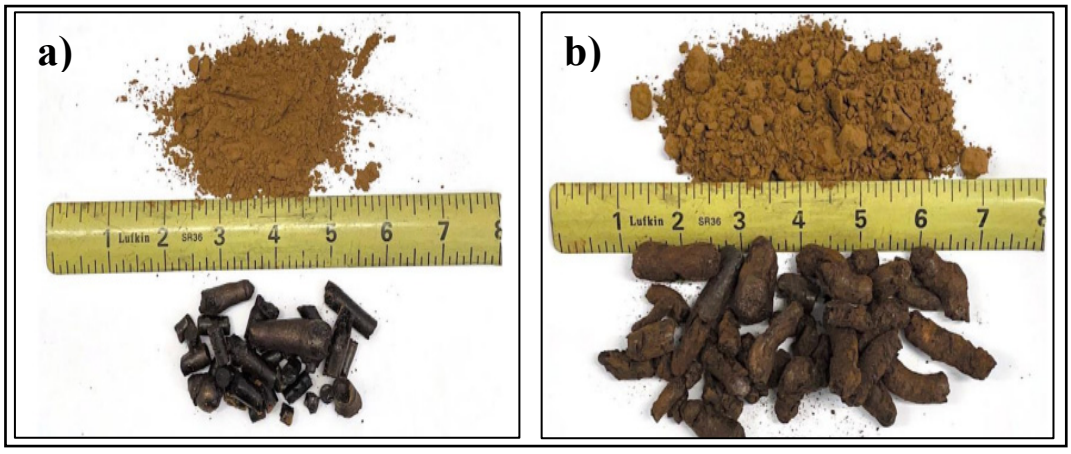


Figure 3.11 High (a) and low (b) durability index pellets

### 3.2.3 Bitumen

Two soft and unmodified bitumens adapted for cold climates and standard traffic level were used in this research: PG 58S-28 and PG 52S-34. According to the Transports Quebec,

PG 58S-28 is specified for Montreal's area. PG 52S-34 was chosen to see the impact of lignin on softer bitumen, compared to PG 58S-28. Table 3.4 shows the main properties of the two bitumens according to the bitumen suppliers, Suncor Energy and McAsphalt.

Table 3.4 Properties of the bitumen PG 58S-28 and PG 52S-34 provided by the suppliers

| Aging level | Test | Property | Value for PG | | Standard or Test method |
|---|---|---|---|---|---|
| | | | 58S-28 | 52S-34 | |
| None [a] | FP | Flash point, FP (°C) | 305 | 305 | ASTM D 92 |
| | SP | Softening point, SP (°C) | 42.5 | 36.0 | LC 25-003 |
| | BRV | Viscosity, η, at 135 °C (mPa·s) | 254.0 | 174.0 | AASHTO T 316 |
| | | Viscosity, η, at 165 °C (mPa·s) | 80.0 | 59.0 | |
| | DSR | \|G*\|/sin (δ) at 58 or 52 °C (kPa) | 1.3 | 1.1 | AASHTO T 315 |
| | | High temperature, $T_{high}$ (°C) | 59.7 | 52.8 | ASTM D 7643 |
| | RTFO | Mass variation (% mass) | -0.415 | -0.717 | AASHTO T 240 |
| Short term [b] | MSCR | Jnr3.2 at 58 or 52 °C ($kPa^{-1}$) | 2.84 | 3.68 | AASHTO T 350 |
| | | Jnrdiff. at 58 or 52 °C (%) | 12.7 | 8.3 | |
| | | R3.2 at 58 or 52 °C (%) | 0 | 0 | |
| | | Traffic level at 58 or 52 °C (n: letter) | S | S | |
| Long term [c] | BBR | Low temperature, $T_{low}$ (°C) | -30.1 | -34.7 | AASHTO T 313 ASTM D 7643 |

[a] The tests were carried out on unaged bitumen.
[b] The tests were carried out on the rolling thin-film oven (RTFO) residue.
[c] The tests were carried out on the RTFO and pressure aging vessel (PAV) residue.

### 3.2.4 Aggregate

The aggregate used in this research to produce the HMA was sampled directly from the quarry and characterized in the laboratory. Table 3.5 shows the type, size and source of each aggregate category. The sieving process of the aggregate was conducted and the results were analyzed. Quebec's Laboratoire des chaussées LC method was employed in order to check the eligibility of the aggregate to be used in the HMA. Figure 3.12 shows the gradation curve of the mix and the LC-4202 requirements (control points and restriction zone) for an ESG-10. According to

Quebec provincial (LC-4202) requirements, the gradation curve must be located between the control points and out of the restriction zone (MTMDET, 2017). For this research program, it was decided to produce and test an ESG-10, which is the most common surface mix used on high traffic roads in Quebec (MTQ, 2015).

Table 3.5 Properties of the aggregate used to produce HMA

| Aggregate type | Aggregate size (mm) | Source |
|---|---|---|
| Limestone | 5-10 | DJL Saint-Bruno |
| | 0-5 | |
| Non-washed limestone | 0-5 | DJL Saint-Philippe |
| Natural sand | 0-1.25 | DJL Saint-Rock |
| Limestone filler | 0-0.315 | DJL coating plant |

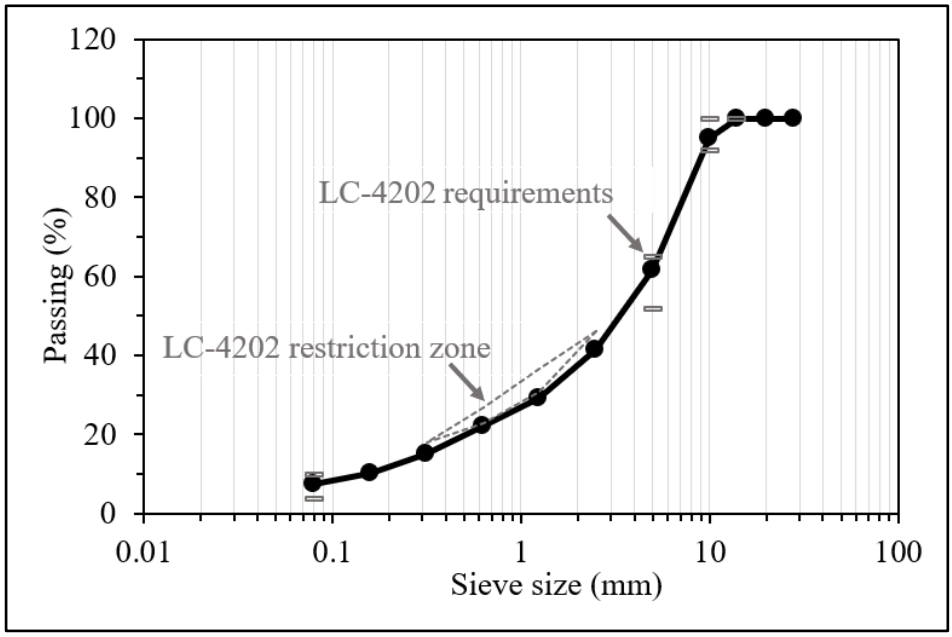


Figure 3.12 Particle size distribution of the aggregate and LC-4202 requirements for ESG-10

## 3.3 Tests methods

The research program is divided into six phases, each represents the corresponding chapter (Figure 3.13). The program starts from phase A which is the wet process incorporation of lignin

into the bitumen and the verification of the wet process incorporation through the corresponding tests (phase B, CH. 4). The lignin modified bitumen was studied at high and low temperatures and the oxidation process as well (phase C, CH. 5). After, the compactability of the HMA produced by wet and dry processes was investigated (phase D, CH. 6). The rheological properties and thermomechanical performance of the HMA at high and low temperatures were examined (phase E, CH. 7). Lastly, three annexes are presented (phase F). Annex I shows the full-scale production of the modified HMA with lignin. Annex II shows the effect of tall oil on the HMA compactability. Annex III shows the fatigue tests results of the lignin-modified HMA.

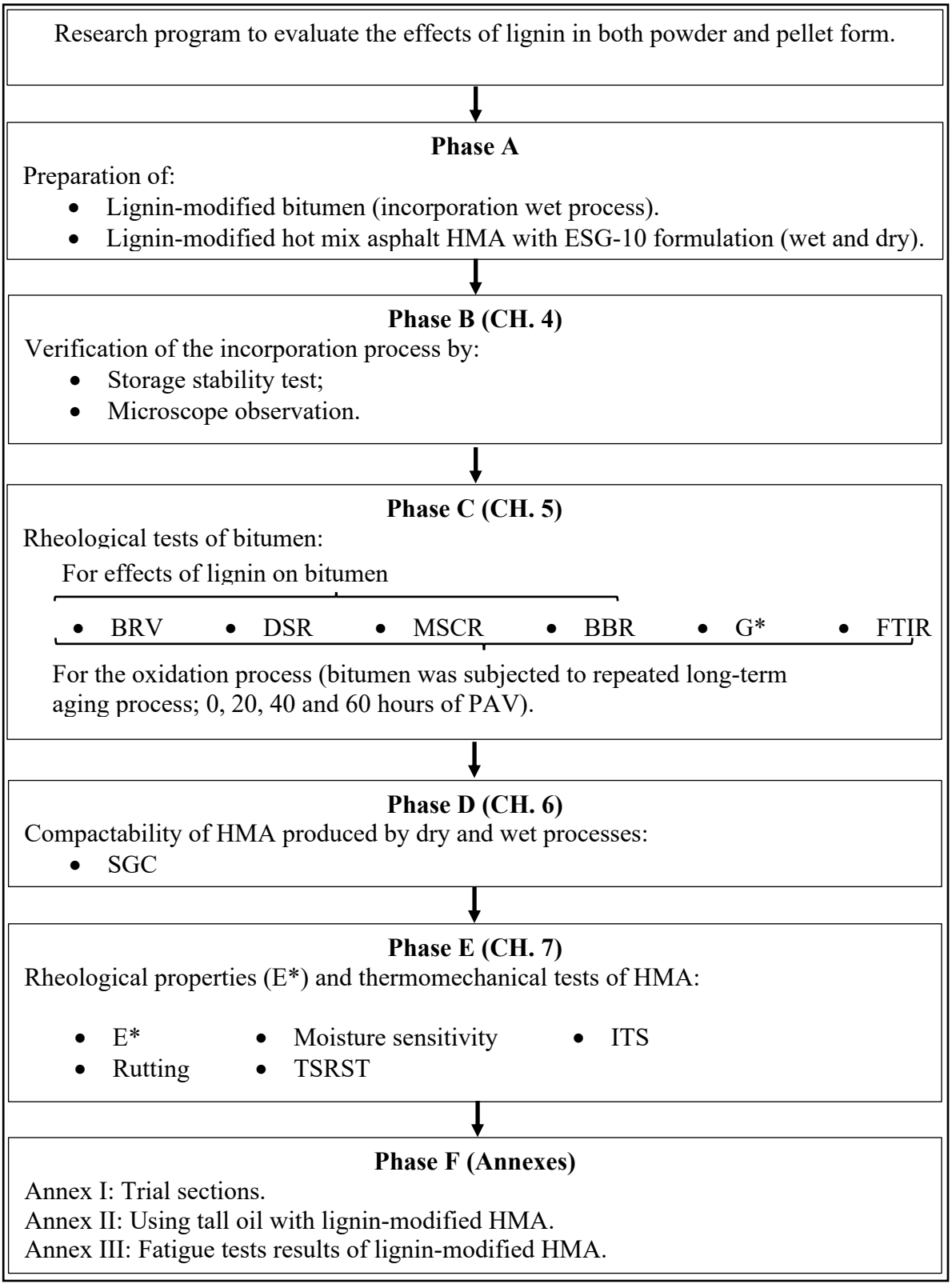


Figure 3.13 Summary of the research program

### 3.3.1 Verification of the incorporation of lignin into the bitumen (wet process)

The lignin was incorporated with the bitumen under different conditions. The incorporation process was verified by performing the storage stability test and with microscope observation in order to check the stability and homogeneity of the lignin modified bitumen.

#### 3.3.1.1 Storage stability test

The purpose of the storage stability test is to provide evidence on how the stability of a product varies with time under the influence of environmental factors such as temperature, humidity and light (Quebec test method LC 25-003 and American standard ASTM D 5892). In this case, the objective of the test was to check the stability of the modified bitumen after the addition of the lignin. If the binder is stable, it means that the dispersion of the lignin does not change over time. Two types of mixers (Figure 3.14) were employed to perform the incorporation process. An overhead stirrer (IKA RW16) and a high shear mixer (HSM SILVERSON L4RT-W). Tubes partly filled (50 ± 0.5 g) with bitumen (modified with lignin or not) were conditioned at 163 °C for 48 hours (Figure 3.15 a) and were then placed in a freezer at -5 °C for 3 hours. After this conditioning, thin discs of bitumen were cut at the top and at the bottom of each tube (separation tube test) and their softening point (SP) was determined (Figure 3.15 b). The softening point (SP) is defined as the temperature at which a bitumen disc can no longer support the weight of a 3.5 g steel ball (ASTM D 36). Finally, the storage stability of the bitumen corresponds to the absolute difference between the SP of the top disc and the bottom disc. The closest the two temperatures are, the better the stability is. Two repetitions are planned to perform for this test. According to LC 25-003 and ASTM D 5892, the difference should be less than 2.0 and 2.2 °C, respectively, to consider the mix as stable.

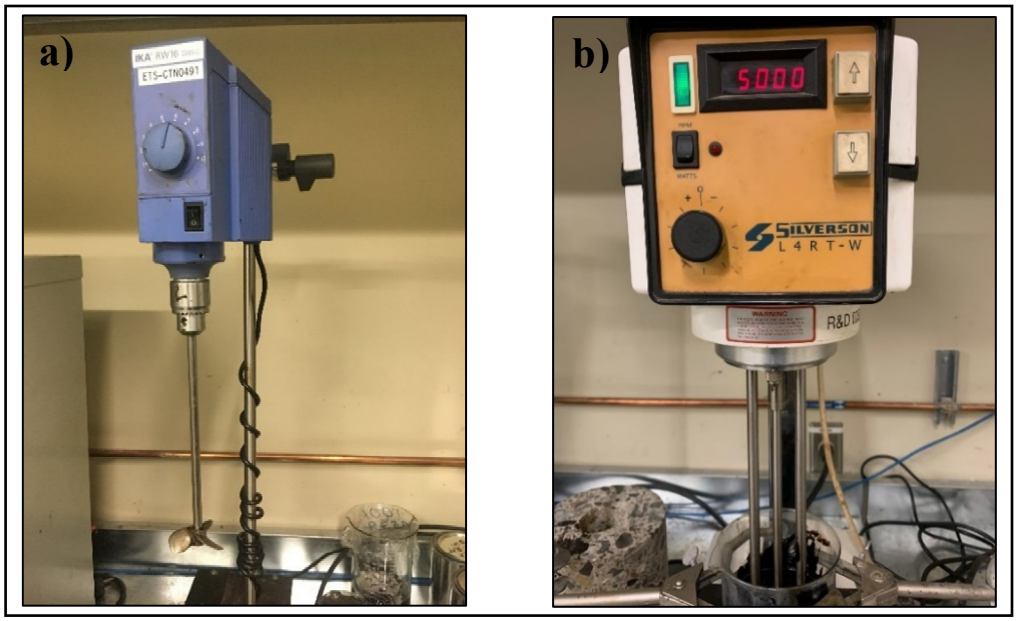


Figure 3.14 Two mixers used in this study. a) IKA RW16 basic overhead stirrer, b) SILVERSON L4RT-W high shear mixer

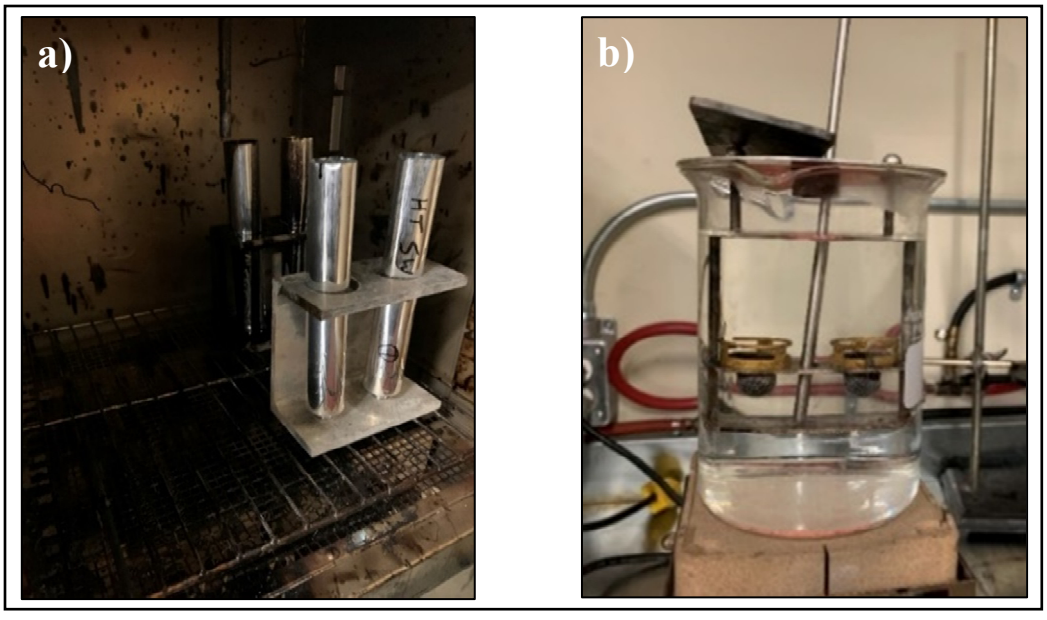


Figure 3.15 Storage stability test. a) tubes for the storage stability test, b) Softening point test

### 3.3.1.2 Microscope observations

The aim of these observations is to verify that the lignin is homogeneously distributed in the bitumen and that there are no lignin clusters in the mixes. For this, a very thin layer (obtained by sliding two hot parallel glass plates) of hot bitumen was spread on a glass plate (Figure 3.16 a) and the microscope (Figure 3.16 b) was used to make a visual evaluation of the homogeneity of the material at room temperature (20-25 °C). There are no standards to evaluate the homogeneity of a modified bitumen with microscopy. In this research program, a software which is called FIJI/IMAGEJ is used for the quantification of the microscope images. This software can detect the solid particles in the images and draw line borders with highlighted colour. In this regard, the most important step for detecting particles is the thresholding which is a technique to separate objects (lignin particles) from the background (bitumen). Due to the sensitivity of this technique, the results of the quantification for those images vary according to the thresholding value of the objects and background. Many trials (thresholding values) can be done to obtain the best thresholding that represents the microscope image. With this thresholding, the lignin particles can be distinguished from the bitumen. Following, with the morphological analysis of the microscope images, the homogeneity of the bitumen is evaluated based on the dispersion of the lignin particles throughout the bitumen. In other words, the distances between the lignin particles can refer to the homogeneity of the lignin-modified bitumen. For further analysis, the shape, surface texture and angularity of the lignin particles can be used to predict the properties (viscosity) and thermomechanical performance of HMA, especially stiffness and resistance to the water damage. One observation is planned to perform for each lignin content.

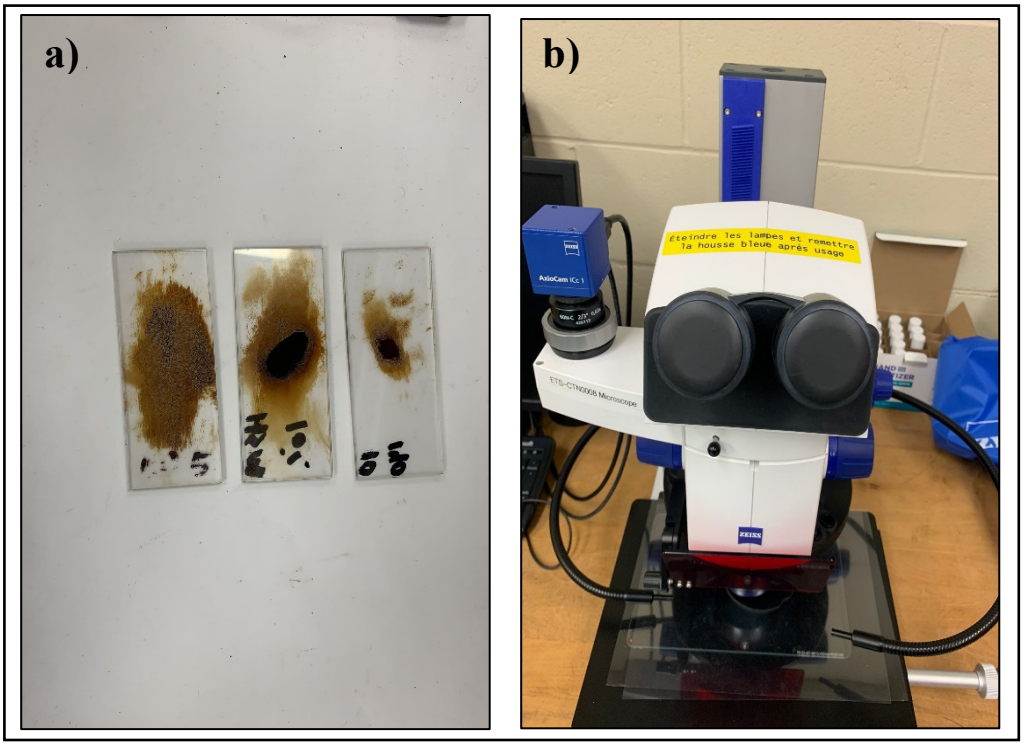


Figure 3.16 Homogeneity tests with microscopy. a) bitumen drops on the glass plates, b) microscope apparatus

### 3.3.2 Aging processes, rheological and chemical tests of bitumen

According to the standards of some rheological tests (AASHTO T 350 and AASHTO T 313), the specimen of the bitumen to be tested should be from the residue of different aging processes. For that specimen which is not required to be aged (AASHTO T 316, LC 25-007 and AASHTO T 315), the test was performed directly upon the completion of the incorporation wet process. However, the time between the incorporation process and testing varies from a few minutes (about 10 minutes) to approximately one hour. It is important to note that the resting period did not change the results, according to the performed repetitions.

#### 3.3.2.1 Rolling Thin Film Oven (RTFO)

The RTFO is the simulation of the short-term aging process that occurred during production and paving operations (AASHTO T 240-13). RTFO ages the bitumen by applying heat and air and it is necessary for predicting the behavior of early age HMA pavements and distresses. For

this purpose, eight glass containers (Figure 3.17 a) were filled with 35 g of bitumen and cooled down for one hour before being arranged in the carriage of the RTFO apparatus (Figure 3.17 b). As specified in the standard, the aging process was conducted for 85 minutes at 163 °C of temperature and 4000 ml/min of airflow.


Figure 3.17 RTFO aging. a) glass containers filled with bitumen, b) RTFO apparatus

### 3.3.2.2 Pressure Aging Vessel (PAV)

The PAV is the simulation of the long-term aging process of the asphalt binder (AASHTO R 28-12). The PAV aging process is always done after completing the RTFO aging process. The asphalt binder is subjected to heat (100 °C) and pressure (2.11 MPa) for 20 hours to simulate in-service aging over a period of 5 to 10 years (AASHTO R 28-12). A stainless steel pan (Figure 3.18 a) was filled with 50 g of the RTFO residue and then placed in the pan holder inside the PAV apparatus (Figure 3.18 b). The vacuuming process should be applied on the PAV residue before being used for the tests in order to remove the air bubbles from the bitumen.

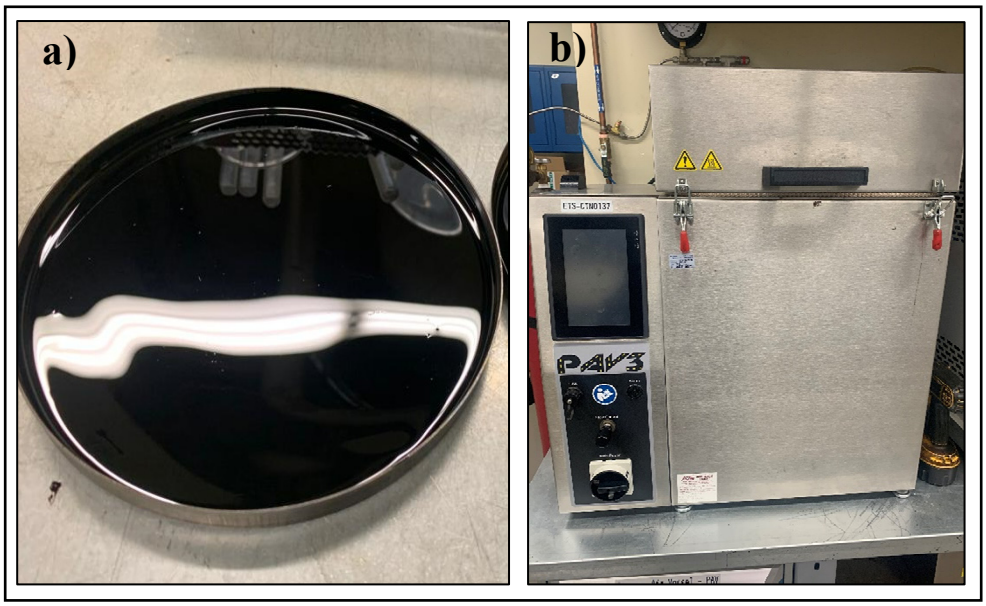


Figure 3.18 PAV aging. a) stainless steel pan, b) PAV apparatus

### 3.3.2.3 Brookfield Rotational Viscometer (BRV) test

The BRV test was carried out by following the AASHTO T 316 standard and Quebec test method LC 25-007. This test was performed on the unaged bitumen. The viscosity (η), which is the flow resistance of the bitumen, has a direct impact on the ability of the bitumen to coat the aggregates during mixing, and on the workability and compactability of the mix afterwards. Some bitumens need to be heated to a higher temperature to reach the viscosity targeted for mixing ($\eta_{\text{targeted for mix.}}$: 170 ± 20 mPa·s) and compaction ($\eta_{\text{targeted for comp.}}$: 280 ± 30 mPa·s) process. According to the standard and test method, the test should be performed at 135 and 165 °C. In this research, the test was also performed at 145 and 155 °C to get more information about the viscosity-temperature relationship of the bitumens since the addition of lignin may impact the normally linear viscosity-temperature relationship. For this purpose, a spindle was immersed in a cylindrical mold filled with 8.16 g of bitumen (Figure 3.19 a) and the BRV apparatus (Figure 3.19 b) allows the spindle to rotate with a speed of 100 rotations per minute. An average of five measurements for one specimen are planned to perform for this test.


Figure 3.19 Brookfield Rotational Viscometer (BRV) test. a) BRV mold, b) BRV apparatus

### 3.3.2.4 Steady shear flow (SSF) method

The SSF method, also known as Reinke method (Almusawi et al., 2019), was also used to measure the viscosity of the unmodified and lignin-modified bitumen. It was decided to have a second viscosity measurement method because we had a problem with the Brookfield device at the beginning of the project which lasted for a long time.

Like for BRV, the tests were performed on the unaged bitumen specimens. SSF method is based on the shear dependency behaviour of the bitumen. The dynamic shear rheometer (DSR) is employed to perform the test (Figure 3.20 a). In this test, a specimen of 25 mm in diameter (Figure 3.20 b) is placed between the two-parallel plate of DSR with 0.5 mm gap. High shear stresses sweep (50 to 1000 Pa) are applied on the specimen at different temperatures (88 to 112 °C). The test starts at 88 °C and 50 Pa and then conducting a constant shear until steady state is achieved at each shear stress level. The duration time of data sampling is 12 seconds. When three consecutive sampling duration generates viscosity values within 2 %, the steady state is achieved. The specimen should be conditioned for 10 minutes at each temperature. In this

method, the targeted viscosity for the mixing process is the same as in BRV (170 ± 20 mPa·s), while the difference is in that for the compaction process (350 ± 30 mPa·s compared to 280 ± 30 mPa·s for BRV). One repetition is planned to perform for this test.

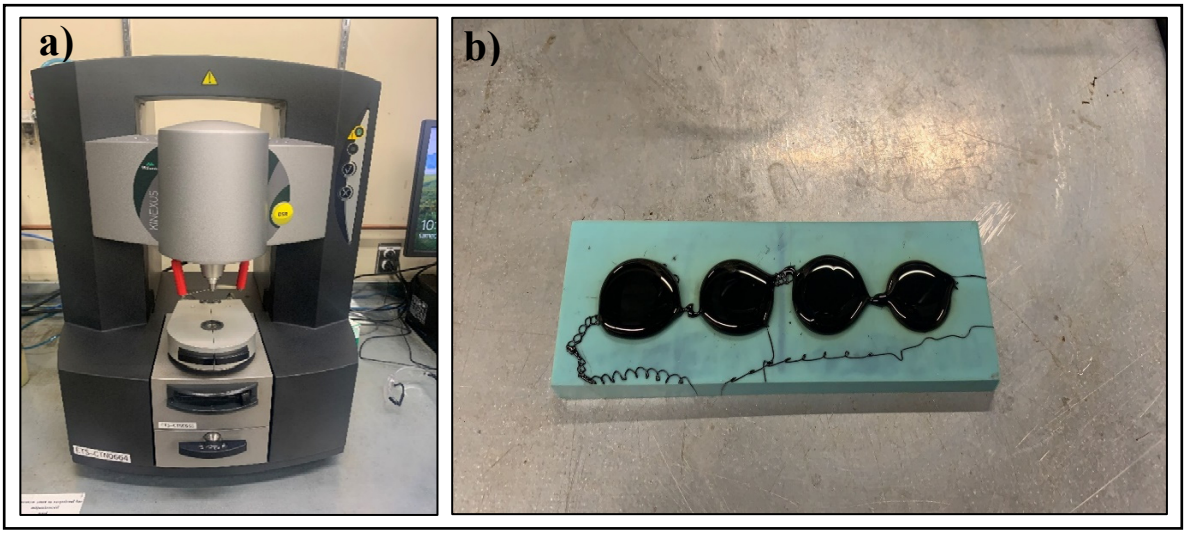


Figure 3.20 Dynamic Shear Rheometer used for the Steady shear flow (SSF) method. a) DSR apparatus, b) 25 mm geometry used for the test

### 3.3.2.5 Dynamic Shear Rheometer (DSR) test

The DSR test was used to evaluate the performance of the bitumen at high temperatures, and it could be utilized to characterize the viscoelastic behaviour of the bitumen (AASHTO T 315). The DSR tests were performed on the unaged bitumens to determine the norm of complex shear modulus ($|G^*|$) and the phase angle ($\delta$) at the frequency of 1.59 rad/s (or 10 Hz) and for different temperatures, starting from the high temperature PG of the bitumen (52 and 58 °C for bitumens PG 52S-34 and PG 58S-28, respectively) and continue with a 6 degrees increment until criterion's failure. $|G^*|$ represents the stiffness of the bitumen, while $\delta$ represents the lag between the applied stress and the material response. According to the standard, the classification of the bitumen is based on the value of the ratio $|G^*|/\sin(\delta)$. It should be higher than 1 kPa at the H temperature of the performance grade (PG) of the bitumen examined. In addition, the value of 1 kPa is used to determine the high temperature ($T_{high}$) of the bitumen. One repetition is planned to perform for this test.

### 3.3.2.6 Multiple Stress Creep Recovery (MSCR) test

The MSCR test evaluates the traffic level (n) class of bitumen, and it is also related to the rutting performance of the bitumen (AASHTO T 350). This test was added recently to the Transports Quebec standard (TQ 4101) that refers to the American standard (AASHTO M 332). The test was carried out on the RTFO residue at two different stress levels: 0.1 and 3.2 kPa. The non-recoverable creep compliance values at the stress level of 3.2 kPa ($Jnr_{3.2}$, $kPa^{-1}$), the difference in non-recoverable creep compliance between 0.1 and 3.2 kPa ($Jnr_{diff}$, %) and the average recovery at 3.2 kPa ($R_{3.2}$, %) were determined at the high (H) temperature grade of the unmodified bitumen. The $Jnr_{3.2}$ value ranges from 0 to 4.5 $kPa^{-1}$ and the lower the value is the better resistance to permanent deformation of the bitumen. The DSR apparatus (Figure 3.20 a) is used to perform the MSCR test using the same geometry of the specimen (25 mm diameter, Figure 3.20 b). Table 3.6 shows the traffic level (n) of the bitumen determined with the parameters of MSCR test according to the standard TQ 4101. One repetition is planned to perform for this test.

Table 3.6 Traffic level (n) class of bitumen determined with the MSCR test specifications

| Traffic level (n) class [a] | $Jnr_{3.2}$ value ($kPa^{-1}$) | $Jnr_{diff}$ (%) [b] | $R_{3.2}$ (%) [c] |
|---|---|---|---|
| Standard (S) | ≤ 4,5 | 75 max. | $\geq 29.371 Jnr_{3.2}^{-0.263}$ |
| Heavy (H) | ≤ 2 | | |
| Very Heavy (V) | ≤ 1 | | |
| Extreme (E) | ≤ 0,5 | | |

[a] The class of bitumen is determined with parameters requirements of MSCR test specified in Transports Quebec standard TQ 4101.
[b] Does not apply to class E bitumen.
[c] Does not apply to bitumens of traffic level S class and is limited to a minimum of 55 % for bitumens with $Jnr_{3.2} < 0.10$ $kPa^{-1}$.

### 3.3.2.7 Bending Beam Rheometer (BBR) test

The BBR test was used to evaluate the performance of the bitumen at low temperatures (AASHTO T 313). Since bitumens are more prone to low temperature cracking with age, this test is performed on PAV residue. Figure 3.21 (a) shows the BBR apparatus used in this

research. In this test, the hot bitumen is poured in a rectangular mold to form the BBR beam (102 mm x 12.5 mm x 6.25) shown in Figure 3.21 (b). The excess of the bitumen on the surface of the beam is trimmed after 45 minutes of cooling down and then the beams are demolded after another 45 minutes of cooling down. The beams are placed in the testing bath and conditioned at the testing temperature for 60 minutes. The load is applied to the bitumen beams to determine the creep stiffness modulus, S(60), and the creep relaxation, m(60), at 60 seconds loading time. Those parameters are used to evaluate the performance of the bitumen at low temperatures. To ensure that the bitumen has a good thermal cracking resistance at temperatures superiors than the L temperature grade, the S(60) value must be lower than 300 MPa and the m(60) value must be higher than 0.3. The low temperature ($T_{low}$) of the bitumen is calculated from the most restrictive of those parameters. Three repetitions are planned to perform for this test.

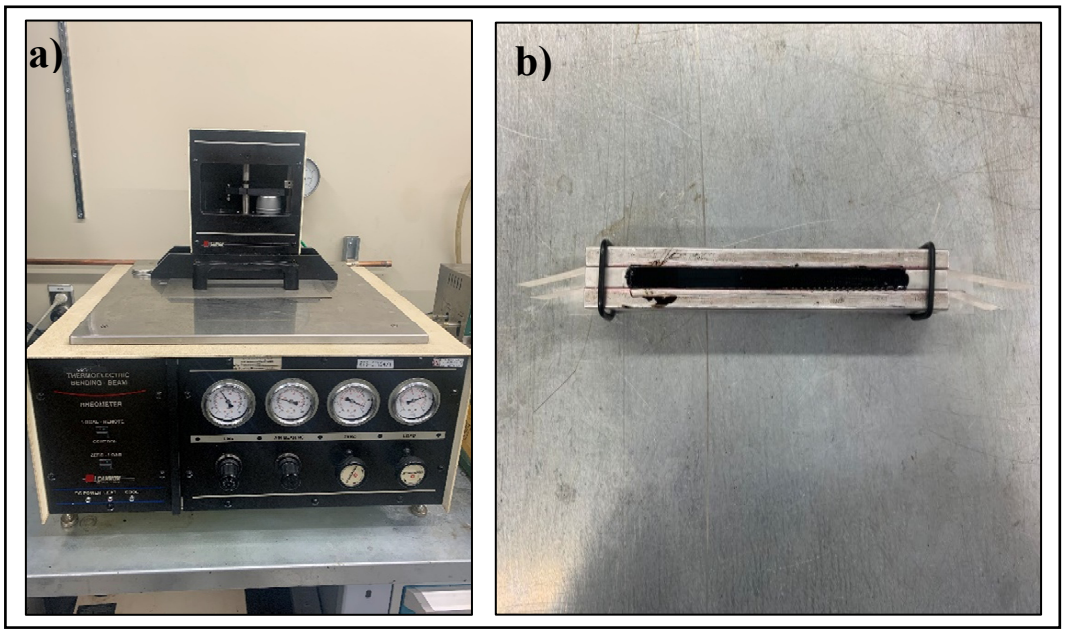


Figure 3.21 Bending Beam Rheometer (BBR) test. A) BBR apparatus,
b) specimen of the beam

### 3.3.2.8 Shear complex modulus G*

The G* tests are performed to characterize the complete linear viscoelastic (LVE) properties of the bitumens. The LVE domain was determined as a prior step to be able to perform the G*

test. To do so, stress-strain curves were obtained at specific temperature and frequency, depending on the G* testing temperatures. In particular, to determine the LVE domain for G* tests at high, intermediate and low temperatures, fixed temperatures were used (40, 4 and -16 °C, respectively) by using specific geometries (25 mm with gap of 1 mm, 8 mm with gap of 2 mm and 4 mm with gap of 2 mm, respectively). The frequency was fixed at 10 Hz. The linearity was determined at which the stiffness decreased to 95 % of its initial value. Following, the G* tests were done at a wide range of temperatures (-30, -18, -6, 0, 10, 22, 34, 46, 58, 70 and 82 °C) and frequencies (10, 8, 6, 4, 2, 1.59, 0.9, 0.7, 0.5, 0.3 and 0.1 Hz). The geometries 25, 8 and 4 mm are shown in Figures 3.20 b and 3.22 a and b, respectively. The chosen rheological model and its graphical representations used to analyze the test results are mentioned in section 3.3.3.3 (complex modulus E* for HMA). One repetition is planned to perform for this test.

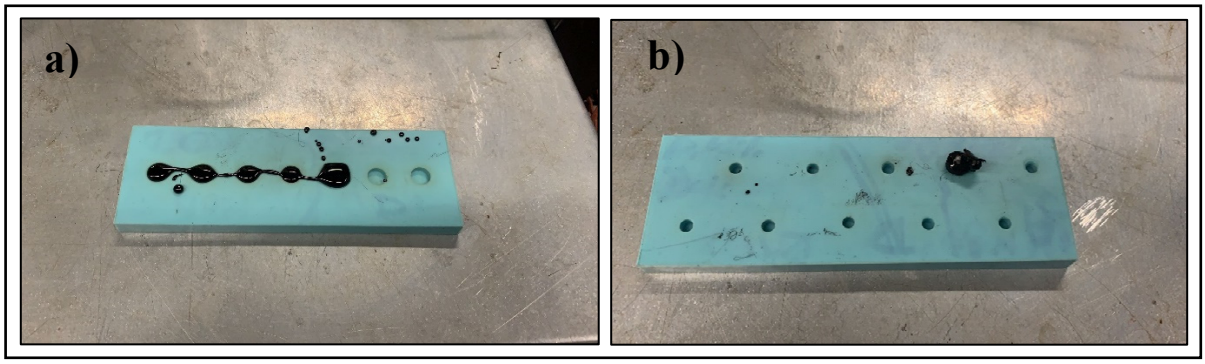


Figure 3.22 Mold for the specimen preparation for G*. a) 8 mm, b) 4 mm geometry used for G* test

### 3.3.2.9 Fourier transform infrared (FTIR)

The FTIR technique was employed to obtain an infrared spectrum of emission or absorption of the lignin. The basis of the chemical composition of the lignin could be provided by the FTIR. More precisely, FTIR is used to determine the components and identify the compounds of the material. It can also be used to highlight if there are new spectra that refers to a new produced component. Data of high spectral resolution could be collected over a wide range (from 10 000 to 400 $cm^{-1}$ wavelength). In this test, the absorbed monochromatic light beam by the specimen is measured. The spectroscopy of FTIR detects functional groups of the specimen

such as N-H, O-H, C-H, C = O, C = C, and C = N. For this purpose, one drop of the bitumen was poured on a thin glass plate to be tested. Figure 3.23 (a) and (b) show the FTIR spectroscopy and the prepared specimen for the test, respectively. One repetition is planned to perform for this test. From the FTIR spectrum, the carbonyl (C=O at 1700 $cm^{-1}$ wavenumbers) and sulfoxide (S=O at 1030 $cm^{-1}$ wavenumbers) indices can be determined by calculating the area under the corresponding peak relatively to a 2-endpoint baseline.

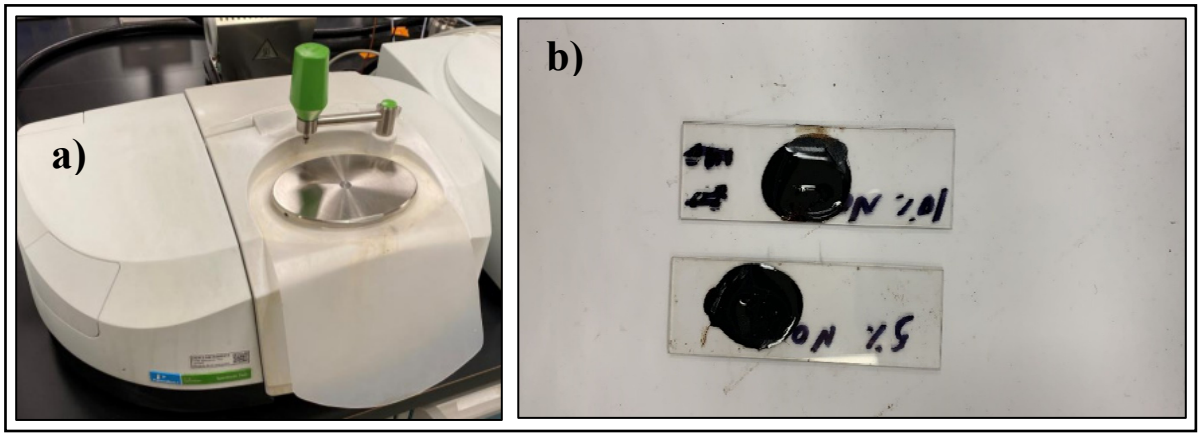


Figure 3.23 Fourier transform infrared (FTIR). a) FTIR spectroscopy apparatus, b) drop of bitumen on a thin glass plate

### 3.3.3 Compactability, rheological properties and thermomechanical performance tests of HMA

This section includes the tests performed on the HMA in order to evaluate the effects of lignin addition on the viscosity, rheological properties and thermomechanical performance at high, intermediate and low temperatures. These tests are shear gyratory compaction (SGC), complex modulus (E*), moisture sensitivity, rutting resistance, thermal stress restrained specimen TSRS for thermal cracking resistance and fatigue cracking resistance.

For the HMA preparation, the aggregates were separated by the mechanical separator in order to have equal portions for each type of the aggregate. Then the aggregates were placed in the oven at 15 °C higher than the mixing temperature (measured using DSR, Reinke method) for around 24 hours. For the bitumen, the oven was programmed to run at the mixing temperature

for 3 hours. The lignin was added, at room temperature, to the bitumen (wet process) or directly to the HMA (dry process). All accessories (bowl, mixer, spoon and pans) that are needed for the mixing process are placed in the oven at the aggregate temperature. A countertop mixer, Hobart model A200, (Figure 3.24 a) was used to prepare the HMA specimens for SGC, moisture sensitivity and moisture-induced damage tests. A thermo-regulated (TR) mixer (InfraTest model 30 l) (Figure 3.24 b) was used to prepare the HMA slabs for the E*, rutting and fatigue tests.


Figure 3.24 Mixers used in this study. a) Hobart model A200 countertop mixer, b) Thermoregulated TR (InfraTest model 30 l) mixer

### 3.3.3.1 Shear gyratory compaction (SGC) test

The SGC test was employed to evaluate the compactability of the modified HMA with lignin (LC 26-003). There are three test standards that are associated with this test; LC 25-007 (Section 3.3.2.3), LC 26-045 and LC 26-010. LC 26-045 is used for the measurement of the maximum theoretical specific gravity $G_{mm}$, while LC 26-010 is used for the separation (reduction) of the HMA specimen. The separation process was done with a sample splitter in

order to obtain two equal portions of HMA. In the first step of the separation process, the difference between the two portions should be less than 3 %, and less than 5 % for the other steps until the end of the process. Upon the completion of the mixing and separation processes, the HMA specimen is placed in the oven at the compaction temperature $T_c \pm 2$ °C (measured using DSR, Reinke method) for a minimum of 30 minutes and a maximum of 2 hours. Then, the specimen was placed in the preheated cylindrical mold at the $T_c$. The test starts to compact the HMA specimen that is placed in an inclined mold of about 1.25° with respect to the horizontal axis. The machine applies a pressure of 600 kPa while rotating at 30 gyrations per minute. The height of the specimen is determined after each gyration in order to calculate the air voids content and the test stops after 200 gyrations. Figure 3.25 (a) and (b) show the scheme of the SGC test and the gyratory shear press, respectively. The compaction curve between the air voids content (%) with the number of gyrations (N) in semi-logarithmic scale can be obtained. According to the LC-4202 requirements for ESG-10, the air voids content at 10 gyrations should be higher than 11 %, between 4 and 7 % at 80 gyrations and higher than 2 % at 200 gyrations. Three repetition is planned to perform for this test.

In this research program, the CEI is calculated between gyration number 10 and the number of gyrations required to reach the target air voids of 5.5 % (average of 4 and 7 %). Herein, to compare the CEI results, it is not useful to consider the area below the target air voids. Therefore, an equation characterized by the parameters $V_m$ (10) and (K) could be used:

$$CEI = \frac{(Vm(10) - Vm.t)^2}{2\ x\ |k|} \tag{3.1}$$

where CEI is compaction energy index, $V_m$ (10) is the air voids in the mix at N=10, $V_{m.t}$ is the target air voids in the mix (5.5 %) and K is the slope of the compaction curve.

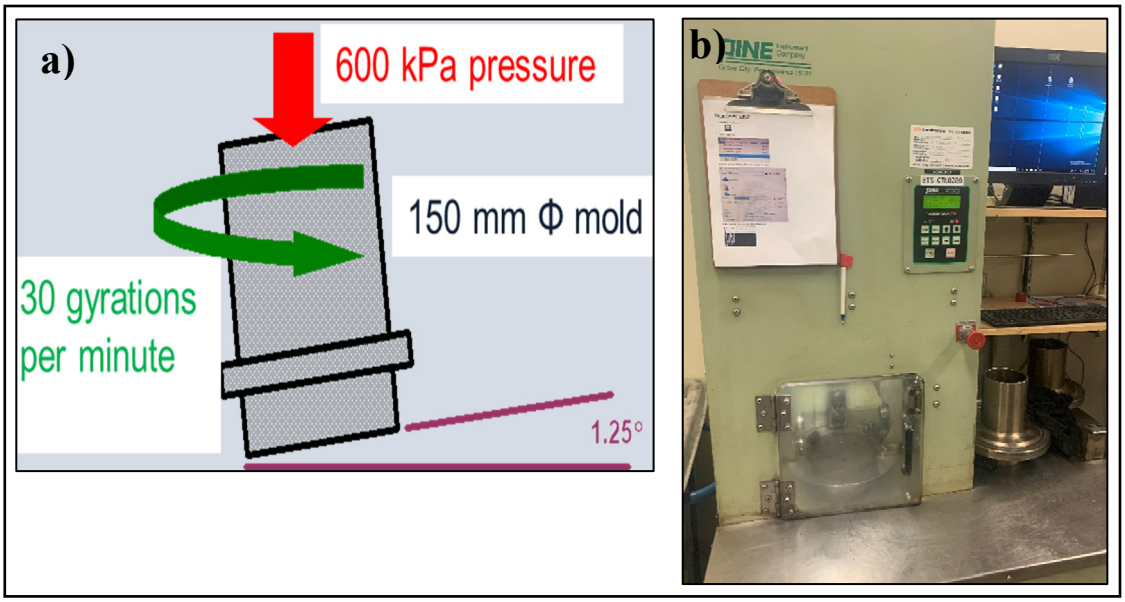


Figure 3.25 Shear gyratory compaction (SGC) test. a) scheme of the SGC test, b) gyratory shear press

### 3.3.3.2 Maximum theoretical specific gravity (Gmm) test

The $G_{mm}$ (LC 26-045) value is needed to determine the required mass for the SGC test. This test is performed on loose (uncompacted) HMA (Figure 3.26). The loose HMA was placed in the oven at $T_c \pm 2$ °C for 2 hours and then cooled down at the room temperature. In order to have the $G_{mm}$ value, the air trapped in the specimen is removed while being subjected to a partial vacuum. For the vacuuming process, the glass container was filled with water of about 2.5 cm above the HMA specimen surface and the process had been conducted for 10 minutes, one minute without shaking and 9 minutes with shaking. Three masses are required to calculate the $G_{mm}$ value. The dry mass of the specimen (at least 1000 g for ESG-10), the mass of the glass container filled with water and its cap and the mass of the specimen and the glass container filler with water and its cap. The last mass should be measured after the vacuuming process. The temperature of water should be 25 ± 0.5 °C. Two repetitions are planned to perform for this test.

Figure 3.26 Loose HMA specimen used for $G_{mm}$

### 3.3.3.3 Complex modulus (E*)

This test method was employed to evaluate the rheological properties of the HMA within the linear viscoelastic LVE domain at a wide range of temperatures and frequencies. The tests done are based on the Laboratoire sur les Chaussées et les Matériaux Bitumineux (LCMB) methodology which is similar to the LC 26-700 method from the MTQ. The standard LC 26-690 was used for the production of the HMA specimens using Laboratoire des Ponts et Chaussées (LPC) compactor. Two specimens (75 ± 1 mm in diameter and 135 ± 1.5 mm in height) were extracted from the compacted slab (500 mm x 180 mm x 100 mm) by LPC compactor. The specimens were placed in a sand container to avoid any deformation and cured for two weeks at room temperature and then the air voids content was measured for each specimen. The test was performed by applying cyclic tension-compression load on the specimen. This test can be performed under stress or strain control mode, but in this research program, the strain control mode was employed. The test was performed at a wide range of temperatures (-35, -25, -15, -5, 5, 15, 25 and 35 °C) and frequencies (10, 3, 1, 0.3, 0.1, 0.03 and 0.01 Hz). One repetition is planned to perform for this test. The 2S2P1D rheological model was used to analyze and evaluate the viscoelastic behaviour of the HMA in the LVE domain. The graphical representations of the 2S2P1D model, Cole-cole diagram and master curves of the norm of complex modulus |E*| and phase angle φ, were employed.

### 3.3.3.4 Moisture sensitivity tests

In this section, two tests are employed to evaluate the resistance to the moisture or the water damage. The tests are the moisture sensitivity LC 26-001 and moisture-induced damage AASHTO T 283. Both tests provide valuable information for ensuring durability and improving the resistance of HMA to common distress modes such as cracking and moisture damage. They also provide a more comprehensive understanding of the HMA performance characteristics by focusing on stability, flow and tensile strength of HMA.

For the moisture sensitivity test, the associated tests standards are LC 26-020, LC 26-040 and LC 26-060. LC 26-020 was used for the preparation of the Marshall specimens by the Marshall compactor (Figure 3.27 a). The specimens were placed in the oven at $T_c \pm 2$ °C for 2 hours before being compacted. After 24 hours of curing time of the compacted specimens at room temperature, the specific gravity for each specimen was measured according to LC 26-040. The air voids content of the specimens was determined and specimens were grouped into two subsets of three specimens having approximately equal average of the air voids content. The specimens in the first subset were subjected to the vacuuming process and then soaked directly in a water bath without contacting the air for 24 hours at 60 ± 1 °C. This condition allows the specimens to undergo accelerated aging by soaking (LC 26-001). The specimens in the second group were placed in a water bath for 30-40 minutes at 60 ± 1 °C. The test was performed at 25 °C after the conditioning of the specimens. LC 26-060 was used to determine the resistance to the deformation by applying a constant speed of load to the jaw of the Marshall apparatus (Figure 3.27 b). The maximum carried load by the specimen is called Marshall stability. The ratio of the average Marshall stability of the soaked specimens divided by the average Marshall stability of the non-soaked specimens is called stability retained or water resistance (WR). To meet the standard requirement, the WR should be higher than 70 %. The moisture-induced damage test includes one cycle of freeze and thaw. An indication of the cracking resistance at low temperatures could be obtained. After mixing, the specimens were cooled down at the room temperature for 2 hours and cured in the oven at 60 °C for 24 hours. The temperature was increased to the $T_c$ for 2 hours. The gyratory shear press was used to compact eight

specimens in order to obtain 7 ± 0.5 % air voids. The compacted specimens were cooled down at the room temperature for 2 hours before being extracted from the mold. The fan was employed to accelerate the cooling process. The specimens were stored at room temperature for 24 hours. The eight Marshall compacted specimens were grouped into two subsets of four specimens having approximately equal average of the air voids content. The specimens in the first subset, which is called conditioned subset, were subjected to a vacuum saturation for 5-10 minutes until obtaining 70-80 % of degree of saturation. The saturated specimens were wrapped with a plastic film and placed in a plastic bag containing 10 ml of water and then placed in the freezer at -16 °C for 18 hours. The plastic bags were removed and the specimens were placed in the water bath at 60 °C for 24 hours. Finally, before starting the test, the specimens were placed in another water bath at 25 °C for 2 hours. The specimens of the dry subset were wrapped with plastic in a heavy-duty, leakproof plastic bag, and then they were placed in the water bath at 25 °C for 2 hours. The load was applied to the specimen by forcing two steel loading strips together at a constant rate of 50 mm per minute (Figure 3.28). The maximum carried load by the specimen is called indirect tensile strength ITS. The indirect tensile strength ratio ITSR at 25 °C was calculated by dividing the average ITS for the conditioned subset by the average ITS for the dry subset.


Figure 3.27 Marshall compaction. a) Marshall compactor,
b) Marshall specimen during the test

Figure 3.28 Marshall specimen during the indirect tensile

### 3.3.3.5 Rutting resistance test

In this test method, the HMA slab undergoes the repeated load of 5 KN to evaluate the rutting performance of the HMA at high temperature (LC 26-410). The LC 26-400 was used for the production of the slabs using the LPC slab compactor (Figure 3.29 a). In addition, this test provides an appreciation of the stress and temperature conditions that are applied on the asphalt pavement (Moghaddam et al., 2011; Perraton et al., 2011). The TR mixer was used to produce 25 kg of HMA for two slabs, each of 500 mm x 180 mm x 50 mm, and then they were compacted by LPC compactor. The slabs were cured at room temperature for 48 hours and the specific gravity of each slab was measured at the end of the curing time. The French Laboratory Rut Tester FLRT (Figure 3.29, b and c) was employed to perform the tests. According to the test standard (LC 26-410), the testing temperature should be 58 ± 2 °C for the asphalt binder PG 58 n-L. FLRT measures the rutting of two slabs that are subjected, at the same time, to the loaded wheel that moves back and forth at a sinusoidal rhythm, including rutting. At the beginning of the test, 1000 cycles were applied at the room temperature to complete the installation of the HMA specimens in the mold and the rut depth as an average of 15 different points was measured. After, the rut depth was measured as an average of 15 different points on the surface after applying 1000, 3000, 10 000 and 30 000 cycles at 58 °C. The plot of the average rut depth of the two slabs in percent with the number of loading cycles could be

obtained. According to the requirements of the standard, the average of the rut depth after 1000 and 3000 cycles should be less than 10 % and 20 %, respectively.

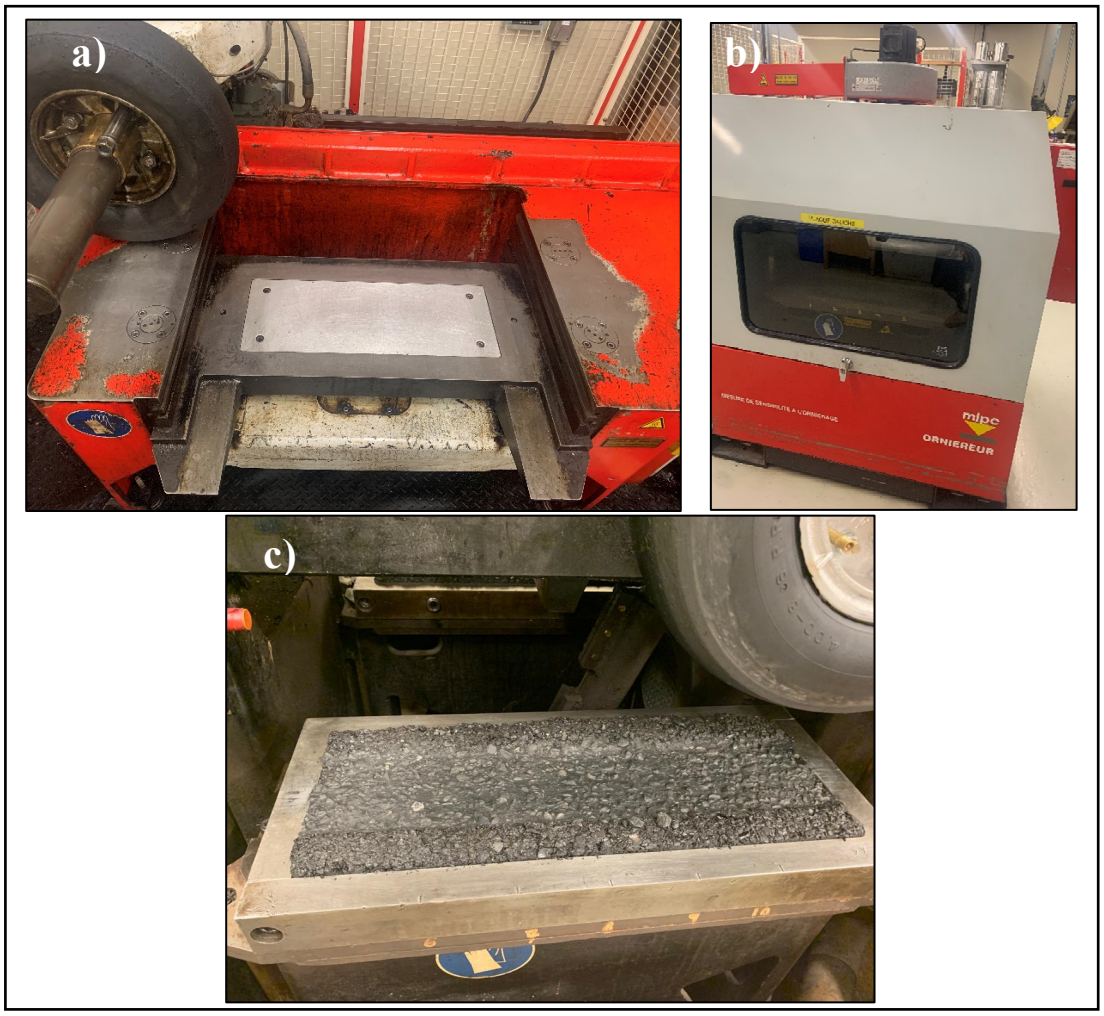


Figure 3.29 Rutting resistance test. a) LPC plate, b) rut tester, c) zoom on the loaded wheel

### 3.3.3.6 Thermal stress restrained specimen test (TSRST)

This test method was used to evaluate the resistance to the low temperature thermal cracking of the HMA (AASTHO TP 10). Three specimens were extracted from the SGC specimen, each of 51±1 mm in diameter and 115±2 mm in length. This is different from the test standard (60±5 mm in diameter and 250±5 mm in length). The specimens were placed in a sand container to avoid any deformation and cured for three weeks and then the air voids were

measured. The two ends of the specimen were glued with slow setting epoxy to the aluminum platens in two stages. The bench stage which was performed for four hours. The other end was glued in the Material Testing System MTS 858 press directly (Figure 3.30 a). A low force of 40 N was applied on the specimen for 4 hours at room temperature. This gluing condition allows the specimen to obtain a perfect alignment with the press. Upon the completion of the gluing process, the specimen was conditioned for 6 hours at 5 °C and then the temperature inside the thermal chamber starts to decrease at a cooling rate of 10 °C/hour measured at the surface of the specimen while the specimen is kept restrained from the longitudinal contraction. The thermal stress inside the HMA specimen starts to build up and increase over the time until it exceeds the strength of the HMA. The specimen starts to crack until breakage and then the test stops automatically (Figure 3.30 b). The evolution of the thermal stress with the decrease of the temperature can be obtained. It is very important to check the starting temperature of the test to better evaluate the relaxation properties of the HMA. According to the evolution of the curve of the thermal stress, the maximum carried thermal stress at the breakage point is called fracture strength ($S_T$) and the associated temperature with $S_T$ is called fracture temperature ($T_F$). The temperature at which the material changes its behavior from viscoelastic to elastic, or vice versa, is called glass-transition temperature (Tg).

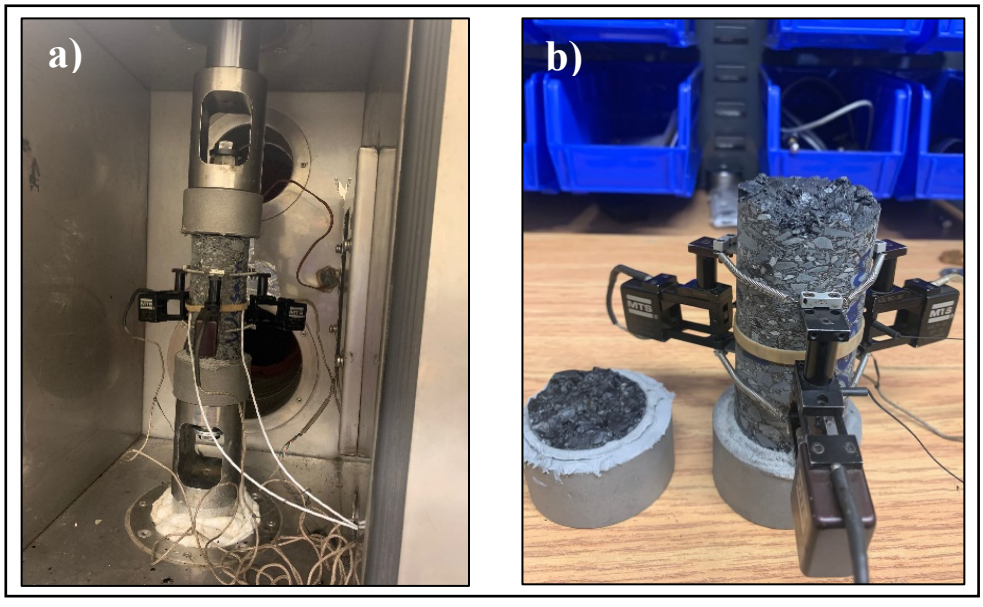


Figure 3.30 Thermal stress restrained specimen test (TSRST) a) specimen inside the thermal chamber, b) broken specimen after the test

#### 3.3.3.7 Fatigue test (DGCB method)

This test was performed to simulate the behaviour of the HMA under actual loads. In this research program, the fatigue behaviour of the HMA was investigated by the uniaxial tension-compression test in strain-controlled mode according to the DGCB method (Département de Génie Civil et Bâtiment) developed at the ENTPE (École Nationale de Travaux Publics de l'État, (Lyon, France)). The preparation of the tested specimens (75 ± 1 mm in diameter and 135 ± 1.5 mm in length) is explained in the E* test (Section 3.3.3.3). The same specimens that were used for the E* tests, are utilized for the fatigue tests since E* is actually a non-destructive test. The test was performed at one temperature and one frequency (10 °C & 10 Hz) and at four strain amplitudes (80, 90, 100 and 120 μm) to develop the Wöhler curve. Two repetitions at each strain amplitude are planned for this test. The results are presented in annex III.

### 3.4 Field sections

In the summer of 2021, four different field sections with HT SW A 1 lignin modified asphalt mixes were built in Canada. Two sections were constructed in the province of Quebec while another one in Ontario and a fourth one in Alberta. Two different processes were used, which are dry and wet process. The amount of lignin from 5 % to 20 % by the weight of asphalt binder was added. Reclaimed asphalt pavement (RAP) content of 10 % was used in Alberta's trial section. For all trials, the aggregates were heated for 30 seconds then the asphalt binder was added and the mixing process was continued for another 30 seconds. This section is presented in annex I where the details are shown such as the dimensions of the field sections for the unmodified and lignin-modified HMA, asphalt binder type, compaction process, number of passes and HMA type. In addition, some photos taken during the construction works are shown.

# CHAPTER 4

# LIGNIN INCORPORATION PROCESS IN BITUMEN

## 4.1 Introduction

This chapter presents the study of the incorporation process of lignin powder and pellets into bitumen. This process is called the wet process. As stated in chapter 2, through the research in the literature, the information about the incorporation process is limited. In other words, there is almost no information on how the lignin is precisely added to the bitumen and the effects of each parameter on the incorporation process, especially the temperature, speed and duration. Therefore, a study considering these issues was done on one type of lignin in order to better understand the incorporation process of lignin in bitumen.

In this chapter, the methodology used to incorporate HT SW A 1 (available in higher amount among than the other types) lignin in powder form into bitumen is first presented. Based on the results of this study, the parameters of the incorporation process for the other types of the lignins and pellets were selected. The incorporation of an inert filler is also discussed in order to compare the lignin-modified bitumen properties with a common filler.

As mentioned in chapter 3 (section 3.2.3), the base bitumen used in this research program is without polymers. This is to avoid seeing any effects other than lignin since it is a biopolymer product. Therefore, it is important to note that the results presented in all chapters should not be assumed for polymer-modified bitumen.

However, the modification of the bitumen needs to be followed by a quality control process that was, here, separated in two steps. Accordingly, upon the completion of the incorporation process, all lignin-modified bitumens were verified in terms of the stability and homogeneity through performing the storage stability test and with microscope observations. Figure 4.1 shows the different steps and the objective of each step.

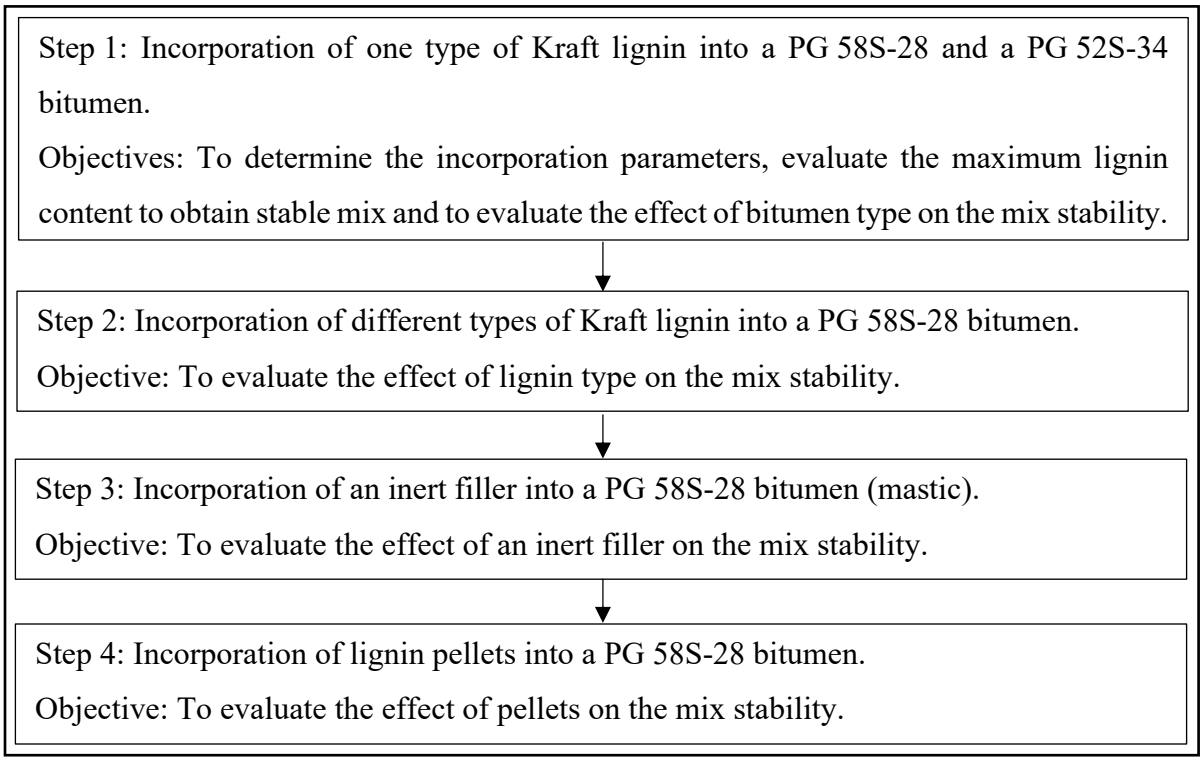


Figure 4.1 Summary of the different steps and the objective of each step

## 4.2 Preparation of the lignin-modified bitumen

This section presents the preparation of the modified bitumens with different types of the lignin in powder form or pellets, and an inert filler (mastic). Three main parameters (temperature, speed and duration) of the incorporation process are discussed. The storage stability tests were performed on the mentioned materials, and the effect of each parameter of the incorporation process is discussed. It should be noted that despite the fact that there is no mention of repetitions in the storage stability test, two repetitions were performed on each material.

The detailed study of the incorporation process that includes the change of the different parameters used in the incorporation process is presented in section 4.2.1, while the part of the study on the incorporation of different lignins into the bitumen is shown in section 4.2.2. This is followed by section 4.2.3 where the incorporation of an inert filler in the bitumen is studied. This is done to investigate if the added lignin, in powder form, behaves like a filler or like a

binder. The last part, section 4.2.4, shows the incorporation of the pellets (HT SW A 1 lignin powder + soybean oil) into the bitumen.

All lignins in powder form and the inert filler were incorporated into the bitumen by using an IKA RW16 basic overhead stirrer: classified as a low shear mixer (LSM). While the pellets-modified bitumens were prepared by using LSM and high shear mixer (HSM) (section 2.4.2). For the pellets, the LSM and HSM are used since the results for LSM are not conclusive. As a prior step to the incorporation process, the bitumen was heated to 165 ± 5 °C, according to the findings from the previous studies (Xu et al., 2017; Batista et al., 2018; Pérez et al., 2019; Zhang et al., 2019; Gao et al., 2020; Norgbey et al., 2020).

For the incorporation process, a beaker of 1000 ml was partially filled with the preheated bitumen and, afterwards, the lignin or pellets were added to the bitumen. Herein, it is worth mentioning that the added lignin powder or pellets were not heated since the moisture content is low (≈1 %) for both (Table 3.2 or 3.3). For some types of the lignin in junk shape, the moisture content was measured and found to be 12-14 %, which made the bitumen foam (as observed visually). So, it was necessary to dry the lignin before incorporating it into the bitumen.

### 4.2.1 Study of the incorporation lignin HT SW A 1 into the bitumen

The conducted study on the incorporation process was done on the first type of lignin powder that is shown in Table 3.1 (HT SW A 1). Based on the findings from this study, the parameters of the incorporation process were selected for the preparation of the modified bitumens with different lignins. This study was divided into three steps. In the first step, 20 % lignin contents were incorporated into the bitumen PG 58S-28 which was used for all mixes in this chapter. The lignin content (e.g. 20 %) represents a percentage of the total weight of the mix (bitumen and lignin). The incorporation temperature and speed were fixed at 165 ± 5 °C and 1000 ± 20 rotations per minute (rpm), respectively. During the mixing, the temperature of the bitumen was maintained constant by a hot plate. For the incorporation duration, three different durations

(15, 60 and 90 minutes) were used. The reason behind those selected durations was that most of the above-mentioned studies (section 4.2) used 60 minutes duration. So, it was decided to select lower (15 minutes) and higher (90 minutes) durations in addition to 60 minutes. For the comparison purpose, one mix was done manually for 60 minutes.

In the second step, three different lignin contents (10, 20 and 30 %) were incorporated into the bitumen. According to the previous studies (Gao et al., 2020), the effect of the lignin is not significant when the content is low (5-8 %). So, it was decided to start with 10 % and keep an increase of 10 % until observing storage stability issues which is not the case for 30 % lignin content at high incorporation temperature (165 ± 5 °C) and, therefore, the increase in percentage was continued in the third step. Regarding the incorporation temperature, in addition to the selected one (165 ± 5 °C) from to the previous studies, another lower temperature was selected (140 ± 5°C). The reason behind this selected temperature, and not lower, is to avoid some issues during the incorporation process such as the low workability (higher viscosity at lower temperature than 140 ± 5 °C) and safety problems (related to the mixer). This step is to evaluate the effect of the temperature on the incorporation process. In this step, the mix was continued for 15 minutes at 900 ± 20 rpm for 10 % lignin content and 1000 rpm for 20 and 30 % lignin contents. In the third step, higher lignin content (50 %) compared to those in the first and second steps was incorporated into the bitumen at temperatures of 140 ± 5 and 165 ± 5 °C with a speed of 1100 ± 20 rpm. The maximum speed of the model of the mixer is 1200 rpm which was not reached due to safety purpose (vibration of the whole mixer). Two different durations were used for these mixes (30 and 60 minutes). The incorporation duration for all mixes starts when all amounts of lignin is incorporated into the bitumen. Following, storage stability tests and microscope observations were performed to check the stability and homogeneity of the lignin-modified bitumen. Moreover, the dispersion of the lignin particles over the bitumen, the tendency of these particles to form clusters and the decomposition of the lignin particles are presented in details by using the morphological analysis of the microscope images (section 4.2.5). Also, these tests were employed to evaluate the effects of different conditions of the incorporation process on these properties (stability and homogeneity). Two repetitions were performed for each test of the storage stability.

During the initial stages of the lignin incorporation process in bitumen, great care was taken to avoid losing lignin. Since lignin has a low density, it's volume can be significant when high content (by mass) is used. Consequently, the lignin was added gradually, for 30 and 50 % of lignin content, and the mixer speed was reduced to avoid lignin being blown out of the mixing pot, and also to avoid bitumen from splashing. As a general guideline, it is advisable to consider these measures as safety precautions during the incorporation process. Based on the visual observation during the incorporation process, the speed was adjusted until it reached the final speed (900, 1000 and 1100 rpm for 10, 20 and 30 and 50 % lignin content, respectively). In other words, the selected incorporation speed is affected directly by the lignin content which governs the viscosity of the bitumen. Table 4.1 shows the summary for all prepared mixes and tests done in this study.

Table 4.1 Summary of the prepared mixes by LSM and tests done to study the incorporation process of lignin HT SW A 1 into the bitumen PG 58S-28

<table>
<tr><td colspan="6">Step 1</td></tr>
<tr><td>Lignin content (%) [a]</td><td>Incorporation temperature (± 5 °C)</td><td>Incorporation duration (± 1 min.)</td><td>Incorporation speed (± 20 rpm)</td><td>Storage stability</td><td>Microscope observation</td></tr>
<tr><td>0</td><td>-</td><td>-</td><td>-</td><td rowspan="5">✓</td><td>✓</td></tr>
<tr><td rowspan="4">20</td><td rowspan="4">165</td><td>15</td><td rowspan="3">1000</td><td>-</td></tr>
<tr><td>60</td><td>✓</td></tr>
<tr><td>90</td><td>-</td></tr>
<tr><td>60</td><td>manually</td><td>-</td></tr>
<tr><td colspan="6">Step 2</td></tr>
<tr><td>10</td><td rowspan="3">140 & 165 [b]</td><td rowspan="3">15</td><td>900</td><td rowspan="3">✓</td><td rowspan="3">✓ [c]</td></tr>
<tr><td>20</td><td rowspan="2">1000</td></tr>
<tr><td>30</td></tr>
<tr><td colspan="6">Step 3</td></tr>
<tr><td rowspan="2">50</td><td>140</td><td rowspan="2">30 & 60</td><td rowspan="2">1100</td><td rowspan="2">✓</td><td rowspan="2">✓ [d]</td></tr>
<tr><td>165</td></tr>
<tr><td colspan="6">[a] Lignin content (%) by the total weight of the mix (bitumen and lignin).<br>[b] The mix of 20 % lignin at 165 °C was prepared in the first step.<br>[c] The microscope observations were performed for the mixes prepared at 165 °C.<br>[d] The microscope observation was not performed for the mix prepared at 140 °C for 60 minutes.</td></tr>
</table>

#### 4.2.1.1 Storage stability tests results of the study on the incorporation process of lignin into bitumen

This section presents the storage stability tests results of the unmodified and modified bitumen with HT SW A 1 lignin. The coefficient of variation (COV) value is low for all repetitions (less than 1.0 %) and, according to the ASTM C 670 standard, it is located within the maximum acceptable range. This applies for the storage stability tests results shown in the next sections. Table 4.2 shows the results for the two repetitions of the storage stability tests of the conducted study on the prepared mixes of the modified bitumen PG 58S-28 with the lignin HT SW A 1 (section 4.2.1, Table 4.1). Mixes are considered stable if the storage stability result is less than 2.0 or 2.2 °C according to standards LC 25-003 and ASTM D 5892, respectively.

In the first step, the storage stability tests results show stable lignin-modified bitumen for each incorporation duration (maximum storage stability value of 0.5 °C). This indicates, indirectly, that the lignin particles are homogeneously spread in the bitumen. The convergence of the density values for bitumen and lignin, approximately 1.0 g/cm$^3$, helps to obtain a stable lignin-modified bitumen. In other words, the lignin stays in suspension within the bitumen. It is interesting that the manual incorporation of the lignin for 60 minutes resulted in a stable lignin-modified bitumen. So, the incorporation of the lignin powder into the bitumen can be done without using advanced equipment. However, according to the tests results in this step, the incorporation duration does not seem to be a key parameter in the incorporation process of 20 % lignin content. Therefore, in order to reduce the energy consumption during the incorporation process, the shortest incorporation duration (15 minutes) was selected for all mixes in the next step.

In the second step, it can be seen that the incorporation temperature has a significant impact on the stability and homogeneity of the lignin-modified bitumen. In particular, the stability of the modified bitumen with 30 % of lignin at 140 °C is negatively impacted by the lower temperature compared to the stability of the mix which was incorporated at 165 °C. In other words, the use of 140 °C as an incorporation temperature resulted in unstable modified bitumen with 30 % of lignin (storage stability value is 2.6 °C which is higher than 2.0 or 2.2 °C). This

finding might be due to the low workability (high viscosity) of the mix and, therefore, the lignin particles may tend to form clusters within the modified bitumen. As a consequence, lignin particles are collected at the bottom of the tube, which indicates that the mix is not stable. On the other hand, the incorporation temperature did not show an effect on the stability of the modified bitumen with 10 % lignin. However, the incorporation temperature of 165 °C was selected to be employed in the incorporation process. Higher incorporation temperature than 165 °C for this lignin content (30 %) was not tried in order to avoid the decomposition of the lignin particles (Table 3.2).

In the third step, as expected, incorporation of high lignin content (50 %) at low incorporation temperature (140 °C) resulted in unstable mix (storage stability of 5.0 °C). This is observed at the lower incorporation temperature (140 °C) used in this study (Table 4.2). Accordingly, this might indicate that the bitumen is not liquid enough to mix the lignin and, therefore, lignin particles are adjoining each other forming a cluster that falls, by its self weight, at the bottom of the tube causing a separation between the lignin and bitumen. On the other hand, incorporation of 50 % lignin at higher temperature and longer duration (165 °C and 60 minutes, respectively) resulted in stable and homogeneous mix compared to what was incorporated for 30 minutes at 165 °C. Regarding the incorporation speed, it was not found to have an impact on the stability of the lignin-modified bitumen. It is mostly governed by the viscosity of the bitumen; the more lignin content the more viscous bitumen. In general, the incorporation of the lignin powder into the bitumen is possible with simple equipment such as LSM and hot plate. Therefore, it was decided to not use more developed equipment such as HSM. To this end, based on the findings of this study, specific values for the parameters of the incorporation process done by LSM are selected for all the following lignin-modified bitumen. In particular, the incorporation temperature and duration are 165 °C and 15 minutes, respectively. For the incorporation speed, 900 ± 20 rpm is selected for 10 % lignin content and 1000 rpm for higher contents.

Table 4.2 Storage stability tests results of the study on the incorporation process of the lignin HT SW A 1 into the bitumen PG 58S-28

| Step 1 | | | | | | | |
|---|---|---|---|---|---|---|---|
| Lignin content (%) | Temperature (± 5 °C) | Duration (± 1 min.) | Speed (± 20 rpm) | Softening point (SP) (°C) | | Storage stability (°C) | Avg. of storage stability (°C) |
| | | | | Top | Bottom | | |
| 0 | - | - | - | 41.1 | 40.8 | 0.3 | 0.5 |
| | | | | 41.3 | 41.9 | 0.6 | |
| 20 | 165 | 15 | 1000 | 44.2 | 43.3 | 0.9 | 0.5 |
| | | | | 44.4 | 44.5 | 0.1 | |
| | | 60 | | 43.9 | 44.0 | 0.1 | 0.1 |
| | | | | 44.8 | 44.9 | 0.1 | |
| | | 90 | | 44.1 | 44.5 | 0.4 | 0.4 |
| | | | | 44.6 | 44.9 | 0.3 | |
| | | 60 minutes (manually) | | 45.0 | 45.2 | 0.2 | 0.2 |
| | | | | 44.9 | 45.1 | 0.2 | |
| Step 2 | | | | | | | |
| 10 | 140 | 15 | 900 | 42.5 | 43.3 | 0.8 | 0.5 |
| | | | | 43.6 | 43.8 | 0.2 | |
| | 165 | | | 42.1 | 42.9 | 0.8 | 1.0 |
| | | | | 41.7 | 42.8 | 1.1 | |
| 20 | 140 | | 1000 | 47.0 | 45.0 | 2.0 | 2.1 |
| | | | | 46.9 | 44.7 | 2.2 | |
| 30 | 140 | | | 48.3 | 50.8 | 2.5 | 2.6 |
| | | | | 48.5 | 51.1 | 2.6 | |
| | 165 | | | 46.0 | 46.1 | 0.1 | 0.1 |
| | | | | 46.6 | 46.7 | 0.1 | |
| Step 3 | | | | | | | |
| 50 | 140 | 30 | 1100 | 64.8 | 63.9 | 0.9 | 5.0 |
| | | | | 61.8 | 70.8 | 9.0 | |
| | | 60 | | 56.5 | - [a] | - [a] | - [a] |
| | | | | 56.9 | - [a] | - [a] | |
| | 165 | 30 | | - [b] | 61.2 | - [b] | - [b] |
| | | | | 61.4 | 62.2 | 0.8 | |
| | | 60 | | 60.3 | 59.6 | 0.7 | 0.4 |
| | | | | 60.1 | 60.2 | 0.1 | |

[a] The mix could not be poured and tested due to the collected specimen at the bottom of the tube (unstable mix).
[b] The sample was lost during the test.

After conducting this study, the same lignin (HT SW A 1) was incorporated into the bitumen PG 52S-34 in order to evaluate the effects of the lignin on the stability and homogeneity of another (different) unmodified bitumen. Three different contents of lignin HT SW A 1 (10, 20 and 30 %) were incorporated at a temperature of 165 ± 5 °C for 15 minutes with a speed of 900 ± 20 rpm for 10 % lignin content and 1000 rpm for 20 and 30 % lignin contents. Following, the storage stability tests were performed on the modified bitumens. In addition, the stability of the unmodified PG 52S-34, as a reference, was checked. Table 4.3 shows the summary of the modified bitumens and tests done. Two repetitions were performed for each test of the storage stability.

Table 4.3 Summary of the prepared mixes of the modified bitumen PG 52S-34 with lignin HT SW A 1 by LSM and tests done

<table>
<tr><th>Lignin content (%) *</th><th>Incorporation temperature (± 5 °C)</th><th>Incorporation duration (± 1 min.)</th><th>Incorporation speed (± 20 rpm)</th><th>Storage stability</th><th>Microscope observation</th></tr>
<tr><td>0</td><td>-</td><td>-</td><td>-</td><td>✓</td><td>-</td></tr>
<tr><td>10</td><td rowspan="3">165</td><td rowspan="3">15</td><td>900</td><td rowspan="3">✓</td><td rowspan="3">-</td></tr>
<tr><td>20</td><td rowspan="2">1000</td></tr>
<tr><td>30</td></tr>
<tr><td colspan="6">* Lignin content (%) by the total weight of the mix (bitumen and lignin).</td></tr>
</table>

Table 4.4 shows the results for the two repetitions of the storage stability tests of the prepared mixes of different modified bitumen (PG 52S-34) with the lignin HT SW A 1. All lignin-modified bitumens are stable and homogeneous. In addition, no significant difference (maximum of 0.6 °C) between the storage stability values of the lignin-modified bitumens PG 58S-28 and PG 52S-34. Accordingly, the type of bitumen does not seem to affect the stability of the lignin-modified bitumen. To this end, the compatibility and suspensibility of the lignin within the two unmodified bitumens is similar with respect to small differences which can be due to the chemical structure of the base bitumens used.

Table 4.4 Storage stability tests results of the modified bitumen PG 52S-34 with the lignin HT SW A 1

| Lignin content (%) | Temperature (± 5 °C) | Duration (± 1 min.) | Speed (± 20 rpm) | SP (°C) | | Storage stability (°C) | Avg. of storage stability (°C) |
|---|---|---|---|---|---|---|---|
| | | | | Top | Bottom | | |
| 0 | - | - | - | 36.2 | 36.1 | 0.1 | 0.1 |
| | | | | 36.4 | 36.3 | 0.1 | |
| 10 | 165 | 15 | 900 | 38.6 | 38.1 | 0.5 | 0.4 |
| | | | | 38.4 | 38.7 | 0.3 | |
| 20 | | | 1000 | 39.1 | 39.2 | 0.1 | 0.2 |
| | | | | 39.6 | 39.9 | 0.3 | |
| 30 | | | | 42.2 | 42.3 | 0.1 | 0.2 |
| | | | | 43.1 | 42.9 | 0.2 | |

Based on the obtained results, it is possible to have stable lignin modified bitumen, and there is very little difference between the results obtained for bitumen PG 52S-34 with the other bitumen (PG 58S-28). Because of this, the bitumen PG 58S-28 will be used in the following parts of this study since it is the specified bitumen for Montreal's area. In the following section, the incorporation of different types of the lignin into one type of the bitumen (PG 58S-28) is presented. These different types include different properties such as the source of the lignin (hard wood (HW) or soft wood (SW)) and potential hydrogen (pH).

### 4.2.2 Preparation of the modified bitumen with different types of the lignin

All other types of the lignin, including acidic (A) and basic (B) types, were incorporated into the bitumen PG 58S-28 by using LSM. Each type was incorporated with a content of 20 % at a temperature of 165 ± 5 °C for 15 minutes with a speed of approximately 1000 rpm. The lignins HT SW B, TB HW A, TB HW B, K SW A and K SW B (Table 4.5) were grinded and dried twice by the supplier. Accordingly, the incorporation process and the storage stability tests for these lignins were performed three times; for the original version (junk), after the first grinding process and after the second grinding process. Herein, the selected parameters of the incorporation process for the original version of these lignins were used in the incorporation process for the lignins that were produced after the first and second grinding process. It was

necessary to place the junk lignin particles in the oven since these particles made the bitumen foam (12-14 % moisture content) in the first trial of the incorporation into the bitumen. For the lignins HT SW A 2, HT SW A-modified and K SW A-modified, the incorporation process and the storage stability tests were performed once since there was no grinding process done. One repetition was performed for each test of the storage stability. Table 4.5 shows the summary of the preparation of the modified bitumens with the lignins and tests done.

Table 4.5 Summary of the prepared (LSM) modified bitumen PG 58S-28 with 20 % of each type of the lignin and tests done

| Lignin type | Incorporation temperature (± 5 °C) | Incorporation duration (± 1 min.) | Incorporation speed (± 20 rpm) | Storage stability | Microscope observation |
|---|---|---|---|---|---|
| HT SW A 2 | 165 | 15 | 1000 | ✓ | - |
| HT SW B | | | | | |
| TB HW A | | | | | |
| TB HW B | | | | | |
| K SW A | | | | | |
| K SW B | | | | | |
| HT SW A-modified | | | | | |
| K SW A-modified | | | | | |

#### 4.2.2.1 Storage stability tests results of the modified bitumen PG 58S-28 with different types of the lignin

Table 4.6 shows the storage stability tests results of the modified bitumen PG 58S-28 with different types of the lignin before and after the first grinding process. As can be seen, only the modified bitumen with HT SW A 2 lignin is stable. This lignin type is similar to the HT SW A 1 type in terms of the color (dark brown) and pH (3-4). For the other types of lignin, many lignin particles are collected at the bottom of the tube, which indicates that these types of lignin are not stable in the bitumen. This finding might be due to the weight of the junk particles. Herein, it was decided to carry out the grinding process of these particles which was done by the lignin producer at their facility. This decision was taken based on the storage

stability test result of the stable modified bitumen with HT SW A 2 lignin. In other words, the size of the lignin particles might be one of the key parameters to achieve a stable lignin-modified bitumen.

The lignins that were grinded, based on the producer availability, are HT SW B, TB HW A, TB HW B, K SW A and K SW B. Following, the storage stability tests were continued on the modified bitumen with the different lignins after the first grinding process. It is worth mentioning that these types have different particle sizes then the HT SW A 2 lignin. However, as expected, it can be seen in the lower part of Table 4.6 that all mixes are unstable. Figure 4.2 shows the lignin particles fall at the bottom of the tube which indicates that the lignin is not stable in the bitumen. The second grinding process with the target of the fine powder form was done at the same facility.

Table 4.7 shows the storage stability tests results of the modified bitumen with the different lignins after the second grinding process. The lignins HT SW B, TB HW A and TB HW B are stable in the modified bitumen (the maximum storage stability value is 0.8 °C). This finding confirms that the size of the lignin particles affects the stability of the modified bitumen. On the other hand, the modified bitumen with the lignins K SW A and K SW B are unstable mixes. This shows that the stability of the modified bitumen is governed by not only the particles size but also other factors. These factors might be the chemical interaction, molecular weight, pH, densities of the lignin and bitumen and the viscosity of the modified bitumen. In this research program, it is possible that the grinding process affects the properties of the lignin particles due to the energy used to grind these particles. In other words, this energy might affect the electrical charge of the lignin particles.

However, to make sure of the effect of the size of the lignin particles, the size of the particles was measured for A and B lignins that were produced after the first and second grinding process, including the lignins HT SW A-modified and K SW A-modified (Figure 4.3).

Table 4.6 Storage stability tests results of the modified bitumen PG 58S-28 with different types of the lignin before and after the first grinding process

| Grinding level | Lignin type | Incorporation of 20 % of each type<br><br>Temperature, duration & speed (± 5 °C, ± 1 min. & ± 20 rpm) | SP (°C) | | Storage stability (°C) |
|---|---|---|---|---|---|
| | | | Top | Bottom | |
| Before (junk particles) | HT SW A 2 | 165, 15 & 1000 | 43.3 | 43.4 | 0.1 |
| | HT SW B | | 43.9 | -* | -* |
| | TB HW A | | 43.5 | | |
| | TB HW B | | 42.9 | | |
| | K SW A | | 44.1 | | |
| | K SW B | | 44.2 | | |
| | HT SW A-modified | | 42.3 | | |
| | K SW A-modified | | 43.5 | | |
| After the first grinding process | HT SW B | | 43.3 | -* | -* |
| | TB HW A | | 43.7 | | |
| | TB HW B | | 43.1 | | |
| | K SW A | | 44.5 | | |
| | K SW B | | 44.6 | | |
| * The mix could not be poured and tested due to the collected specimen at the bottom of the tube (unstable mix). | | | | | |

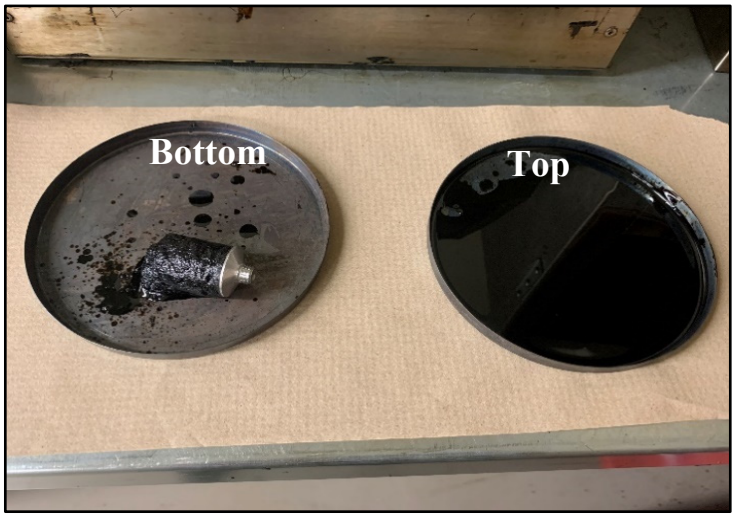


Figure 4.2 The bottom (left) and top (right) of the tube for the modified bitumen with K SW B lignin after the first grinding process

Table 4.7 Storage stability tests results of the modified bitumen PG 58S-28 with different types of the lignin after the second grinding process

| Lignin type | Incorporation of 20 % of each type<br><br>Temperature, duration & speed (± 5 °C, ± 1 min. & ± 20 rpm) | SP (°C) | | Storage stability (°C) |
|---|---|---|---|---|
| | | Top | Bottom | |
| HT SW B | 165, 15 & 1000 | 43.6 | 44.3 | 0.7 |
| TB HW A | | 43.5 | 44.1 | 0.6 |
| TB HW B | | 44.1 | 44.9 | 0.8 |
| K SW A | | 45.0 | 47.6 | 2.6 |
| K SW B | | 44.6 | 47.3 | 2.7 |

Figure 4.3 shows Dx (50) parameter used to compare the particle size of each lignin. This parameter represents the median diameter of the particles (50% of the particles are greater and 50% are smaller). It is chosen to facilitate the comparison with what is observed from the analysis of microscope observation (section 4.2.5). It should be noted that Dx (90) is checked and it shows similar trend as Dx (50). Regarding the variability of Dx (50), the software itself performs automatically five repetitions for each test. The COV value is checked for each test and it is found to be maximum of 2 % which is acceptable according to the ASTM C 670 standard. It can be seen that the HT SW B lignin after the second grinding process is finer (32.3 µm) compared to the first grinding process (55.4 µm). Therefore, the particles size for this lignin seems to have an effect on the stability of the modified bitumen. While it is interesting to see that even the K SW A lignin is finer after the second grinding process, it is unstable in the modified bitumen. That being said the particle size of the lignin is not the only or the most important parameter for the stability of the modified bitumen, but it still needs to be as small as possible (powder form) since the particle size of other types showed an influence on the stability of the lignin-modified bitumen. The lignin HT SW A-modified (unstable) in comparison with the HT SW A 1 and HT SW A 2 lignins (stable) can be considered a good example to show the effect of the particle size. For the TB HW A lignin, despite it is stable in the modified bitumen after the second grinding process, the particle size is similar after both grinding processes. For TB HW B lignin, the average particle size (Dx (50)) is coarser after the second grinding process which is not expected. This might be due to the way how the grinding process was done at the facility of the lignin producer. These findings for TB HW A

and TB HW B lignins might be due to the effects of the other factors such as pH. Finally, according to Figure 4.3 and the storage stability tests results, it is difficult to determine a threshold value of the particle size that guarantees a stable lignin-modified bitumen, considering the effect of the other factors.

In general, incorporation a powder of the lignin into the bitumen has many advantages such as better compatibility and suspensibility within the bitumen and making the storage stability test possible to be completed, leading to the final result (stable or unstable).

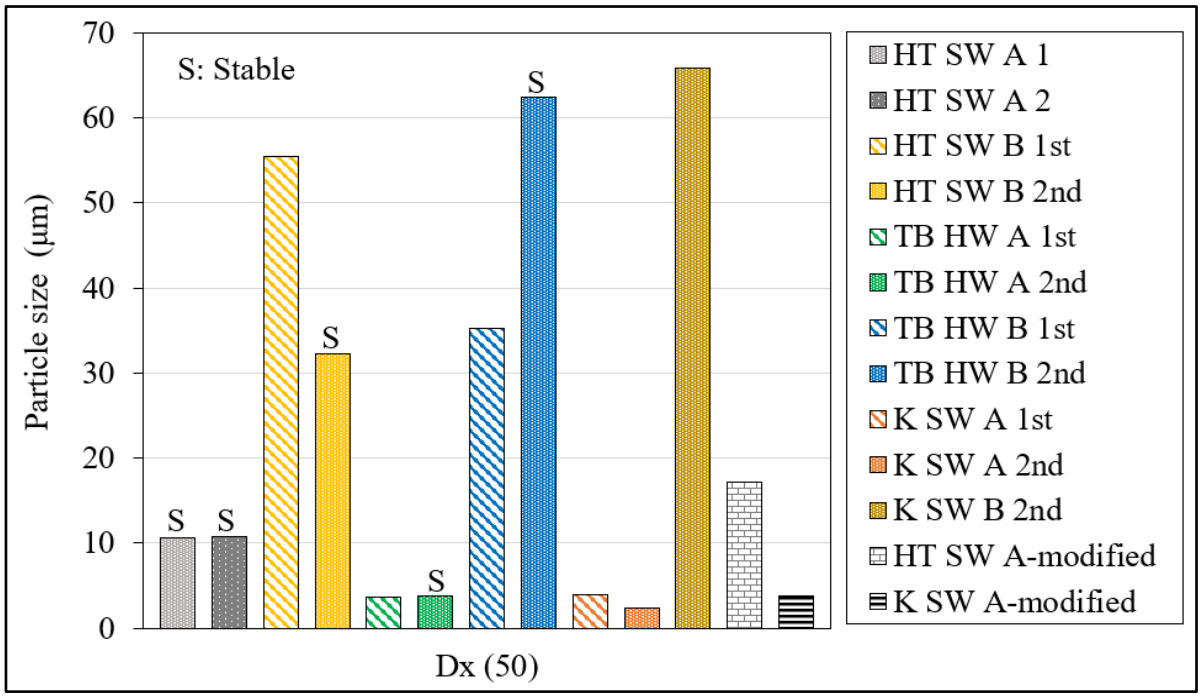


Figure 4.3 Particles size based on Dx (50) value for A (including modified types) and B lignins after the first and second grinding process

Since the compatibility between the lignin and the bitumen is improved, it is expected that the lignin will change the properties of the bitumen. In other words, the presence of the lignin in powder form might modify the bitumen in a way to produce a stable lignin-modified bitumen. Herein, it is worth investigating the effect of the powder of a standard inert filler on the stability of the modified bitumen with inert filler (mastic).

### 4.2.3 Preparation of the mastic

In order to investigate the effect of the inert filler on the bitumen, two mastics (modified bitumen with inert filler) were prepared by using LSM. Herein, it is worth mentioning that the same bitumen (PG 58S-28) was used as that for the lignin-modified bitumen. In addition, the same apparatus, equipment and tools that were employed in the incorporation process of the lignin-modified bitumen were used. To do so, due to the significant difference of the density between the lignin (≈1.25 g/cm$^3$) and inert filler (≈2.70 g/cm$^3$), the equivalent in volume of the inert filler to 10 % and 20 % lignin of the total weight of the mastic were prepared. To facilitate the comparison, the corresponding percentage weight of filler in the mastic is 22 % and 44 % for 10 % and 20 % of lignin, respectively. As observed, the values for filler are twice that for lignin which is expected according to the density values for filler (≈2.70 g/cm$^3$) and lignin (≈1.25 g/cm$^3$). These mixes of mastic were incorporated into the bitumen at 165 ± 5 °C for 15 minutes with a speed of approximately 900 and 1000 rpm for 10 % and 20 % inert filler content, respectively. The preparation of the mixes of mastic was followed by performing only the storage stability tests. It was decided that checking the stability and homogeneity of the mixes of mastic is enough to distinguish between the lignin, as a powder, and the inert filler. One repetition of the test was performed. Table 4.8 shows the summary of the prepared mixes of mastic with the bitumen PG 58S-28 and tests done.

Table 4.8 Summary of the prepared mixes of mastic with the bitumen PG 58S-28 by LSM and tests done

| Inert filler content (%) * | Incorporation temperature (± 5 °C) | Incorporation duration (± 1 min.) | Incorporation speed (± 20 rpm) | Storage stability | Microscope observation |
|---|---|---|---|---|---|
| 10 | 165 | 15 | 900 | ✓ | - |
| 20 | | | 1000 | | |
| * The filler content corresponds to the equivalent in volume to 10 % or 20 % of the lignin by the total weight of the mastic. | | | | | |

#### 4.2.3.1 Storage stability tests results of the mastic

Table 4.9 shows the storage stability tests results of the modified bitumen PG 58S-28 with the inert filler (mastic). It can be seen that the mix with 10 % filler content is unstable (storage stability value of 3.3 °C). For 20 % filler content, the collected specimen at the bottom of the tube made the test not possible to be completed, because the filler and the bitumen were separated (Figure 4.4). It is worth reminding that these filler contents, 22 % and 45 %, correspond to the equivalent in volume to 10 % and 20 %, respectively, of the lignin by the total weight of the mastic. The incorporation of the lignin into the bitumen with these contents (10 and 20 %) did not show what is observed here (unstable mastic). The lignin showed a good compatibility with the bitumen (0.5-1 °C storage stability values) which is completely the opposite of the mastic. The important factor here is probably the density of the two components of the mastic, inert filler and bitumen. The density of the inert filler particles is higher than that for the bitumen, causing them to settle at the bottom due to their higher molecular weight. Herein, in comparison with 10 and 20 % of lignin content, it might indicate that at least part of the lignin, as a powder, does not behave as a filler. In other words, the lignin may play both roles: filler and bitumen modifier. However, further investigation to better describe the status of the lignin in the bitumen is highly recommended for future studies. In addition, performing the rheological and thermomechanical tests should help to understand the behaviour of the lignin in the bitumen and HMA.

Table 4.9 Storage stability tests results of the modified bitumen PG 58S-28 with the inert filler

| Filler content (%) | Temperature (± 5 °C) | Duration (± 1 min.) | Speed (± 20 rpm) | SP (°C) | | Storage stability (°C) |
|---|---|---|---|---|---|---|
| | | | | Top | Bottom | |
| 10 | 165 | 15 | 900 | 43.1 | 46.4 | 3.3 |
| 20 | | | 1000 | 43.5 | -* | -* |
| * The mix could not be poured and tested due to the collected specimen at the bottom of the tube. | | | | | | |

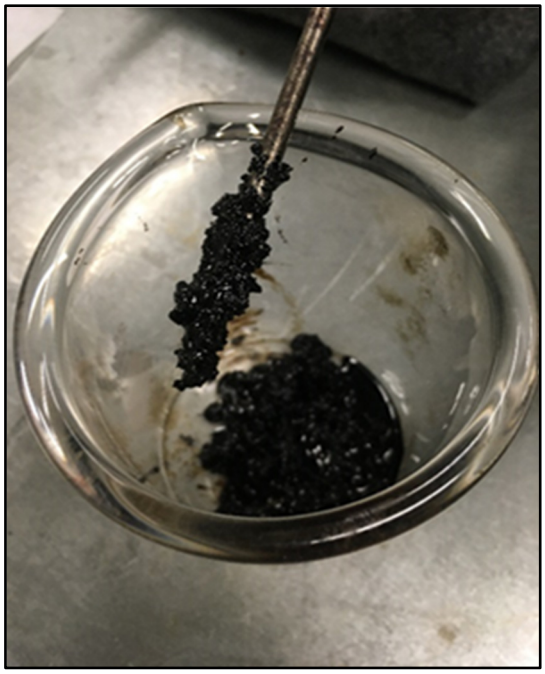

Figure 4.4 Collected filler at the bottom
of the tube for storage stability test

As mentioned in previous sections (4.2.1, 4.2.2 and 4.2.3), the use of lignin in powder form may be problematic for health and safety reasons. Based on that, it was decided to test lignin in pellet form. The pellets within the bitumen will help to reduce the health risks. In particular, some dust was generated from the incorporation process of the lignin and inert filler (materials in powder form). Therefore, this issue is believed to be a major concern, especially in a larger scale than the laboratory scale (field scale). The following section shows the effect of using pellets on the storage stability of the unmodified bitumen.

### 4.2.4 Preparation of the modified bitumen with pellets

This section presents the incorporation process of two types of the pellets into the bitumen. As mentioned before, HT SW A 1 lignin is used with the soybean oil to form pellets. These types are the high durability index (HDI) pellets and low durability index (LDI) pellets. The HDI pellets contain 10 % of soybean oil and has a durability index of 79.2, while the LDI pellets contain 5 % of soybean oil and has a durability index of 43.4. Both types of the pellets were

incorporated into the bitumen PG 58S-28 by using both mixers, LSM and HSM. The content of 10 % of both types of pellets was incorporated at a temperature of 165 ± 5 °C.

For LSM, the incorporation process was continued for a total of 90 minutes with a speed of approximately 700 rpm. For HSM, the total incorporation duration was 40 minutes at a range of speed of 5000-7000 rpm. The mix was inspected every 15 minutes during the incorporation process in order to observe the existence of the particles of pellets in the bitumen. After 90 minutes of incorporation by LSM, the particles of the HDI pellets can still be seen in the mix despite they were broken down into small solid particles. Figure 4.5 shows a photo which explains this observation. It is worth mentioning that the particles of the HDI pellets incorporated by HSM disappeared after the first 15 minutes of the visual observation. Therefore, the use of the HSM showed the effectiveness of its principle for the incorporation process of pellets into the bitumen.

For the incorporation of the LDI pellets, it was necessary to increase the speed of the HSM at the beginning of the process from 5000 rpm to 7000 rpm to allow the particles get mixed with the bitumen. This observation was found for only the LDI pellets which can be explained due to its low density, compared to the HDI pellets, that resulted in a higher amount of the added pellets. Then, the speed was decreased to 5000 rpm which was used for the whole duration of the incorporation of the HDI pellets into the bitumen. One repetition was performed for each test of the storage stability. Table 4.10 shows the summary of the prepared modified bitumens with pellets and tests done.

For future investigation, it is strongly recommended to perform tests on the bitumen with soybean oil only. This will help to differentiate between the effect of the lignin and the effect of the soybean oil on the bitumen.

Figure 4.5 A photo taken during the incorporation process of the HDI pellets by LSM showing the presence of pellets

Table 4.10 Summary of the modified bitumen with pellets prepared by LSM and HSM and tests done

| Pellets type | Pellets content (%) | Incorporation temperature (± 5 °C) | Total duration of incorporation (± 1 min.) | | Incorporation speed (± 20 rpm) | | Storage stability |
|---|---|---|---|---|---|---|---|
| | | | LSM | HSM | LSM | HSM | |
| HDI | 10 | 165 | 90 | 40 | 700 | 5000-7000 | ✓ |
| LDI | | | | | | | |

#### 4.2.4.1 Storage stability tests results of the modified bitumen with pellets

Table 4.11 shows the storage stability tests results of the modified bitumen PG 58S-28 with the HDI and LDI pellets incorporated by LSM and HSM. Both types that were incorporated by both mixers showed instability in the bitumen. In particular, the tests were not possible to be completed due to the collected specimen at the bottom of the tube. The presence of the oil used to compress the lignin powder, forming pellets, affects the stability and homogeneity of the pellet-modified bitumen. In particular, the density of the soybean oil is approximately 0.92

g/cm$^3$ which helps to dilute the bitumen and, therefore, reduces the density of the bitumen. As a result, the ratio of lignin density to bitumen density becomes higher, leading to the settling of lignin particles at the bottom due to their molecular weight. Herein, it is worth investigating, in future studies, some methods such as using an agent that helps to improve the compatibility between the pellets and bitumen, leading to obtain a stable pellets-modified bitumen.

Table 4.11 Storage stability tests results of the modified bitumen PG 58S-28 with different types of the pellets incorporated by LSM and HSM

| Mixer type | Pellets type | Incorporation of 10 % of each type<br>Temperature, duration & speed (± 5 °C, ± 1 min. & ± 20 rpm) | SP (°C) | | Storage stability (°C) |
|---|---|---|---|---|---|
| | | | Top | Bottom | |
| LSM | HDI | 165, 90 & 700 | 42.1 | -* | - |
| | LDI | | 41.8 | -* | - |
| HSM | HDI | 165, 40 & 5000-7000 | 41.3 | -* | - |
| | LDI | | 41.5 | -* | - |

* The mix could not be poured and tested due to the collected specimen at the bottom of the tube.

According to the results of the storage stability tests shown in the previous studies, it is necessary to perform the morphological analysis of the microscope images taken. This will help to quantify the effect of the incorporation of lignin into the bitumen. The following section shows the microscope observations of the lignin-modified bitumen.

### 4.2.5 Microscope observations

Figures 4.6 to 4.13 show the microscope images for the HT SW A 1 lignin, unmodified and modified bitumen PG 58S-28 with different contents. In addition, Table 4.12 summarizes the diameter of the particles, the mean, total and maximum area of the lignin particles in addition to their area in the bitumen specimen in percent (all values are rounded to the unity). It is important to note that each figure presented in this section, including the calculation, represents one zone of the bitumen specimen laid on the glass plate shown in Figure 3.16 a. Moreover, thresholding and detecting lignin particles in those images is not easy to control which implies variation in the results, especially for lignin alone (Figure 4.6). In order to reduce this effect,

many thresholding attempts were done and the one with better detected particles (all lignin particles can be seen clearly) is presented. All images of the lignin-modified bitumen are those for which the lignin was incorporated at 165 °C except the mix shown in Figure 4.11 for which it was incorporated at 140 °C. The difference in the background color between the photos is due to the passing light which was affected by the thickness of the bitumen layer laid on the glass plate. It is interesting to see, based on visual evaluation, that the shape of the lignin particles did not change when they were incorporated into the hot bitumen. This indicates that the lignin particles did not decompose nor break during the incorporation process at high temperature. The images showed that the lignin particles were re-distributed during the incorporation process in a way to present a good dispersion over the bitumen. According to the storage stability tests results, the lignin is in suspension in the bitumen.

The summary of the results (Table 4.12) of microscope images for the modified bitumen with 10 and 20 % lignin (Figure 4.8 and 4.9) shows that the mean value of the area is 406 and 489 $\mu m^2$, respectively, which is an increase of 20 %. This means that the lignin particles tend to agglomerate with each other. However, the agglomeration of lignin particles is marginal compared to 30 % lignin content. Also, the percentage area of those particles (Table 4.12) is 11 % and 22 % for 10 % and 20 % lignin, respectively. This is expected and reflects the lignin content incorporated into the bitumen. To put it differently, this shows that all lignin particles are detected by the software and the results of quantifying the studied zone of those images are representative.

For the modified bitumen with 30 % lignin (Figure 4.10), the mean area increased significantly (784 $\mu m^2$) compared to 10 and 20 % lignin (406 and 489 $\mu m^2$, respectively). It is worth mentioning that the white circles in Figure 4.10 are not included in the calculation for the analysis of the lignin particles since they are air bubbles. The significant increase in the mean area indicates the agglomeration of some lignin particles, forming a cluster. To confirm this, it can be seen from Figure 4.10 that the presence of the lignin clusters in this modified bitumen is clear. As can be seen from the figure, it is difficult to define what is considered a cluster based on the number of particles agglomerated together. However, according to the results for

20 % and 30 % lignin at which the particles agglomerate, an average area for lignin clusters can be assumed. Herein, in order to define the cluster in this study based on what is observed, the lignin particles that have an average area of 635 $\mu m^2$ (midpoint of 489 $\mu m^2$ for 20 % and 784 $\mu m^2$ for 30 %) or higher is considered a cluster. The clusters might be considered as a concern for the homogeneity of the lignin-modified bitumen. Despite that, the storage stability tests results showed a stable modified bitumen with 30 % of lignin. Generally, the presence of the lignin clusters limits the movements of the bitumen molecules which result in a viscous modified bitumen. However, it is expected to have homogeneity issues for higher lignin contents than 30 % in the bitumen. The area and diameter values shown in Table 4.12 for 50 % lignin content are much higher than 30 % which confirm the homogeneity and stability issues. In this case, the lignin is almost in a continuous phase of suspension instead of the bitumen. This is due to the agglomeration of lignin particles in a big cluster. As can be seen, the incorporation of 50 % lignin at 165 °C for 60 minutes showed smaller values of the diameter compared to 30 minutes (49 µm compared to 56 µm, respectively). This finding might be due to long incorporation time that result in a better dispersion of the lignin particles in the bitumen. Combining this with the storage stability tests results that showed stable lignin-modified bitumen, it is recommended to increase the incorporation duration for high lignin content while maintaining high incorporation temperature. In general, the rough edges of lignin particles help to improve the adhesion property of the bitumen and other characteristics such as the resistance to the water damage and high temperature performance. This improvement is due to a three-dimensional multi-directional spatial network that is formed by the lignin with the bitumen. The rough edges of the lignin particles can be observed through the photos shown in Figures 4.8 to 4.13.

Finally, it is interesting to compare the average particle size (diameter) of HT SW A 1 lignin based on Dx (50) parameter shown in Figure 4.3 with what is observed from the microscope observation. From the mean area values shown in Table 4.12 for Figures 4.6 to 4.13, the diameter can be determined assuming that the lignin particles are circular in shape (applying the mathematical equation used to calculate the area of a circle). Depending on the lignin content, the lignin particles in those figures obtained from the microscope observations show

bigger diameter values (Table 4.12: ranges from 23 to 56 µm) than that observed from the laser gradation shown in Figure 4.3 (11 µm). This confirms the formation of lignin clusters within the bitumen. It can be seen that the values of the mean area and diameter for lignin alone are higher than that for 10 % and 20 % lignin content which can be due to the sampling of lignin (many particles stick together).

Table 4.12 Summary of the microscope observations obtained from ImageJ for the lignin alone and modified bitumen PG 58S-28 with different contents of HT SW A 1 lignin

| Material (lignin content %) | Area ($\mu m^2$) | | | Diameter (µm) [A] | Area of lignin particles in percent of specimen surface (%) |
|---|---|---|---|---|---|
| | Mean | Total | Maximum | | |
| Lignin alone | 561 | 361,842 | 13,881 | 27 | 20 |
| Bitumen PG 58S-28 | - | - | - | - | - |
| 10 | 406 | 660,629 | 6,108 | 23 | 11 |
| 20 | 489 | 990,912 | 9,636 | 25 | 22 |
| 30 | 784 | 1,160,540 | 26,432 | 32 | 33 |
| 50 (30 min at 140 °C) | 2,244 | 3,020,679 | 437,397 | 54 | 49 |
| 50 (30 min at 165 °C) | 2,501 | 2,638,884 | 196,324 | 56 | 43 |
| 50 (60 min at 165 °C) | 1,889 | 2,603,136 | 444,672 | 49 | 43 |

[A] This value is determined based on the mathematical equation used to calculate the area of a circle assuming that the lignin particles have circular shape.

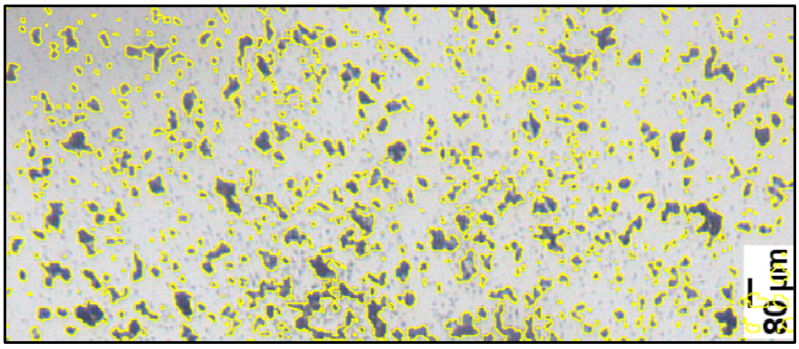


Figure 4.6 Microscope image for HT SW A 1 lignin alone

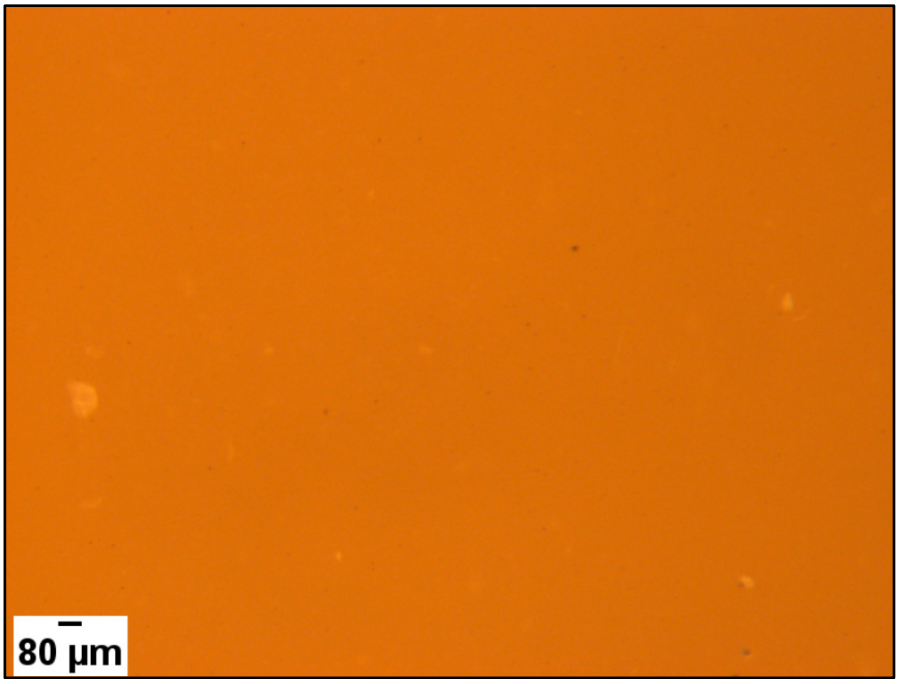


Figure 4.7 Microscope image for the unmodified bitumen PG 58S-28

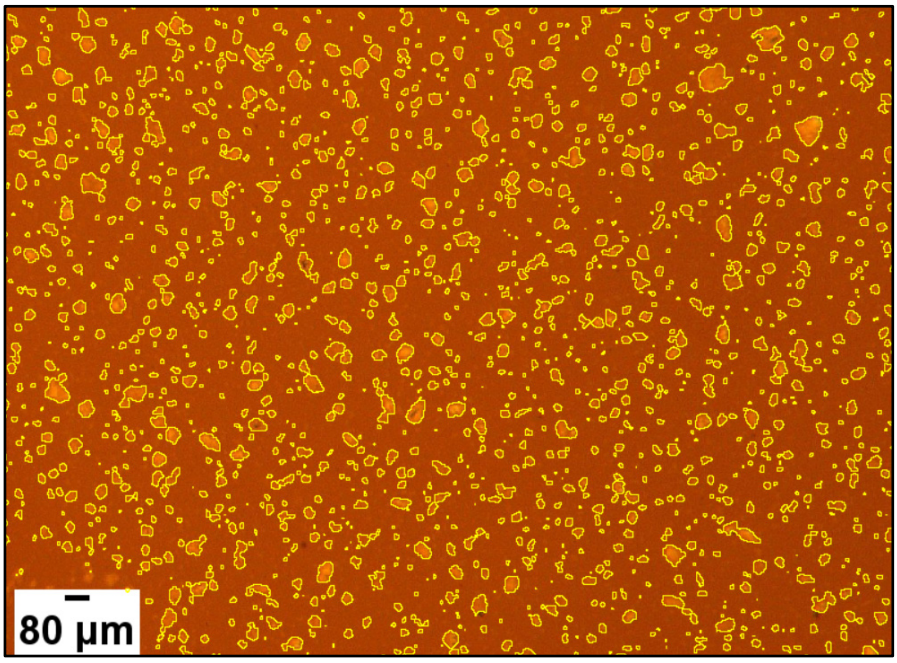


Figure 4.8 Microscope image for the modified bitumen PG 58S-28 with 10 % of the HT SW A 1 lignin

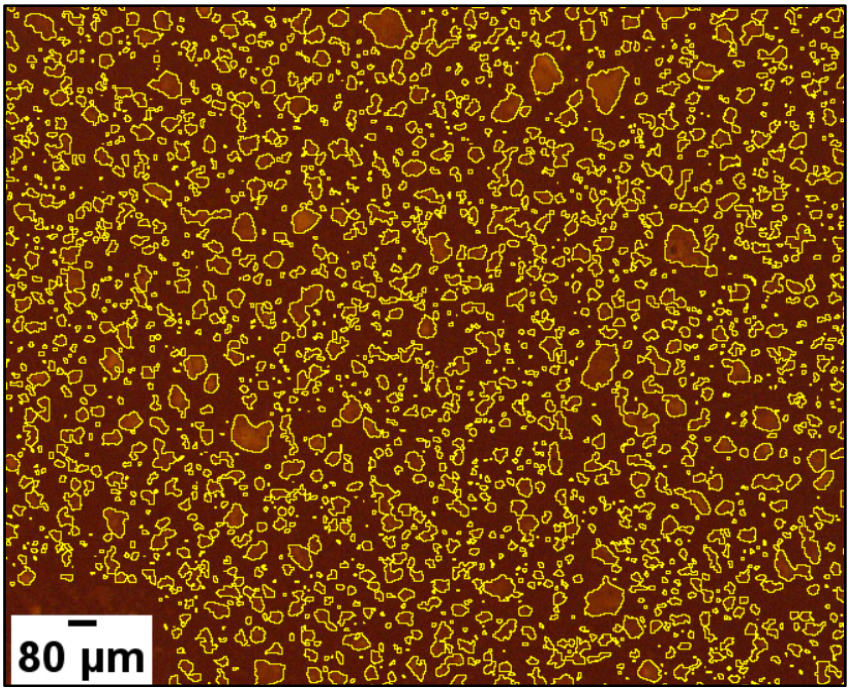


Figure 4.9 Microscope image for the modified bitumen
PG 58S-28 with 20 % of the HT SW A 1 lignin

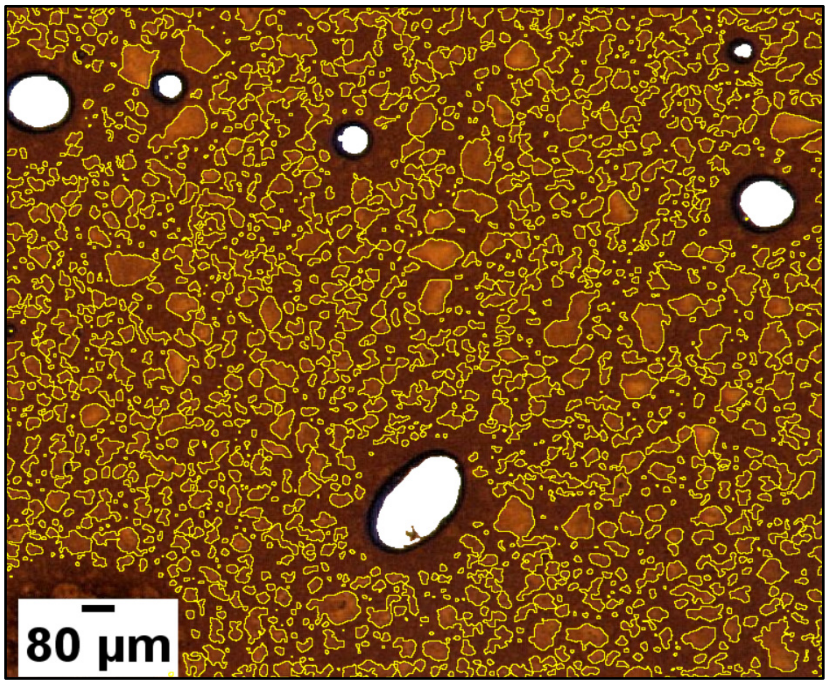


Figure 4.10 Microscope image for the modified bitumen
PG 58S-28 with 30 % of the HT SW A 1 lignin

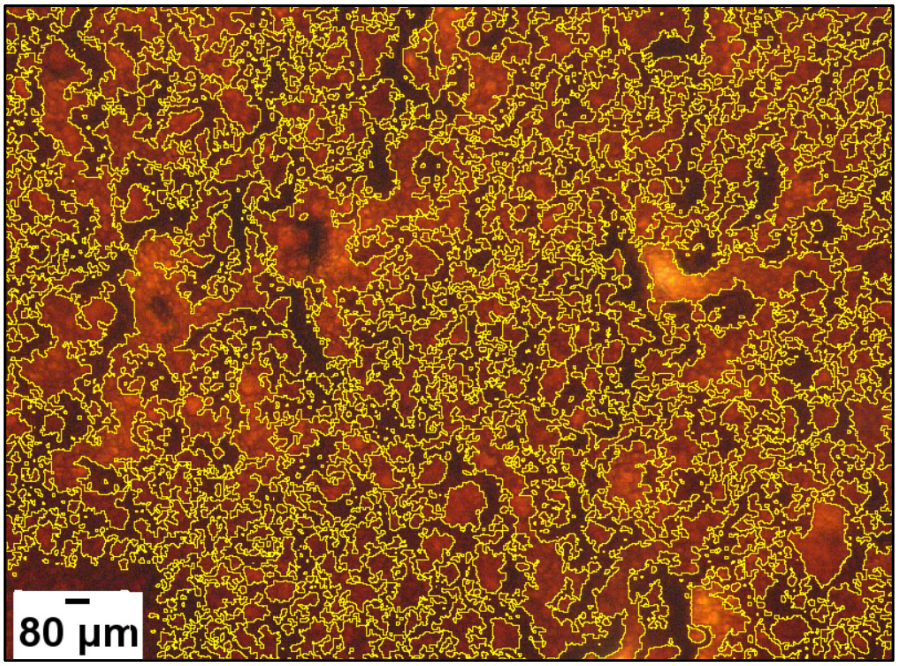


Figure 4.11 Microscope image for the modified bitumen PG 58S-28 with 50 % of the HT SW A 1 lignin (30 min at 140 °C)

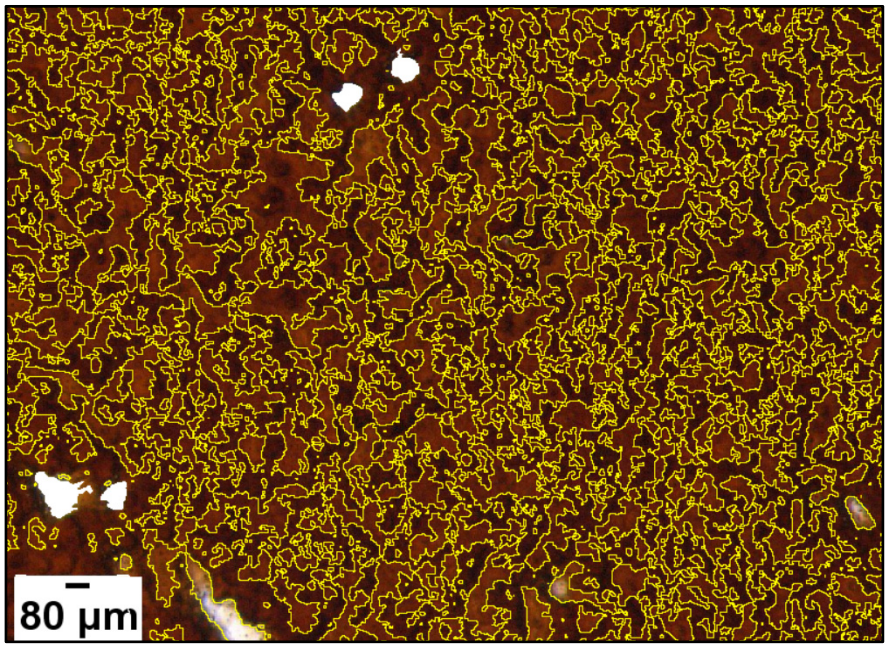


Figure 4.12 Microscope image for the modified bitumen PG 58S-28 with 50 % of the HT SW A 1 lignin (30 min at 165 °C)

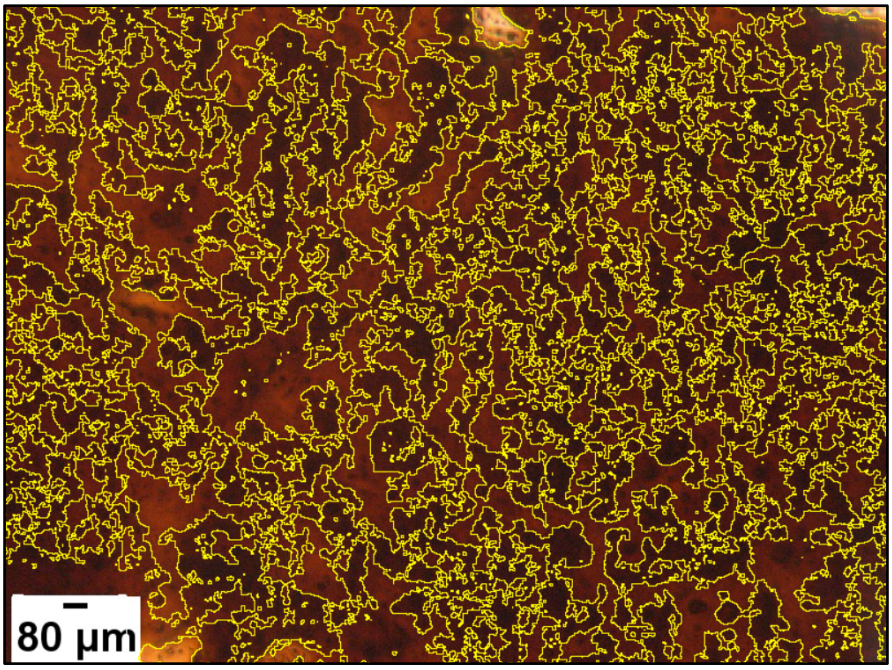


Figure 4.13 Microscope image for the modified bitumen PG 58S-28 with 50 % of the HT SW A 1 lignin (60 min at 165 °C)

## 4.3 Summary

This chapter discussed the incorporation process of different types of lignins, inert filler and pellets into the bitumen. In particular, a study of the incorporation process with different parameters (temperature, duration and speed) was done with one type of lignin in order to characterize the effects of these parameters on the stability and homogeneity of the lignin-modified bitumen. Afterwards, according to the results of this study, specific values for the parameters of the incorporation process were selected for the incorporation of the inert filler and pellets into the bitumen. Following, the storage stability tests and microscope observations were performed to verify of the incorporation process in terms of the stability and homogeneity of the lignin-modified bitumen. The results have shown that it is possible to add lignin in bitumen. More specifically, the following conclusions can be drawn:

- Incorporation of the lignin, in powder form, with the bitumen by using simple equipment (LSM and hot plate) is possible.
- Lignin-modified bitumens are stable and homogeneous for up to 30 % lignin content.

- The effect of the incorporation temperature on the stability of the modified bitumen is not significant for low lignin contents (10 and 20 %).
- The incorporation duration is not a key parameter in the incorporation process for up to 30 % lignin content. For 50 %, it is recommended to increase the duration while maintaining high temperature. Since lignin is a biopolymer, longer duration (up to 4 hours used for polymers) should be used to evaluate the effect on the stability of the modified bitumen.
- The type of bitumen does not seem to affect the stability of the lignin in the mix.
- The size of the lignin particles is not a major factor for the stability of the lignin-modified bitumen. Other parameters such as the molecular weight, pH, densities of the lignin and bitumen, viscosity of the modified bitumen and the electrical charges of the lignin particles should be taken into account.
- The lignin did not decompose during the incorporation process at high temperature.
- The lignin is well dispersed and homogeneously distributed in the bitumen for lignin contents less than 20 %. However, for higher lignin contents, lignin particles tend to agglomerate and form clusters, leading to unstable mix.
- The inert filler is not stable in the bitumen which can be due to its high density.
- The modified bitumens with 10 % of HDI and LDI pellets incorporated by LSM and HSM mixers are unstable. This might be due to the presence of the soybean oil within the pellets.

According to the findings and drawn conclusions of this chapter, a specific value of each parameter of the incorporation process can be selected. The incorporation temperature and duration are 165 ± 5 °C and 15 minutes, respectively, for 10, 20 and 30 % lignin contents. A duration of less than 15 minutes can be studied in future. For 50 % lignin content, the duration should be increased to 60 minutes. For the incorporation speed, it is 900 ± 20 rpm for 10 % lignin content, 1000 ± 20 rpm for 20 and 30 % and 1100 ± 20 rpm for 50 %. The incorporation process of the lignin powder into the bitumen can be done by using LSM. Using HSM is highly recommended for the pellets. The incorporation temperature, speed and duration should be 165 ± 5 °C, 5000-7000 rpm and 40 minutes, respectively, for 10 % pellets content. Using agents to obtain stable pellets-modified bitumen is recommended for future investigation.

# CHAPTER 5

# ANTIOXIDATION PROPERTIES AND EFFECTS OF LIGNIN ADDITION ON THE BITUMEN PROPERTIES

## 5.1 Introduction

After having established the incorporation process of the lignin into bitumen as presented in Chapter 4, it is now important to quantify the effect of the lignin on the properties of the lignin-modified bitumen. This chapter presents the effects of the different types of lignin powder and pellets on the rheological properties of the bitumen. In particular, a study on the effects of one type of lignin on two different grades of unmodified bitumen was done. More specifically, the effects on the viscosity, the mechanical behaviour and the performances at high and low temperatures are studied.

Afterwards, according to the findings of this study, the effects of different types of lignin powder and pellets on the same mentioned rheological properties of one bitumen type were evaluated. The work with different types of lignin powder was aimed at seeing if the different lignins have the same effect on the bitumen and if a specific combination of lignin and bitumen performs better than the others.

Last but not least, a study on the effect of the aging process on the properties of the lignin-modified bitumen is presented in order to evaluate the antioxidation capacity of lignin. In this study, different contents of one type of lignin were incorporated into the bitumen. Following, three consecutive 20 hours long-term aging processes (PAV) were applied on the RTFO residue of the lignin-modified bitumen. The related tests were performed to evaluate the antioxidation properties of the aged lignin-modified bitumen. In addition, the FTIR test was performed to assess the evolution of the chemical composition of the lignin-modified bitumen during the aging process. Finally, the drawn conclusion of the main findings of this chapter is presented in the last section.

## 5.2 Effects of lignin on the rheology and oxidative aging properties of bitumen

The work in this section is divided into four consecutive steps. Thus, the bitumen grade used and lignin contents incorporated were determined based on the results of the previous step. The following diagram is a summary of these four steps that are described in details in the next sections.

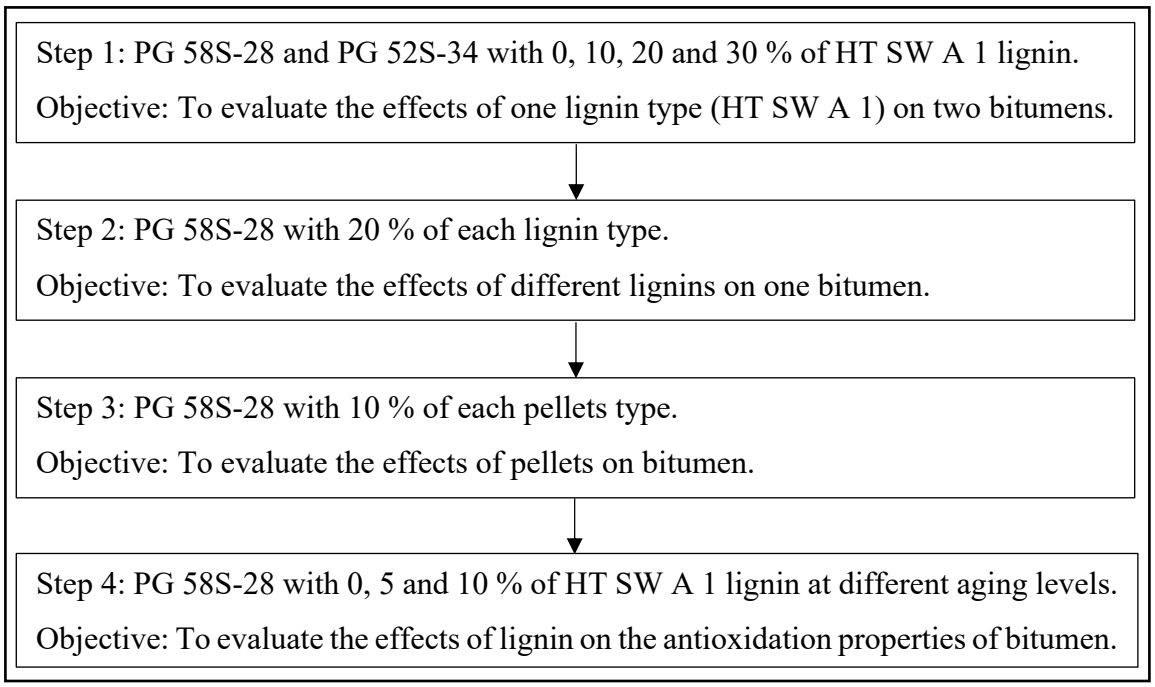


Figure 5.1 Summary of the four steps and the objective of each step

In the first step, the work aims to characterize the rheological properties of lignin-modified bitumen. In this regard, this study investigates the incorporation of different contents (0, 10, 20 and 30 % by total mass of the modified bitumen) of HT SW A 1 lignin powder into two unmodified bitumens adapted for cold climates and a standard traffic level (PG 58S-28 and PG 52S-34). Different tests were performed to evaluate the effects of the lignin incorporation on the performance of those two bitumens, based on Superpave classification (the PG classification: PG Hn-L), at high to low temperature for a more complete characterization. In particular, the BRV test is used to evaluate the effects on the viscosity (η) of the lignin-

modified bitumen and to determine the mixing ($T_{mix}$) and compaction ($T_{comp}$) temperatures of the two bitumens. The DSR, the MSCR and the BBR tests are used to determine the high temperature ($T_{high}$: determined high temperature of PG based on ASTM D 7643) and the high temperature grade (H: high temperature PG), the traffic level (n) and the low temperature ($T_{low}$: determined low temperature of PG based on ASTM D 7643) and the low temperature grade (L: low temperature PG) of the bitumens, respectively. Table 5.1 shows the lignin contents (by total mass of the modified bitumen) incorporated into both bitumen and the tests performed.

Table 5.1 Summary of the experimental campaign of the tests performed on the modified bitumen with HT SW A 1 lignin (step 1)

| Bitumen PG (Hn-L) | Lignin content (%) [A] | Testing temperatures, $T_T$ (°C) and number of repetitions for each test [#] | | | |
|---|---|---|---|---|---|
| | | BRV | DSR | MSCR | BBR |
| 58S-28 and 52S-34 | 0 | 135 [1+3] [B] | H [1+3] [B] | H [1+3] [B] | L + 4 [2-3] [C] |
| | 10 | 145 [1+3] [B] | H + 6 [1+3] [B] | | L + 10 [3] [D] |
| | 20 | 155 [1+3] [B] | | | L + 16 [3] [E] |
| | 30 | 165 [1+3] [B] | | | |

[A] Lignin content in relation to the total mass of the modified bitumen (lignin + bitumen) and lignin is there to substitute the bitumen.
[B] The first repetition was performed about a year before the three other repetitions.
[C] For PG 58S-28 (0, 10 and 20 % of lignin) and PG 52S-34 (0 % of lignin).
[D] For both bitumen.
[E] For PG 58S-28 (20 and 30 % of lignin) and PG 52S-34 (10, 20 and 30 % of lignin).

In the second step, the work done aims to evaluate the effect of using different lignins, including different physical and chemical properties, on the rheological properties of the unmodified bitumen PG 58S-28. The same tests (BRV, DSR, MSCR and BBR) used in the previous study (first step) were employed in this work. Some of these lignins are extracted from the hard wood (HW) while others from the soft wood (SW). In addition, some of them are in acid (A) form (pH=3) while others are in base (B) form (pH=10). The most interesting point in this section is that the differences between the lignins show whether they have the same effect or not on a fixed bitumen, in addition to see if there is a specific combination of lignin, among the others, and bitumen that performs better than the others. For this purpose, the lignin content within the bitumen is 20 % for all types of lignin. This content was selected

based on the results of the study performed on HT SW A 1 lignin. In contrast to the previous study, BRV tests were performed at the two temperatures specified in the standard, 135 and 165 °C. This is due to the linear relationship, in a semi-logarithmic scale, between the testing temperatures and the viscosity. However, the results, an average of three repetitions, of the rheological tests for the unmodified bitumen (0 % lignin) used in this step were taken from the previous step. Herein, it is worth mentioning that only one repetition was considered for BRV, DSR and MSCR tests performed on the modified bitumen with different types of lignin. This is due to the small variability (COV values) of the three repetitions performed in the previous study. In other words, the difference in the values between the different repetitions is small. For BBR tests, three repetitions were kept due to the long duration of time required for the conditioning and preparation of the beams. Table 5.2 shows the lignin content (by total mass of the modified bitumen) incorporated into the bitumen and the tests performed.

Table 5.2 Summary of the experimental campaign of the tests performed on the modified bitumen with different lignins (step 2)

| Bitumen PG (Hn-L) | Lignin type | Lignin content (%) [A] | Testing temperatures, $T_T$ (°C) and number of repetitions for each test [#] | | | |
|---|---|---|---|---|---|---|
| | | | BRV | DSR [B] | MSCR [B] | BBR |
| 58S-28 | HT SW A 2 | 20 | 135 [1]<br>165 [1] | H [1]<br>H + 6 [1] | H [1] | L + 10 [3]<br>L + 16 [3] |
| | HT SW B | | | | | |
| | TB HW A | | | | | |
| | TB HW B | | | | | |
| | K SW A | | | | | |
| | K SW B | | | | | |
| | HT SW A-modified | | | | | |
| | K SW A-modified | | | | | |

[A] Lignin content in relation to the total mass of the modified bitumen (lignin + bitumen) and lignin is there to substitute the bitumen.
[B] DSR and MSCR tests were not performed for the HT SW A-modified and K SW A-modified lignins.

In the third step, the work aims to evaluate the effect of using pellets on the rheological properties of the unmodified bitumen PG 58S-28. In this study, the HT SW A 1 lignin powder was mixed with the soybean oil to form the pellets. The pellets were prepared for us by a third party. The same tests (BRV, DSR, MSCR and BBR) are employed in this work. Two types of

the pellets are studied in this section. The first one is the high durability index (HDI) type that has a durability index of 79.2 and a soybean oil content of 10 %. The second one is the low durability index (LDI) type that has a durability index of 43.4 and a soybean oil content of 5 %. Only one content (10 %) of each type of the pellet is incorporated into the unmodified bitumen. This was due to the fact that the work was started lately, compared to the work on the lignin in powder form. More specifically, the pellets materials were involved at the end of this research. The reason behind the selected content (10 %) is that it is the same as the first content studied for the HT SW A 1 lignin. The benefit of this point is to have a base layer of tests results which will help the subsequent studies to continue on studying the pellets-modified bitumen and having a comparison with the results of the modified bitumen with the lignin in powder form. Table 5.3 shows the content of both types of the pellets (by total mass of the modified bitumen) incorporated into the bitumen and the tests performed in this experimental campaign.

Table 5.3 Summary of the experimental campaign of the tests performed on the modified bitumen with HDI and LDI pellets (step 3)

| Bitumen PG (Hn-L) | Pellets type | Pellets content (%) [A] | Testing temperatures, $T_T$ (°C) and number of repetitions for each test [#] | | | |
|---|---|---|---|---|---|---|
| | | | BRV | DSR | MSCR | BBR |
| 58S-28 | HDI | 10 | 135 [1]<br>165 [1] | H [1]<br>H + 6 [1] | H [1] | L + 4 [3]<br>L + 10 [3] |
| | LDI | | | | | |

[A] Pellets content in relation to the total mass of the modified bitumen (pellet + bitumen) and pellets are there to substitute the bitumen.

In the fourth step, the use of lignin as an antioxidant product within bitumen is discussed. In particular, to see whether the lignin accelerates or slows down the effect of the aging on the modified bitumen. To do so, different HT SW A 1 lignin contents (0, 5 and 10 %) were incorporated into the bitumen PG 58S-28. According to Zhang et al. (2019) and Xu et al. (2017), the lignin content to show antioxidation properties is low (7-8 %). In addition, higher lignin content than 10 % was not used in order to limit the stiffening effect of lignin on the bitumen. Moreover, the high stiffness of the aged-modified bitumen with lignin requires a caution in handling equipment, especially DSR, and avoiding damage to them (safety measures

to not break the equipment). First, short-term aging process (RTFO) is applied once and then different long-term aging processes (PAV) (0, 20, 40 and 60 hours) are applied. The unaged bitumens (0 hours of PAV) are tested with the BRV, DSR, full G* and FTIR tests. For G* and FTIR, this was decided to get the chance of having a complete image (at a wide range of temperatures and frequencies) of the LVE behaviour (full G*) and to see the effect of lignin on the chemical composition of the unaged bitumen (FTIR). The other tests (BRV, DSR, MSCR and BBR) on the unaged bitumen are presented before G* and FTIR sections. It should be noted that the 40 hours and 60 hours PAV are not standard tests. However, since lignin is considered to have antioxidant capacities, it is decided to prolong the artificial aging to verify if it is possible to better quantify the impact of the lignin on the aging properties. Table 5.4 shows the campaign of the tests performed on the unmodified and modified bitumen with different contents of HT SW A 1 lignin at each conducted PAV aging process.

Table 5.4 Summary of the experimental campaign of the tests performed on the modified bitumen with different contents of HT SW A 1 lignin and aging levels of PAV (step 4)

| Bitumen PG (Hn-L) | Lignin content (%) [A] | Testing temperatures, $T_T$ (°C) and number of repetitions for each test [#] after each aging level (20, 40 and 60 hours of PAV) | | | | | |
|---|---|---|---|---|---|---|---|
| | | BRV | DSR | MSCR | BBR | Full G* [E] | FTIR [F] |
| 58S-28 | 0 | 135 [1]<br>150 [1]<br>165 [1] | H [1]<br>H+6 [1]<br>H+12 [1]<br>H+18 [1]<br>H+24 [1] | H [1]<br>H+6 [1]<br>H+12 [1]<br>H+18 [1]<br>H+24 [1] | L+4 [3] [B]<br>L+10 [3] [C]<br>L+16 [3] [D] | -30-82 [1] | 20-25 [1] |
| | 5 | | | | | | |
| | 10 | | | | | | |

[A] Lignin content in relation to the total mass of the modified bitumen (lignin + bitumen) and lignin is there to substitute the bitumen.
[B] For all unmodified aged bitumens, modified bitumens with 5 % after 20 and 40 hours of PAV and modified bitumen with 10 % after 20 hours of PAV.
[C] For all aged bitumens, including unmodified and modified ones.
[D] For modified bitumen with 5 % after 60 hours of PAV and modified bitumens with 10 % after 40 and 60 hours of PAV.
[E] The $T_T$ for the low, intermediate and high temperature ranges are (-30, -18, -6 and 0 °C), (-6, 0, 10, 22 and 34 °C) and (34, 46, 58, 70 and 82 °C), respectively, at the frequencies of 0.1, 0.3, 0.5, 0.7, 0.9, 1.59, 2, 4, 6, 8 and 10 Hz.
[E, F] Applied for the unaged (0 hours of PAV) and aged (20, 40 and 60 hours of PAV) unmodified and modified bitumens with 5 and 10 % of lignin.

### 5.2.1 Results and analysis

This section contains the test results of the unmodified and lignin-modified bitumens for all steps. Therefore, the variability of the results should be addressed and controlled by repeating the test more than once. Each value shown in the Tables and Figures of the first step is the average value of more than one repetition. Table 5.1 shows the number of repetitions ([#]) for each test. The repetitions for BRV, DSR and MSCR tests were not all performed at the same time. The first repetition was performed about a year before the three other repetitions. Consequently, a small difference between the first and the other three results is observed for these tests because the bitumen was aged during the period separating the two series of tests. For the rest of the tests, the repetitions were all performed at the same time. Regarding the variability of the results, the COV is a well-known statistical tool which evaluates the variability of the results. The COV of the three (3) repetitions, which are performed at the same period, ranges from 0.2 % to 0.9 % for all tests results. Combining the first (1) repetition with the three (3) repetitions increases the COV to a maximum of 3.2 %. ASTM C 670 standard is used to check the acceptability of the variability since the standard for the test indicates the acceptable variability range for only two (2) repetitions. According to this standard, the variability of the results is within the maximum acceptable range of 3.5 %.

As mentioned earlier, the results are presented in terms of the tests performed. More specifically, for example, the results of BRV tests for all steps are presented in one section: effects of HT SW A 1 lignin on two different unmodified bitumens (first step), effects of different types of lignin on fixed unmodified bitumen (second step), effects of pellets on the unmodified bitumen (third step) and effects of HT SW A 1 lignin on the oxidative aging properties of bitumen (fourth step).

#### 5.2.1.1 BRV tests

This section shows the viscosity results of the different steps. The effect of lignin on the viscosity of bitumen is discussed firstly in general. Then, more details for the results of each step are presented.

*General considerations*

Since lignin, a powder, is mixed with the bitumen, it is expected that there will be an effect on the viscosity. Figure 5.2 shows the viscosity (η) values, obtained with the BRV tests, for the PG 58S-28 bitumen with different HT SW A 1 lignin contents, 20 % of other lignins and 10 % of pellets. As can be seen and as expected, the viscosity of the bitumen increases with the addition of all lignins in powder form except for the lignin in pellets form. This means that the lignin in powder form increase the resistance to flow and hinder the movement of the bitumen at high testing temperatures ($T_T$ = 135 to 165 °C). The increase in viscosity will lead to the increase of the mixing ($T_{mix}$) and compaction ($T_{comp}$) temperatures of the bitumen. In this regard, the lignin-modified bitumen should be heated more to well coat the aggregate and to meet the air voids requirements of the asphalt mix during the compaction process.

Many studies showed that the addition of mineral filler increases the stiffness and viscosity of the bitumen (Robati et al., 2015). This effect depends on the concentration and properties of mineral filler used and the bitumen content within the mastic (filler + bitumen). However, the overall trend observed for the results presented in this section fits with the findings of the literature for a filler. Despite that, more work is needed to fully understand how the addition of lignin affects the viscosity. The viscosity would probably be less impacted if the lignin behaves fully as a binder, but at this point and with the results available, it is not possible to state with confidence if the lignin should be considered as a binder, a filler or a bit of both in the bitumen. It is believed that depending on the amount used, part of the lignin may not work as a filler. The rheological tests such as DSR, MSCR and BBR should help to better understand that.

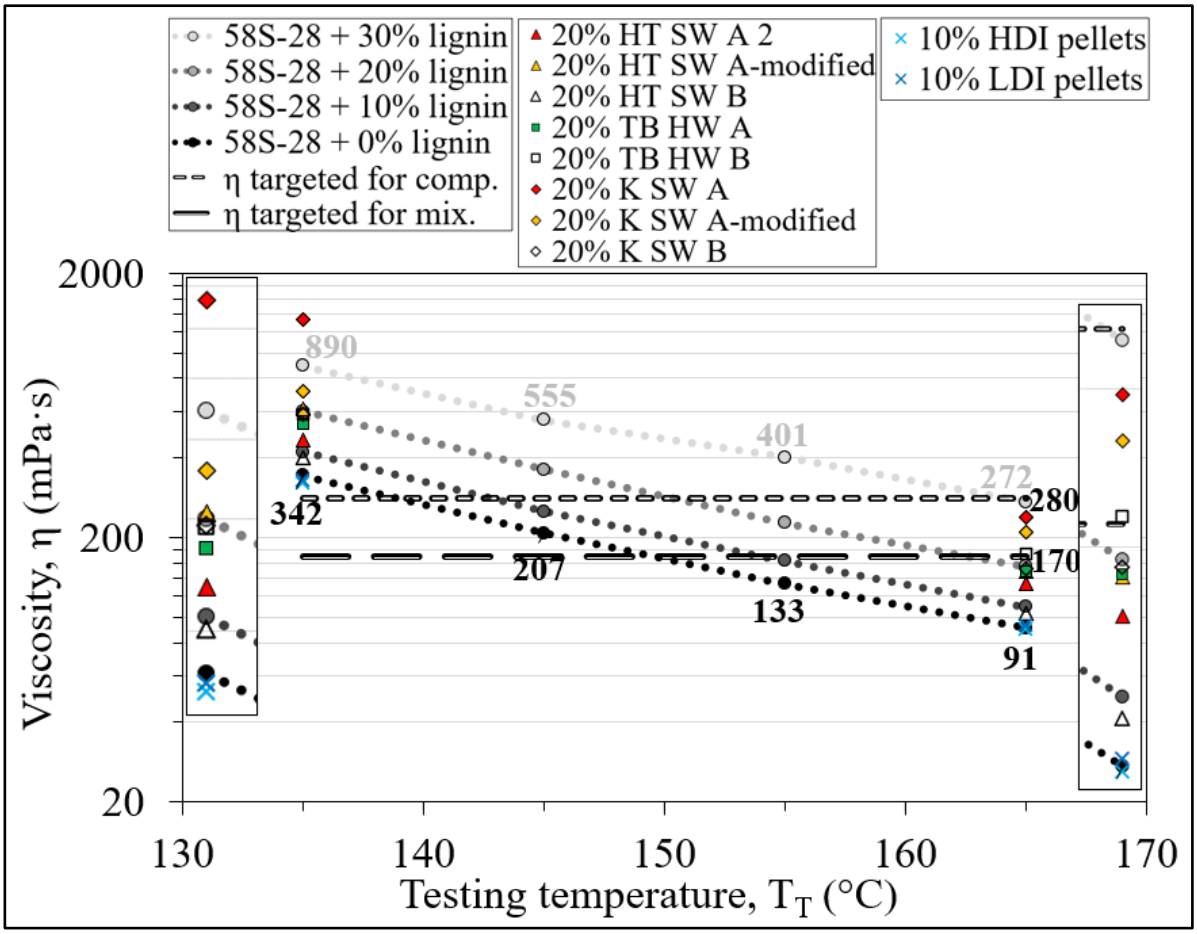


Figure 5.2 Viscosities (η) of PG 58-28 with different HT SW A 1 lignin contents, 20 % of different lignins and 10 % of pellets as a function of testing temperature ($T_T$) and lignin content (% in relation to the total mass of bitumen) and targeted viscosities for mixing ($\eta_{targeted\ for\ mix}$: 170 mPa·s) and for compaction ($\eta_{targeted\ for\ comp}$: 280 mPa·s)

*Step 1 (effects of one lignin type on two bitumens)*

Figure 5.3 shows the viscosity (η) values for the PG 52S-34 bitumen with different contents of HT SW A 1 lignin. The addition of lignin to the PG 52S-34 bitumen shows the same overall trend as observed for the PG 58S-28 bitumen. Table 5.5 shows the $T_{mix}$ and the $T_{comp}$ for the two bitumens with HT SW A 1 lignin corresponding to the targeted viscosities that are shown in Figures 5.2 and 5.3. The $T_{mix}$ increases from 150 to 173 °C and from 138 to 170 °C for the PG 58S-28 and the PG 52S-34 bitumen, respectively, with increasing lignin content (Table 5.5). These temperatures for the unmodified bitumens (0 % lignin) fit with those proposed in LC 26-003 Annex A. The $T_{comp}$ increases from 140 to 164 °C and from 127 to

159 °C for the PG 58S-28 and the PG 52S-34 bitumen, respectively, with increasing lignin content (Table 5.5).

In Figures 5.2 and 5.3, it can be easily observed that the PG 58S-28 with 10 % of HT SW A 1 lignin has almost the same viscosity values as the PG 52S-34 with 20 % of the same lignin. Also, for HT SW A 1 lignin, the $T_{mix}$ and $T_{comp}$ are almost the same (154 and 143 °C, respectively) for PG 58S-28 with 10 % of lignin and (154 and 142 °C, respectively) for PG 52S-34 with 20 % of lignin (Table 5.5).

It is important to mention that increasing the construction temperatures will result in more energy consumption and it can cause safety issues. However, increasing the construction temperatures is acceptable if compared with other bitumen modifiers: for example, the $T_{mix}$ of bitumen modified with crumb rubber could reach up to over 170 °C (Wu et al., 2021; Xie et al., 2019). Despite the additional gas emissions due to the increase in the construction temperatures, performance and environmental benefits could still be gained by lignin addition. Since the addition of lignin increases the viscosity and stiffness of the bitumen, it becomes interesting or necessary to use warm mix asphalt (WMA) technology, which uses a lower production temperature, in order to limit the increase in bitumen heating due to the addition of lignin and to limit the aging and stiffness of the bitumen, as proposed and confirmed by Rubio et al. (2012) and Al-Qadi et al. (2012).

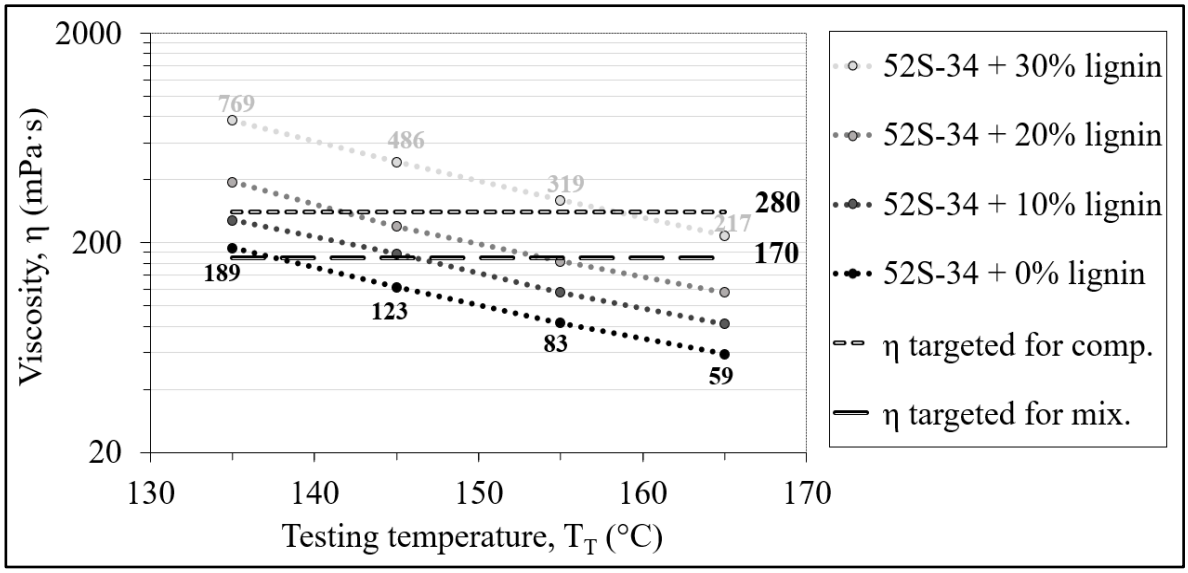


Figure 5.3 Viscosities (η) of PG 52-34 with different HT SW A 1 lignin contents as a function of testing temperature ($T_T$) and lignin content (% in relation to the total mass of bitumen) and targeted viscosities for mixing ($\eta_{targeted\ for\ mix}$: 170 mPa·s) and for compaction ($\eta_{targeted\ for\ comp}$: 280 mPa·s)

Table 5.5 Mixing ($T_{mix}$) and compaction ($T_{comp}$) temperatures for both bitumens corresponding to the targeted viscosities

| Lignin content (%) | Targeted viscosity, η (mPa·s) | Bitumen PG 58S-28 | | Bitumen PG 52S-34 | |
|---|---|---|---|---|---|
| | | $T_{mix}$ [A] (°C) | $T_{comp}$ [A] (°C) | $T_{mix}$ [A] (°C) | $T_{comp}$ [A] (°C) |
| 0 | 170 for mixing; 280 for compaction | 150 | 140 | 138 | 127 |
| 10 | | 154 | 143 | 146 | 132 |
| 20 | | 163 | 151 | 154 | 142 |
| 30 | | 173 [B, C] | 164 | 170 [B, C] | 159 |

[A] $T_{mix}$ and $T_{comp}$ were determined mathematically with viscosities at 135 and 165 °C in accordance with Quebec test method (Laboratoire des chaussées: LC 25-007).
[B] Value outside the measurement area.
[C] For your information, in Quebec, the maximum $T_{mix}$ is limited to 170 °C for polymer modified bitumen.

Figure 5.4 shows the increase of $T_{mix}$ and $T_{comp}$ for both bitumens (PG 58S-28 and PG 52S-34 modified with HT SW A 1 lignin) by calculation the difference between the temperature for the reference mix and the temperature for a modified mix (the $\Delta T_{mix}$ and $\Delta T_{comp}$). The $\Delta T_{mix}$

increases from 0 to 23 °C and from 0 to 32 °C for PG 58S-28 and PG 52S-34, respectively. The $\Delta T_{comp}$ increases from 0 to 24 °C and from 0 to 32 °C for PG 58S-28 and PG 52S-34, respectively. Although, the unmodified PG 52S-34 is less viscous than the unmodified PG 58S-28, the $\Delta T_{mix}$ and the $\Delta T_{comp}$ of PG 52S-34 is bigger compared to the PG 58S-28. Accordingly, the effect of the lignin addition is greater on PG 52S-34 than PG 58S-28 for $T_{mix}$ and $T_{comp}$ (Figure 5.4). This difference might be due to the nature of the physical interactions and/or chemical reactions occurring between the lignin and the different bitumens. It is worth mentioning that the lignin addition has a greater effect on the $T_{mix}$ ($\Delta T_{mix}$), where the viscosity of the bitumen is lower than the $T_{comp}$ ($\Delta T_{comp}$), where the viscosity of the bitumen is higher.

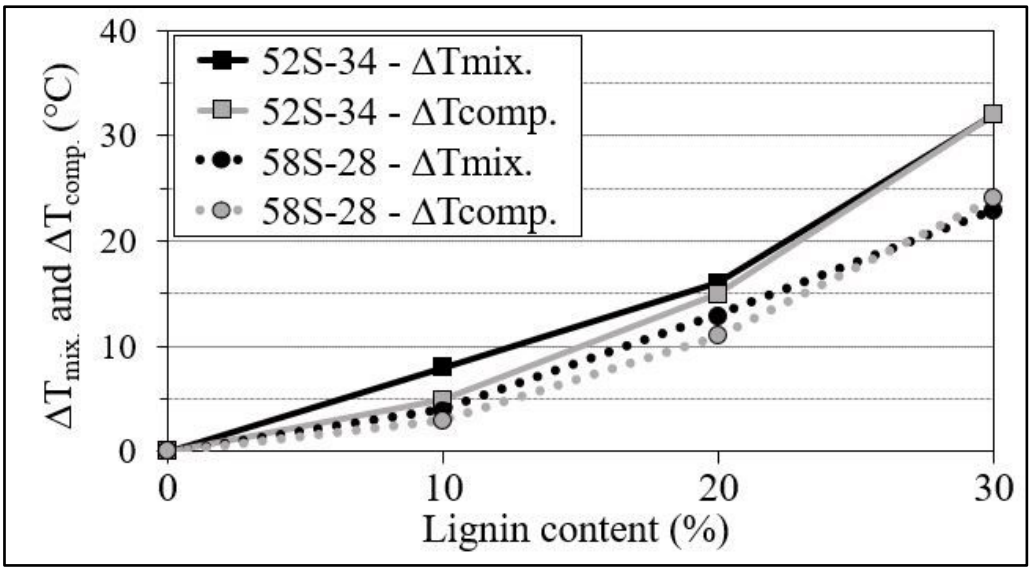


Figure 5.4 Increase of mixing ($\Delta T_{mix}$) and compaction ($\Delta T_{comp}$) temperatures of the modified bitumens compared to the unmodified bitumen (0 % of lignin)

*Step 2 (effects of different types of lignin)*

As can be seen in Figure 5.2, the different lignins all increase the viscosity of the bitumen but with different magnitudes. These differences can be interpreted by the different chemical and physical properties of each type of lignin. In particular, the difference in pH (acid or base), gradation (Figure 4.3) and other properties of the different types of lignin which result in a production of different levels of bitumen's viscosity. However, there is no clear trend between the different viscosities of the modified bitumens and the lignin supplier (HT or TB or K) or

from hard (HW) or soft wood (SW) or have acid (A) or base (B) form. This means that there is no variable seems to have more influence on the viscosity results than the other variables (supplier or type of wood or pH). It is interesting to see that the variation of viscosity at 135 °C for the use of different types of lignin is bigger than what is observed for the use of different contents of HT SW A 1 lignin (Figure 5.2). This is not the case at higher temperature (165 °C). Finally, it can be easily observed that the combination of bitumen PG 58S-28 and 20 % of K SW A lignin shows the highest viscosity (1333 mPa.s) among all modified bitumens with 20 % of other lignins and even higher than 30 % of HT SW A 1 lignin, including unexpected trend of result at 135 °C compared to other bitumens. This might be due to different patterns of the chemical interaction in a way to create very strong bonds between the bitumen molecules. In this regard, according to this observation, it is expected that the workability and compactability issues of the modified HMA with this lignin type (K SW A) will be greatly challenged. However, it was decided to modify this lignin at the facility of the producer in order to reduce the viscosity. Following, the modified version of K SW A lignin (K SW A-modified) was tested and it shows expected results as other lignins except K SW A lignin. This confirms that the properties, chemical and/or physical, of the lignin have a significant effect on the viscosity of the bitumen.

*Step 3 (effects of pellets)*

As can be seen in Figure 5.2, the modified bitumens with 10 % of both pellet types show similar viscosities to the unmodified bitumen. Therefore, the mixing and compaction temperatures for 10 % pellets are similar to those for the unmodified bitumen. It is worth mentioning that the same lignin (HT SW A 1) in powder or pellet form does not show the same effect on the viscosity of the bitumen. This is mostly due to the presence of soybean oil within the pellets. Herein, the exact lignin content in pellets form is not 10 % since the pellets contain a portion of oil. The soybean oil is a low-density oil that dilutes the bitumen and decreases the viscosity caused by the addition of lignin in powder form in the bitumen. Also, the oil facilitates the movement of the bitumen molecules and reduces its density. The presence of soybean oil is expected to improve the workability and compactability of HMA. It should be noted that the only difference between the LDI and HDI pellets is the soybean oil content (5 and 10 %,

respectively). This difference is not significant enough to show consequences on the viscosity results of the bitumen.

*Step 4 (anti-oxidation properties)*

It is well known that the increase of the viscosity of bitumen is not only due to the addition of the modifiers, but also the aging process of the bitumen itself. In this context, it is interesting to see the behaviour of the aged lignin-modified bitumen. In other words, to see what happens when the modified bitumen gets aged and if the lignin behaves as an antioxidant product within the bitumen. Figure 5.5 shows the Viscosities (η) obtained from the BRV tests for the aged unmodified and modified bitumens with 5 and 10 % of HT SW A 1 lignin. According to the test standard, the test should be performed at 135 and 165 °C. In this study, the average temperature (150 °C) is used to see if the aging process will affect the normally linear viscosity-temperature relationship. As can be seen from Figure 5.5, the linear relationship can be observed which means that there is no effect of the aging on the normal viscosity-temperature relationship.

Generally speaking, increasing the aging level from 0 to 60 hours of PAV increased the viscosity of the bitumen which is expected due to the effect of the aging process itself. This leads to increase the construction temperatures, $T_{mix}$ and $T_{comp}$, of the bitumen in order to have coated aggregates and compactable HMA. However, in this study, these observations are due to not only the effect of the aging but also the effect of the lignin. It is interesting to see that the curves of the different bitumens at each aging level are grouped together (Figure 5.5). This means that the effect of aging is greater than the effect of lignin.

According to the location of the curves of the bitumens at 20 hours of PAV aging level, it can be seen that the modified bitumen with 10 % lignin has higher viscosity (472 mPa.s at 150 °C) than the modified bitumen with 5 % lignin (427 mPa.s at 150 °C) and the unmodified one (360 mPa.s at 150 °C) at the same aging level (20 hours of PAV). Comparing those bitumens at the unaged level (0-hour PAV), in addition to the effect of lignin, this increase in the viscosity can be due to the oxidation that occurs during the aging process. That being said that

both effects, lignin addition and aging, produce more viscous bitumen, resulting in more reduction in the movement of the bitumen molecules.

On the other hand, it is interesting to see that the modified bitumen with 10 % lignin at 40 hours of PAV aging level shows lower viscosity than the modified bitumen with 5 % lignin at the same aging level (755 and 810 mPa.s at 150 °C, respectively). It also shows the same trend at 60 hours of PAV aging level, even with bigger difference (1047 mPa.s at 150 °C for 10 % lignin and 1514 mPa.s at 150 °C for 5 % lignin). Herein, one possible hypothesis can be assumed for this observation is that the presence of lignin within bitumen creates a defense line to the aging effect, leading to protect the bitumen from being aged or retard the hardening effect resulted from the aging process. However, comparing the results for 0 % lignin with 5 and 10 %, lignin does not show the anti-oxidation properties.

Figure 5.6 shows the ratio of viscosity at 150 °C for all bitumens at different aging levels referenced to the unaged level (0 hours of PAV). It is interesting to see that the aging effect occurred at 40 and 60 hours of PAV is bigger than that at 20 hours of PAV. As can be seen, the modified bitumen with 5 % lignin shows the highest ratio among all bitumens. Accordingly, the use of 5 % lignin does not show anti-oxidative aging properties. For 10 % lignin, the ratio is slightly lower than that for the unmodified bitumen. However, based only on this, the use of lignin as antioxidant product cannot be stated with a confidence.

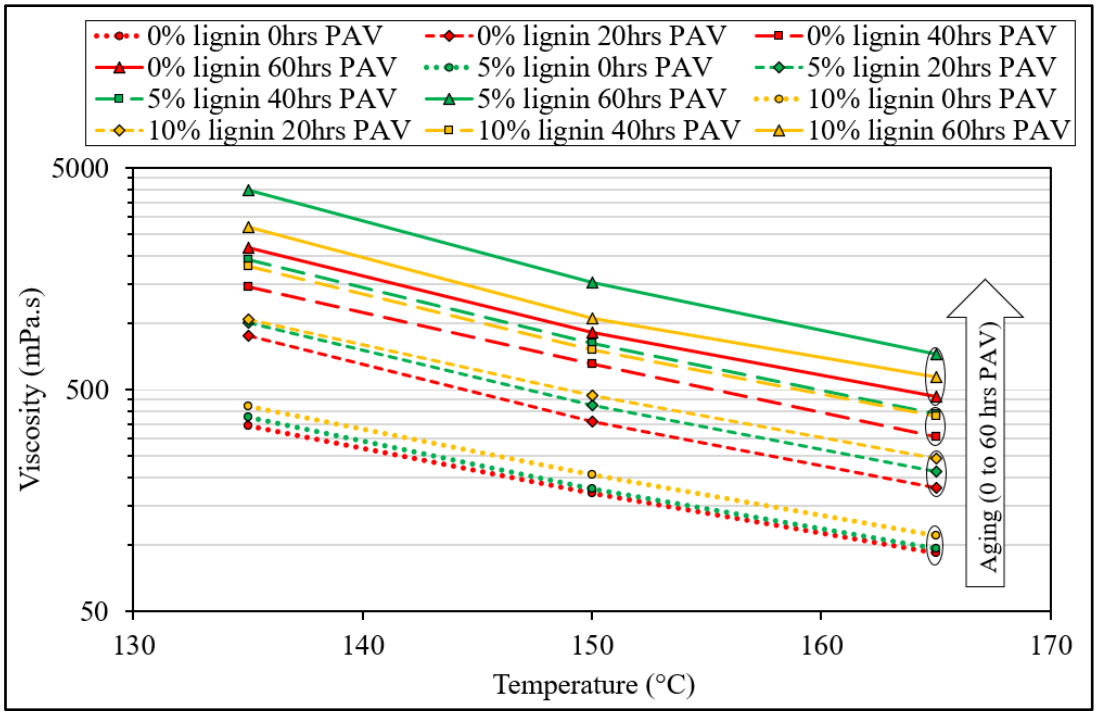


Figure 5.5 Viscosities (η) of the unmodified and modified bitumens with different contents of HT SW A 1 lignin at different aging levels

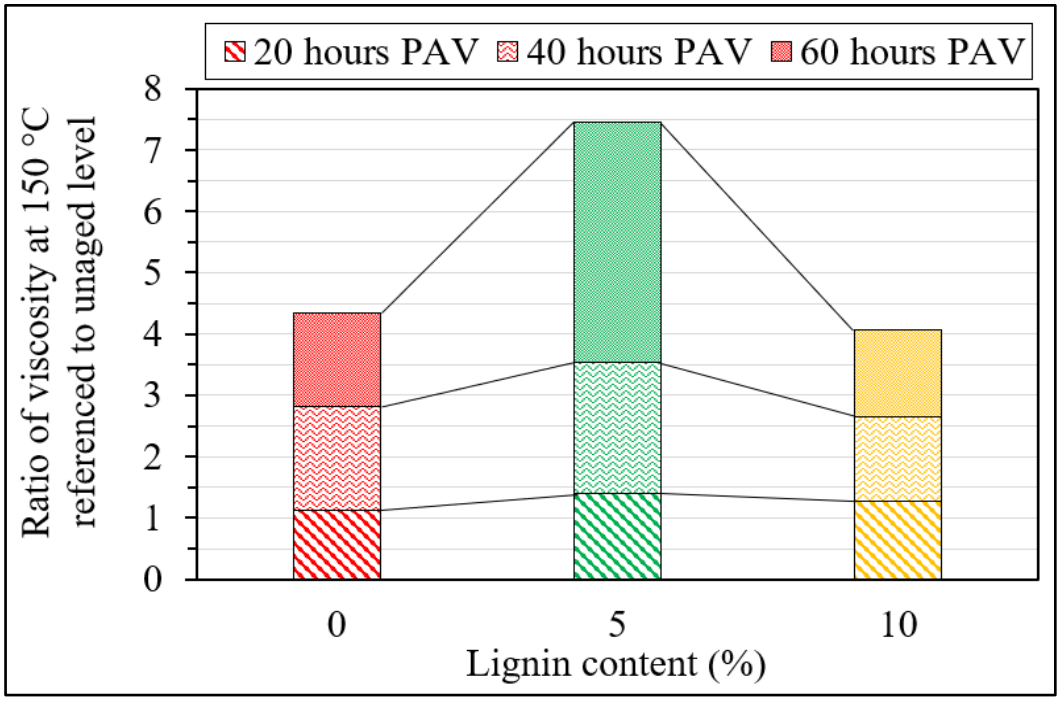


Figure 5.6 Ratio of viscosity at 150 °C of the unmodified and modified bitumens with different contents of HT SW A 1 lignin referenced to unaged level

Generally speaking, as presented in this section, the addition of lignin increases the viscosity of the bitumen. This effect varies according to the type of lignin. Using pellets decreases the viscosity of the bitumen which is due to the presence of the soybean oil. The aged lignin-modified bitumen shows higher viscosity than the unaged bitumen. However, the use of lignin within the bitumen does not show antioxidation properties. Higher lignin contents could be used to better investigate the use of lignin as an antioxidant product. Finally, according to the results, lignin changes the properties of the bitumen and, therefore, the behaviour. In this context, the stiffness of the bitumen is expected to be affected. DSR tests can be used to examine the effect of the addition of lignin on the bitumen's stiffness.

#### 5.2.1.2 DSR tests

This section shows the DSR results of the different steps. The effect of lignin on the high temperature performance of the bitumen is discussed firstly in general. Then, in more details for the results of each step are presented.

*General considerations*

Lignin increases the viscosity (η) of the bitumen, which results in stiffer bitumen. As mentioned before, the stiffness of the bitumen, a viscoelastic material, can be measured with the DSR. All lignins increase the $|G^*|/\sin(\delta)$ value of the bitumen except for the 10 % of HDI pellets type (Figure 5.7). Lignin addition shifted the high temperature ($T_{high}$) performance grade to higher temperature for which the $|G^*|/\sin(\delta)$ specification (1.0 kPa) is satisfied. Overall, the addition of lignin produced stiffer bitumen and higher viscosity (η) which results in an improvement of the performance at high temperatures.

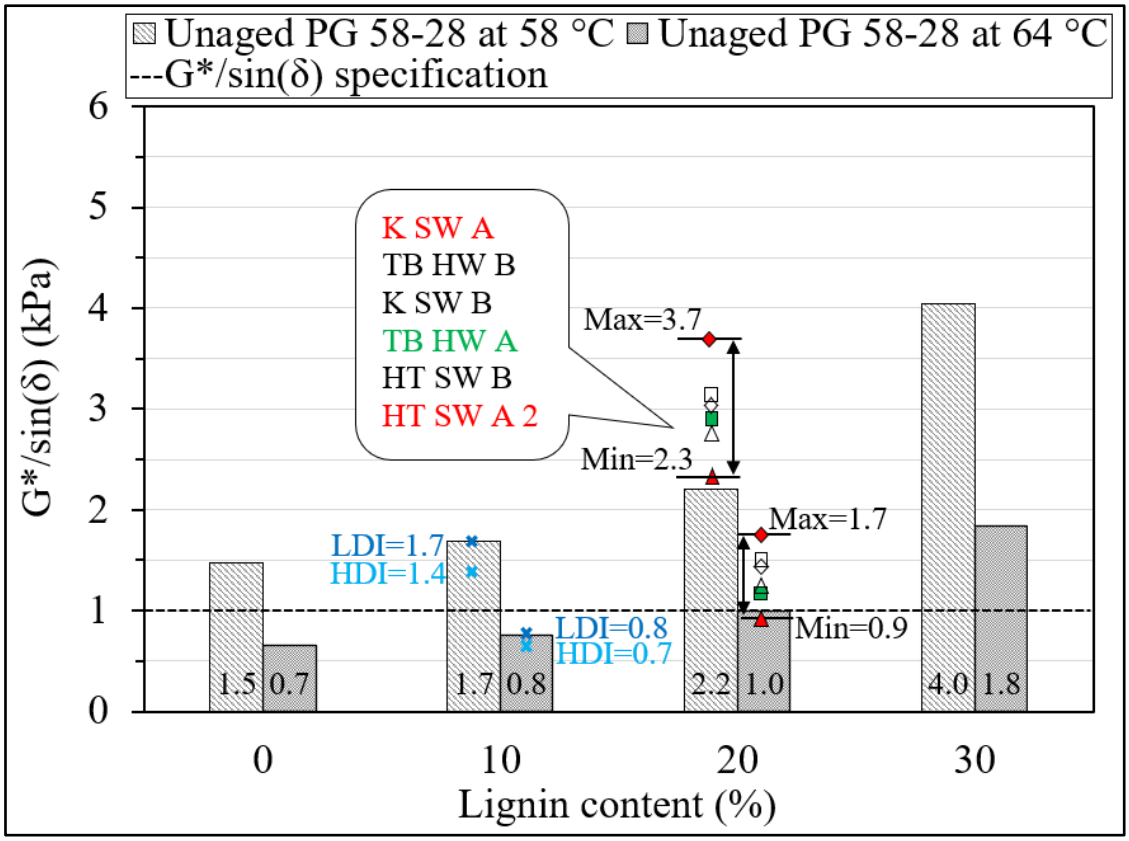


Figure 5.7 DSR test results for PG 58-28 with different HT SW A 1 lignin contents, 20 % of different lignins and 10 % of pellets

*Step 1 (effects of one lignin type on two bitumens)*

As can be seen from Figures 5.7 and 5.8, the effect of HT SW A 1 lignin on both PG 58S-28 and PG 52S-34 bitumens is roughly similar: the $|G^*|/\sin(\delta)$ value increases as the lignin content increases. The DSR test results ($|G^*|/\sin(\delta)$) are used to determine the $T_{high}$ of both bitumens (Table 5.6). It can be seen that using 20 and 30 % of lignin shifted $T_{high}$ to higher temperature for both bitumens, while it is not the case for 10 % lignin.

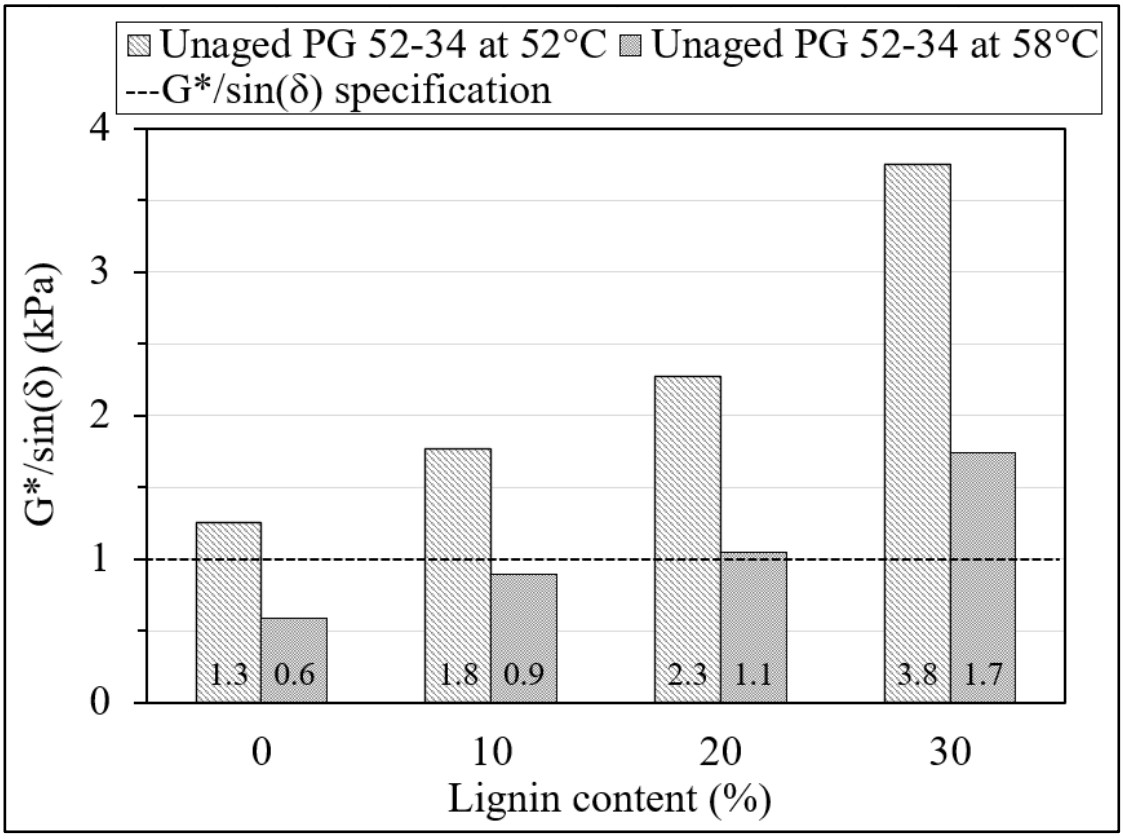


Figure 5.8 DSR test results for PG 52-34 with different HT SW A 1 lignin contents

Table 5.6 Specification and DSR test results for both bitumens modified with HT SW A 1 lignin

| Lignin content (%) | Values of $\|G^*\|/\sin(\delta)$ [a] and corresponding high temperature ($T_{high}$) | | | | | | | |
|---|---|---|---|---|---|---|---|---|
| | Bitumen PG 58S-28 | | | | Bitumen PG 52S-34 | | | |
| | At 58 °C (kPa) | Phase angle, δ (°) at 58 °C | At 64 °C (kPa) | $T_{high}$ [b] (°C) | At 52 °C (kPa) | Phase angle, δ (°) at 52 °C | At 58 °C (kPa) | $T_{high}$ [B] (°C) |
| 0 | 1.5 | 87.2 | 0.7 | 60.9 | 1.3 | 87.2 | 0.6 | 53.8 |
| 10 | 1.7 | 87.0 | 0.8 | 61.9 | 1.8 | 86.9 | 0.9 | 57.0 |
| 20 | 2.2 | 86.7 | 1.0 | 64.3 | 2.3 | 86.1 | 1.1 | 58.4 |
| 30 | 4.0 | 85.9 | 1.8 | 68.7 | 3.8 | 85.3 | 1.7 | 62.3 |

[a] Specification for $|G^*|/\sin(\delta)$ at the $T_{high}$=1 (kPa).
[b] $T_{high}$ is determined according to ASTM D 7643 standard.

Figure 5.9 shows the increase of $T_{high}$ (the $\Delta T_{high}$) with the HT SW A 1 lignin content for both bitumens. The $\Delta T_{high}$ of the lignin-modified PG 52S-34 is higher (0 to 8.5 °C) than the lignin-modified PG 58S-28 (0 to 7.8 °C) where the lignin content varies from 0 to 30 %, which means

that the stiffening effect of the lignin is slightly greater for the PG 52S-34, which has a lower viscosity. The trend observed here, for DSR, is the same trend as for the BRV tests results for the modified bitumens with HT SW A 1 lignin (greater effect on PG 52S-34 than PG 58S-28). The difference in the stiffening effect between both bitumens may be due to the different physical and chemical interactions with the lignin. In general, lignin changes the viscoelastic behaviour of the bitumen.

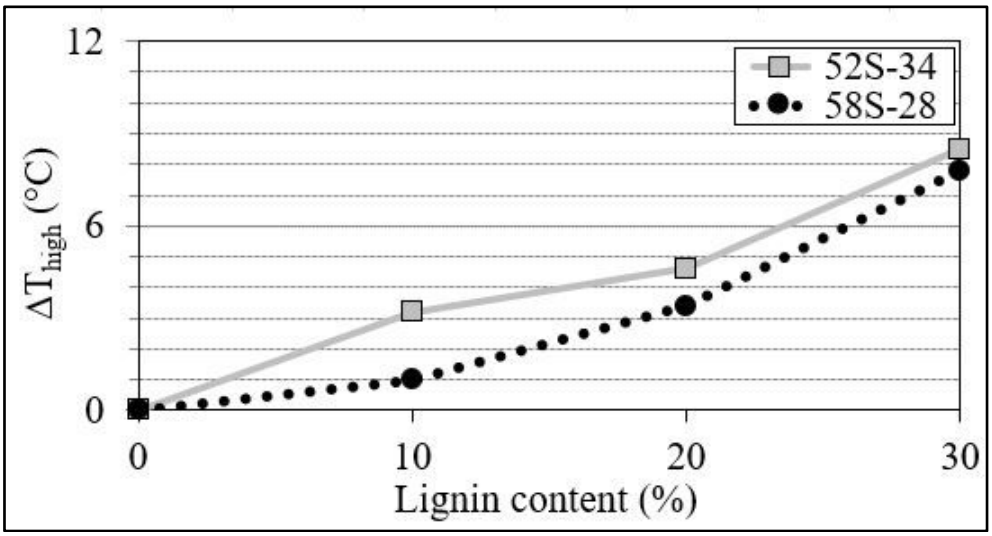


Figure 5.9 Increase of high temperature ($\Delta T_{high}$), compared to the bitumen with 0 % of lignin, according to the lignin content for both bitumens

*Step 2 (effects of different types of lignin)*

The different types of lignin increase the |G*|/sin (δ) value with different magnitudes. The increase is sufficiently important to result in a shift of $T_{high}$ to a higher temperature (from 58 to 64 °C) except for HT SW A 2 lignin. As observed for the BRV results, there is no clear tendency if the lignin supplier or the type of wood or pH has more influence on the |G*|/sin (δ) value. The variation of |G*|/sin (δ) values between different lignins is higher than what is observed for 0 to 20 % of HT SW A 1 lignin only. It is interesting to see that the increase in |G*|/sin (δ) follows the same order as for the viscosity results (e.g. K SW A lignin shows the highest |G*|/sin (δ) value and highest viscosity results). Therefore, the combination of bitumen PG 58S-28 and K SW A lignin is expected to show the best rutting performance.

The DSR tests on the HT SW A-modified and K SW A-modified lignins are not presented here due to the abnormal and out of the ordinary results. This is strongly related to the presence of the big solid particles, compared to powder, of lignin on the DSR plate (Figure 5.10). This observation raises doubts about the results, including the representativeness issue and questionable results.

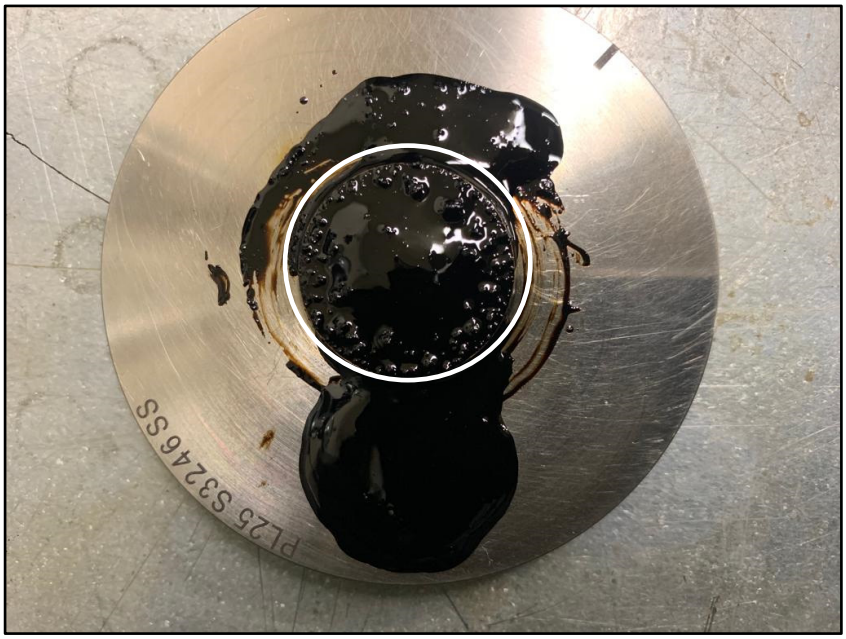


Figure 5.10 A photo shows the particles of HT SW A-modified lignin on the plate used for the DSR test

*Step 3 (effects of pellets)*

As can be seen from Figure 5.7, the modified bitumens with 10 % of each pellets type show similar |G*|/sin (δ) values than the unmodified bitumen. Also, those values for 10 % pellets are similar to those for 10 % of HT SW A 1 lignin in powder form. This includes small variation of |G*|/sin (δ) values for 10 % pellets compared to 10 % of HT SW A 1 lignin in powder form. This observation is a little different from what is observed for the BRV tests results. However, it is worth mentioning that the modified bitumen with LDI pellets (5 % soybean oil) is slightly stiffer than that with HDI pellets (10 % soybean oil). Therefore, the content of the soybean oil affects not only the durability of the pellets, but also the stiffness of the bitumen. Both modified bitumens remain in the same high temperature PG (58 °C) as the unmodified one. This can be

due to the presence of soybean oil that dilutes the bitumen. Therefore, the rutting performance at high temperature will not be significantly improved compared to the unmodified bitumen. However, the effect of the pellets type is clearer, here with DSR, than with BRV.

*Step 4 (anti-oxidation properties)*

Figure 5.11 shows the values of |G*|/sin (δ) obtained from the DSR tests at different temperatures for the unaged and aged-unmodified and modified bitumens with 5 and 10 % of HT SW A 1 lignin. It can be seen, as expected, that all bitumens show higher values of |G*|/sin (δ), at a specific temperature, with the increase of the aging level. This leads to increase the high temperature PG from 58 to 82 °C for all bitumens except for those tested at 82 °C with 20 hours of PAV aging level. This indicates that the rutting performance for the aged bitumens is better than that for the unaged ones. However, the modified bitumens show higher |G*|/sin (δ) values than the unmodified bitumen at all aging levels. It is important to note that the hardening effect due to the lignin addition is completely negligible compared to the effect of aging.

Both lignin contents (5 and 10 %) show higher |G*|/sin (δ) values than the bitumen without lignin (0 %). It is interesting to look at the ratio of these values at different levels of aging. Figure 5.12 shows the ratio of |G*|/sin (δ) values at 58 °C for all bitumens at different aging levels referenced to the unaged level (0 hours of PAV). This temperature (58 °C) is chosen since it is the high temperature PG of the bitumen used. However, it should be noted that the ratio at the other testing temperatures shown in Figure 5.12 is checked and it shows the same trend as 58 °C. It can be seen that the difference in this ratio is not significant between all bitumens at 20 hours of PAV aging level. The ratio at 40 hours of PAV is bigger compared to 20 hours of PAV. At 60 hours of PAV, the ratio is much greater than that at 20 and even 40 hours of PAV. This means that the rate of increase of the aging (oxidation) increases at higher aging levels. This observation is the same as what is observed for BRV tests. As can be seen, comparing the ratio values for 0 % lignin with those for 5 and 10 %, the lignin does not show anti-oxidative aging properties within bitumen.

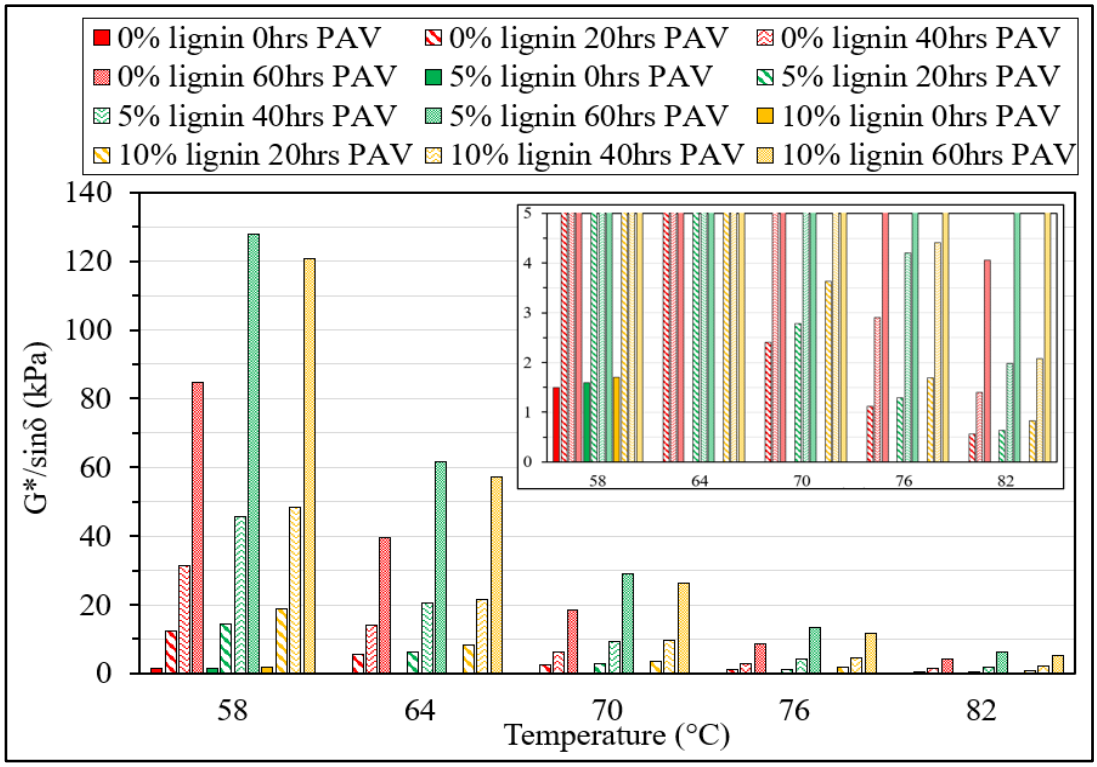


Figure 5.11 G*/sin (δ) values at different temperatures for the bitumen modified with different contents of HT SW A 1 lignin at different aging levels

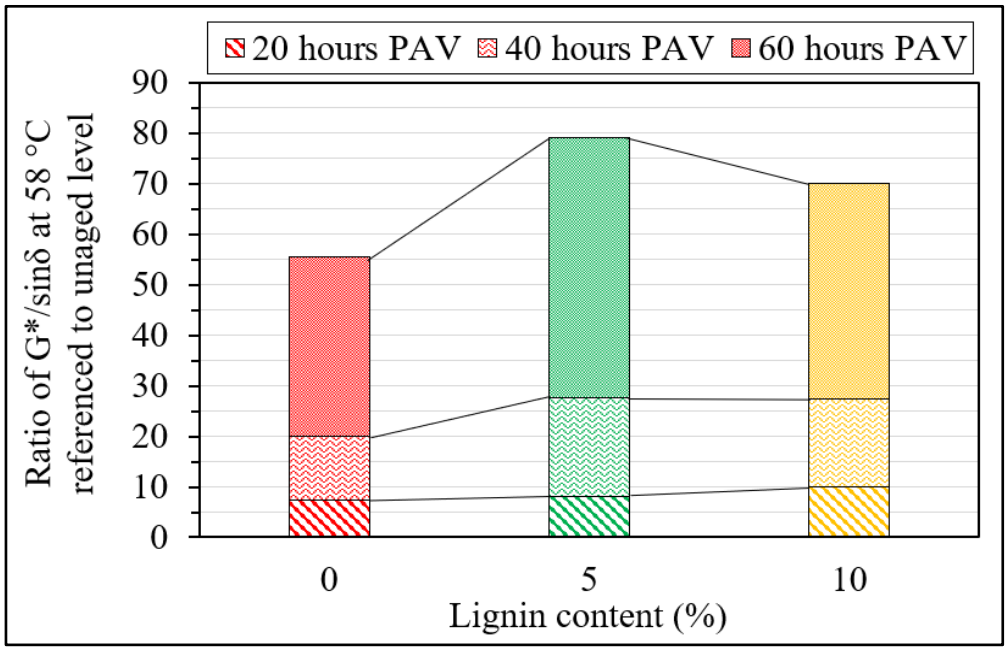


Figure 5.12 Ratio of G*/sin (δ) at 58 °C of the bitumen modified with different contents of HT SW A 1 lignin referenced to unaged level

Overall, the effect of lignin on the stiffness (DSR results) of the bitumen follows the same trend as for the viscosity (BRV results), including an increase of the bitumen's stiffness. This includes the effect of different types of lignin in powder form on the unaged bitumen, pellet-modified bitumen and antioxidative aging properties. However, despite the fact that the |G*|/sin (δ) parameter is the rutting parameter in SHRP (Xu et al., 2017), conducting MSCR test is needed since it evaluates the permanent deformation resistance of the bitumen under loading and the relaxation time which better characterizes the accumulated permanent strain, the rutting, that is associated with the stress levels (0.1 and 3.2 kPa). The phase angle (δ) values for the modified bitumen with HT SW A 1 lignin presented in Table 5.6 are shown at only the H temperature grade of bitumen (58 or 52 °C) to help in the interpretation of MSCR tests results. It is well known that the phase angle (δ) increases as the temperature increases and, however, the lower it is, the more elastic the bitumen behaves, which is beneficial in reducing permanent deformation (or rutting).

#### 5.2.1.3 MSCR tests

This section shows the MSCR tests results of the different steps. The effect of lignin on the bitumen resistance to permanent deformation is discussed firstly in general. Then, more details for the results of each step are presented.

*General considerations*

Lignin increases the stiffness of the bitumen, |G*|/sin (δ) value from DSR test, which will affect the rutting performance. The non-recoverable creep compliance ($Jnr_{3.2}$) values are obtained with MSCR tests for the bitumen PG 58S-28 modified with different contents of HT SW A 1 lignin and are shown in Figures 5.13. It can be seen that all lignins decrease $Jnr_{3.2}$ value except for the 10 % HDI pellets. This indicates better resistance of the bitumen to permanent deformation. Accordingly, lignin improves the rutting performance at high temperature. This finding is in accordance with the study by Zhang et al. (2022).

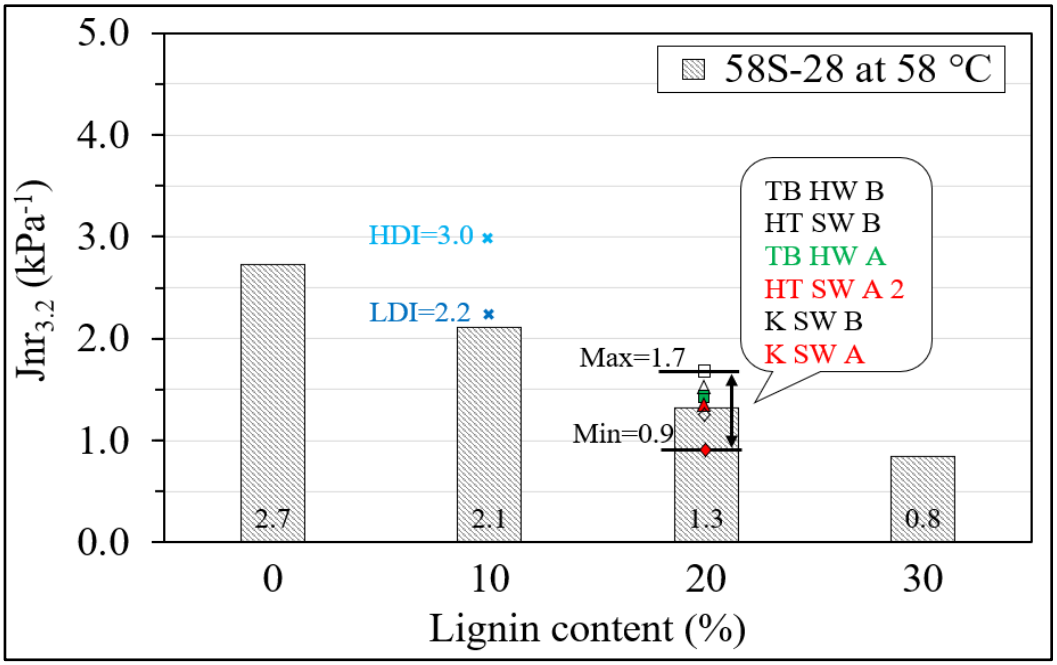


Figure 5.13 $Jnr_{3.2}$ values at 58 °C for PG 58-28 with different HT SW A 1 lignin contents, 20 % of different lignins and 10 % of pellets

*Step 1 (effects of one lignin type on two bitumens)*

Figure 5.14 shows the $Jnr_{3.2}$ values for the bitumen PG 52S-34 modified with different contents of HT SW A 1 lignin. As can be seen, the $Jnr_{3.2}$ value decreases as lignin content increases which is the same trend observed for the PG 58S-28 bitumen. The difference in non-recoverable creep compliance between 0.1 and 3.2 kPa ($Jnr_{diff}$), the average recovery of strain ($R_{3.2}$) and the traffic level (n) values for both bitumens are presented in Table 5.7. Based only on $Jnr_{3.2}$: the unmodified bitumens and lignin-modified bitumens with 10 % lignin have a standard (S) resistance to traffic. Lignin-modified bitumens with 20 % and 30 % lignin have a heavy (H) and very heavy (V) resistance to traffic, respectively. Nevertheless, if all test parameters are considered, all bitumens will have standard (S) resistance to traffic (Table 5.7). For both modified bitumens with 20 and 30 % of lignin, the tests should have been performed at 64 °C, for PG 58S-28, and 58 °C, for PG 52S-34, according to the results obtained by the DSR tests (see Table 5.6). As shown by Cardone et al. (2015), increasing the temperature will increase the $Jnr_{3.2}$ value. In this regard, the traffic level "n" class obtained for the $Jnr_{3.2}$ (H and V) are surely overestimated.

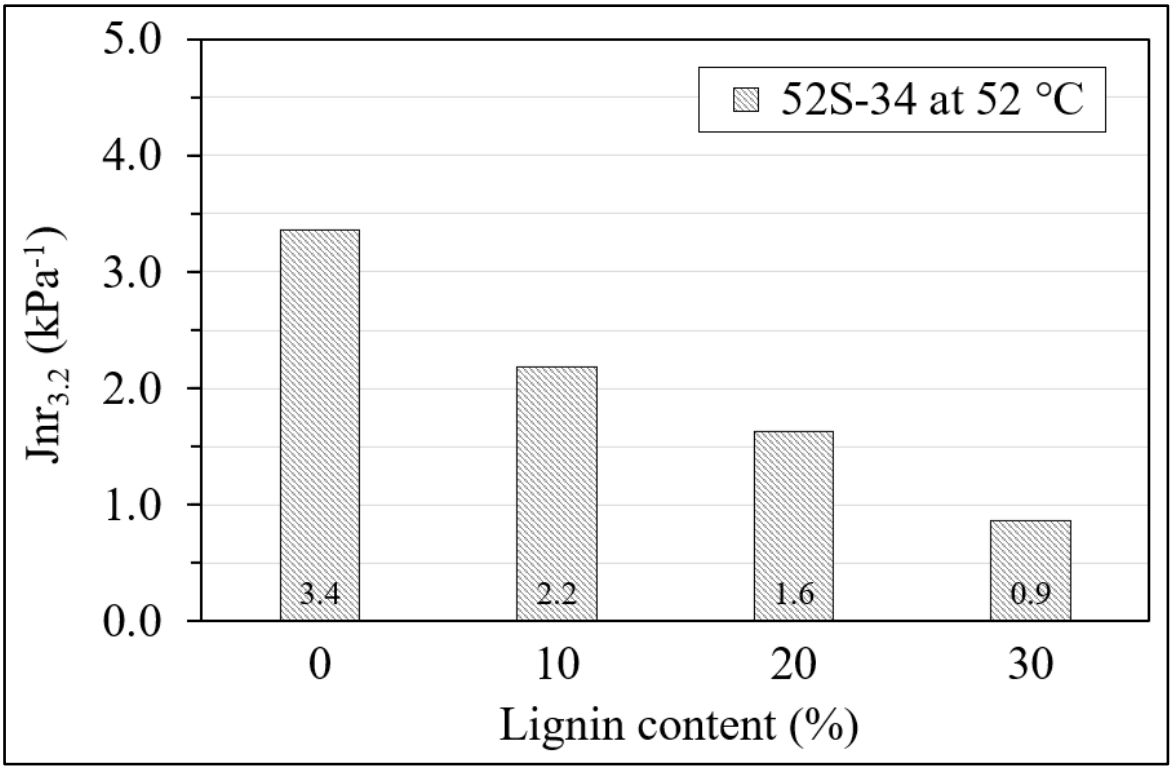


Figure 5.14 $Jnr_{3.2}$ values at 52 °C for PG 52-34 with different HT SW A 1 lignin contents

Table 5.7 MCSR test results, requirements and traffic level (n) class obtained for both bitumens

| Lignin content (%) | Bitumen PG 58S-28 | | | | Bitumen PG 52S-34 | | | |
|---|---|---|---|---|---|---|---|---|
| | MSCR at 58 °C [a] | | | | MSCR at 52 °C [a] | | | |
| | $Jnr_{3.2}$ ($kPa^{-1}$) | $Jnr_{diff}$ (%) | $R_{3.2}$ (%) | $n_{obtained}$ (letter) | $Jnr_{3.2}$ ($kPa^{-1}$) | $Jnr_{diff}$ (%) | $R_{3.2}$ (%) | $n_{obtained}$ (letter) |
| 0 | 2.73 ≤ 4,5 (S) | 12.5 (ok) | 0.5 [b] (S) | S | 3.36 ≤ 4,5 (S) | 15.8 (ok) | 0 (S) | S |
| 10 | 2.11 ≤ 4,5 (S) | 14.0 (ok) | 0.5 [b] (S) | S | 2.18 ≤ 4,5 (S) | 14.5 (ok) | 0.6 (S) | S |
| 20 | 1.32 ≤ 2.0 (H) | 12.8 (ok) | 1.0 [b] (S) | S | 1.63 ≤ 2.0 (H) | 14.9 (ok) | 1.1 (S) | S |
| 30 | 0.84 ≤ 1.0 (V) | 12.9 (ok) | 0.8 [b] (S) | S | 0.86 ≤ 1.0 (V) | 16.3 (ok) | 0.8 [b] (S) | S |

[a] Tests performed at the high temperature grade (H).
[b] Due to the very low values for $R_{3.2}$, it is possible to put the bitumen only in traffic level "Standard" class.

When combining and analyzing the MSCR results with the DSR's, the addition of lignin increases the stiffness (Table 5.6: DSR results) and does not significantly change the capacity to recover at high stress level, which means a small increase in the resistance to permanent

deformation of the bitumen. This is in accordance with what is observed in a few studies (Gao et al., 2020; Pérez et al., 2020; Zhang et al., 2019) which is that the addition of lignin means a better performance at high temperature.

*Step 2 (effects of different types of lignin)*

Regarding the effects of the different lignin types, the resistance to permanent deformation is improved with different levels. There is no clear pattern if the lignin producer or wood type or pH shows more influence on the bitumen resistance to permanent deformation. On the contrary to what is observed for the DSR tests results, the variation of $Jnr_{3.2}$ values for using different types of lignin is lower than that for using of 0 to 20 % of HT SW A 1 lignin. As observed for the DSR tests, the combination of bitumen PG 58S-28 and K SW A lignin shows the lowest $Jnr_{3.2}$ value. Therefore, this combination has the highest capacity of the resistance to permanent deformation. Finally, the effect of the type of lignin is less visible with the MSCR test than with the DSR test.

*Step 3 (effects of pellets)*

It can be seen from Figure 5.13 that the type of pellets has an impact on the bitumen resistance to permanent deformation. The 10 % HDI pellets shows higher $Jnr_{3.2}$ value than the 10 % LDI pellets. This highlights the key role of the soybean oil that reduces the resistant to permanent deformation of the bitumen by diluting it. This means that the lignin in pellets form shows a different trend from what is observed for the powder form.

*Step 4 (anti-oxidation properties)*

Regarding the antioxidative aging properties, when the bitumen ages, it shows higher stiffness (DSR results) and, therefore, its resistance to permanent deformation (MSCR results) is improved. Figure 5.15 shows the values of $Jnr_{3.2}$ parameter obtained from the MSCR tests at different temperatures, same as those that are used for the DSR tests, for the aged unmodified and modified bitumens with 5 and 10 % of HT SW A 1 lignin. Based on what is seen from BRV and DSR tests (big part of the aging effect occurs at high PAV aging levels), it possible

to evaluate the antioxidative aging properties of lignin considering the 20 hours of PAV aging level as a reference.

At a specific temperature, the $Jnr_{3.2}$ values for the aged lignin-modified bitumens are lower than those for the unmodified bitumen. Therefore, the combination of the effects of aging and lignin indicates superior resistance to the permanent deformation at high temperatures. However, comparing 0 % lignin with 5 and 10 %, lignin does not show anti-oxidation properties.

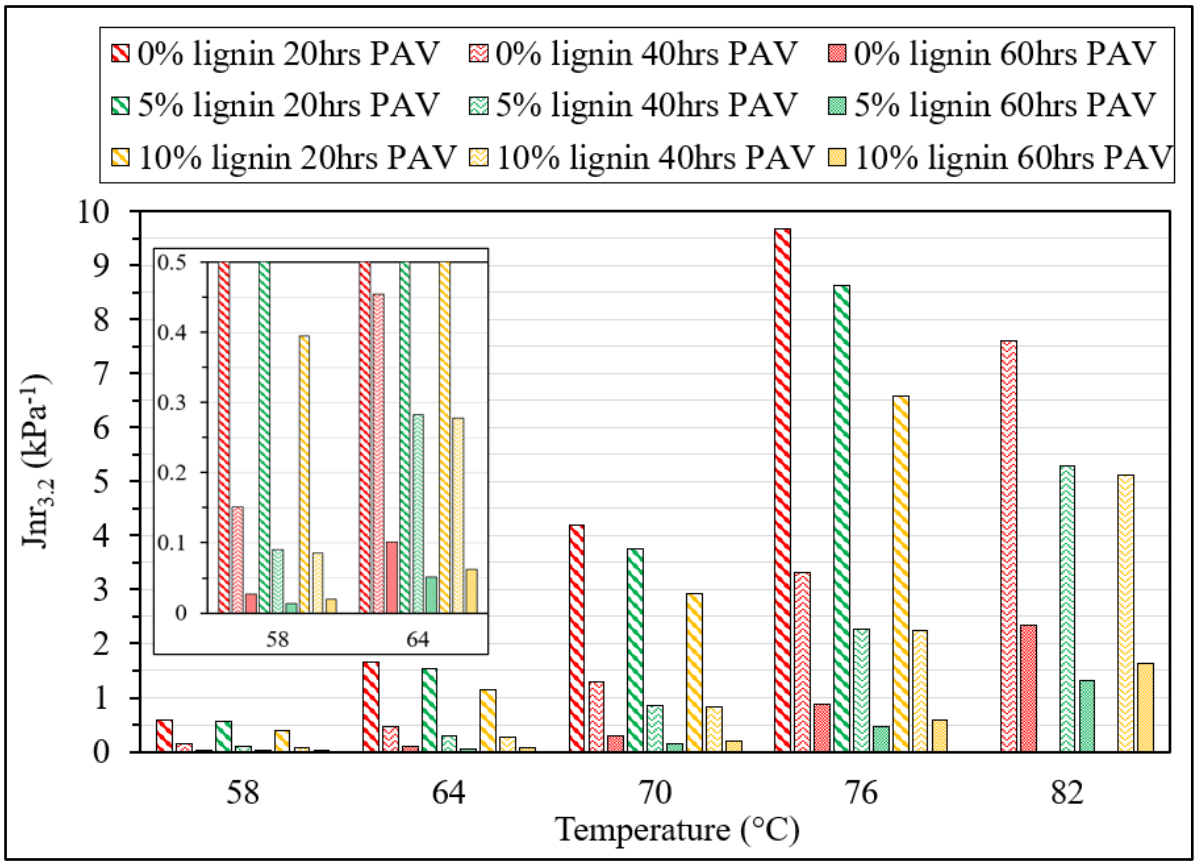


Figure 5.15 $Jnr_{3.2}$ values at different temperatures for the unmodified and modified bitumens with different contents of HT SW A 1 lignin at different aging levels

According to the presented results in this section, lignin increases the resistance to permanent deformation of the bitumen. As mentioned before, this increase differs according to the type of lignin. For the pellet-modified bitumen, the presence of the soybean oil affects the resistance

to permanent deformation. Regarding the antioxidative aging properties for the lignin-modified bitumen and comparing it with the unmodified one, using lignin does not show anti-oxidation properties. Finally, since lignin improves the high temperature performance, replacing part of the bitumen by lignin would be beneficial. However, investigating the effect of lignin on the bitumen at low temperature would be interesting. In particular, to see if lignin shows the same trend as for the tests at high temperature.

#### 5.2.1.4 BBR tests

This section shows the BBR tests results of the different steps. The effect of lignin on the low temperature performance of the bitumen is discussed firstly in general. Then, more details for the results of each step are presented.

*General considerations*

The stiffness and the relaxation characteristics at low temperature of the bitumen are indicators for the low temperature performance. Figures 5.16 and 5.17 show stiffness (S(60)) and slope (m(60)) values, respectively, for the bitumen PG 58S-28 modified with different contents of HT SW A 1 lignin, 20 % of different lignins and 10 % of pellets. As can be seen, all lignins increase the stiffness of the bitumen and decrease the relaxation properties except for the HDI pellets where the trend is slightly different. In general, the lignin-modified bitumens are stiffer and less able to dissipate the thermal stresses, and therefore are more fragile at low temperatures and have less resistance to the thermal cracking compared to the unmodified bitumen. The lignin addition shifts the low temperature ($T_{low}$) to higher temperature. These findings are in accordance with Batista et al. (2018), Wu et al. (2021) and Yu et al. (2021).

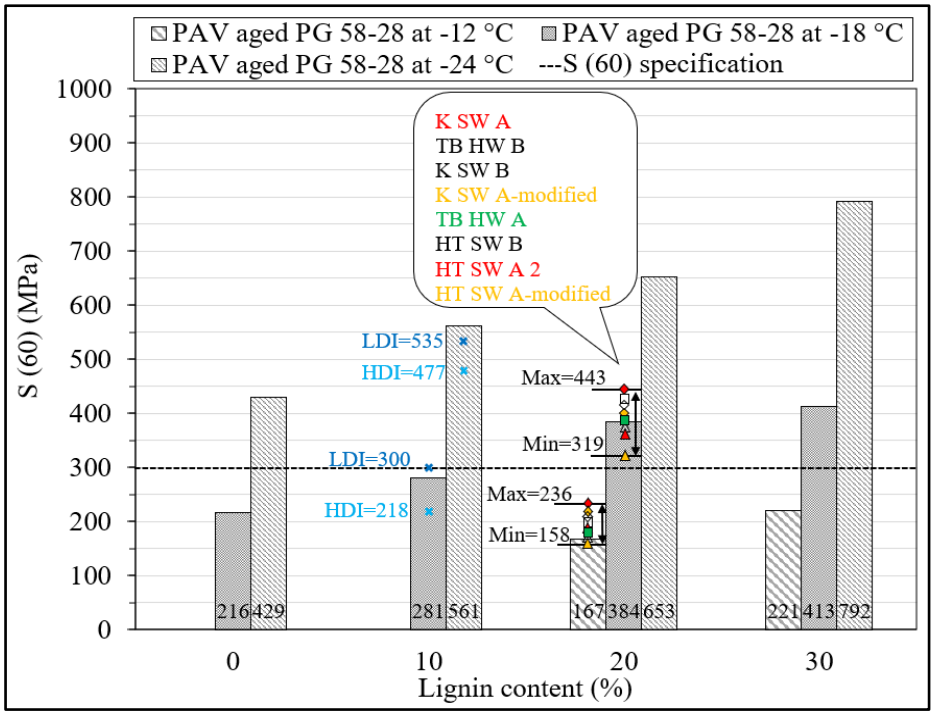


Figure 5.16 Stiffness values for PG 58S-28 with different HT SW A 1 lignin contents, 20 % of different lignins and 10 % of pellets

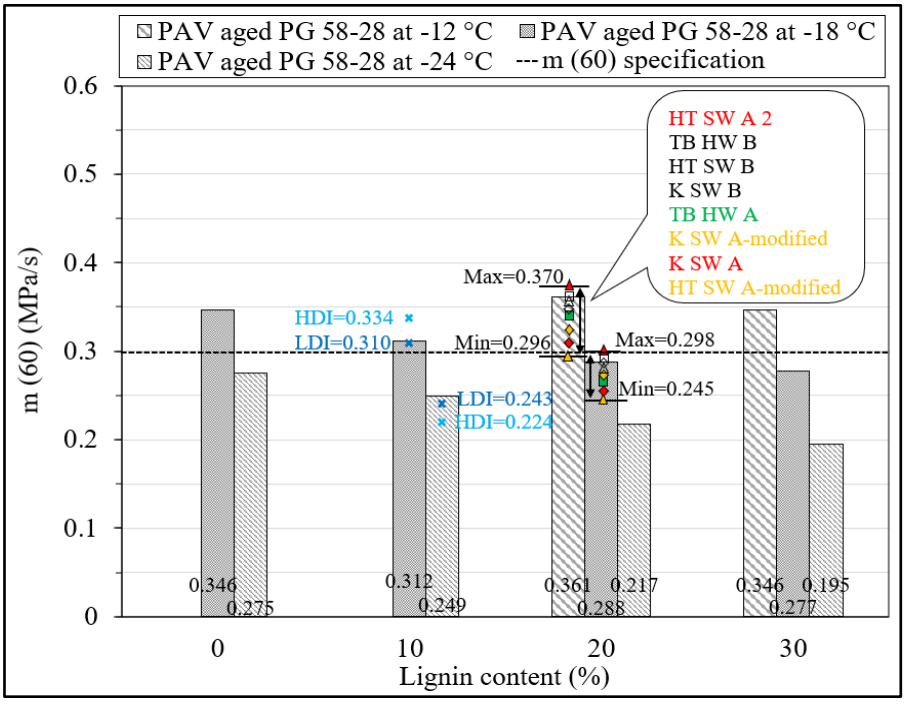


Figure 5.17 Slope values for PG 58S-28 with different HT SW A 1 lignin contents, 20 % of different lignins and 10 % of pellets

*Step 1 (effects of one lignin type on two bitumens)*

Figures 5.18 and 5.19 show stiffness (S(60)) and slope (m(60)) values, respectively, for the bitumen PG 52S-34 modified with different contents of HT SW A 1 lignin. As can be seen for PG 58S-28 and PG 52S-34 bitumens, as the lignin content increases, the creep stiffness, S(60), increases, and the relaxation parameter, m(60), decreases. Table 5.8 shows the $T_{low}$ values according to S(60) and m(60) values obtained with the BBR for the modified bitumen with HT SW A 1 lignin, averaged from two or three repetitions of the test at each temperature. All lignin-modified bitumens PG 52S-34 are shifted to higher grade (-28 °C) in addition to modified bitumens PG 58S-28 with 20 % and 30 % of lignin (-22 °C). As shown by Badeli et al. (2018), the resistance to thermal cracking of the bituminous materials depends mainly on the low temperature PG of the bitumen.

Considering the determined $T_{low}$ (Table 5.8) of lignin-modified bitumen, a negative impact on the low temperature performance of the bituminous materials is possible. Figure 5.20 shows the increase of $T_{low}$ (the $\Delta T_{low}$) with the lignin content for both bitumens. The $\Delta T_{low}$ is similar for both bitumens (Figure 5.20: varies from 0.0 to 6.1 °C with the lignin content). This means that the effect of lignin is similar for both bitumens.

In general, in terms of PG classification, the tests results performed at high temperatures (BRV, DSR and MSCR) exhibit slightly more pronounced differences compared to what is observed here at low temperature (BBR). This indicates that the behaviour at low temperature is mostly controlled by the bitumen.

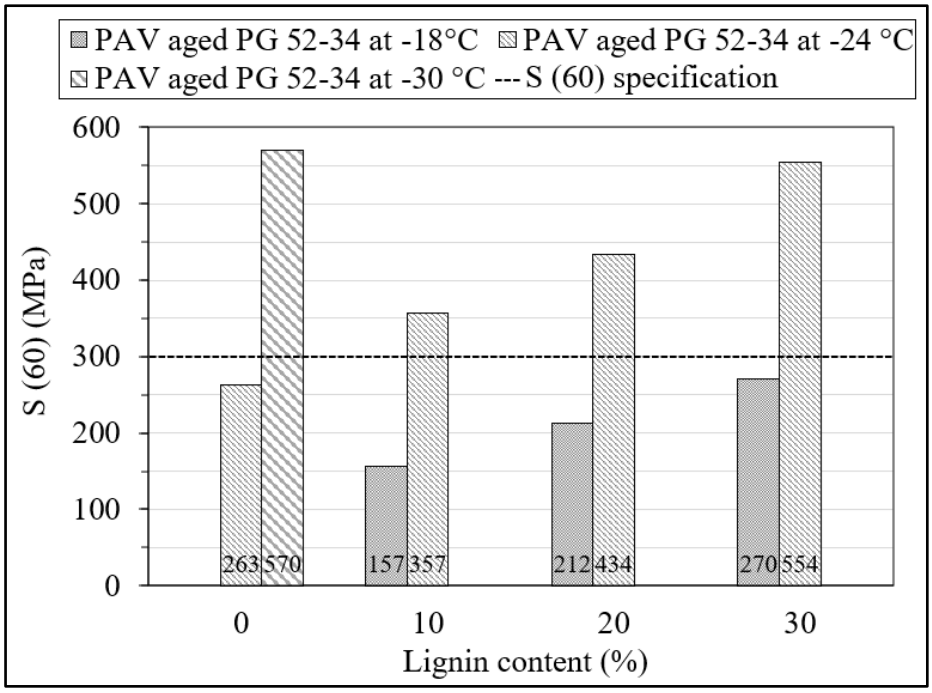


Figure 5.18 Stiffness values for PG 52S-34 with different HT SW A 1 lignin contents

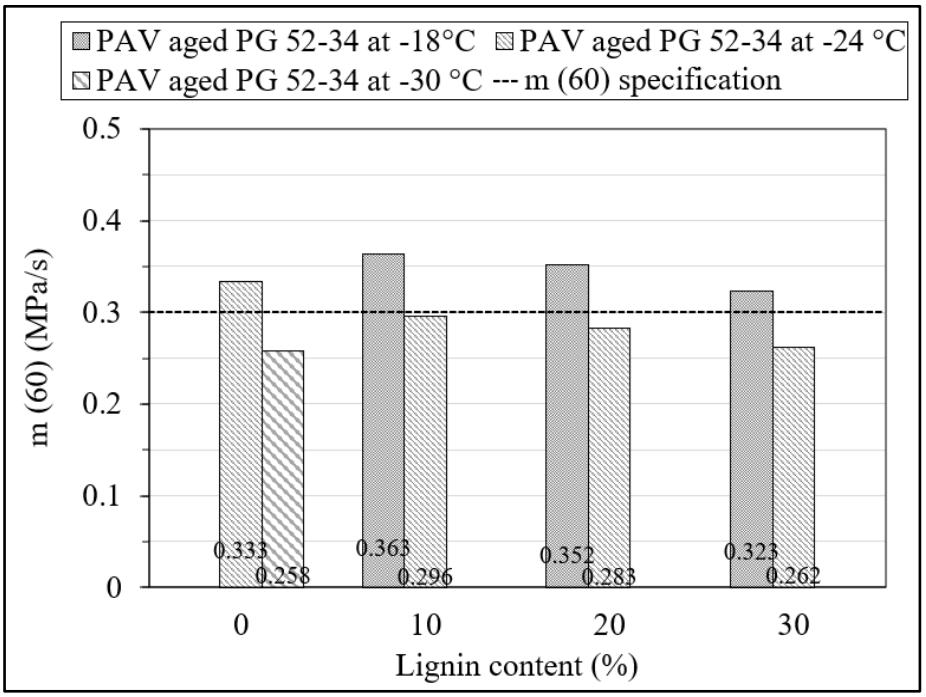


Figure 5.19 Slope values for PG 52S-34 with different HT SW A 1 lignin contents

Table 5.8 Specifications and BBR test results for both bitumens with different HT SW A 1 lignin contents

| Lignin content (%) | $T_T$ [A] (°C) | Bitumen PG 58S-28 | | | Bitumen PG 52S-34 | | | Specifications |
|---|---|---|---|---|---|---|---|---|
| | | S(60) (MPa) | m(60) (MPa/s) | $T_{low}$ [B] (°C) | S(60) (MPa) | m(60) (MPa/s) | $T_{low}$ [B] (°C) | |
| 0 | -30 | --- | --- | --- | 570 | 0.258 | -35.0 | S(60) ≤ 300 and m(60) ≥ 0.3 |
| | -24 | 429 | 0.275 | -30.9 | 263 | 0.333 | -36.6 | |
| | -18 | 216 | 0.346 | -31.9 | --- | --- | --- | |
| 10 | -24 | 561 | 0.249 | -28.6 | 357 | 0.296 | -32.7 | |
| | -18 | 281 | 0.312 | -29.1 | 157 | 0.363 | -33.6 | |
| 20 | -24 | 653 | 0.217 | -26.2 | 434 | 0.283 | -30.9 | |
| | -18 | 384 | 0.288 | -27.0 | 212 | 0.352 | -32.5 | |
| | -12 | 167 | 0.361 | --- | --- | --- | --- | |
| 30 | -24 | --- | --- | --- | 554 | 0.262 | -28.9 | |
| | -18 | 413 | 0.277 | -24.9 | 270 | 0.323 | -30.3 | |
| | -12 | 221 | 0.346 | -26.0 | --- | --- | --- | |

[A] Through correlations, it was determined that it was possible to test the bitumen at a temperature 10°C above the target temperature as specified in the standard.

[B] Determined the two $T_{low}$ based on S(60) and m(60) according to ASTM D 7643 standard [29].
The highest $T_{low}$ value is used (underlined value) for the PG classification.

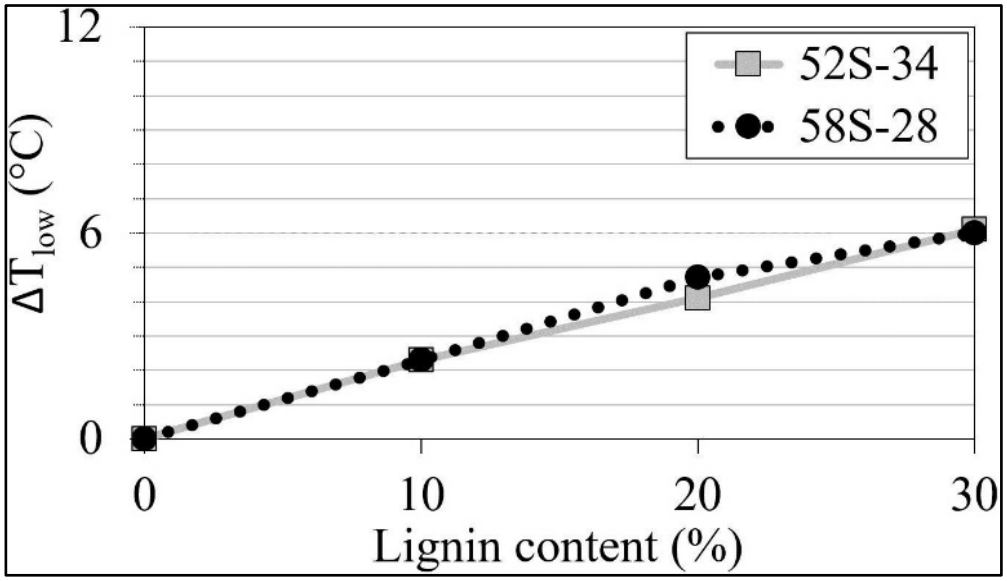


Figure 5.20 Increase of low temperature ($\Delta T_{low}$), compared to the bitumen with 0 % of lignin, according to the lignin content for both bitumens

*Step 2 (effects of different types of lignin)*

The different types of lignin have different stiffening effect on the bitumen. Regarding the variation of S(60) and m(60) values, it is lower for the use of different types of lignin than that for the use of 0 to 20 % of HT SW A 1 lignin (Figures 5.16 and 5.17). There is no clear pattern weather the lignin supplier or the wood type or pH has more impact on the stiffness and relaxation properties of the bitumen. The low temperature PG of all modified bitumens increases to higher temperature (from -28 to -22 °C). It is interesting to see that the combination of bitumen PG 58S-28 and K SW A lignin still show the highest stiffness which indicates the worst low temperature performance among the other lignin-modified bitumens. The effect of lignin type is less visible here in the BBR than that with the DSR. However, due to the observation in Figure 5.10 that leads to not test the HT SW A-modified and K SW A-modified lignins for the DSR and MSCR tests, the results from the BBR tests need to be verified by performing more tests with more repetitions.

*Step 3 (effects of pellets)*

The HDI pellets show different trend from the LDI pellets which is due to the presence of higher content of the soybean oil that dilutes the bitumen. Herein, the oil decreases the stiffness of the bitumen at low temperature and increases the relaxation properties. So, the HT SW A 1 lignin in pellets form, compared to the powder form, improves the ability of the bitumen to dissipate the thermal stresses and increases the resistance to the thermal cracking. It is interesting to see that the low temperature PG for the HDI pellets remains at -28 °C, while for the LDI pellets, it increases to higher temperature (-22 °C). More work is required to understand the results obtained here.

*Step 4 (antioxidation properties)*

Figures 5.21 and 5.22 show, respectively, the stiffness (S(60)) and slope (m(60)) values at different temperatures (-12, -18 and -24 °C) obtained from the BBR tests for the aged unmodified and modified bitumen with different contents (5 and 10 %) of HT SW A 1 lignin. The 20 hours of PAV aging level is used as a reference in order to evaluate the antioxidative aging properties of lignin at low temperature (based on BRV and DSR tests: big part of the

aging effect occurs at high PAV aging levels). It can be seen that the stiffness, at a specific temperature, of all bitumens increases as the aging level and lignin content increase. It should be noted that the effect of lignin addition itself seems not negligible in comparison to the effect of aging, especially for S(60). It is interesting to see that there is a smaller shift, for each bitumen, to higher low temperature PG of the bitumen compared to that observed at the high temperature PG. Both effects, aging and lignin addition, reduce the ability of the bitumen to dissipate the thermal stresses. In comparison with what is observed at high temperature, the effect of lignin and aging is limited at low temperature which is due to the statues of the bitumen where the matrix of bitumen molecules is frozen. Combining both parameters of the BBR tests, S(60) and m(60), lignin does not show antioxidative aging properties on the bitumen at low temperature.

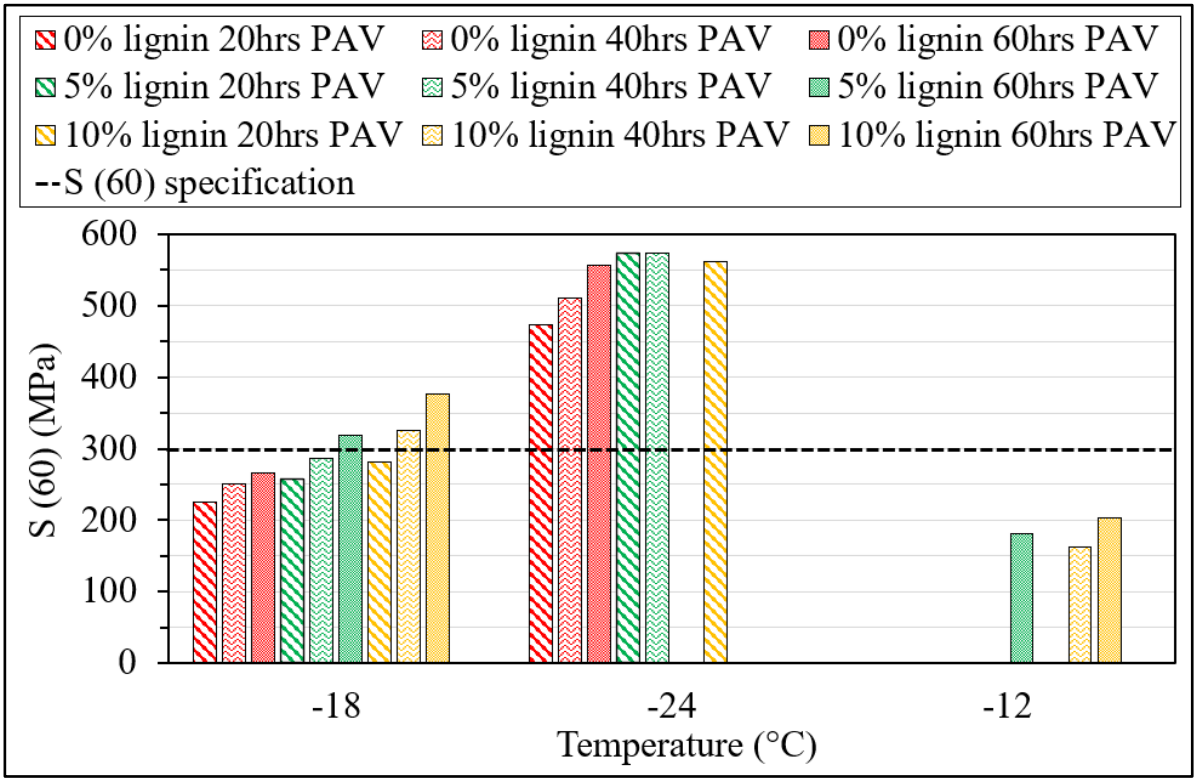


Figure 5.21 Stiffness (S(60)) values at different temperatures for the unmodified and modified bitumens with different contents of HT SW A 1 lignin at different aging levels

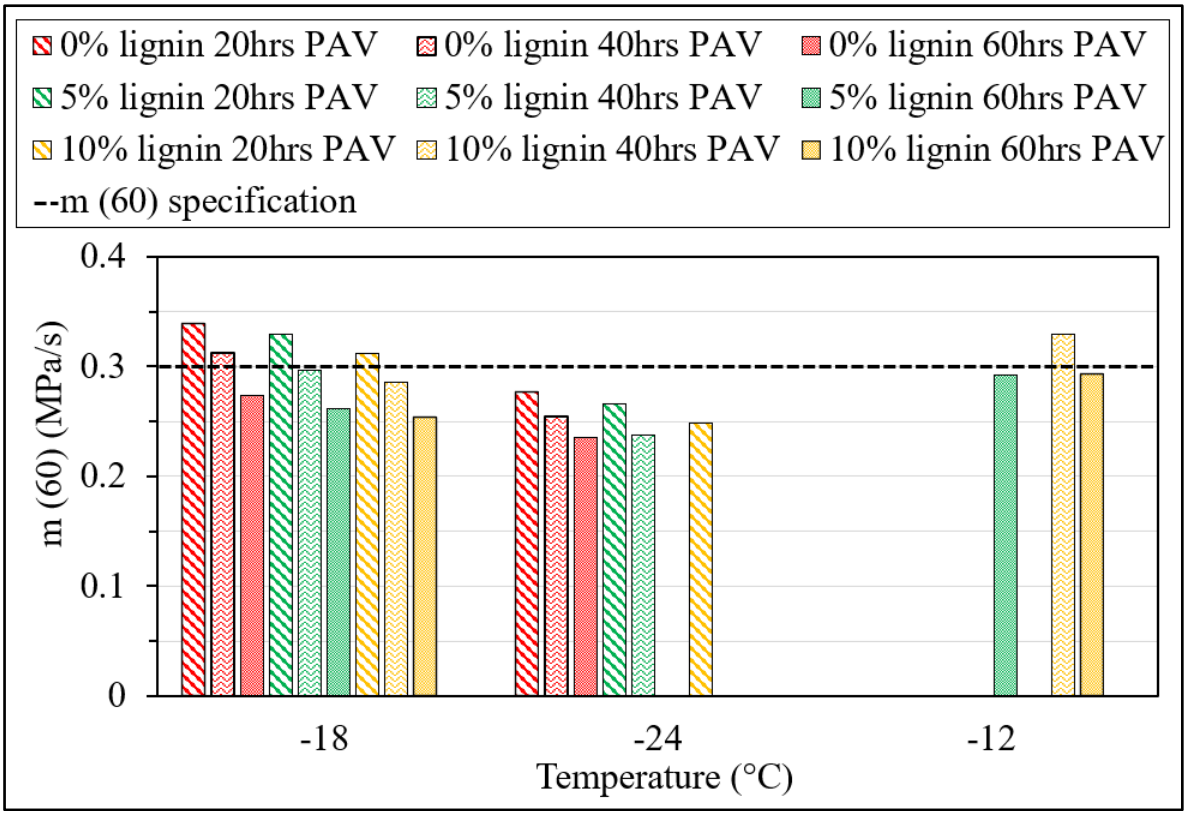


Figure 5.22 Slope (m(60)) values at different temperatures for the unmodified and modified bitumens with different contents of HT SW A 1 lignin at different aging levels

Generally, the effect of lignin is similar for PG 58S-28 and PG 52S-34 bitumens. All lignins increase the stiffness of the bitumen and decrease the relaxation properties. Using different types of lignin affects these properties with different magnitudes. The pellets show the opposite trend which is due to the soybean oil. Using lignin within the bitumen does not show the antioxidation properties.

For further investigations, direct tension tests (DTT) could also be performed for materials with stiffness values between 300 and 600 MPa to evaluate the strain failure of the bitumen which is the criterion of the test. This is recommended for future studies since most of the lignin-modified bitumens show stiffness values within this range (300-600 MPa). So, combining BBR and DTT tests results should provide better evaluation of the low temperature performance of lignin-modified bitumen.

As mentioned earlier, the lignin addition affects the PG of the bitumen by shifting it to higher grade. Depending on how much the shift is, the thermal sensitivity of the bitumen is affected. The DSR, MSCR and BBR tests results are used to determine the PG of the bitumen. In particular, the high temperature PG (DSR), traffic level (MSCR) and low temperature PG (BBR).

#### 5.2.1.5 Evolutions of the thermal range ($T_{high}$-$T_{low}$) and the performance grade (PG Hn-L) of bitumens with the lignin content

The evolution of the thermal range indicates the gap between the high ($T_{high}$) and the low ($T_{low}$) temperatures. The standard for the determination of the $T_{high}$ and the $T_{low}$ temperatures and, the performance grade (PG Hn-L) is ASTM D 7643. Figure 5.23 displays the $T_{high}$-$T_{low}$ which represents the thermal range of bitumen at which the DSR and BBR tests criteria are satisfied. As can be seen, the thermal range ($T_{high}$-$T_{low}$) does not significantly change with the addition of HT SW A 1 lignin for both bitumens. Yet, the lignin increases both $T_{high}$ and $T_{low}$ (Figure 5.23) which means that lignin-modified bitumens perform better at high temperatures but worse at low temperatures.

In addition, this evolution of $T_{low}$ and $T_{high}$ inevitably translates into a change (or a shift) in the performance grade (PG Hn-L) of bitumen. Also, it can be noted that the lignin addition does not improve much the thermal sensitivity of the bitumen which is in accordance with Batista et al. (2018). In this regard, Table 5.9 shows the summary of the PG (Hn-L) for all bitumens tested. For example, the modified bitumen PG 52S-34 with 20 % of HT SW A 1 lignin meets the requirements to classify as a PG 58S-28. Finally, the thermal range of use of bitumen (H-L) is presented in Table 5.9.

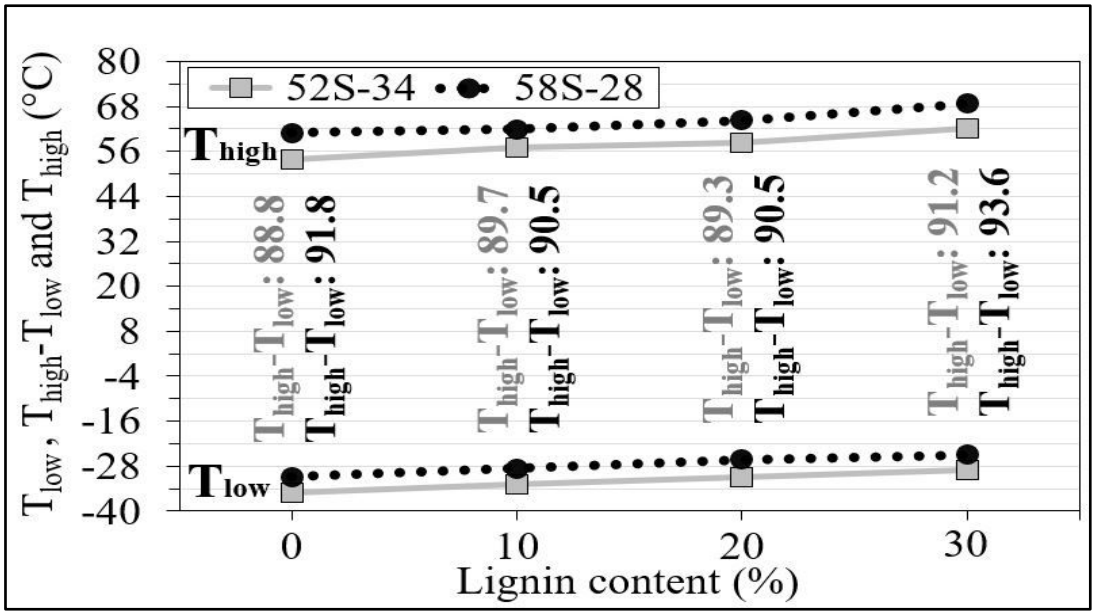


Figure 5.23 High ($T_{high}$) and low ($T_{low}$) temperatures and the resulted gap ($T_{high}$-$T_{low}$: the thermal range) for both bitumens modified with HT SW A 1 lignin

Table 5.9 Summary of the high ($T_{high}$) and low ($T_{low}$) temperatures, the thermal range ($T_{high}$-$T_{low}$), the performance grade (PG Hn-L) and the thermal range of use of bitumen (H-L) for all bitumens modified with HT SW A 1 lignin

| Original bitumen type | Lignin content (%) | $T_{high}$ (°C) | n (-) | $T_{low}$ (°C) | $T_{high}$-$T_{low}$ (°C) | PG (Hn-L) | H-L (°C) |
|---|---|---|---|---|---|---|---|
| PG 58S-28 | 0 | 60.9 ≥ 58 | S | -30.9 ≤ -28 | 91.8 | 58S-28 | 86.0 |
| | 10 | 61.9 ≥ 58 | S | -28.6 ≤ -28 | 90.5 | 58S-28 | 86.0 |
| | 20 | 64.3 ≥ 64 | S | -26.2 ≤ -22 | 90.5 | 64S-22 | 86.0 |
| | 30 | 68.7 ≥ 64 | S | -24.9 ≤ -22 | 93.6 | 64S-22 | 86.0 |
| PG 52S-34 | 0 | 53.8 ≥ 52 | S | -35.0 ≤ -34 | 88.8 | 52S-34 | 86.0 |
| | 10 | 57.0 ≥ 52 | S | -32.7 ≤ -28 | 89.7 | 52S-28 | 80.0 |
| | 20 | 58.4 ≥ 58 | S | -30.9 ≤ -28 | 89.3 | 58S-28 | 86.0 |
| | 30 | 62.3 ≥ 58 | S | -28.9 ≤ -28 | 91.2 | 58S-28 | 86.0 |

According to the results of the tests performed on the HT SW A 1 lignin-modified bitumen, lignin has almost the same effects on both bitumens. All previous tests performed so far are at specific temperatures and frequencies. So, it is interesting to see the effect of lignin on the bitumen (PG 58S-28) at a wide range of temperatures and frequencies which provides better

evaluation and links with the results of the previous tests. This can be done by performing more complex tests.

#### 5.2.1.6 Complex modulus G* tests

This section shows different graphical representations of the G* tests for the unmodified and modified bitumens with different contents (5 and 10 %) of HT SW A 1 lignin and different aging levels (0, 20, 40 and 60 hours of PAV). In particular, Cole-Cole diagrams, master curves of the norm of complex modulus (|G*|) and phase angle (φ) at 22 °C as a reference temperature ($T_{ref}$). In addition, graphs indicate the ratios of the |G*| and the absolute difference of phase angle for the modified bitumens referenced to the unmodified bitumen (0 % lignin) at all aging levels. Finally, a graph shows the difference in percentage of the |G*| between the experimental data and 2S2P1D model referenced to the experimental data of |G*|.

The Cole-Cole diagrams (Figure 5.24) for all unmodified and modified bitumens, including unaged and aged ones, show unique curves. Accordingly, the lignin did not create any polymer effects within the bitumen.

Generally, the loss modulus (viscous component of G*) of the base bitumen (imaginary G*) increases with aging due to the increase in the storage modulus (elastic component or real G*) and stiffness (G*). In addition, the storage modulus increases because the increase in the stiffness compensates the reduction in the phase angle. Herein, the stiffening effect observed for the aged lignin-modified bitumen at different levels is due to not only the presence of lignin but also the effect of the aging process. The effect of the aging on the hardening of the bitumen is major due to the oxidation mechanism.

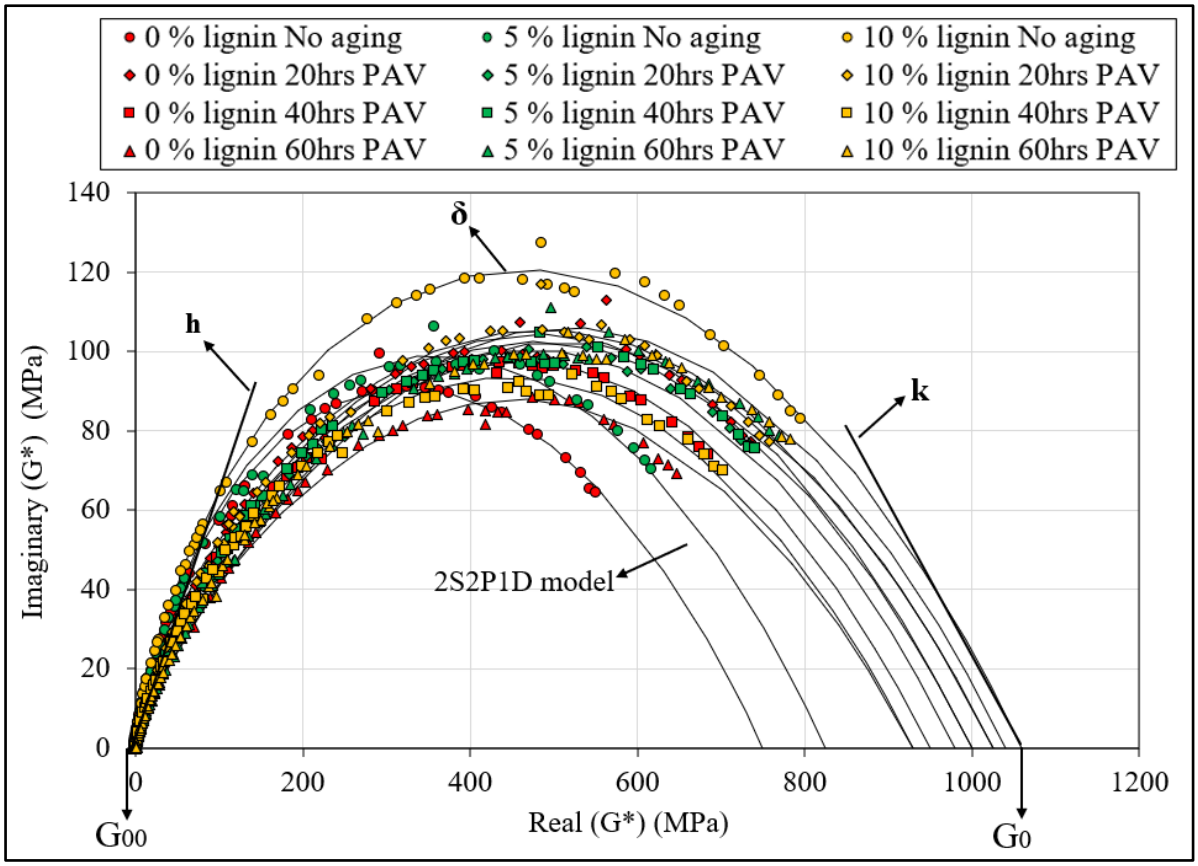


Figure 5.24 Cole-Cole diagram for the unmodified and modified bitumen with different contents of HT SW A 1 lignin at different aging levels, 2S2P1D model and its parameters

All unaged and aged unmodified and lignin-modified bitumens are thermo-rheological simple materials. Thus, the time-temperature superposition principle (TTSP) is valid. Therefore, TTSP can be applied on all bitumens in order to construct the master curves of the |G*| (Figure 5.25) and phase angle (Figure 5.26). It can be seen from the master curves of the |G*| for all bitumens that the aging and lignin increase the stiffness of the bitumen. This can be observed through the shift in the master curves and at the same time the distortion (flattening change in the shape) of these curves compared with the curves for the unaged bitumens. The curves for all bitumens (0, 5 and 10 % of lignin) at each aging level are grouped together which makes them easy to be distinguished. In other words, the effect of aging is clearer than the effect of lignin addition.

Lignin decreases the phase angle of the bitumen at high temperature (low frequency). In addition to the increase in the stiffness, this improves significantly the performance of the bitumen at high temperature. In particular, it increases the resistance of the bitumen to the permanent deformation. This observation confirms what is observed from the DSR and MSCR tests. In terms of the antioxidant capacity of the lignin to the aging effects on the bitumen, no anti-oxidation properties can be seen when comparing 0 % lignin to 5 and 10 %.

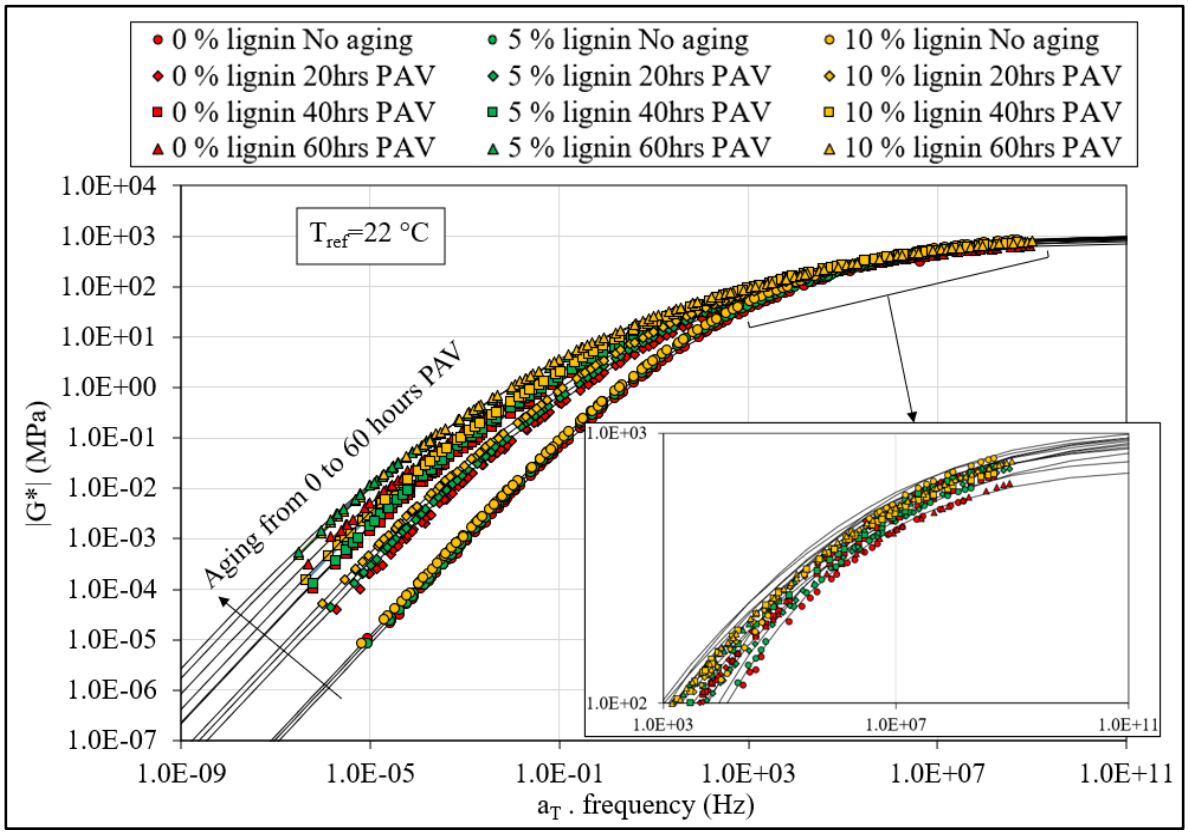


Figure 5.25 Master curves of the norm of complex modulus (|G*|) at $T_{ref}$=22 °C for the unmodified and modified bitumens with different contents of HT SW A 1 lignin at different aging levels and 2S2P1D model

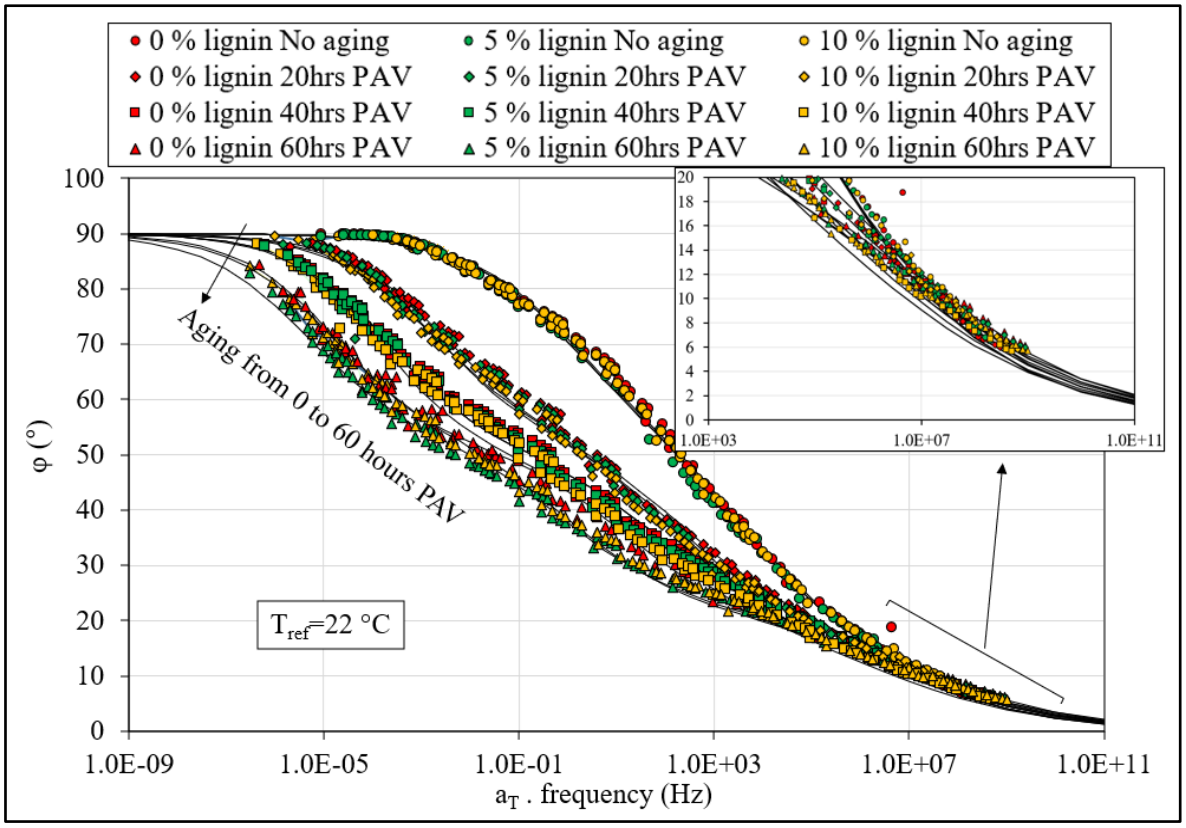


Figure 5.26 Master curves of the phase angle (φ) at $T_{ref}$=22 °C for the unmodified and modified bitumens with different contents of HT SW A 1 lignin at different aging levels and 2S2P1D model

For the 2S2P1D model, it was calibrated with the experimental data, and it fits these data correctly with calibration errors between +10 % and -20 % for most of the data (Figure 5.27). The results of the G* tests, especially the main findings, are not affected significantly for -20 % calibration error.

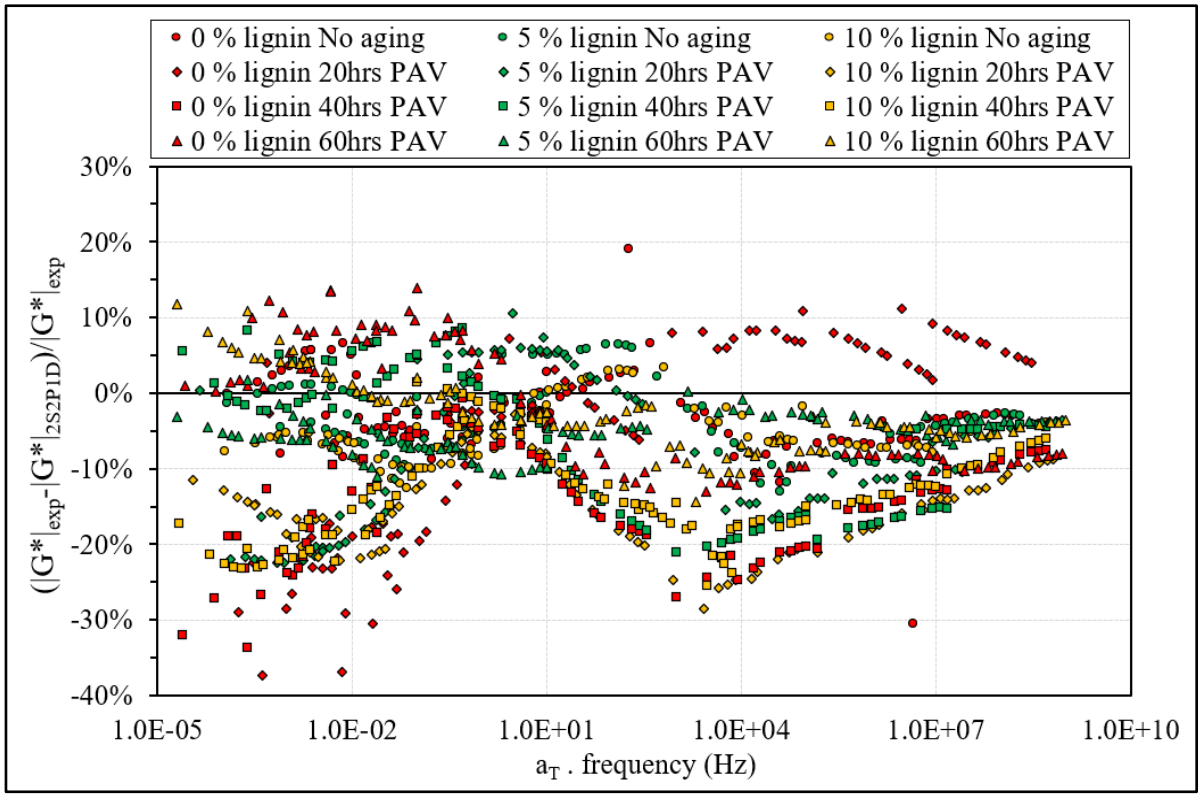


Figure 5.27 Difference in percentage of the norm of complex modulus (|G*|) between the experimental data and 2S2P1D model referenced to the experimental data of |G*| for the unmodified and modified bitumens with different contents of HT SW A 1 lignin at different aging levels

Table 5.10 shows the summary of the 2S2P1D model parameters (shown in Cole-Cole diagrams) and the constants of WLF equation (C1 and C2) for the unmodified and modified bitumens with different contents (5 and 10 %) of HT SW A 1 lignin and aging levels (0, 20, 40 and 60 hours of PAV). Due to the small differences of the values for some parameters such as $G_0$, k and h, it is difficult to observe the antioxidative aging properties of these bitumens. The low lignin content might explain these small differences. It can be seen that the characteristic time ($\tau_E$) is more affected by the aging than the lignin addition (similar values for the unaged bitumens).

Table 5.10 Summary of the parameters of 2S2P1D model and the constants of WLF equation for the unmodified and modified bitumens with different contents of HT SW A 1 lignin at different aging levels

| Lignin content (%) | Aging level (hours of PAV) | Parameters of 2S2P1D model | | | | | | | WLF constants | |
|---|---|---|---|---|---|---|---|---|---|---|
| | | $G_{00}$ (MPa) | $G_0$ (MPa) | k | h | δ | $\tau_E$ | β | C1 | C2 |
| 0 | 0 | 0 | 750 | 0.270 | 0.62 | 2.7 | 0.0000026 | 70 | 13.4 | 134.3 |
| | 20 | | 1000 | 0.255 | 0.60 | 5.0 | 0.000008 | 550 | 25.6 | 230.2 |
| | 40 | | 950 | 0.250 | 0.58 | 5.0 | 0.000025 | 1450 | 26.4 | 230.4 |
| | 60 | | 930 | 0.235 | 0.58 | 6.5 | 0.00005 | 2900 | 21.4 | 179.9 |
| 5 | 0 | | 825 | 0.270 | 0.62 | 2.8 | 0.0000029 | 70 | 25.1 | 230.5 |
| | 20 | | 980 | 0.250 | 0.60 | 4.8 | 0.000012 | 550 | 25.3 | 217.7 |
| | 40 | | 1000 | 0.250 | 0.58 | 5.0 | 0.000025 | 1450 | 26.4 | 230.4 |
| | 60 | | 1040 | 0.255 | 0.60 | 10.5 | 0.00021 | 2000 | 27.3 | 230.1 |
| 10 | 0 | | 1060 | 0.260 | 0.62 | 3.0 | 0.0000025 | 75 | 14.0 | 134.2 |
| | 20 | | 1030 | 0.250 | 0.61 | 4.5 | 0.000024 | 380 | 18.8 | 161.6 |
| | 40 | | 930 | 0.245 | 0.57 | 4.8 | 0.00005 | 1450 | 26.7 | 230.2 |
| | 60 | | 1030 | 0.250 | 0.60 | 9.5 | 0.00023 | 1200 | 26.7 | 223.3 |

As can be seen from the figure of the master curves of |G*| (Figure 5.25), the effect of the aging and lignin at the low temperatures (high frequencies) is limited and it increases with the increase of temperature. Since this effect is limited, it is difficult to observe it through the logarithmic scale of the master curves of the |G*|. Therefore, the ratios of the |G*| of the aged unmodified and lignin-modified bitumens referenced to the unaged (0-hour PAV) bitumens are presented in Figure 5.28. Generally speaking, these ratios are bigger at high temperatures (low frequencies) than those at low temperatures (high frequencies). This is due to the low stiffness of bitumen at high temperature that results in a huge ratio. This ratio becomes clearer as the aging level increases which confirms the finding observed from Figure 5.25 (the effect of aging is clearer than the effect of lignin addition). As can be seen from Figure 5.28, the ratio of stiffness for 5 and 10 % lignin is higher than that for 0 %. This indicates that the lignin does not show the anti-oxidation properties.

For the phase angle, the results of the absolute difference presented in Figure 5.29 for all bitumens referenced to the unaged level confirm what is observed for the ratio of |G*| (Figure

5.28). In addition to the aging and lignin addition effects, it should be noted that some of the results shown in Figures 5.28 and 5.29 are due to the differences (discrepancy range) of the calibration of 2S2P1D model (Figure 5.27).

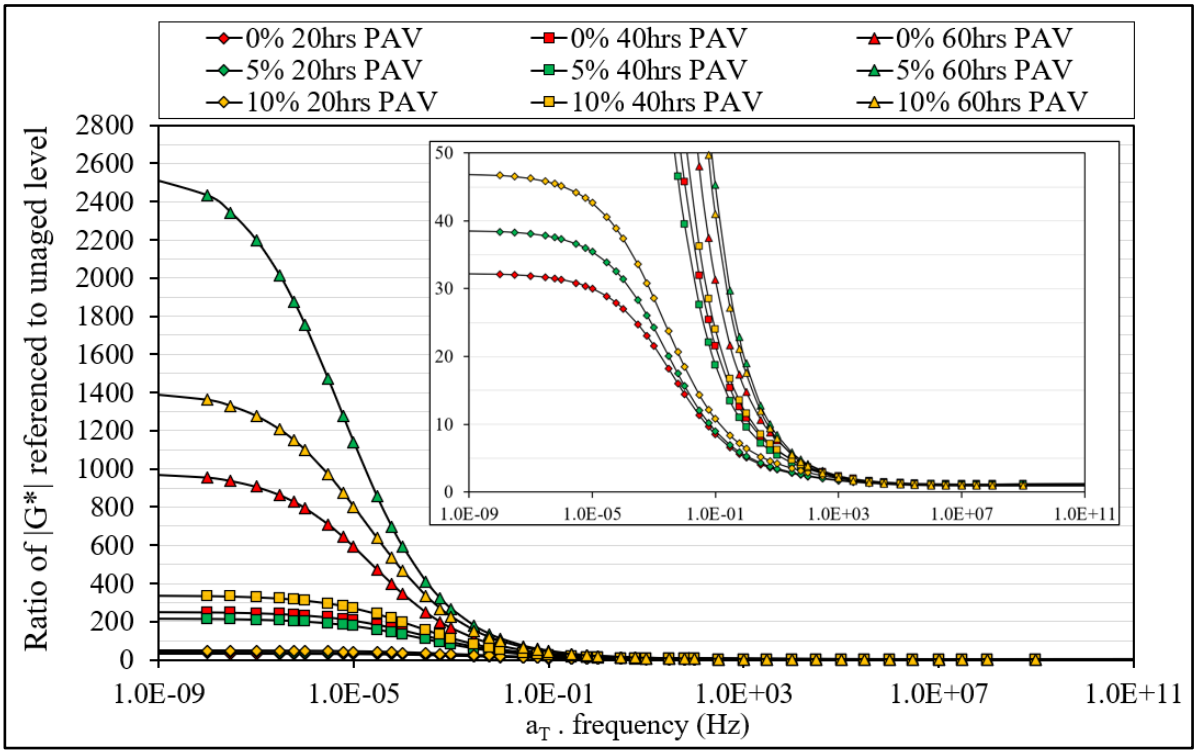


Figure 5.28 Ratio of the norm of complex modulus (|G*|) of the unmodified and modified bitumen with different contents of HT SW A 1 lignin referenced to unaged level

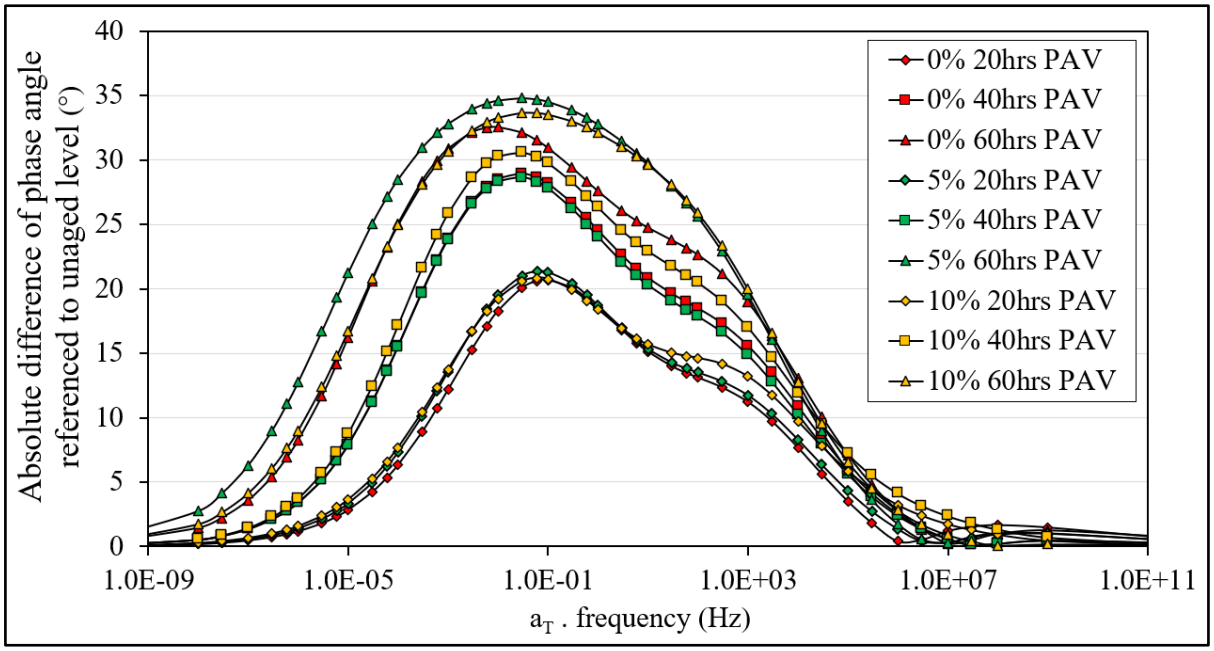


Figure 5.29 Absolute difference of phase angle of the unmodified and modified bitumen with different contents of HT SW A 1 lignin referenced to unaged level

According to the results presented, lignin does change the properties and behaviour of the unaged and aged bitumen. This may indicate that some changes/modifications have been done by the addition of lignin. In particular, the chemical structure of the bitumen, including its molecules. Therefore, performing chemical tests is necessary to investigate the chemistry of the lignin-modified bitumen.

#### 5.2.1.7 FTIR tests

Figure 5.30 shows the FTIR tests results for the unmodified and modified bitumens with different contents (5 and 10 %) of HT SW A 1 lignin and aging levels (0, 20, 40 and 60 hours of PAV). As illustrated in this figure, several peaks can be observed at different wavenumbers. Typically, each peak represents a specific chemical identification for a specific component. In this study, in addition to the qualitative analysis purpose that can be obtained by this test, a quantitative analysis can also be obtained since the results of the reference materials are available.

It is worth mentioning that the preparation and testing conditions were kept the same for all bitumen specimens in order to avoid the effects of the external factors such as temperature and storage duration of the specimens (i.e. interaction with the atmosphere). All tests were performed within one hour (12-15 specimens can be tested within an hour). This helps to increase the accuracy of the intensity of the transmittance/absorbance that is correlated to the quantity of the chemical components in both regions, especially the functional group one.

Generally speaking, Figure 5.30 shows that there are no new peaks introduced or disappeared from the existing ones in both regions, functional group (from 4000 to 1450 $cm^{-1}$ wavenumbers) and fingerprint (from 1450 to 500 $cm^{-1}$ wavenumbers). This means that there are no new chemical components produced for all bitumens. Therefore, there is no indication of any chemical modifications of the bitumen due to the incorporation of lignin. In addition, all peaks of the different curves in the functional group region are close to each other, including small effects of the aging and lignin.

These effects are more obvious in the fingerprint region since the differences, at a given wavenumber, between the peaks are bigger. However, since no new chemical components produced, these differences can be explained by the change of the ratio or the content of these bitumen components. To this end, according to these differences and changes, the bitumens are aged due to the oxidation and lignin effects. Herein, as a result of the oxidation process, the bitumen starts to lose an electron $H^-$ which leads to transform to another structure such as unsaturated compounds (e.g. C=C and C≡C), including strong bonds between the molecules that are resulted in stiffer bitumen.

Many researchers stated that the peaks of the FTIR spectra introduced at 1030 $cm^{-1}$ and 1700 $cm^{-1}$ wavenumbers correspond to the vibrations of sulfoxide (S=O) (fingerprint region) and carbonyl (C=O) (functional group region) bonds, respectively, which are the two major products of bitumen aging (Ouyang et al., 2006; Yao et al., 2013). In other words, the observed differences at these peaks can be presented due to the effect of aging itself.

According to the whole FTIR spectra of all bitumens shown in Figure 5.30, it is difficult to see clearly the effect of lignin on the anti-oxidation properties. Herein, in order to have a better conclusion from the FTIR spectra, the area under the curve at 1700 and 1030 $cm^{-1}$ wavenumbers can be calculated to obtain the carbonyl and sulfoxide indices, respectively. This requires the absorbance value at each wavenumber which can be easily obtained by having the logarithm of the transmittance value shown in Figure 5.30. Figures 5.31 and 5.32 show the carbonyl and sulfoxide indices, respectively, for all bitumens at different aging levels. As can be seen, the values of both indices for 5 and 10 % lignin at different aging levels are slightly higher than that for 0 % lignin. This means that the lignin does not show the anti-oxidation properties.

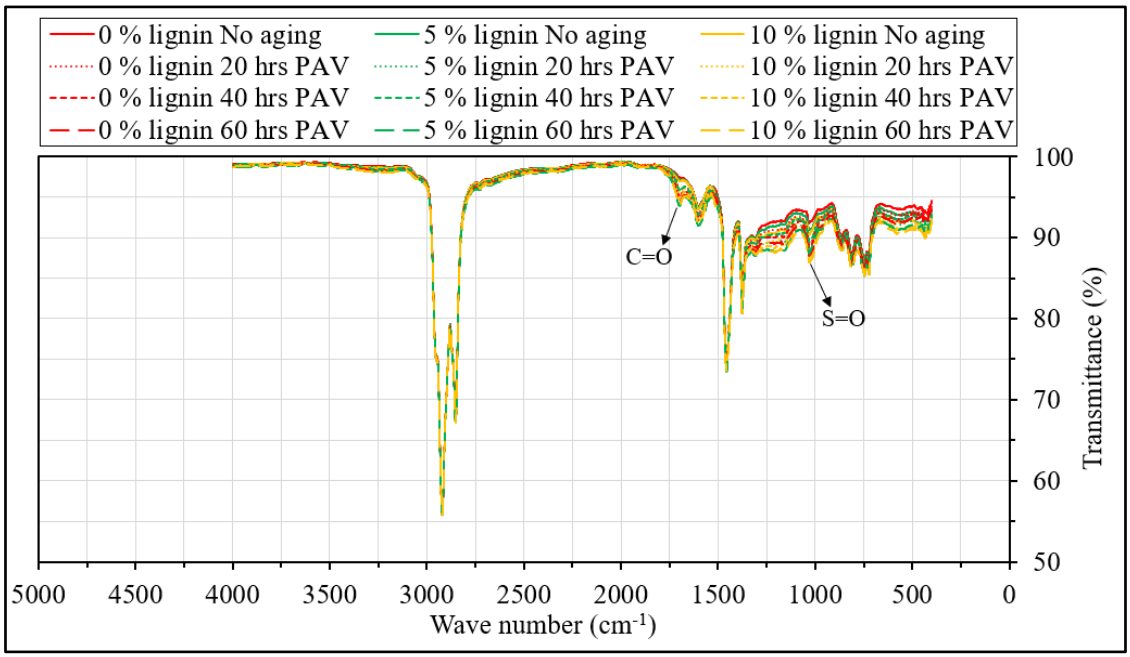


Figure 5.30 FTIR results for the unmodified and modified bitumens with different contents of HT SW A 1 lignin at different aging levels

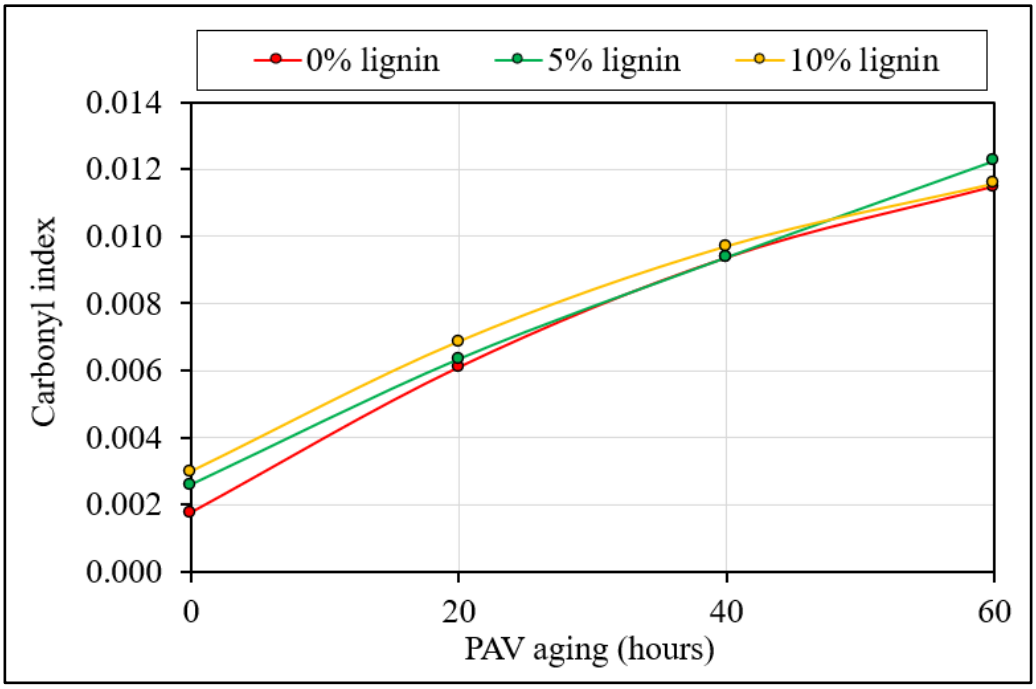


Figure 5.31 Carbonyl index for the unmodified and modified bitumens with different contents of HT SW A 1 lignin at different aging levels

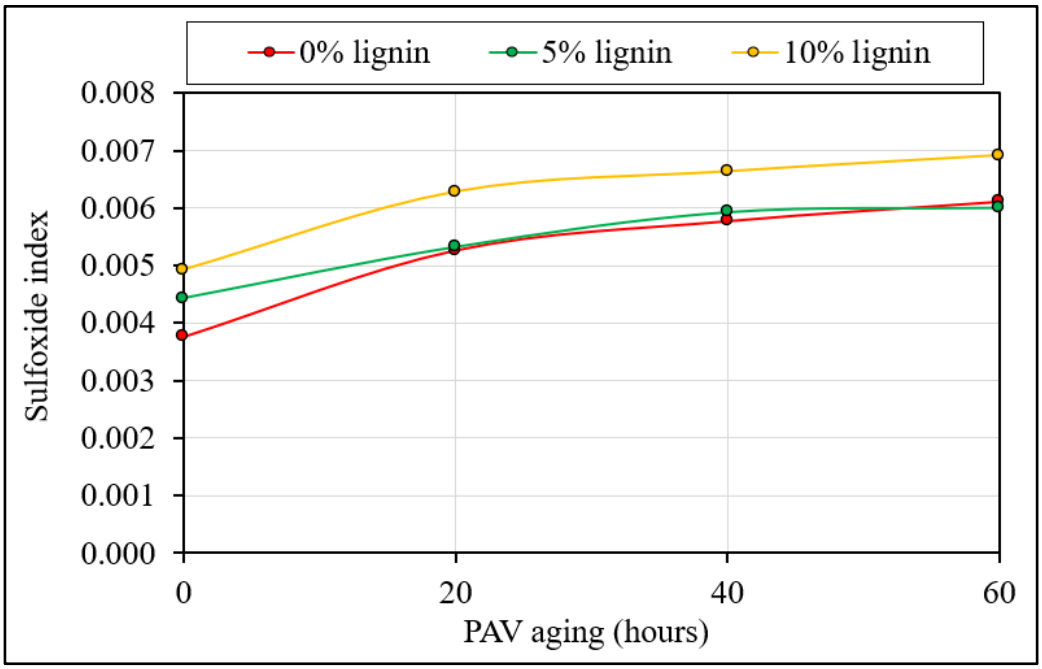


Figure 5.32 Sulfoxide index for the unmodified and modified bitumens with different contents of HT SW A 1 lignin at different aging levels

Based on the findings shown, the lignin addition does not produce new chemical components, including no new peaks observed. The difference observed of the peaks within both regions, functional group and fingerprint, can be due to the change of the components of bitumen. Regarding the antioxidative aging properties of the aged modified bitumen with lignin, no visible effect can be observed.

## 5.3 Summary

This chapter discusses the effects of using different types of lignin in both forms, powder and pellets, and the anti-oxidation properties of the lignin-modified bitumen. Regarding the first step (effect of lignin on two bitumens), a paper is published in the international journal of pavement research and technology (DOI:10.1007/s42947-023-00302-1). The main conclusions of this chapter can be drawn as follows:

- At high temperature, lignin in powder form increases the viscosity, stiffness and resistance to permanent deformation and decreases the phase angle of the bitumen. At low temperature, lignin increases the stiffness and decreases the relaxation properties.
- Using different types of lignin shows the same trend but with different magnitudes.
- Lignin shows similar effects on PG 58S-28 and PG 52S-34 bitumens.
- Lignin shifts the high and low temperature PG to the higher temperature.
- Lignin in pellets form shows a different behaviour which is due to the presence of soybean oil that dilutes the bitumen.
- Lignin does not show anti-oxidation properties on the bitumen. The effect of lignin addition is negligible in comparison with the effect of aging.
- Incorporation of lignin does not show any chemical modifications of the bitumen.

Finally, lignin can be used to replace part of the bitumen and it affects the properties and behaviour of the bitumen. Accordingly, the performance of the HMA is expected to be affected. Although the results of the bitumen tests provide indications regarding the HMA performance, it is still necessary to perform the tests on the HMA itself to better evaluate the effects of the lignin addition on the HMA.

# CHAPTER 6

# EFFECTS OF THE LIGNIN ON THE COMPACTION PROCESS OF THE ASPHALT MIXTURE

## 6.1 Introduction

After presenting the effects of lignin addition on the bitumen which provide indications of the effects on the HMA, it is still necessary to perform the tests on the HMA itself for better evaluation of the lignin impact. The viscosity of the lignin-modified bitumen was discussed in chapter 5. According to the BRV tests results (section 5.2.1.1), the compactability of the lignin-modified HMA is expected to be affected since lignin increases the viscosity of the bitumen. This chapter presents the work done on the compaction process of the HMA. In particular, the evaluation of the effects of using the wet and dry process, different compaction temperatures and different types of lignin in powder and pellets form on the compactability and workability of HMA which are the three objectives of this chapter. To do so, the shear gyratory compaction (SGC) test was employed in this study. The test to determine the value of the maximum theoretical specific gravity ($G_{mm}$) of HMA was also performed as a prior step of the SGC test in order to determine the mass of HMA needed to compact the SGC specimens. Also, the $G_{mm}$ test is used to evaluate the effects of lignin on the density of HMA. The bitumen PG 58S-28 was used as the specified one for Montreal's area. A ESG-10 (*enrobé semi-grenu*) formulation was selected since it is one of the most used HMA in Quebec. In this chapter, the major hypothesis that was made is that the lignin fully replaces the bitumen and therefore behaves only as a binder.

In the first section (section 6.2), the evaluation of the effect of the lignin HT SW A 1 on the compactability of the HMA produced by using the wet and dry processes is presented (section 6.2.1). In section 6.2.2, since the lignin increases the air voids content, it was decided to study the possibility of solving this issue by increasing the compaction temperature of lignin-modified HMA. Then, the effect of different types of lignin in powder and pellets forms on the compaction of HMA produced by the dry process at fixed compaction temperature is shown

(section 6.3). In each section, different parameters (workability, compactability and compaction energy index) of each compaction curve are used for better evaluation of SGC tests results. Lastly, a summary shows the main findings of this chapter is presented (section 6.4).

In addition to the viscosity measured with the BRV, it was also measured with the DSR (Reinke method). As mentioned in chapter 3 (section 3.3.2.4), this second measurement is used due to a problem with the Brookfield device at the beginning of the project (it was broken for a long time). Two contents (0 and 20 %) of HT SW A 1 lignin are incorporated into the bitumen PG 58S-28 to measure the viscosity with the DSR. Using these contents (0 and 20 %) was enough to start with the project, considering the absence of BRV (more accurate than DSR).

Table 6.1 shows the mixing ($T_{mix}$) and compaction ($T_{comp}$) temperatures of the unmodified and modified bitumen PG 58S-28 with 20 % of HT SW A 1 lignin measured with the BRV and DSR tests. As can be seen, the DSR shows different values from the BRV. This is expected and can be interpreted by the different nature of each test in addition to the conditions applied on the material during the test.

Table 6.1 Mixing ($T_{mix}$) and compaction ($T_{comp}$) temperatures measured with BRV and DSR corresponding to the targeted viscosities for the unmodified and modified bitumen with 20 % of HT SW A 1 lignin

| Lignin content (%) | Targeted viscosity (mPa·s) | | | | Bitumen PG 58S-28 | | | |
|---|---|---|---|---|---|---|---|---|
| | Mixing | | Compaction | | $T_{mix}$ [A] (°C) | | $T_{comp}$ [A] (°C) | |
| | BRV | DSR | BRV | DSR | BRV | DSR | BRV | DSR |
| 0 | 170 | | 280 | 350 | 150 | | 140 | 135 |
| 20 | | | | | 163 | 155 | 151 | 145 |
| [A] $T_{mix}$ and $T_{comp}$ are obtained from the DSR using Reinke method at the targeted viscosities for mixing and compaction. | | | | | | | | |

## 6.2 Effect of the lignin on the compactability of HMA

This section shows the effect of the lignin HT SW A 1 on the HMA compactability. In particular, specimens of ESG-10 with different contents of lignin (0, 5 and 20 %) were

produced with the wet and dry process. Afterwards, different compaction temperatures were employed in order to evaluate the effect of increasing the compaction temperature on the compactability of lignin-modified HMA.

### 6.2.1 Comparison between the wet and dry processes

Various HT SW A 1 lignin contents were added to the conventional HMA. The lignin was added to the HMA by using two processes, wet and dry. In the wet process, the lignin was incorporated into the bitumen before being mixed with the aggregate. While in the dry process, the lignin was added directly to the mix. These contents were selected based on the results that are presented in section 5.2.1.1 (Figure 5.1). Table 6.2 shows the summary of the performed SGC tests on the different mixes produced by wet and dry processes at different mixing and compaction temperatures measured with the DSR (Table 6.1). The mixing and compaction temperatures for the unmodified HMA (0 % lignin) are 150 and 135 °C, respectively. For the modified HMAs with 5 and 20 %, it is decided to use the temperatures obtained for 20 % which are 155 and 145 °C, respectively, in order to facilitate the comparison between the modified HMAs. It is necessary to mention that the $G_{mm}$ test was performed on each lignin content shown in Table 6.2. Two specimens were used for each $G_{mm}$ test. The $G_{mm}$ value was employed to determine the mass of HMA to compact in the SGC molds.

Table 6.2 Summary of the performed SGC tests of the unmodified and HT SW A 1 lignin-modified HMA produced by wet and dry processes with different mixing ($T_m$) and compaction ($T_c$) temperatures

| Lignin content (%) [A] | Incorporation process of lignin (wet or dry) and $T_m$ | $T_c$ of SGC tests and repetitions number for each test [#] |
|---|---|---|
| 0 | $T_m$=150 °C | $T_c$=135 °C [3] |
| 5 | Wet and dry at $T_m$=155 °C | $T_c$=145 °C [3] |
| 20 | | |
| [A] Lignin substitution by the asphalt binder mass. | | |

#### 6.2.1.1 Results and analysis

Table 6.3 shows the $G_{mm}$ values of each mixture. Each value represents the average of two specimens. Generally speaking, the $G_{mm}$ value increases with the quantity of lignin in the HMA. This is expected since the density of the lignin (1200-1300 kg/m$^3$) is higher than that of the bitumen (≈ 1020 kg/m$^3$). As can be seen, the effect of the wet or dry process on the $G_{mm}$ value is not significant for both lignin contents (difference of 0.001 for 5 % lignin content and 0.005 for 20 % lignin content). These differences are less than the maximum acceptable difference (0.011 according to LC 26-045) between two specimens of the same mixture. Herein, as expected, there is no difference observed for the $G_{mm}$ values between the wet and dry process since the same quantities of each material are put together. According to the standard of the SGC test (LC 26-003, equation 1), the $G_{mm}$ value was used to calculate the mass of HMA that is required to produce the SGC specimens.

Table 6.3 Summary of the $G_{mm}$ values for each mix produced by wet and dry process

| Lignin content (%) | Incorporation process of lignin (wet or dry) and $T_m$ | $G_{mm}$ |
|---|---|---|
| 0 | $T_m$=150 °C | 2.555 |
| 5 | Wet at $T_m$=155 °C | 2.562 |
| | Dry at $T_m$=155 °C | 2.563 |
| 20 | Wet at $T_m$=155 °C | 2.585 |
| | Dry at $T_m$=155 °C | 2.580 |

Figure 6.1 shows the compaction curves of the HMAs obtained from the SGC tests. In particular, the air voids content (%) (average of three repetitions) with the number of gyrations (N) of the unmodified and modified HMAs with different contents of HT SW A 1 lignin produced with the wet and dry processes. For each lignin content, the standard deviation and maximum difference of the air voids are checked and they meet the requirements of the SGC standard (0.25 for standard deviation and 0.7 for the maximum acceptable difference, according to Table 1 of LC 26-003). This applies for all results presented in the different

sections of this chapter. The coefficient of variation (COV) was calculated for each set of repetitions in order to control the variability of the results. The COV values range from 0.004 to 0.53. The standard of the SGC test (LC 26-003) considers the variability of only two repetitions. So, since three repetitions were performed on the SGC test, the ASTM C 670 standard was used to check the variability of the results. The previous-mentioned COV values are located within the maximum acceptable range (3.3), according to ASTM C 670.

As can be seen (Figure 6.1), the lignin increased the air voids content within the HMA. This means, as expected, that the lignin increased the viscosity of the bitumen which will negatively affect the workability and compactability of the lignin-modified HMAs. As shown in Figure 6.1, only the unmodified and modified HMAs with 5 % lignin content produced by both processes (wet or dry) met the LC-4202 requirements for ESG-10 formulation although the compaction temperature is 10 °C higher (145 °C instead of 135 °C for 5 and 0 % lignin content, respectively). According to this observation, it is necessary to increase the compaction temperature by almost 10 °C for the use of 5 % lignin within the HMA in order to compensate for the increase in the viscosity of the bitumen due to the presence of lignin and, more importantly, the slight reduction in the volume of bitumen, especially the effective volume. As mentioned previously, the density of lignin is higher than that of bitumen. Herein, it is worth mentioning that the increase in the bitumen density due to the presence of lignin translates into a slight reduction in the effective volume of bitumen for the same mass content. The lignin-modified HMAs with 5 % produced by the wet and dry processes showed similar air voids content. Therefore, the effect of the use of the wet or dry process is not significant for 5 % lignin content.

Based on the results for 5 % lignin content, and as expected, increasing the lignin content results in higher viscosity which leads to lower compactability and workability of HMA. In this regard, the modified HMA with 20 % lignin showed the highest air voids content among the other HMAs. It is interesting to see the difference in the air voids content between the modified HMAs with 20 % lignin produced by using the wet and dry processes. This difference in the air voids content ranges from 1.3 % to 2 % which is significant according to the SGC

standard (higher than 0.7). Therefore, the production process (wet or dry) used to produce the modified HMA with 20 % lignin affects the compactability and workability of HMA, including the air voids content. This might be due to the higher viscosity of bitumen in the wet process where the lignin is trapped in bitumen compared to the viscosity in the dry process where the lignin and bitumen are separated at the beginning of the mixing process with the aggregates. Consequently, in the wet process, there is maybe less absorption of bitumen by aggregate which means more effective bitumen volume available to fill the voids within the HMA (less voids). Despite that, the dry process (more voids) to produce the lignin-modified HMA is selected to be used in the following sections of this chapter. This is due to its ease, practicality and the fact that there is no need to check the stability of the lignin-modified bitumen.

There are agents that can be used in order to reduce the viscosity of the bitumen by diluting it which will positively reflect on the HMA workability, leading to lower air voids content. In this regard, tall oil (an oil that is a derivative of wood) was used with different lignin-modified bitumens used to produce HMAs. The results of the SGC tests performed on the modified HMAs with lignin and added tall oil are presented in annex II.

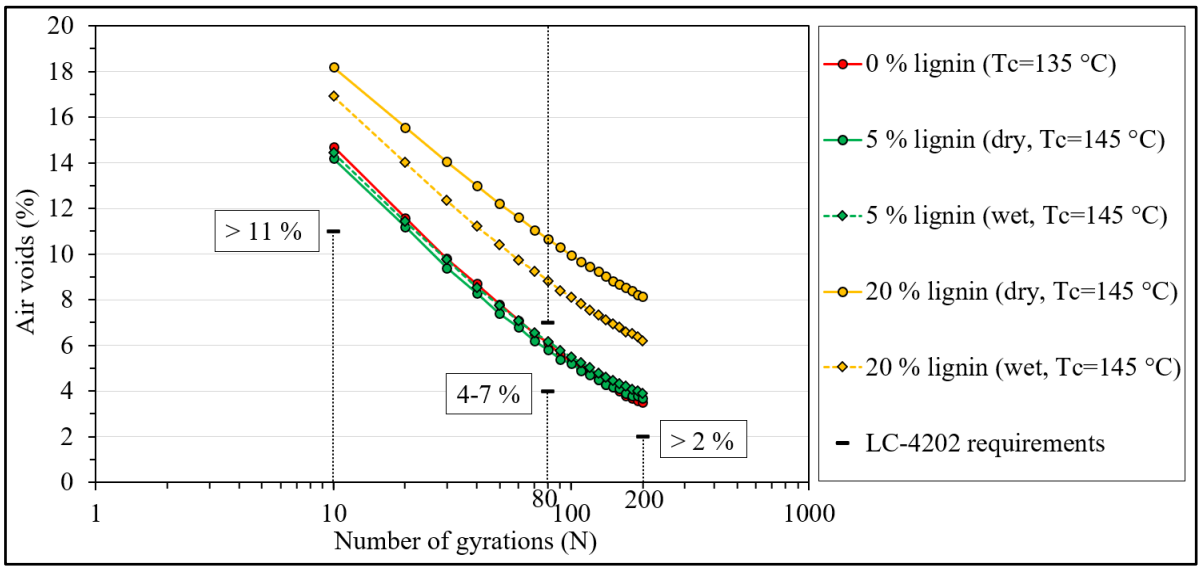


Figure 6.1 Air voids content (%) of the unmodified (0 %) and modified HMA with different contents (5 and 20 %) of HT SW A 1 lignin using wet and dry processes and LC-4202 requirements for ESG-10 formulation

Figures from 6.2 to 6.4 show the parameters of the compaction curve for each HMA. These parameters are the air voids in mix ($V_m$) at 10 gyrations which represents the workability of HMA (Figure 6.2), slope of the compaction curve (K) in semi-logarithmic graph (Figure 6.3) which represents the compactability of HMA and compaction energy index (CEI) (Figure 6.4) which represents the work applied and energy consumed by a roller to reach the target compaction degree of HMA (5.5 % was selected in this research program which represents the average of the air voids content at 80 gyrations (4.0-7.0 %)). In addition, the air voids content at 80 (design number of gyrations ($N_{design}$) for ESG-10 formulation) and 200 ($N_{final}$) gyrations is presented in Figure 6.2. As can be seen, the difference between the workability, compactability and CEI parameters for 0 and 5 % lignin is not significant, maybe because the compaction temperature was increased by 10 °C for 5 % lignin (145 °C for 5 % instead of 135 °C for 0 %). For 20 % lignin, as pointed out by the corresponding compaction curves, the use of dry process resulted in lower workability (high $V_m$ value at 10 gyrations) and higher energy required (high CEI value) to compact the HMA (Figures 6.2 and 6.4, respectively). Although, as mentioned earlier, the dry process was selected for all lignin-modified HMA.

It is difficult to differentiate between the modified HMAs with different lignin contents through the compactability parameter K (slope of the compaction curve). All lignin-modified HMAs show similar K values to each other at the same compaction temperature (Figure 6.3). This means that the lignin addition has almost the same effect on the compactability of the HMA. Moreover, this confirms that the HMA compactability is mostly affected by, first, the quantity of bitumen and its effective volume and, secondly, by the skeleton of the aggregate at the early-stages of the compaction process when the machine starts applying pressure. Finally, as can be observed from Figure 6.2, the air voids content at 80 ($N_{design}$) and 200 ($N_{final}$) gyrations is increased with the increase of lignin content within the HMA.

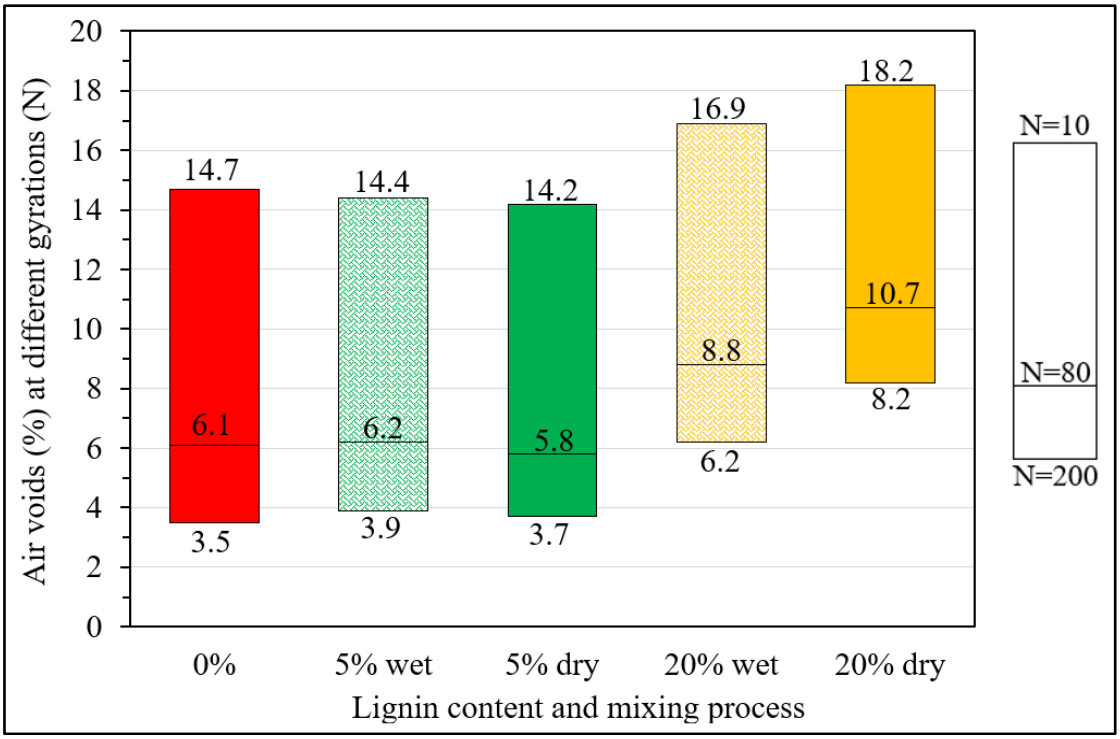


Figure 6.2 Air voids in mix at different gyrations for the unmodified and HT SW A 1 lignin-modified HMA produced by wet and dry processes

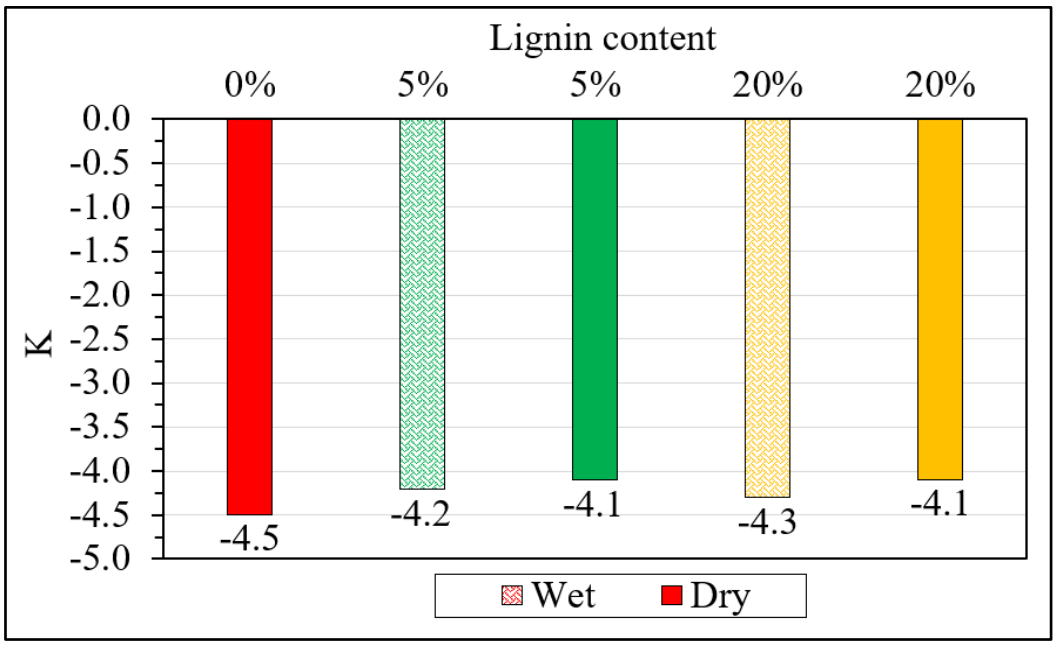


Figure 6.3 K values for the unmodified and HT SW A 1 lignin-modified HMA produced by wet and dry processes

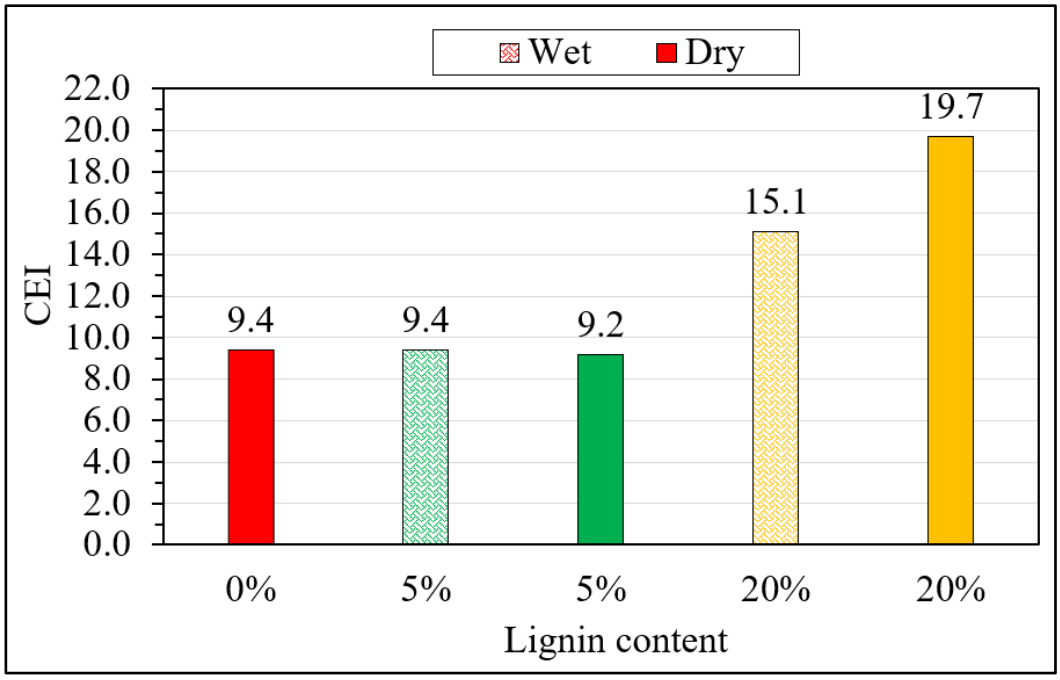


Figure 6.4 Compaction energy index (CEI) values for the unmodified and HT SW A 1 lignin-modified HMA produced by wet and dry processes

According to the results presented in this section, lignin increases the air voids content within the HMA. Herein, it is possible to increase the compaction temperature in order to improve the workability of HMA and, therefore, decrease the air voids content.

### 6.2.2 Effect of compaction temperature

As mentioned earlier, the compaction temperature is measured with the DSR and BRV tests. This shows different results which is expected due to the different natures of both tests. However, it is important to note that the main objective of this section is to see if the compaction issue observed in the previous section can be solved by using higher compaction temperature. In this section, different SGC tests were performed on the unmodified (0 %) and modified HMA with 10 and 20 % of HT SW A 1 lignin produced by the dry process at different compaction temperatures. For 0 % lignin, 135 and 145 °C compaction temperatures are used. For 10 % lignin, 145 and 160 °C compaction temperatures are used while 135 and 151 °C for 20 % lignin. Table 6.4 shows the summary of the performed SGC tests on the unmodified and

modified HMAs with 10 and 20 % of HT SW A 1 lignin produced at different compaction temperatures.

Table 6.4 Summary of the performed SGC tests of the unmodified and modified HMA with 10 and 20 % of HT SW A 1 lignin produced at different compaction temperature ($T_c$)

| Lignin content (%) [A] | $T_m$ | $T_c$ of SGC tests and repetitions number for each test [#] |
|---|---|---|
| 0 | 150 °C | $T_c$=135 °C [3] |
| | | $T_c$=145 °C [3] |
| 10 | 155 °C | $T_c$=145 °C [3] |
| | | $T_c$=160 °C [3] |
| 20 | 155 °C | $T_c$=135 °C [3] |
| | 163 °C | $T_c$=151 °C [3] |
| [A] Lignin substitution by the asphalt binder mass. | | |

### 6.2.2.1 Results and analysis

Figure 6.5 shows the air voids content of the unmodified and modified HMAs with 10 and 20 % of HT SW A 1 lignin tested at different compaction temperatures. As can be seen, the compaction curves of the unmodified HMA (0 % lignin) show significant difference in the air voids (ranges from 0.8 to 1.8 % which is higher than 0.7), including lower air voids at higher compaction temperature. While for the modified HMAs with 10 and 20 %, the compaction curves of the two tested temperatures are close to each other. In other words, the difference in the air voids content is not significant between the two different compaction temperatures (the difference ranges from 0.1 to 0.3 % which is lower than 0.7). Comparing to what is observed for 0 % lignin, this mean that the increase in air voids for lignin-modified mixtures is not only a consequence of the viscosity increase of the bitumen, but it is related to the reduction in the effective volume of bitumen due to the presence of lignin. Therefore, increasing the compaction temperature is not an effective solution to improve the compactability of the modified HMA with lignin, but is necessary to also consider mix design aspects, especially the volumetric approach. Moreover, it should be noted that increasing the compaction temperature

does not result in meeting the LC-4202 requirements (4.0-7.0 % at 80 gyrations). However, increasing the compaction temperature can be a solution in some cases to reduce the air voids within HMA, especially when the lignin content is low, as it was observed in the previous section for 5 %.

For 10 % lignin content, despite the fact that it showed a slight effect, compared to 0 %, on the viscosity of the bitumen itself (section 5.2.1.1: Figure 5.2), it showed an observable effect on the air voids content within the HMA. This confirms again that the reduction in the effective volume of bitumen within lignin-modified HMA plays an important role in the air voids increase. Consequently, since the higher compaction temperature did not show significant effects on the compaction process of the HMA, the lower compaction temperature (obtained from the DSR tests) will be employed in the next sections of this chapter.

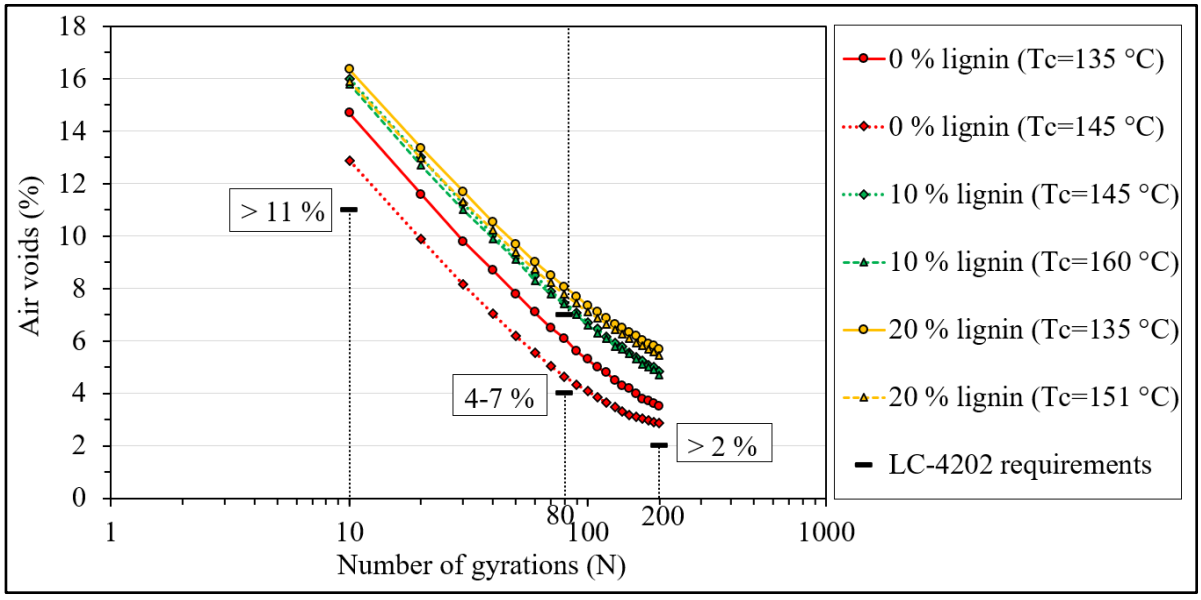


Figure 6.5 Air voids content (%) of the unmodified and modified HMA with 10 and 20 % of HT SW A 1 lignin produced at different compaction temperatures and LC-4202 requirements for ESG-10 formulation

Figures 6.6 to 6.8 show the parameters of the compaction curves for the unmodified and modified HMA with 10 and 20 % lignin produced at different compaction temperatures. In addition, the air voids content at 80 and 200 gyrations for each HMA is presented (Figure 6.6).

As can be seen, according to the values of the parameters presented in Figures 6.6 to 6.8, the effect of the different compaction temperatures on the compaction process of the modified HMA is not significant, including not significant difference, compared to the unmodified HMA where the compaction temperature affects those parameters. Moreover, the air voids content at 80 and 200 gyrations confirms that (a slight difference between the values for the modified HMA compared to the unmodified ones). This confirms that the mix design aspects should be considered in order to improve the workability and compactability of lignin-modified HMA. However, it is interesting to see that the air voids at 10 gyrations and CEI parameters are more affected than K parameter by the use of different compaction temperatures.

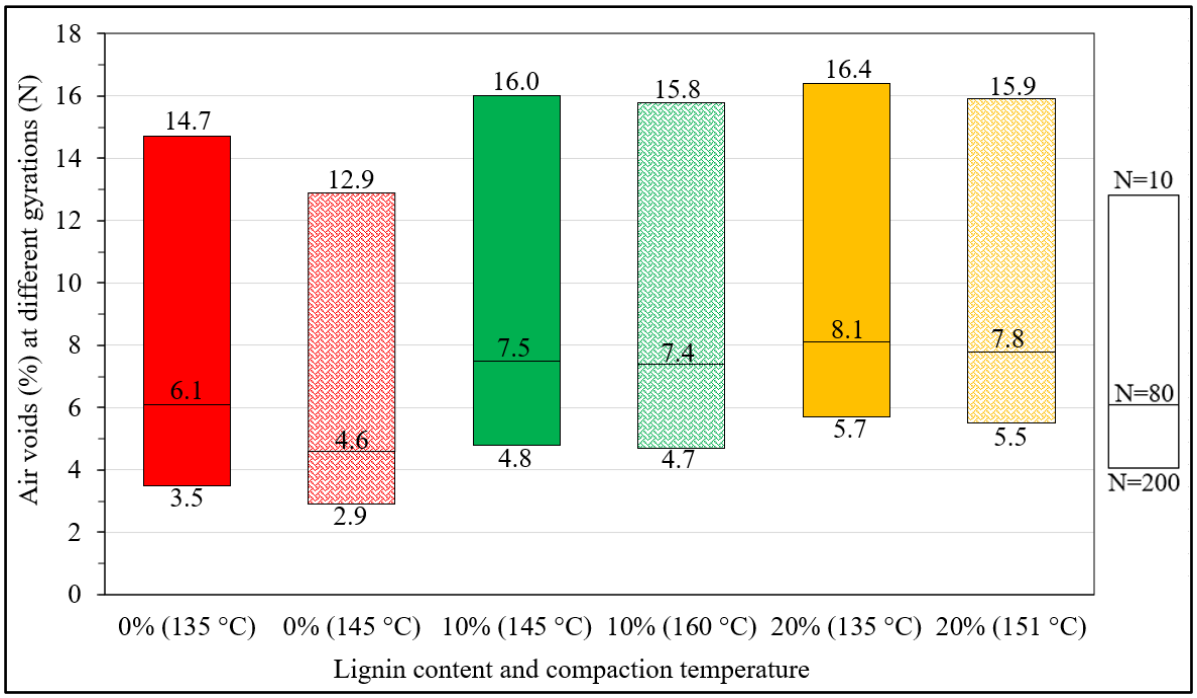


Figure 6.6 Air voids in mix at different gyrations for the unmodified and HT SW A 1 lignin-modified HMA produced by dry process at different compaction temperatures

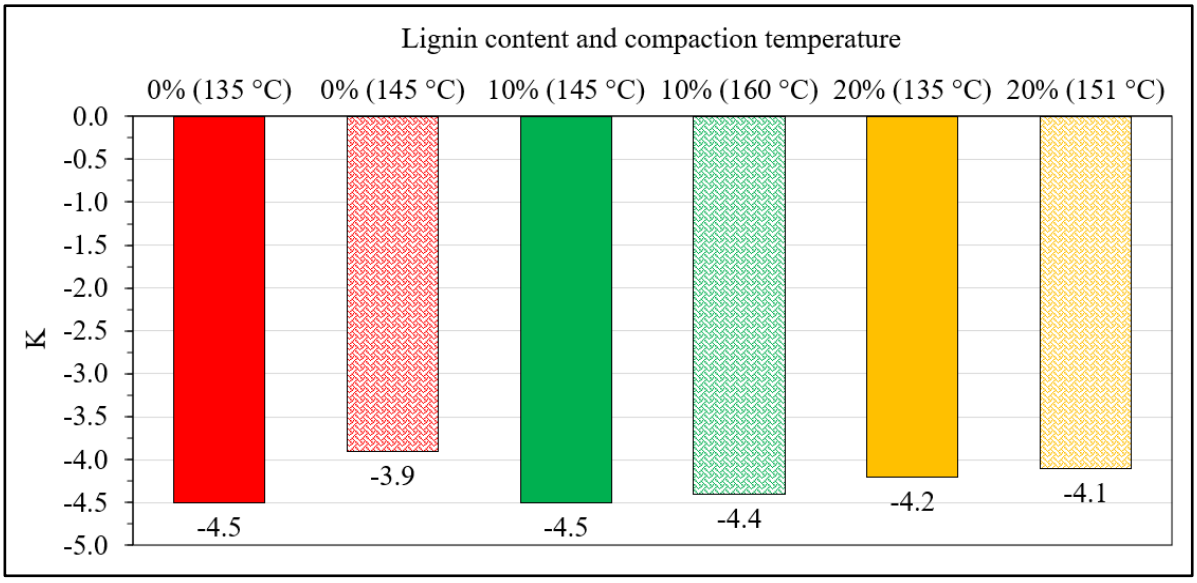


Figure 6.7 K values for the unmodified and HT SW A 1 lignin-modified HMA produced by dry process at different compaction temperatures

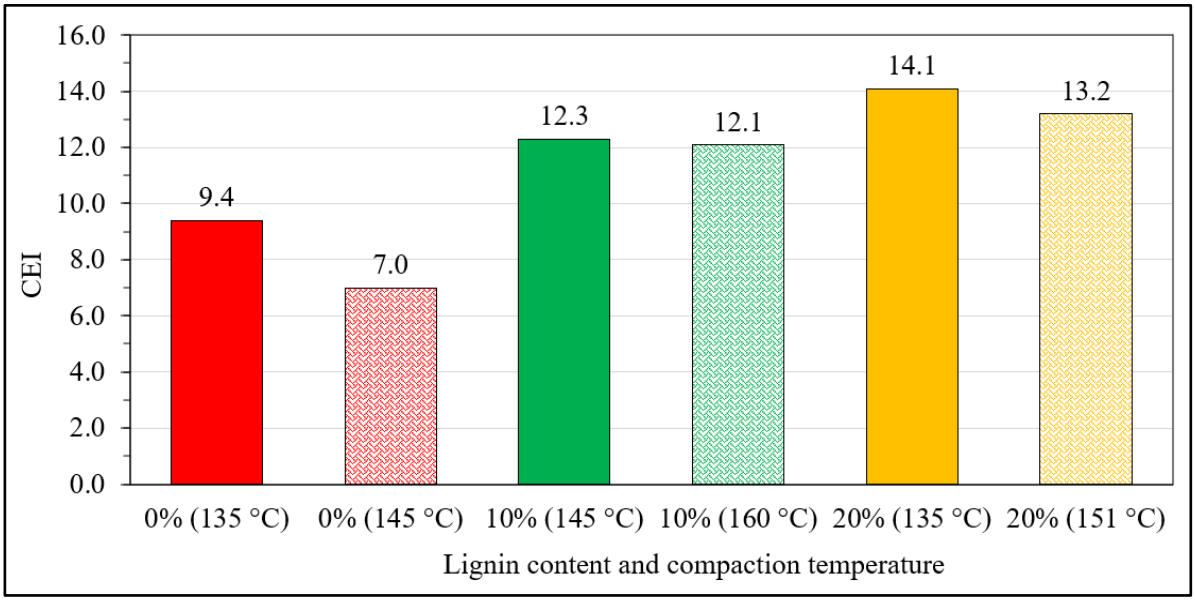


Figure 6.8 Compaction energy index (CEI) values for the unmodified and HT SW A 1 lignin-modified HMA produced by dry process at different compaction temperatures

According to the findings presented in this section, the lower mixing and compaction temperatures, the ones measured with the DSR tests will be employed for all HMAs. More

specifically, for the unmodified HMA (0 % lignin), the mixing and compaction temperatures are 150 and 135 °C, respectively, while 155 and 145 °C for the modified HMA.

## 6.3 Effect of different types of lignin in powder and pellets forms on the compactability of HMA

In this section, different modified HMAs (ESG-10) were produced with different types of lignin powder at constant mixing and compaction temperatures by using the dry process. In particular, based on the findings from the previous section (6.2.2), the mixing and compaction temperatures were selected to be 155 and 145 °C, respectively. This allows to evaluate the effect of the lignin type, including different properties, on the HMA compactability. Moreover, the lignin content was selected to be constant in all mixes, 20 % of each lignin type, in order to have comparable results. The reason behind this selected content is to have more visible results and at the same time to have a link with what was done in chapter 5 (section 5.2.1.1). It was also decided to study the use of pellets (HT SW A 1 lignin powder + soybean oil), because this form of lignin reduces potential health and safety risks associated to the powder form, and it is believed that the presence of soybean oil in the pellets may help to reduce compaction issues. Two types of pellets (HDI and LDI) were added to the HMA by using the dry process. As mentioned previously, the HDI and LDI pellets contain 10 and 5 % of soybean oil, respectively, and have 79.2 and 43.4 durability index (for more details see section 3.2.2). The selected content of the pellets (10 %) is the same as used for the bitumen study in chapter 5 (section 5.2.1.1). The unmodified HMA is used in this section to facilitate the comparison with other HMAs. Regarding the mixing and compaction temperatures, since the viscosity results of bitumen are similar for 0 and 10 % pellets, the unmodified and modified HMAs with pellets were produced at the same mixing and compaction temperatures (150 and 135 °C, respectively). This allows to compare the results with each other and to evaluate the effect of the presence of the soybean oil within the pellets which is expected to improve the HMA compactability. One SGC test was performed on each modified HMA with lignin in powder and pellets forms. This was decided due to the low COV values which were observed in the previous section (6.2). For the $G_{mm}$ tests, two specimens were used for each HMA. Table 6.5 shows the summary of the performed SGC tests of the unmodified and modified HMA with

20 % of different types of lignin powder and 10 % of each pellets type produced by the dry process.

Table 6.5 Summary of the performed SGC tests of the unmodified and modified HMAs with 20 % of different types of lignin and 10 % of pellets types produced by dry process

| Lignin content (%) [A] | Lignin or pellets type | Incorporation process of lignin and $T_m$ | $T_c$ of SGC tests and repetitions number for each test [#] |
|---|---|---|---|
| 0 | - | $T_m$=150 °C | $T_c$=135 °C [3] |
| 10 | HDI | Dry at $T_m$=150 °C | $T_c$=135 °C [1] |
| | LDI | | |
| 20 | HT SW A 1 | Dry at $T_m$=155 °C | $T_c$=145 °C [1] |
| | HT SW A 2 | | |
| | HT SW A-modified | | |
| | HT SW B | | |
| | TB HW A | | |
| | TB HW B | | |
| | K SW A | | |
| | K SW A-modified | | |
| | K SW B | | |
| [A] Lignin substitution by the asphalt binder mass. | | | |

### 6.3.1 Results and analysis

As a prior step for the SGC test, the $G_{mm}$ tests were performed on each HMA. Table 6.6 shows the summary of the $G_{mm}$ values for the unmodified and modified HMAs with 20 % of each type of lignin powder and 10 % of each pellets type produced by using the dry process. As can be seen for lignins powder, all $G_{mm}$ values are close to each other, including small differences. These differences may be due to the slight differences between the densities of the different types of lignin powder, but the results vary between 2.572 and 2.587 so the differences may

also be only due to experimental variability. It is interesting to see that the $G_{mm}$ values for all types of lignin are similar.

For pellets, the $G_{mm}$ value of the HDI type (2.570) is higher than that for the LDI type (2.563). As observed for lignins in powder form, this difference may be due to the difference in the density of pellets type. However, as mentioned previously, this difference is most probably nothing else than the variability of the test itself since it is within the maximum acceptable range of variation for the test repetition.

Table 6.6 Summary of the $G_{mm}$ values for the unmodified and modified HMAs with 20 % of each type of lignin and 10 % of pellets types produced by the dry process

| Lignin content (%) | Lignin or pellets type | Incorporation process of lignin and $T_m$ | $G_{mm}$ |
|---|---|---|---|
| 0 | - | $T_m$=150 °C | 2.555 |
| 10 | HDI | Dry at $T_m$=150 °C | 2.570 |
| | LDI | | 2.563 |
| 20 | HT SW A 1 | Dry at $T_m$=155 °C | 2.580 |
| | HT SW A 2 | | 2.578 |
| | HT SW A-modified | | 2.572 |
| | HT SW B | | 2.582 |
| | TB HW A | | 2.575 |
| | TB HW B | | 2.586 |
| | K SW A | | 2.577 |
| | K SW A-modified | | 2.577 |
| | K SW B | | 2.587 |

Figure 6.9 shows the air voids content of the unmodified and modified HMAs with 10 % of each pellets type and 20 % of each type of lignin powder using the dry process and compacted at 135 and 145 °C, respectively, in addition to the LC-4202 requirements for ESG-10 formulation. The air voids content for 20 % of different lignins powder is located between the

minimum and maximum results, the two dashed lines shown in Figure 6.9. That being said, the addition of different types of lignin resulted in different compaction curves. In other words, the workability and compactability of the modified HMAs were affected differently according to the lignin type and its properties. The minimum line represents the results for TB HW A lignin while the maximum one represents those for K SW B lignin. As can be seen, and expected, the HT SW A 1 lignin fits with the trend observed for the other types of lignin powder. However, it should be noted that none of the modified HMAs with 20 % of each lignin type met the requirements of LC-4202. It is interesting to see that the difference between the air voids of the 20 % HT SW A 1 lignin mix and the 0 % (2.5 %) is higher than the observed difference between the different 20 % lignin mixes (2.0 %). However, the type of lignin generates a relatively high variability that seems to be equivalent to increase the lignin content from 0 to 10 % (Figure 6.5). Similarly to what is observed for the BRV tests on bitumen modified with different lignins, there is no clear pattern if the lignin producer or type of wood or pH has more influence on the workability and compactability of HMA.

For pellets form, as can be seen, only the unmodified and modified HMA with LDI type met the requirements of LC-4202, including air voids content between 4.0 and 7.0 % at 80 gyrations. It is interesting to see that the use of HDI type shows, unexpectedly, higher air voids content compared to the LDI type although the soybean oil content within the HDI type is higher (10 %) than that within the LDI type (5 %). This is unexpected since the presence of higher content of the soybean oil is supposed to reduce the viscosity of the bitumen by diluting it, leading to lower air voids content within the HMA. This observation might be due to the high durability of the pellets that requires longer duration of time of mixing in order to crush the pellets. Indeed, a study conducted by another student showed that a much longer mixing time (5 minutes) than what was used in this study (90 seconds) is required to crush the HDI pellets type while 90 seconds is sufficient to crush the LDI pellets type.

Another possible explanation of the difference between HDI and LDI pellets is the bitumen absorption. In particular, compared to LDI pellets, the bitumen with HDI pellets has a lower viscosity since it contains more soybean oil, which may result in more bitumen absorption and

less effective bitumen. Combining this with the impact of the effective volume of bitumen could interpret the observation of the higher air voids content for the modified HMA with HDI type compared to LDI type.

However, since HT SW A 1 lignin powder is used with the soybean oil to form pellets, it is expected that using pellets compared to powder form will result in lower air voids content when using the same content and compaction temperature for both forms. This is duo to the presence of the soybean oil that decreases the viscosity of the bitumen and, therefore, the workability of the HMA will be improved.

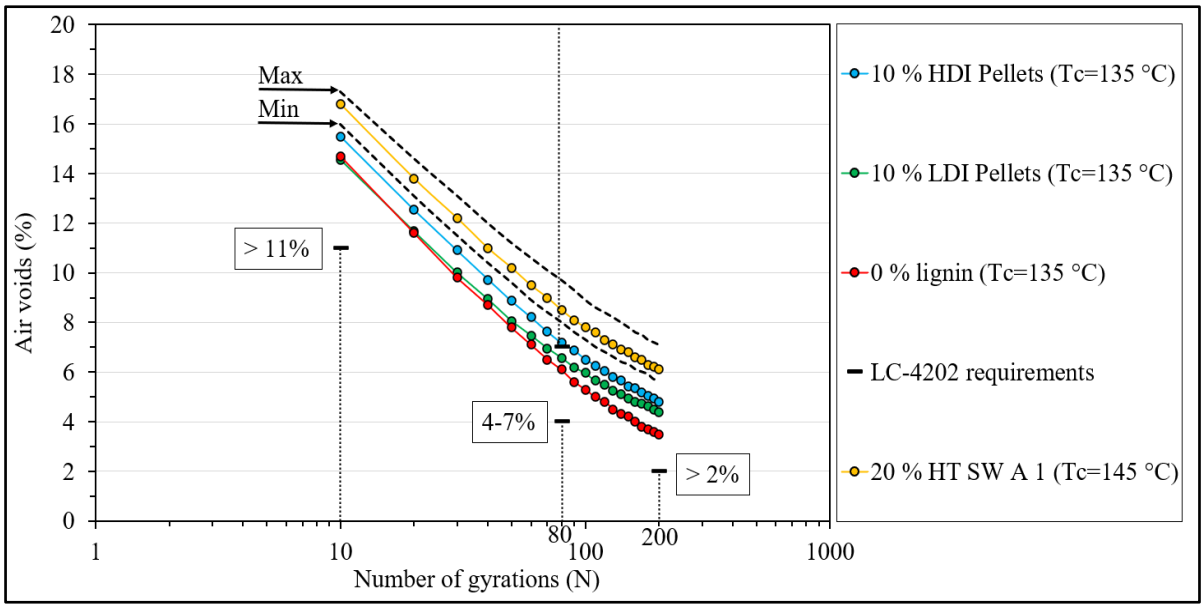


Figure 6.9 Air voids content (%) of the unmodified, minimum and maximum air voids of the modified HMAs with 20 % of each type of lignin and 10 % of each pellets type using dry process and LC-4202 requirements for ESG-10 formulation

Figures 6.10 to 6.12 show the parameters of the compaction curve for the unmodified and modified HMAs with 20 % of each lignin powder type and 10 % of each pellets type produced by using the dry process. Comparing the different lignins in powder form with each other, as expected, the workability and CEI parameters are slightly affected (including not significant difference) according to the chemical and physical properties of each type of lignin. The compactability parameter (K) shows similar values (small differences compared to the

workability and CEI) which means that it is less affected by the type of lignin and its properties compared to the other parameters. Combining this with what is observed from Figure 6.9, the parameters of compaction curves (especially workability and CEI) are more affected by the lignin content than the lignin type. Also, the air voids content at 80 and 200 gyrations is not significantly affected by using different lignins in powder form.

As observed from Figure 6.9, the use of TB HW A lignin showed the highest workability and lowest CEI among the other types of lignin. On the other hand, the K SW B lignin showed the lowest workability and, therefore, the highest energy required in the compaction process (CEI). In addition, the highest air voids content at 80 and 200 gyrations can be seen for this lignin (K SW B). Comparing those parameters of the modified HMAs with 20 % of lignins in powder form with 0 %, the differences between the values are significant.

For the pellets, the difference in the values of the compaction curve parameters (especially workability and CEI) between 10 % of LDI pellets and 0 % is not significant while it is higher for 10 % of HDI pellets, including significant difference. Moreover, the use of HDI pellets resulted in the highest air voids content at 80 and 200 gyrations compared to 0 % and 10 % of LDI pellets which means the lowest workability and, therefore, the highest CEI (Figures 6.10 and 6.12). This seems to be due to the high durability of HDI pellets that are not fully crushed, so the soybean oil does not dilute the bitumen enough to improve the workability. For K values, as observed for the previous sections, it is less affected than the workability and CEI parameters. However, it looks like the lignin in pellets form can be utilized to solve the workability issue of HMA.

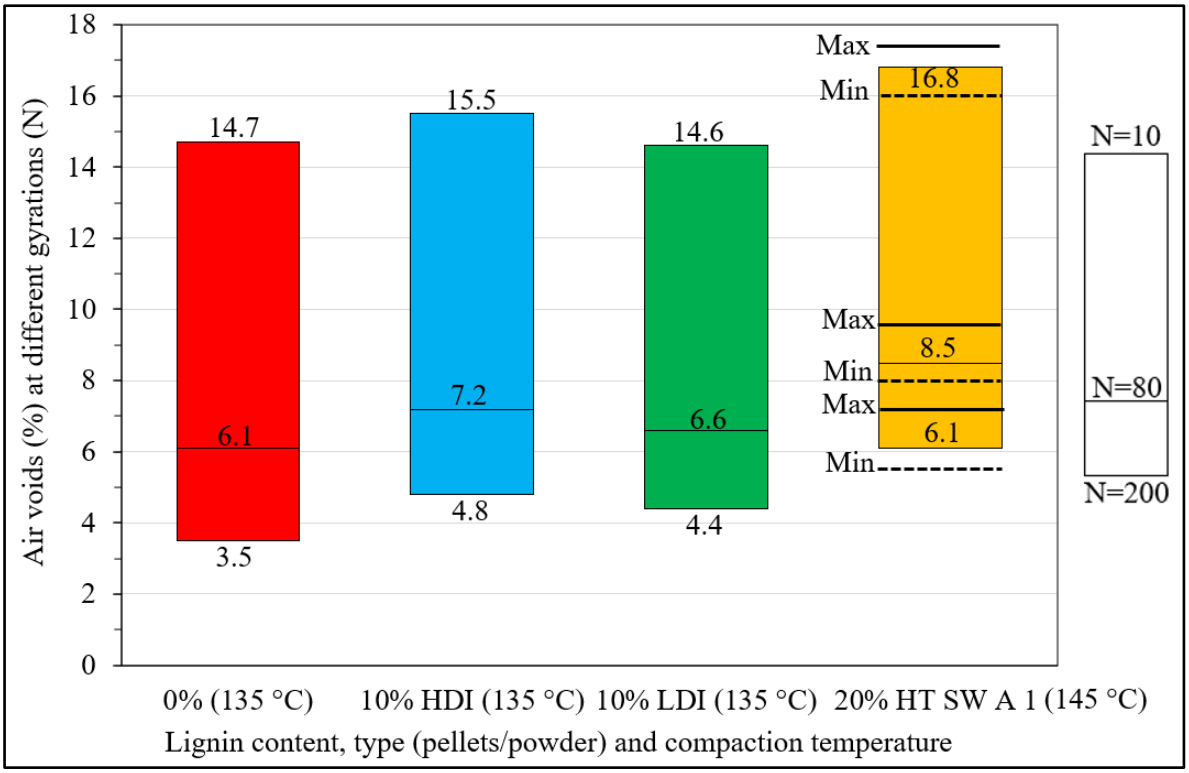


Figure 6.10 Air voids in mix at different gyrations for the unmodified, minimum and maximum air voids of the modified HMAs with 20 % of each type of lignin and 10 % of each pellets type using dry process

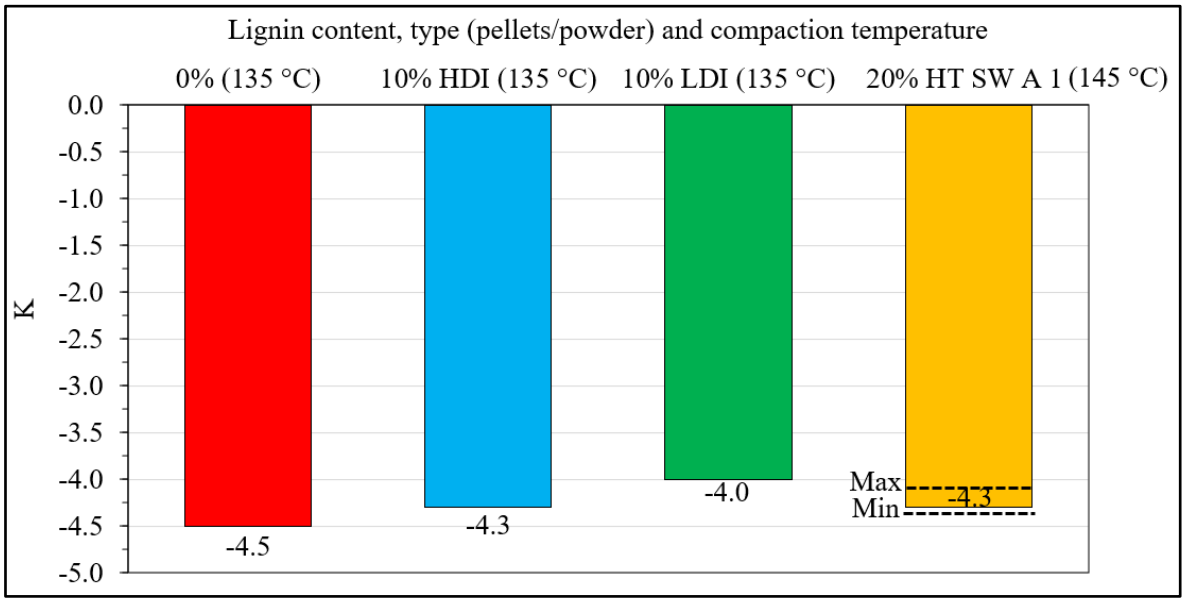


Figure 6.11 K values for the unmodified and modified HMAs with 20 % of each type of lignin (min and max) and 10 % of each pellets type using dry process

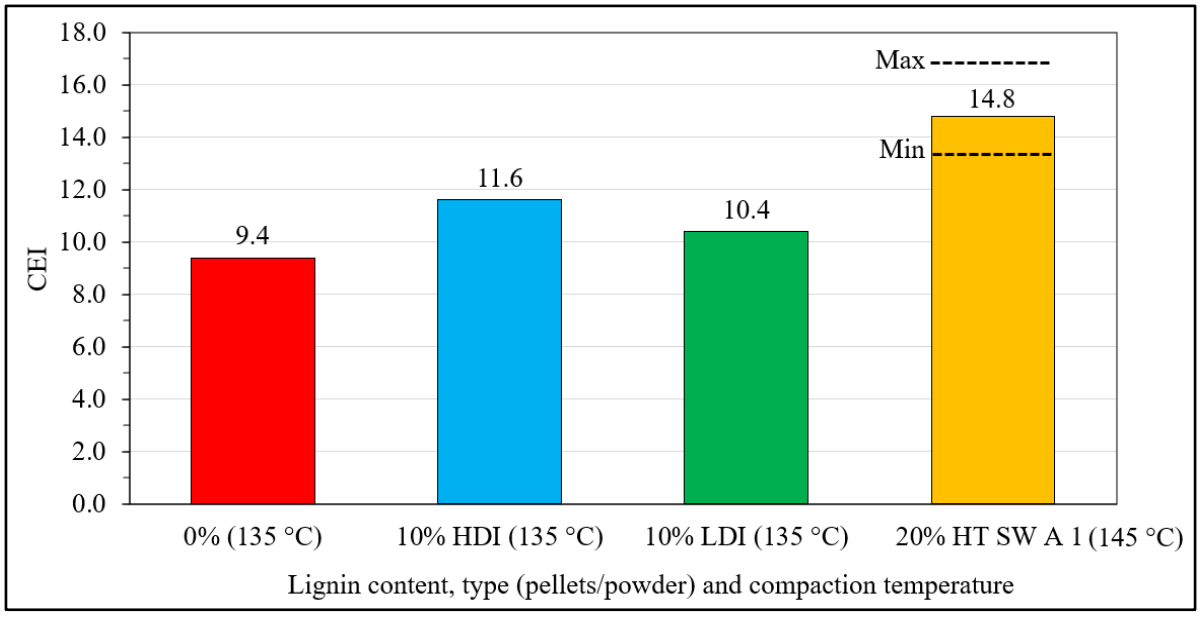


Figure 6.12 Compaction energy index (CEI) values for the unmodified and modified HMAs with 20 % of each lignin type (min and max) and 10 % of each pellets type using dry process

As mentioned in chapter 5, the pellets were involved at the end of this research program. This means that the work on pellets material was not continued although it showed positive effects. However, according to the previous studies and the findings presented in this study, it is worth investigating higher contents of the pellets due to the benefits on the compactability of HMA. Moreover, this helps to better understand and evaluate the effect of the soybean oil on the compaction process of HMA.

## 6.4 Summary

This chapter presented the work done on the compaction process of the unmodified (0 % lignin) and modified HMAs with different contents of the lignin in powder and pellets forms. The SGC test was employed to evaluate the compaction process of HMA. The main conclusions of this chapter can be drawn as follows:

- Lignin decreases the workability and compactability of HMA and increases the air voids within the HMA.

- The difference of the air voids between the wet and dry processes is small for 5 % lignin, while it is significant for 20 % where the dry process showed higher air voids than the wet process.
- Increasing the compaction temperature did not result in a significant reduction of the air voids within the lignin-modified HMA. This might be due to the reduction of the effective volume of bitumen with the presence of lignin.
- All lignin types in powder form increase the air voids content. This increase differs from one type to another which is due to the different properties of each type.
- For the lignin in pellets form, it shows different behaviour which is due to the presence of soybean oil that dilutes the bitumen.

According to the results presented in this chapter, the air voids content of the modified HMA is increased due to the addition of lignin. Herein, it is interesting to see how lignin affects the performance of HMA where the air voids content has an impact. The evaluation of the thermomechanical performance of the lignin-modified HMA is presented in the next chapter.

# CHAPTER 7

# EFFECTS OF THE LIGNIN ON THE THERMOMECHANICAL BEHAVIOUR AND PERFORMANCE OF THE ASPHALT MIXTURE

## 7.1 Introduction

As discussed in chapter 6, the air voids content is an important volumetric factor of HMA. Without mix design adjustments, which was not the purpose of this study, the modified HMA with lignin have higher air voids contents than the unmodified one. In this context, since this factor affects the HMA behaviour and performance, the tests results shown in this chapter are not only due to the effect of lignin addition, but also the effect of the different air voids contents. This chapter presents the work done on the thermomechanical properties and performance of the lignin-modified HMA. In particular, the evaluation of the effects of lignin on the moisture susceptibility, LVE behaviour and HMA performance at high and low temperatures by conducting the corresponding thermomechanical tests.

## 7.2 Effects of HT SW A 1 lignin on the thermomechanical performance of HMA

This section presents the effects of the addition of HT SW A 1 lignin on the resistance of HMA to the moisture damage, rheological behaviour and the performance at high and low temperatures. In particular, the moisture sensitivity and indirect tensile strength (ITS) tests were employed to evaluate the moisture susceptibility, while tension-compression complex modulus (E*) tests at a wide range of temperatures (-35, -25, -15, -5, 5, 15, 25 and 35 °C) and frequencies (10, 3, 1, 0.3, 0.1, 0.03 and 0.01 Hz) were employed in the evaluation of the rheological behaviour of HMA within the LVE domain. The rutting and thermal stress restrained specimen tests (TSRST) were used to evaluate the HMA performance at high and low temperatures, respectively. For the fatigue cracking resistance of HMA at intermediate temperatures, the results are presented in annex III which is due to the problem with the tests results. As studied in chapter 6, the lignin contents 5 and 20 % are selected in this chapter to evaluate the effects of the addition of low and high lignin contents, respectively. The PG 58S-

28 bitumen is used with aggregate to produce HMAs following the ESG-10 formulation (Quebec's HMA) by using the dry process (section 6.2.1) at the mixing and compaction temperatures obtained from the DSR tests (Table 6.1). Table 7.1 shows the summary of the mechanical tests performed on the unmodified and lignin-modified HMAs.

Table 7.1 Summary of the mechanical tests performed on the unmodified and modified HMA with different contents of HT SW A 1 lignin produced by using the dry process

<table>
<tr><td rowspan="2">Lignin content (%) [A]</td><td rowspan="2">Mixing process</td><td colspan="5">Performed tests and number of repetitions for each test [#]</td></tr>
<tr><td>Moisture sensitivity</td><td>ITS</td><td>E*</td><td>Rutting</td><td>TSRST</td></tr>
<tr><td>0</td><td>$T_m$ =150 °C and $T_c$ = 135 °C</td><td rowspan="3">[3] S [B]<br>[3] N [B]</td><td rowspan="3">[4] C [C]<br>[4] D [C]</td><td rowspan="3">[1]</td><td rowspan="3">[2]</td><td rowspan="3">[3] [D]</td></tr>
<tr><td>5</td><td rowspan="2">$T_m$ =155 °C and $T_c$ = 145 °C</td></tr>
<tr><td>20</td></tr>
<tr><td colspan="7">[A] Lignin substitution by the asphalt binder mass.<br>[B] S: soaked specimens. N: non-soaked specimens.<br>[C] C: conditioned specimens. D: dry specimens.<br>[D] Three specimens were extracted from one SGC specimen for each lignin content.</td></tr>
</table>

### 7.2.1 Results and analysis

This section shows the results of the mechanical tests presented in Table 7.1 and performed on the unmodified and modified HMAs with different contents of HT SW A 1 lignin. The COV value was calculated for those tests that had been repeated (moisture sensitivity, ITS, rutting and TSRST). The COV ranges from 0.01 % to 0.27 % but no mention of acceptable COV values are specified in the corresponding test standards. Though, according to the general ASTM C 670 standard, these COV values are located within the maximum acceptable range which is 3.5 %. For rutting tests, the results meet the acceptability criteria shown in Table 2 of the test standard (LC 26-410).

#### 7.2.1.1 Moisture sensitivity

Figure 7.1 shows the moisture sensitivity tests results (average of 3 results) of the unmodified and modified HMAs with different contents of HT SW A 1 lignin. In particular, the Marshall stability at 60 °C, water resistance (WR) and the air voids content (underlined value in %). All HMAs meet the requirements of the standard (LC 26-001) for the moisture sensitivity test (WR is higher than 70 %). The error bars (calculated based on the standard deviation of the experimental data obtained as tests results) shown in Figure 7.1 indicate that the differences between all HMAs are statistically significant (no overlap). These significant differences can indicate that the properties of HMA are changed/modified due to the lignin addition. Generally speaking, the lignin addition increases the Marshall stability of HMA although the air voids content of the lignin-modified HMAs is higher than that for the unmodified HMA. Thus, the WR is increased (90.8 and 86.5 % for 5 and 20 % lignin content, respectively, compared to 82.2 % for 0 %).

Figure 7.2 shows the ITS tests results (average of 4 results) of the unmodified and modified HMAs with different contents of HT SW A 1 lignin. More specifically, ITS at 25 °C, ITS ratio (ITSR) and the air voids content (underlined value in %). According to the standard of ITS test (AASHTO T 283), the air voids content is maintained at 7.0 ± 0.5 % which is not the case in the moisture sensitivity tests. This leads to better evaluation of the effects of the lignin addition on the resistance of HMA to the damage caused by the moisture. The error bars show, statistically, significant differences between the HMAs (no overlap). As can be seen, lignin increases the indirect tensile strength of the HMA (Figure 7.2). Also, the ITSR is increased (0.98 for 5 % and 0.91 for 20 % compared to 0.88 for 0 %).

Since the Marshall stability and ITS are increased, the lignin increases the adhesion bonding between the aggregates which helps to retard the appearance of the stripping distress within the asphalt pavement. This can be due to the viscous and strong film (lignin-modified bitumen) that coats the aggregates and increases the friction angle between them which requires more energy to separate the aggregates mixed by lignin-modified bitumen. Therefore, the lignin

addition results in the increase of the HMA strength. However, it should be noted that there is no clear trend observed from Figures 7.1 and 7.2 (the HMA with 5 % performs better than the one with 20 %) and although the differences shown from these figures are statistically validated, they remain slight variations for both, Marshall stability and ITS.

As highlighted by Omar et al. (2020) in his research, the increase in the viscosity of the bitumen due to the lignin addition affects positively the adhesion of the HMA. This improvement can lead to an increase in the HMA resistance to the abrasion (disintegration and degradation of the aggregates). As stated by Zhang et al. (2020), the increase in the adhesion between the aggregates will help to delay the development of the fatigue cracking within the asphalt pavement. In other words, the lignin increases the durability and stability of the HMA which leads to longer service life of the asphalt pavement.

Finally, according to the results obtained from both tests, it is possible that the lignin increases the surface tension of the bitumen which means high resistance to the penetration of water into the aggregates. In this regard, the use of lignin can retard the degradation of aggregate caused by weathering and, especially, freeze-thaw (FT) cycles. However, ITS test includes one FT cycle so the conclusion regarding the resistance of HMA to the FT can’t be drawn without applying more FT cycles.

The results of both tests show the same overall trend. However, it is still recommended to perform both tests since the moisture sensitivity test focuses on stability and deformation of HMA, while the moisture-induced damage test focuses on tensile strength of HMA which is critical for understanding its resistance to cracking. Overall, lignin-modified HMA is less sensitive to the moisture damage and water effects compared to the unmodified one despite the high air voids content within the HMA.

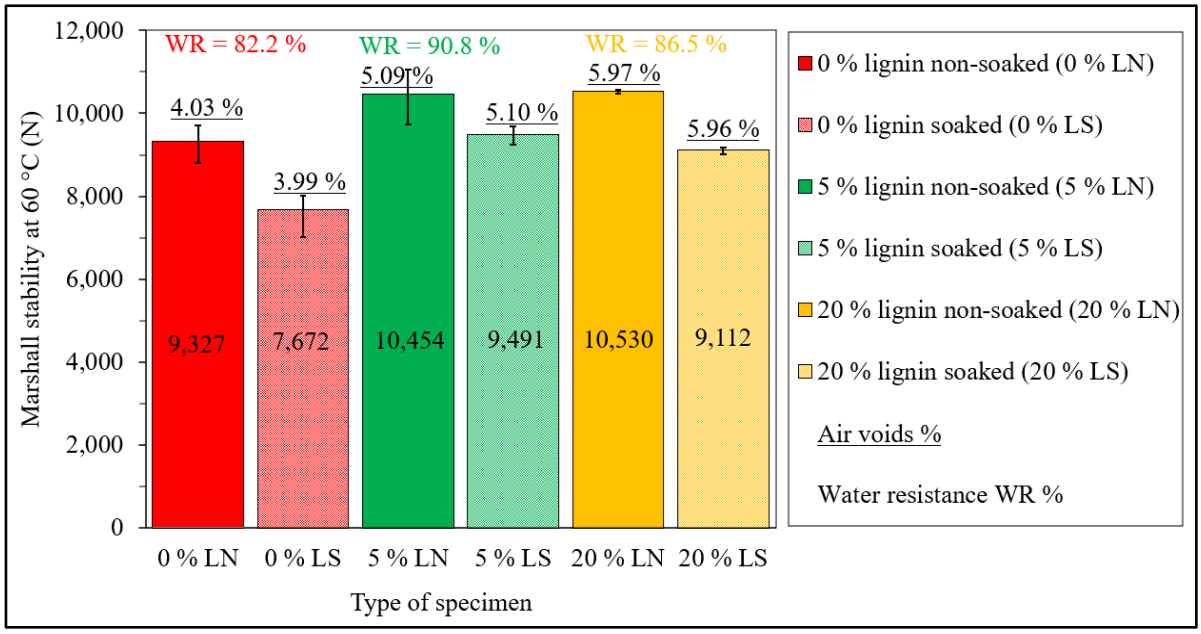


Figure 7.1 Moisture sensitivity test results for the non-soaked (N) and soaked (S) specimens of the unmodified and modified HMA with different contents of HT SW A 1 lignin: Marshall stability at 60 °C, water resistance (WR) and air voids content (underlined value in %)

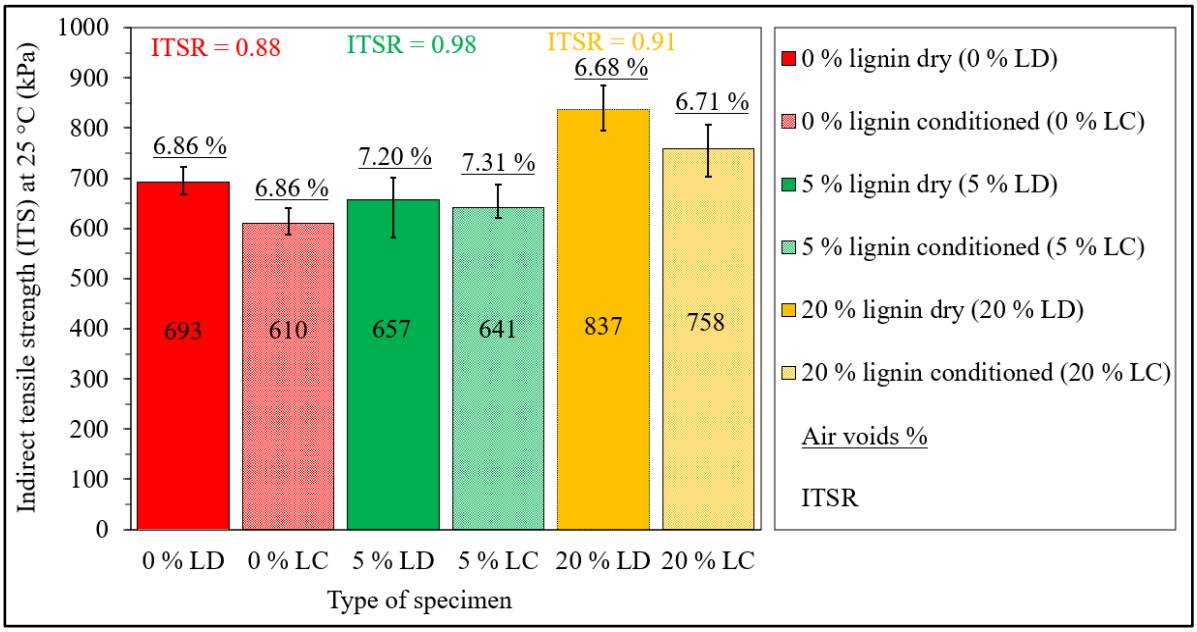


Figure 7.2 Indirect tensile strength (ITS) test results for the dry (D) and conditioned (C) specimens of the unmodified and modified HMA with different contents of HT SW A 1 lignin: ITS at 25 °C, ITS ratio (ITSR) and air voids content (underlined value in %)

Since the tests results show that the lignin changes the properties of HMA, it is expected that the behaviour of the modified HMA will be also changed/modified. To confirm this, more complex tests should be performed to better understand the effects of lignin addition. Herein, complex modulus tests were performed to see the lignin effects on the rheological behaviour of HMA.

#### 7.2.1.2 Complex modulus (E*)

Figure 7.3 shows Cole-Cole diagram of the unmodified and modified HMA with different contents of HT SW A 1 lignin in addition to 2S2P1D model parameters ($E_{00}$, $E_0$, h, k and δ). As can be seen, the data is continuous which results in unique curves. The modified HMAs with lignin are thermo-rheological simple materials. Therefore, the Time-Temperature Superposition Principle (TTSP) is valid and lignin does not create any biased effects observed with mixes with high polymer content.

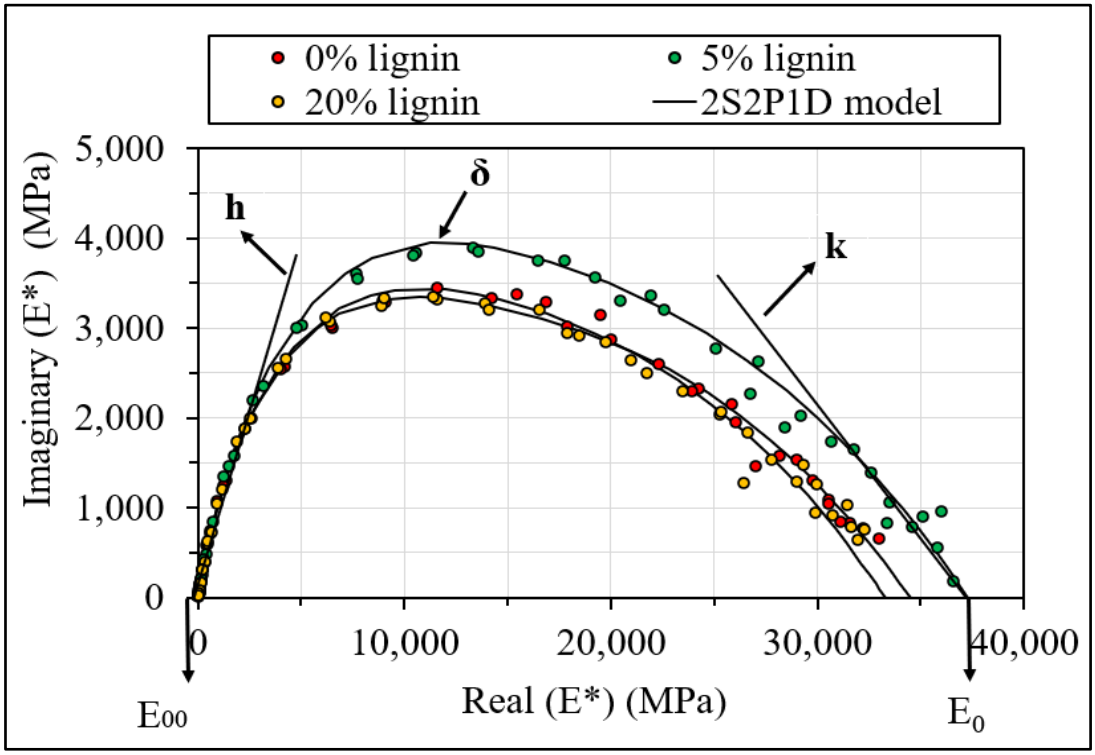


Figure 7.3 Cole-Cole diagram for the unmodified and modified HMA with different contents of HT SW A 1 lignin and 2S2P1D model parameters (E00, E0, h, k and δ)

TTSP is used to construct the master curves of the norm of complex modulus (|E*|) (Figure 7.4) and phase angle (Figure 7.7) for all HMAs. Generally speaking, lignin increases the stiffness despite that the lignin-modified HMA specimens have greater air voids. The effect of lignin addition on the stiffness at high temperatures (low frequencies) is clearer than that at the low temperatures (high frequencies) (Figure 7.4). According to the results, it is difficult to see a difference between the different contents of lignin. It seems that there are 2 trends; one without lignin and one with lignin (5 % or 20 %).

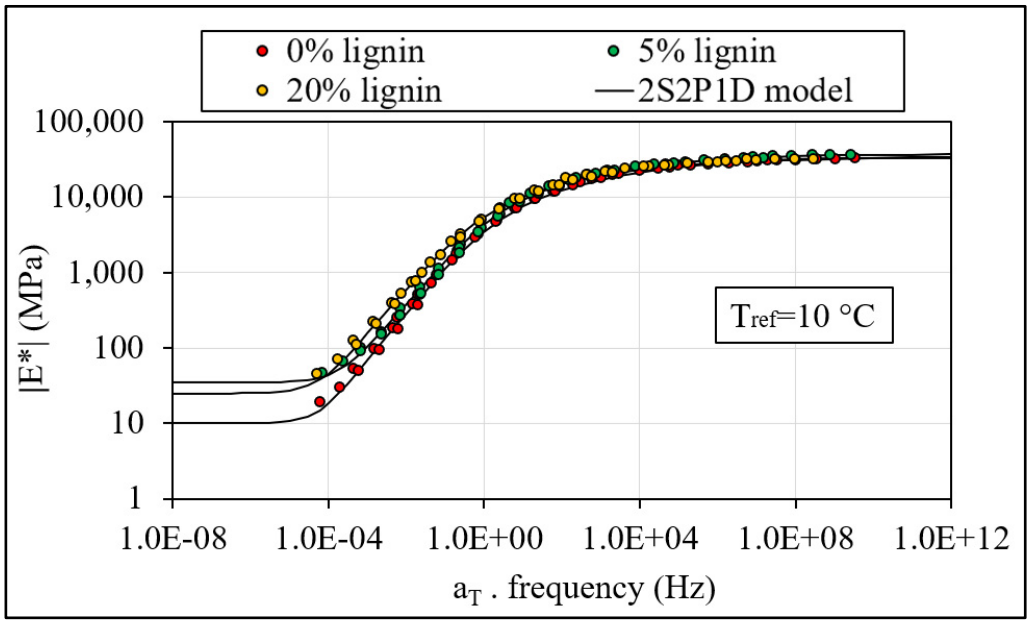


Figure 7.4 Master curves of the norm of complex modulus (|E*|) at $T_{ref}$=10 °C for the unmodified and modified HMA with different contents of HT SW A 1 lignin and 2S2P1D model

As mentioned previously, the three considered HMAs have different air voids (5.4 % for 0 % lignin, 4.3 % for 5 % lignin and 6.9 % for 20 % lignin), which greatly impact stiffness results. Herein, the use of the normalized Cole-Cole diagram is strongly suggested (Figure 7.5). The purpose of this diagram is to visualize the results with less influence of the different air voids. As can be seen, the normalized Cole-Cole diagram for all HMAs show small differences. In other words, the use of this diagram shows its effectiveness to get rid of the air voids effect but the lignin effects are still visible.

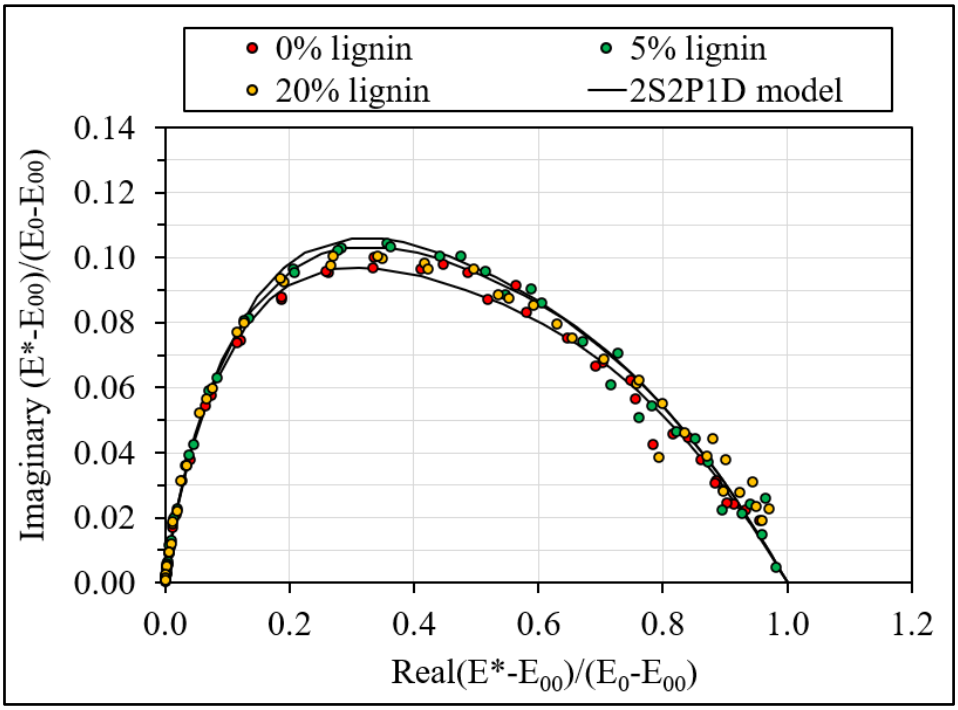


Figure 7.5 Normalized Cole-Cole diagram for the unmodified and modified HMA with different contents of HT SW A 1 lignin

The ratio of |E*| of the lignin-modified HMA to the unmodified one can be used to better show the effect of lignin addition on the stiffness at low temperatures (high frequencies). Figure 7.6 shows the ratio of |E*| of 5 and 20 % to 0 % of lignin. At low temperatures (high frequencies), the ratio of 20 % to 0 % lignin is lower than that for 5 % to 0 % lignin. This means that the modified HMA with 20 % lignin has lower stiffness than that modified with 5 % lignin. As mentioned above, and expected, this reduction in the stiffness is strongly related to the high air voids content within the modified HMA with 20 % lignin. At high temperatures (low frequencies), it is interesting to see that the ratio of |E*| for 20 % to 0 % lignin increases rapidly compared to 5 % to 0 % lignin. This confirms the finding observed from the plot of |E*| shown in Figure 7.4 (higher stiffness for the modified HMA with 20 % lignin). However, in addition to the lignin effect, it should be noted that the results shown in Figure 7.6 are also influenced by the calibration of 2S2P1D model (Figure 7.8), especially at low frequencies where there is more difference between the model and experimental data.

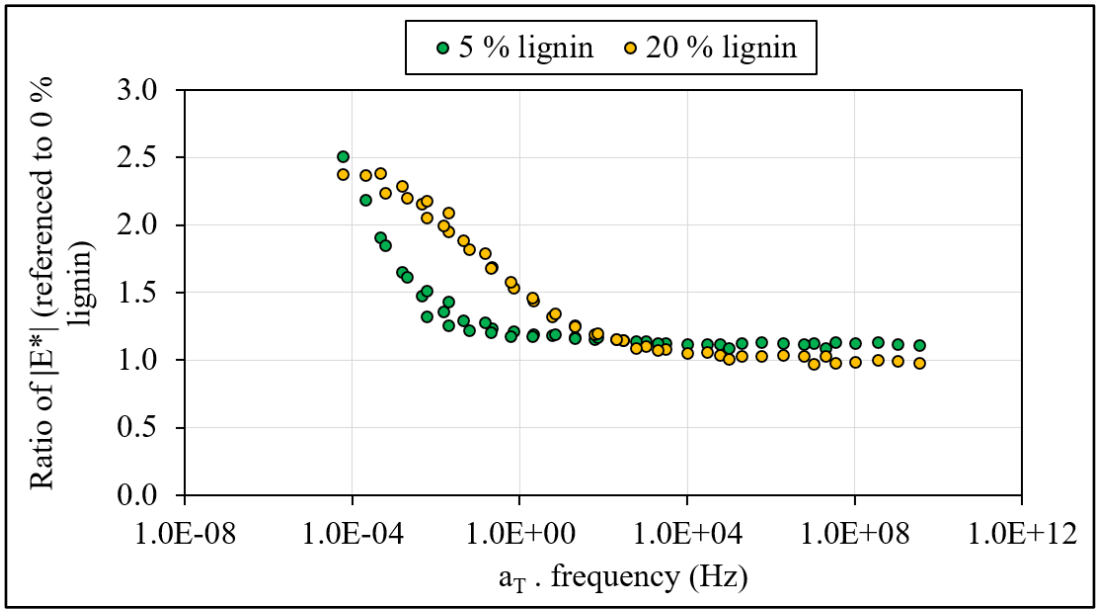


Figure 7.6 Ratio of the norm of complex modulus (|E*|) for the modified HMA with different contents of HT SW A 1 lignin referenced to the unmodified HMA

Besides the effects of lignin addition on the stiffness of HMA, it is interesting to see also the effect on the phase angle. Figure 7.7 shows the master curves of the phase angle at $T_{ref}$=10 °C for the unmodified and lignin-modified HMAs with different contents and 2S2P1D model. As can be seen, the lignin addition caused a shift and reduction in the master curves of the phase angle for the modified HMAs. Accordingly, the lignin-modified HMAs show lower phase angle than the unmodified one. This means that the lignin addition reduces the viscous component of the behaviour, so the material loses ability to relax stress, while the elastic component of the behaviour becomes greater.

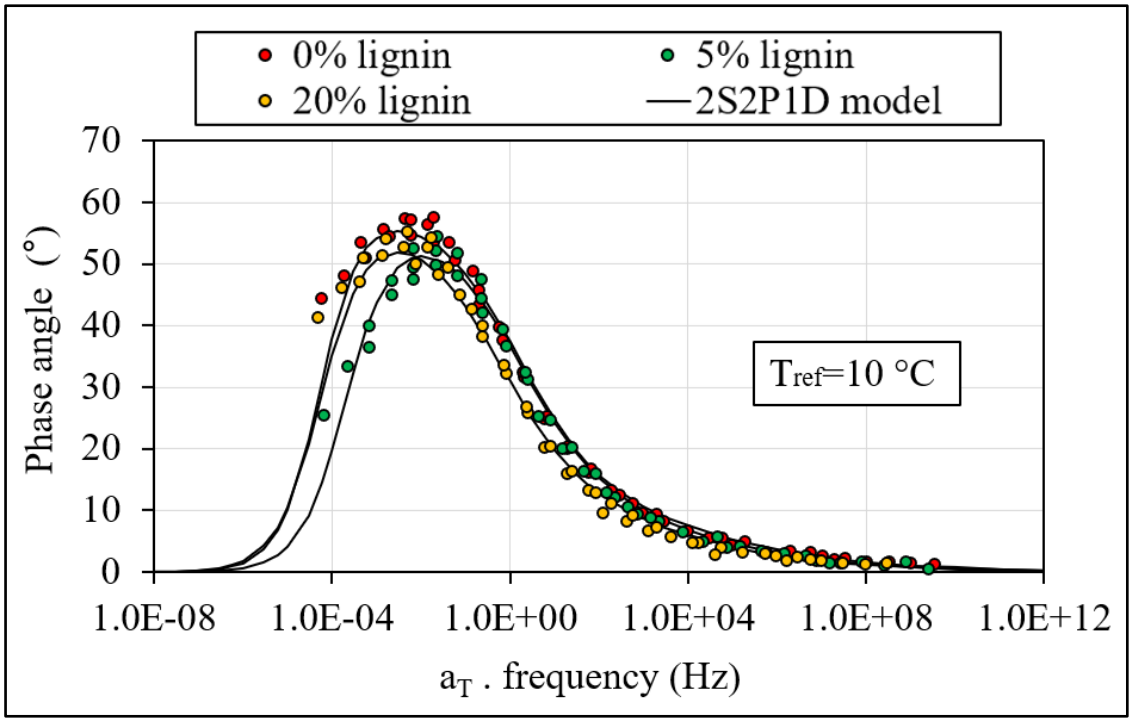


Figure 7.7 Master curves of the phase angle (φ) at $T_{ref}$=10 °C for the unmodified and modified HMA with different contents of HT SW A 1 lignin and 2S2P1D model

As can be seen from Figure 7.8, the 2S2P1D model was calibrated on the experimental data, and it fits the data correctly. Most of the data lies in the discrepancy range of ± 10 % which means that the calibration of the model is good. Few points are out of this range, but they do not impair the calibration of the 2S2P1D model.

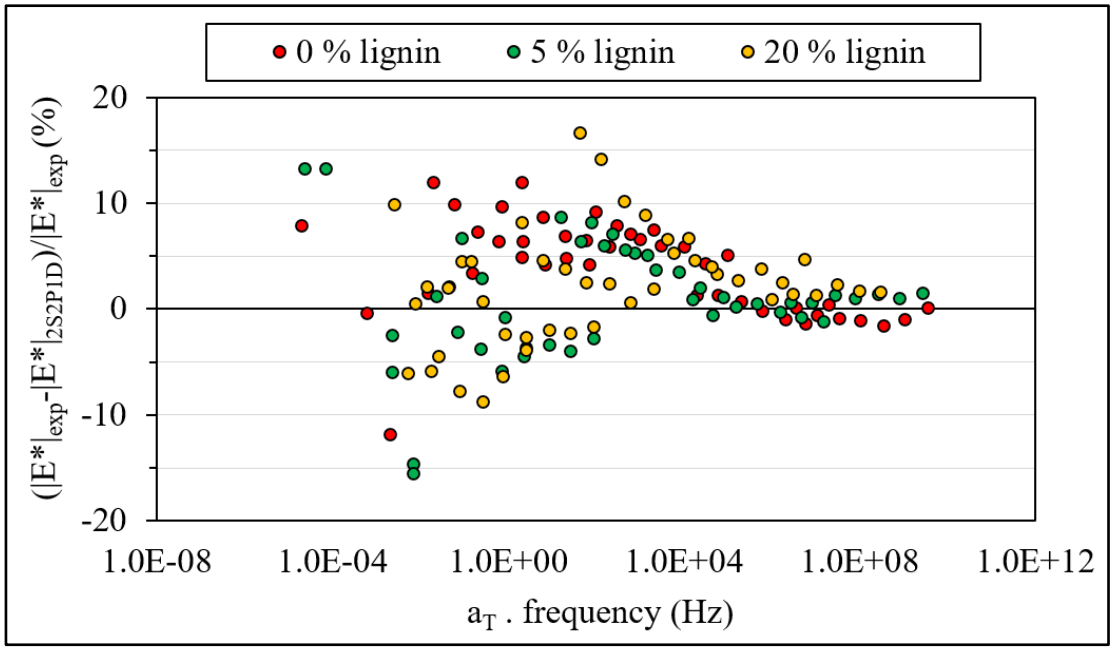


Figure 7.8 Difference in percentage of the norm of complex modulus (|E*|) between the experimental data and 2S2P1D model referenced to the experimental data of |E*| for the unmodified and modified HMA with different contents of HT SW A 1 lignin

Table 7.2 shows the summary of the air voids content, 2S2P1D model parameters (shown in Cole-Cole diagram, Figure 7.3) and the constants of WLF equation for the unmodified and modified HMAs with different contents (5 and 20 %) of HT SW A 1 lignin. As can be seen from Table 7.2, the modulus ($E_0$ and $E_{00}$) is affected by not only the lignin content but also the air voids contents. Also, since lignin is used to replace part of the bitumen, it is believed that the amount of added bitumen affects the modulus. The parameters h, k and δ are related to the rheology of the bitumen. For the h parameter, all values are the same (0.63) and, also, the values for the k parameter are similar (0.20 for 0 % and 0.21 for 5 and 20 % lignin). On the other hand, the difference for the δ parameter is more visible (2.32, 2.10 and 2.20 for 0, 5 and 20 % lignin) compared to k and h parameters, but it remains not significant. Herein, with the small differences for h, k and δ, a big part of the lignin probably acts as a filler and does not modify the bitumen which aligns with the FTIR results. However, it is important to look at the mastic (filler + bitumen) as a binder and not only the bitumen. In other words, it is possible that the bitumen remains unchanged, but the mastic holding the aggregates together is different. For the characteristic time (τ), the effect of lignin addition on it can be observed (0.01, 0.013

and 0.035 for 0, 5 and 20 % lignin) and attributed to the viscosity of the modified HMAs with lignin. However, it is still important to evaluate the effects of lignin addition away from the effects of the air voids content.

Table 7.2 Summary of the air voids content, parameters of the 2S2P1D model and constants of WLF equation for the unmodified and modified HMA with different contents of HT SW A 1 lignin

| Lignin content (%) | Air voids (%) | $E_0$ (MPa) | $E_{00}$ (MPa) | k | h | δ | τ | β | C1 | C2 |
|---|---|---|---|---|---|---|---|---|---|---|
| 0 | 5.4 | 10 | 34500 | 0.20 | 0.63 | 2.32 | 0.01 | 150 | 19.4 | 148.1 |
| 5 | 4.3 | 35 | 37300 | 0.21 | 0.63 | 2.10 | 0.013 | 150 | 17.7 | 139.8 |
| 20 | 6.9 | 25 | 33300 | 0.21 | 0.63 | 2.20 | 0.035 | 150 | 23.7 | 180.1 |

As can be seen from Table 7.1, one repetition is used for this test due to a shortage in the materials. The quality index (QI) is checked and found to be acceptable (less than 15 %). However, more repetitions are needed for this test. As mentioned earlier, the E* tests results are used to show the behaviour of HMA at all temperatures. Regarding the thermomechanical performance of HMA, it is necessary to perform the corresponding test in order to better evaluate the effects of lignin addition on the HMA performance at high and low temperatures.

#### 7.2.1.3 Rutting

Figure 7.9 shows the results of the rut depth at 58 °C versus the number of loading cycles for the unmodified and lignin-modified HMAs with different contents in addition to the requirements of LC 26-410. As can be seen, lignin-modified HMAs meet the LC 26-410 requirements (< 10 % at 1000 cycles and < 20 % at 3000 cycles). At 1000 cycles, the rut depth is 4.1 % for both lignin contents, 5 and 20 %, compared to 6.1 % for 0 % lignin. At 3,000 cycles, it is close to 6.0 % for 5 and 20 % and 8.0 % for 0 % lignin content (less rut depth in percent at 58 °C for the modified HMAs with lignin). In the evaluation of the rutting performance of HMA, the air voids content has a significant influence and the rutting resistance

tends to decrease with increasing air voids. Despite the air voids content (average of the results for two slabs) is higher for lignin-modified HMAs (5.3 % for 0 % lignin, 6.4 % for 5 % lignin and 8.2 % for 20 % lignin), they show better rutting performance. Besides this, since lignin is used to substitute bitumen, these modified HMAs contain less bitumen. It is well known that the rutting resistance increases when the bitumen content decreases.

It can be seen from Figure 7.9 that the rut depth (%), for all HMAs, increases rapidly at the early stage of the test, which is due to the compressive loading pressure on the loose HMA. Then, the rut depth reduces gradually, which can be attributed to the shear flow of the HMA. The slope of the rut depth located between 10,000 and 30,000 cycles is lower for the modified HMA with 5 and 20 % of lignin (0.016 for both contents) than that for 0 % lignin (0.025). Lower slope means higher dynamic stability and rutting resistance of the HMA (Zhang et al., 2020). In conclusion, the use of lignin within the HMA improves the resistance to permanent deformation. These findings, obtained from the rut tests, confirm the results of DSR and MSCR tests (sections 5.2.1.2 and 5.2.1.3, respectively) performed on the bitumen itself.

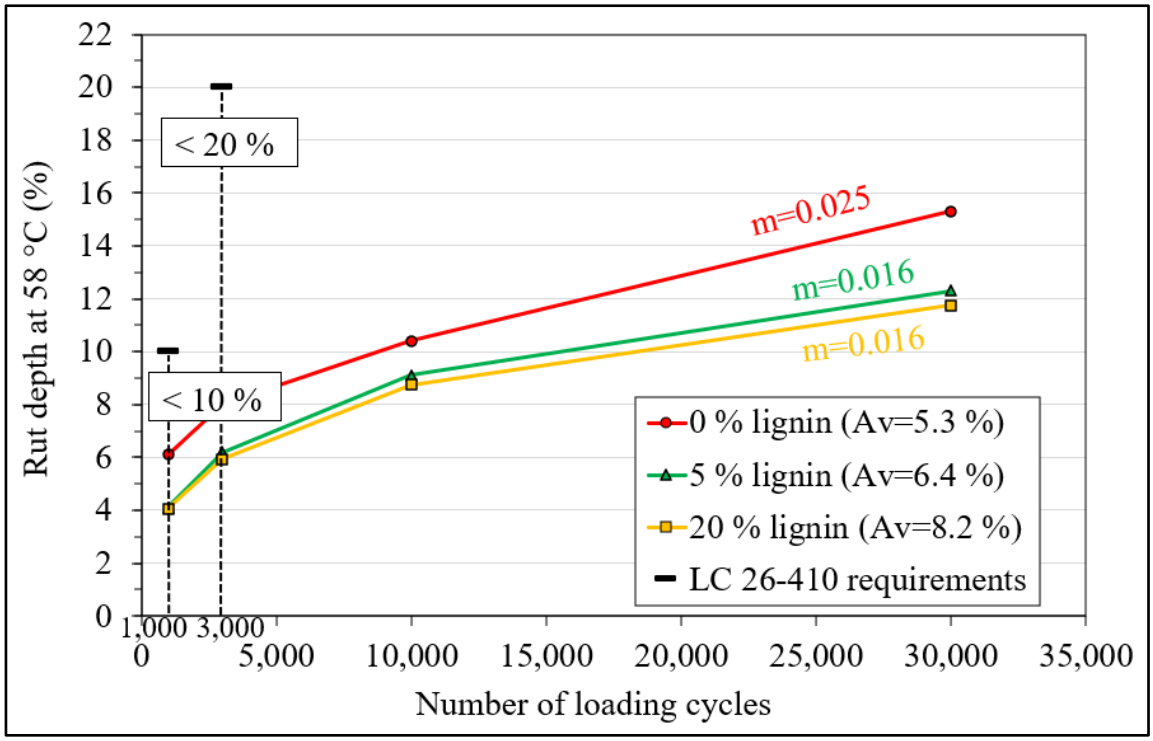


Figure 7.9 Rut depth at 58 °C for the unmodified and modified HMA with different contents of HT SW A 1 lignin, air voids (Av) and requirements of LC 26-410

Since the lignin shows effects on the performance of the HMA at high temperatures, it is expected to see effects on the low temperature performance as well. Performing the corresponding test can be used to evaluate the thermal cracking resistance of HMA at low temperatures.

#### 7.2.1.4 TSRST

Figure 7.10 shows the evolution of the thermal stress versus the decrease in the temperature for the unmodified and lignin-modified HMAs with different contents (three specimens for each lignin content). All tests started at almost the same temperature (5.6-5.8 °C). This is very important to be checked to better evaluate the performance of HMA at low temperatures. As can be seen, at the beginning of the test, the thermal stress increases slowly with the decrease in the temperature, which is mostly due to the relaxation of the HMA. Then, at specific temperature, the HMA changes its behaviour and the relationship between the thermally induced stresses and the temperature is approximately linear. This temperature is called the glass-transition temperature ($T_g$) at which the material changes its behavior from viscoelastic to elastic, or vice versa. Then, the thermal stresses continue increasing, with decreasing of the temperature, up to the maximum stress (upper left corner of Figure 7.10), defined as fracture strength. The corresponding temperature of the fracture strength is called the fracture temperature.

All above-mentioned parameters are determined from the results of the TSRSTs (Figure 7.10) for each specimen of the unmodified and lignin-modified HMAs. Since the size of the specimens is different from what is in the standard for TSRST, it is worth discussing the effect of the specimen size on the tests results. As stated by Jung & Vinson (1994), the fracture temperature is mostly affected by the bitumen type and barely followed by the specimen size. The only dimension that can influence the tests results is the diameter (51 ± 1 mm in this study) and not the length. This comes from the direction of the heat transfer through the specimen inside the thermal chamber (horizontally from the outer to the inner surface). This affects the time required to reach the thermal equilibrium inside the specimen. In particular, the shorter

time that is needed for smaller diameter may result in higher fracture and glass-transition temperatures (Jung & Vinson, 1994).

Figure 7.11 shows the average value (three results) for the fracture and glass-transition temperatures and fracture strength of each lignin content. The fracture temperatures for 0, 5 and 20 % lignin content are -29.6, -29.7 and -28.2 °C, respectively. This temperature is affected by the performance grade (PG) of the bitumen (PG 58S-28 is used). Herein, it is interesting to present the values of the low temperature PG obtained from the BBR tests (section 5.2.1.4) and compare them with what is obtained here. Thus, the link between the BBR and TSRSTs can be better highlighted. The low temperature PG for 0, 5 and 20 % lignin contents are -30.9, -29.1 and -26.2 °C, which are similar to the temperatures obtained from the TSRSTs. This indicates that both tests, BBR and TSRST, are strongly linked with each other. It should be noted that the TSRSTs for all HMAs show good repeatability.

The mixture with 5% lignin shows similar fracture temperature to 0 % lignin (-29.7 and -29.6 °C, respectively), while for 20% lignin the fracture temperature is slightly higher (-28.2 °C for 20 % compared to -29.6 °C for 0 %). This means that there is a negative effect on the low temperature performance of HMA due to the use of 20 % lignin, but it is limited. Regarding the fracture strength, the addition of lignin does not show an effect since all values are similar to each other (3.4 MPa for 0 and 5 % lignin content and 3.3 MPa for 20 %).

Due to the test principle and set up that leads to a failure of the bitumen film, TSRSTs results are not much affected by the different air voids contents of the mixtures (1.0, 1.5 and 2.4 % for 0, 5 and 20 % lignin, respectively). The glass-transition temperatures for 0, 5 and 20 % lignin are -15.3, -16.7 and -11.7 °C, respectively. According to this, the addition of lignin shows more visible effects than on the fracture temperature. However, these effects show the same trend as for the fracture temperature (slight improvement for 5 % lignin and visible negative effect for 20 %).

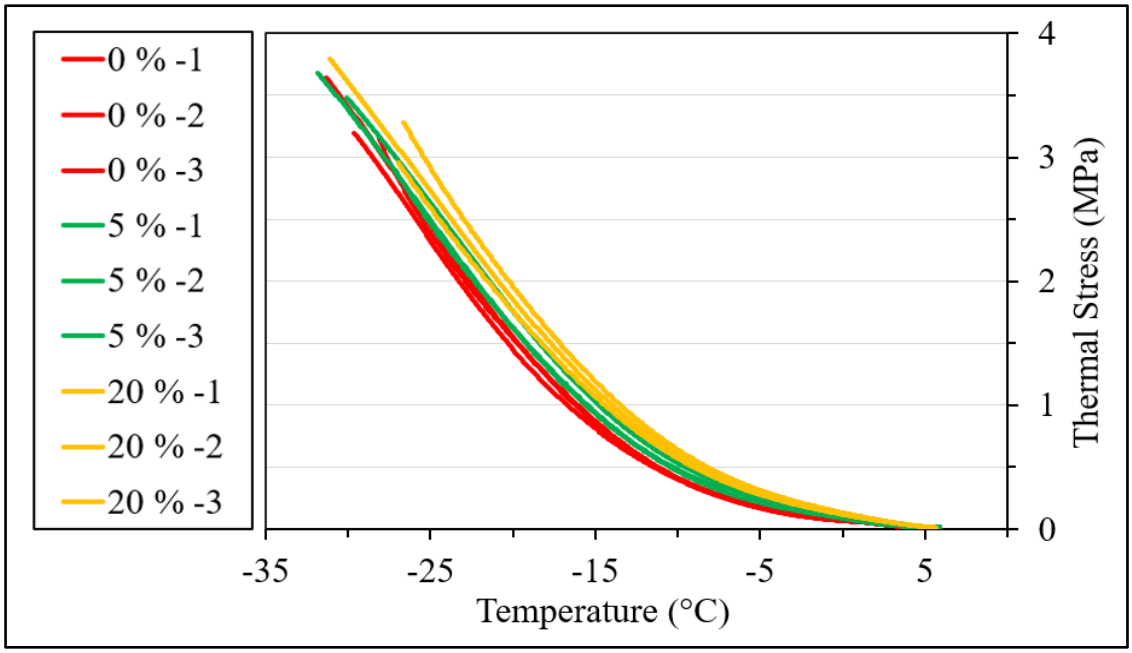


Figure 7.10 Evolution of the thermal stress versus the decrease in the temperature for each specimen of the unmodified and lignin-modified HMAs with different contents

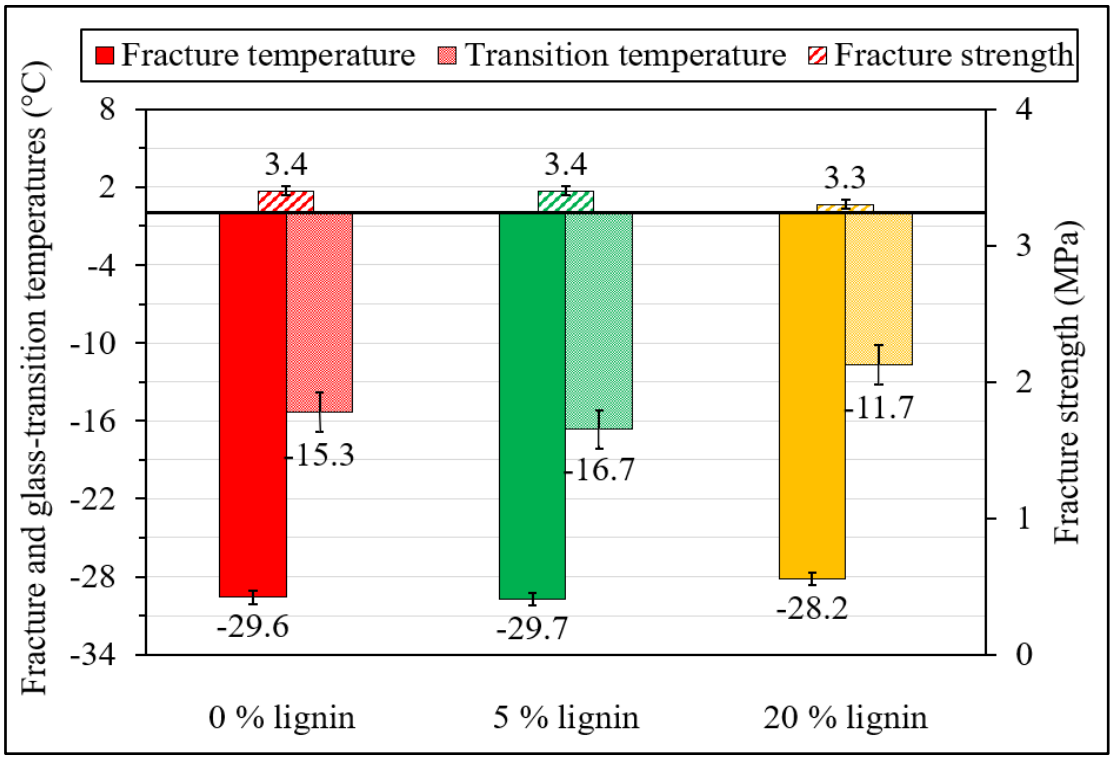


Figure 7.11 Fracture and glass-transition temperatures and fracture strength for the unmodified and lignin-modified HMAs with different contents (average of 3 results)

In conclusion, for high lignin contents (20 % or more) the resistance to thermal cracking is decreased. On the other hand, for low lignin content (5 % or less), there is not a significant change of the performance at low temperatures.

## 7.3 Summary

This chapter presents the evaluation of the effects of lignin addition on the moisture susceptibility, LVE behaviour and thermomechanical performance of HMA at different temperatures. The main conclusions of this chapter can be drawn as follows:

- Lignin addition increases the Marshall stability, indirect tensile strength and water resistance of HMA.
- Lignin increases the stiffness of HMA and decreases the phase angle.
- Lignin improves the HMA resistance to permanent deformation at high temperature.
- Using 20 % of lignin decreases the HMA resistance to thermal cracking at low temperatures, while the 5 % of lignin does not show significant change.

Finally, according to the presented findings of the thermomechanical tests performed in this chapter, the lignin can replace part of the bitumen and improve the thermomechanical performance of HMA.

# CONCLUSION

This research program investigates the effects of lignin on the behaviour and performance of bitumen and HMA. In particular, a methodology to incorporate lignin into bitumen is established. Following, the effects of lignin on bitumen in addition to the anti-oxidative aging properties are evaluated. Then, the effect of lignin addition on the workability and compactability of HMA is evaluated. Afterwards, the behaviour and thermomechanical performance of lignin-modified HMA are evaluated. Herein, the main and specific objectives of this research program are achieved. Accordingly, the main conclusions of this research program can be drawn as follows:

- The incorporation process of lignin into bitumen is possible;
- The lignin-modified bitumen is stable and homogeneous for up to 30 % lignin content;
- Increasing the incorporation temperature does not have a significant effect on the stability for low lignin content (up to 20 %). For high lignin content (50 %), the incorporation temperature, speed and duration should be increased;
- Changing the lignin type impacts the storage stability in the bitumen;
- The microscope observations show that the lignin is well distributed in bitumen. Clusters of lignin are observed for 30 % lignin content and higher;
- Incorporating pellets into bitumen results in unstable modified bitumen which can be due to the presence of soybean oil;
- Lignin in powder form increases the viscosity, stiffness at high and low temperatures and resistance to permanent deformation of the bitumen, while for pellets form, the behaviour is different which is due to the presence of soybean oil;
- Lignin shows similar overall impact on two different grades of unmodified bitumen;
- Using different types of lignin affects the bitumen properties differently, according to the physical and chemical properties of each type;
- Lignin does not show anti oxidative aging properties of the bitumen;
- Lignin in powder form increases the air voids content within HMA while the pellets decrease this content which is due to the soybean oil that dilutes the bitumen;
- The dry process results in higher air voids compared to the wet process;

- Increasing the compaction temperature is not an effective solution to improve the compactability of the modified HMA with lignin, but is necessary to also consider mix design aspects, especially the volumetric approach;
- The use of different types of lignin affects the air voids content within HMA differently;
- Lignin improves the moisture sensitivity of HMA;
- Lignin increases the HMA stiffness and decreases the phase angle;
- Lignin improves the resistance of HMA to the permanent deformation at high temperature;
- At low temperature, the low lignin content (5 %) does not show a significant change, while the high content (20 %) reduces the HMA resistance to thermal cracking;

According to the main findings presented in this research program, lignin can be used to replace part of the bitumen. These results fill some of the research gaps such as establishing a methodology for incorporating lignin into bitumen, investigating the effects of each parameter of the incorporation process, evaluating the anti oxidation properties for the long-term aging process and evaluating the effects of lignin on the rheological behaviour and fatigue cracking resistance of HMA. Based on those findings, it is believed that the lignin, as a powder, behaves as a binder and filler within the bitumen and HMA.

Finally, the results of this research program are useful and should be used for further research. This implies more work with more lignin contents, and different lignins, and more tests are required for a more comprehensive understanding of how lignin addition affects the bitumen and HMA. In addition, a mix design study to determine the optimum lignin content within the HMA is highly recommended. Also, a study to better understand the behaviour of lignin is suggested. In other words, to see if lignin in powder form behaves as a binder or filler or both in addition to determine the percentage of each role. Lastly, since lignin is a biopolymer, it is recommended to use polymer-modified bitumen (PmB) in order to evaluate the effect of lignin on unmodified bitumen and PmB.

# ANNEX I

# FIELD TRIAL SECTION AND LIFE CYCLE ASSESSMENT

## Introduction

After presenting the effects of lignin addition on the properties and performance of HMA produced in laboratory scale, it is interesting to translate the production process into a bigger scale. This annex, as a part of this research program, shows the use of lignin within the asphalt pavement on a full scale. In this context, four field trial sections were executed in different provinces across Canada, one in Alberta, one in Ontario and two in Quebec (one in Laval University and one in Quebec City). This is decided based on what is seen in the lab, including tests results shown in different chapters of this research program. Similar to the work done in the laboratory, the trial sections were done with two different lignin addition process; the wet process and the dry process. In the wet process, the lignin is added directly in the bitumen by the bitumen supplier. In the dry process, the lignin is added in the HMA at the asphalt plant by the contractor.

It is important to mention that in all four trial sections, unmodified HMAs (reference mix) were placed beside the lignin modified HMAs in order to have a good comparison in terms of properties and performance under the same climatic conditions, the same traffic and built on the same pavement structure. Also, except for the Laval University trial section, only a surface course was built with the lignin modified HMA. For the Laval University trial section, a lignin modified HMA was built as a base course layer. For all trial sections, the aggregates were heated for 30 seconds, then the bitumen was added and the mixing time was 30 seconds. The mixing temperature for all sections is 150 °C.

For the three sections using the dry process, the lignin was added in the asphalt plant directly. To do that, pre-weighted plastic (LDPE) bags of lignin were prepared by the lignin producer and a specific number of bags were just thrown into the mixer in order to get the desired percentage of lignin, which was 5%, 10% or 20% depending on the section. The lignin was put

in plastic bags which melted when in contact with the hot aggregates and the bitumen, therefore releasing the lignin. The impact of the presence of plastic was considered insignificant because of the small quantity. For the three sections built on road sections, no gauges were installed in the pavement to measure precisely the properties of the HMA under load. However, for the Laval University section, strain gauges and thermocouples were installed in the test pit. The main advantage of the Laval University test pit is the fact that the temperature and humidity are controlled and that it is possible to accelerate the loading. The results are not available yet. However, the initial observations have shown that the lignin modified HMA did perform better than the unmodified HMA in terms of rutting resistance. Another important aspect to note is the use of recycled asphalt (Reclaimed Asphalt Pavement: RAP) in two of the trial sections. For the field trial section in Alberta and the one at Laval University, RAP was used in the HMAs. As expected, no issues were observed in the HMA production because of the use of RAP and no issues were observed for the placement of the lignin-modified HMA with RAP, even with 20% RAP for the base layer at Laval University. Even if no long-term performance data is available yet, this is good since the combination of RAP and lignin means an even lower amount of unmodified bitumen is used in the mixes. It should be noted that though some compaction issues were observed in the laboratory, the compaction process of the lignin-modified HMA in the field did not cause any problem and the operators of the compaction rollers did not notice a significant difference between the unmodified and the lignin-modified HMA. Table-A I-1 shows the details for each trial section. Figures-A I-1 to 4 show photos of the trial section paved in Alberta, Ontario, Laval University and Quebec City, respectively.

Table-A I-1 Summary for the trial sections

| | Alberta (Sturgeon County) | Ontario (Thunder Bay) | Quebec (Quebec City) | Laval University |
|---|---|---|---|---|
| Date | 26, Aug, 2021 | 20, Sep, 2021 | 14, Oct, 2021 | 13, Oct, 2021 |
| Type | Mill & overlay | New paving | Mill & overlay | |
| Dimensions of unmodified section (length, width, depth) (m) | 279.5*7*0.065 | 296*7*0.05 | 250*3*0.055 | 3*2*0.14 |
| Dimensions of modified section (length, width, depth) (m) | 140.5*7*0.065 | 215*7*0.05 | | |
| HMA (type) | 10mmHT | HL4 | ESG10 | ESG10 (top) and GB20 (bottom) |
| Lignin content (%) | 5 | 5 | 10 | 10 (top) and 20 (bottom) |
| RAP content (%) | 10 | - | - | 20 (bottom) |
| Addition process | Wet | Dry | Dry | Dry |
| Laydown temperature | 125-145 °C | 120-150 °C | 135-155 °C | 125-145 °C |
| Compaction procedure | Double steel roller (breakdown) Pneumatic rubber tire roller Double steel roller for Alberta and small double steel roller for Ontario (finishing) | | Double steel roller (breakdown) Small double steel roller (finishing) | Small double steel roller (finishing) |
| Number of passes | 2-5 (breakdown) 16-22 (pneumatic) 2-5 (finishing) | 4-6 | - | 15-22 |
| Bitumen (type) | PG 58-28 | PG 52-34 | PG 58-34 | PG 58-34 |

Figure-A I-1 Alberta’s trial

Figure-A I-2 Ontario’s trial

Figure-A I-3 Quebec city's trial

Figure-A I-4 Laval University's trial

**Observations**

A follow-up over several years will be carried out to verify if the durability of the sections with lignin is similar to that of the reference sections. However, the preliminary observations for the four trial sections are positive. First, it was shown that it is simple to make lignin modified HMA in the field. For both processes, wet and dry, there was very little modification to the process. For the wet process, the only change was the modification of the bitumen by the supplier. So, except that extra step, nothing was different for the contractor who constructed the trial section. For the dry process, the only difference was the addition, manually, of the bags of lignin in the mixer. It is believed that setting up an automated process to deliver the bags of lignin in the mixer would not be complicated. However, it would be better if no plastic were used in terms of sustainability. To that end, it would be required to modify the lignin, to change its format from a powder to something bigger that is not blown away by the wind. Herein, using pellets is possible.

As mentioned earlier, for HMA mixing and compacting, the temperature of the HMA was not modified to take into account the presence of lignin, i.e. the lignin-modified HMAs were considered as usual HMAs. For Ontario and Quebec field trial sections, no compaction issues were perceived by the construction crews. For Alberta sections, the lignin modified HMA behaved stiffer than the reference HMA, and it was difficult to remove rubber-tired roller marks with the finishing roller and required a higher compaction effort, similar to a polymer-modified bitumen. Here, it is questionable whether it was the combination of RAP and lignin that generated this phenomenon. Other than the process of the addition of the lignin itself, the mix preparation process and the pavement construction was done without modifications. Visually no difference between the unmodified HMAs and the lignin-modified HMAs were observed, and the properties of the lignin HMA prepared in the field are comparable than the reference HMAs.

For the trial section at Laval University, as shown on Figure-A I-4 (left), strain gauges were installed for this trial section in order to better evaluate the behaviour of the lignin modified

HMA compared to the unmodified HMA under loading. The main observations obtained from this trial section are, firstly, slight better rutting resistance for the lignin-modified section and, secondly, lower strain under the load for the section with lignin-modified HMA, which means higher stiffness. Those two aspects are very important and positive results. There were not enough loading cycles to see cracking fatigue, but it is worth mentioning that neither unmodified section nor modified sections have shown surface distresses related to cracking. A conference paper specifically on the trial sections was presented at the Canadian Technical Asphalt Association (CTAA) in 2022. The paper is titled: *Field Trial Sections of Kraft Lignin-Modified Hot Mix Asphalt*.

**Summary**

This annex shows the use of lignin with HMA on a field scale. Lignin-modified HMA can be produced on a full scale using either wet or dry process without major difficulties. Establishing an automated set up to deliver lignin into the mixer would not be complicated. Also, no real challenges during the construction process were observed by the contractors crew.

# ANNEX II

# EFFECT OF TALL OIL ON THE COMPACTIBILITY OF LIGNIN-MODIFIED HMA

## Introduction

As shown in chapter 6, lignin addition in powder form increases the viscosity of the HMA and, therefore, the air voids content within the HMA because it increases the difficulty of the compaction process. To this end, using agents to reduce the viscosity of HMA is possible. This annex shows the effects of the tall oil on the compactibility of lignin-modified HMA. Tall oil is used since it is an oil that is a derivative of wood, like lignin. This oil is used in the paper and pulp industry and it is obtained from the black liquor which is a mixture of lignin, water and other by-products that result from the Kraft pulping process. The primary components of tall oil are fatty acids, resin acids and neutral materials.

Tall oil was used with the same modified HMA with different lignins (HT SW A 2, TB HW A and K SW B) that were employed in chapter 6 (section 6.3). Herein, it should be noted that the same lignin content (20 %) is used in order to have comparable results and, thus, better evaluation of the tall oil effects. Also, SGC test is employed in this study. These lignins were selected due to the low workability and compactability observed among the other types of lignin. Tall oil is added to the lignin-modified HMA with different contents (3, 4 and 5 % by the bitumen mass), so less unmodified bitumen is used within the HMA. More specifically, adding 20 % lignin and 3 % tall oil (for TB HW A lignin) means a replacement of the unmodified bitumen by 23 %. The tall oil content used with K SW B lignin type is 5 % since it shows the highest air voids content within the HMA compared to the other types of lignin, which means low workability. The same mixing (155 °C) and compaction (145 °C) temperatures as used in chapter 6 are employed here.

**Summary of the results**

In order to facilitate the comparison process, the SGC tests results for the lignin-modified HMAs with (dashed line) and without (solid line) tall oil are presented in Figure-A II-1. It can be seen that the tall oil addition decreases the viscosity of the HMA which results in lower air voids content, including better workability. This refers to the presence of the fatty acids within the tall oil that act as rejuvenators. Despite that, none of the lignin-modified HMAs met the LC-4202 requirements except the HT SW A 2 with 4 % tall oil. Adding more tall oil is possible and it is expected to help in reducing the viscosity. However, the effect of the tall oil on the compactibility of the HMA is different. Particularly, as shown in Figure A II-1, adding tall oil to the modified HMA with HT SW A 2 lignin shows bigger effect than that on the K SW B lignin, including bigger reduction of the air voids content. This can be due to the difference in the chemical interaction between tall oil and different types of lignin that have different chemical properties. For TB HW A lignin, tall oil did not show a reduction of the air voids content. This might indicate that this lignin (with its properties) needs longer duration of mixing time with tall oil in order to have sufficient chemical interaction.

Overall, adding tall oil shows some benefits on the compactibility of the HMA which may reflect on the performance of HMA. To this end, more work is needed to better evaluate the effect of tall oil on the HMA and to find the optimum dosage of tall oil which helps to avoid the negative impact on HMA properties. Finally, since the tall oil replaces part of the bitumen, the consequent environmental impact should be investigated in future researches.

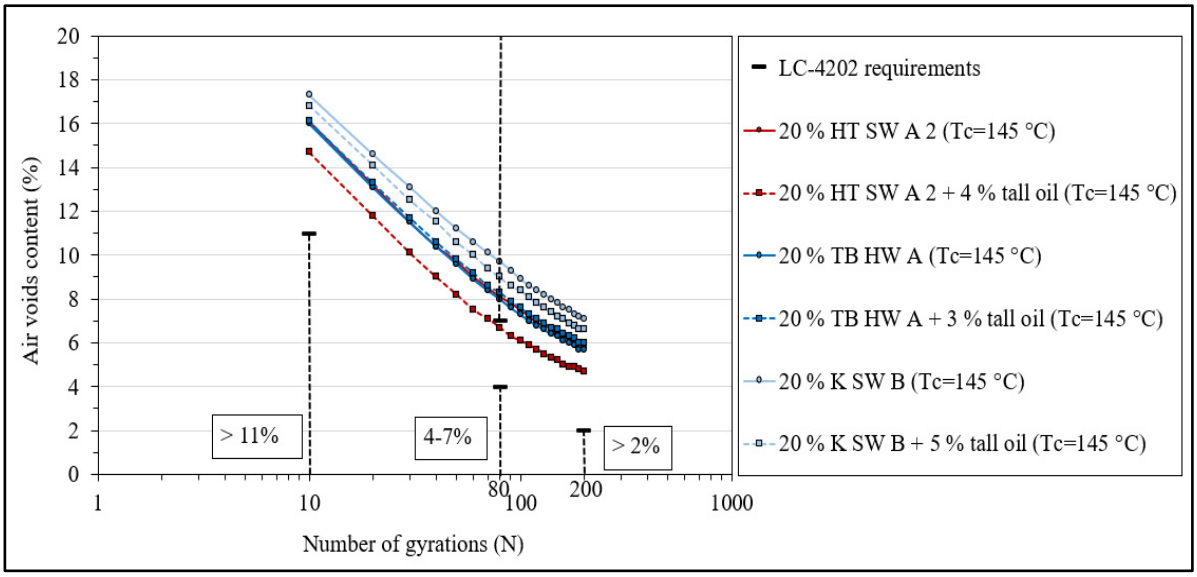


Figure-A II-1 SGC tests results for the lignin-modified HMA with and without tall oil

# ANNEX III

# EFFECTS OF LIGNIN ON FATIGUE CRACKING RESISTANCE OF ASPHALT MIXTURE

## Introduction

This annex shows the work done to evaluate the effects of lignin on the HMA performance at intermediate temperature, particularly fatigue cracking resistance. Fatigue (tension-compression) tests were performed at a temperature of 10 °C and a frequency of 10 Hz and at different strain levels (80, 90, 100 and 120 μdef). The same bitumen (PG 58S-28), HMA formulation (ESG-10) and lignin contents (0, 5 and 20 %) as used in chapter 7 are employed in this work. The same applies for the mixing process (dry) and construction temperatures (mixing and compaction temperatures measured with the DSR). Two specimens were tested at each strain level.

## Results and analysis

This section shows the fatigue tests results for the unmodified and lignin-modified HMAs at each imposed strain level. One tested specimen is considered for some lignin contents and strain levels. This is due to the heterogeneity of the tested specimen and thus indicating the presence of a crack, including failed tests/specimens. The non-homogeneous distribution of the air voids content within the specimen can interpret this heterogeneity. In general, this observation can generate a variability in the stiffness of the material and, subsequently, a non-uniform deformation of the specimen under the applied stress.

However, only the good tests results are shown in the analysis of this section. Table-A III-1 shows the summary of the fatigue tests results and the air voids content within each tested specimen for each lignin content. It should be noted that the tests results in red color are not considered in Wöhler curves shown in Figures A III-1 and A III-2. This is due to issues with the fatigue tests.

For all tests, the same imposed strain level was applied on the two specimens (e.g. A1 and A2) cored from the same slab (e.g. slab number 1 (S1)). As can be seen from Table-A III-1, and expected, increasing the imposed strain level results in shorter fatigue life. In addition, the use of 20 % lignin content leads to reduce the fatigue resistance of the HMA which is not unexpected for an increase in the stiffness, as observed for the complex modulus tests. In order to better evaluate the effects of the addition of lignin on the fatigue cracking resistance of HMA, the imposed strain (deformation) level and fatigue life ($Nf_{50\%}$ criterion) were used to construct the Wöhler curve for each lignin content used within the HMA.

Table-A III-1 Summary of the air voids content and fatigue tests results for each specimen of the unmodified and lignin-modified HMAs

| Lignin content (%) | Tested specimen | Air voids (%) | Real deformation (μdef) | $Nf_{50\%}$ (cycles) | $\lvert E_0^* \rvert$ (MPa) | Average of $\lvert E_0^* \rvert$ (MPa) [A] |
|---|---|---|---|---|---|---|
| 0 | S2A1 | 4.1 | 97.5 | 225,446 | 9,413 | 8,732 |
| | S3A1 | 4.8 | 86.9 | 1,238,849 | 8,300 | |
| | S4A2 | 4.4 | 77.7 | 2,299,527 | 8,483 | |
| | S1A1 | 4.5 | 116.6 | 367,687 | 9,097 | |
| | S2A2 | 3.7 | 96.3 | 413,662 | 9,131 | |
| | S4A1 | 5.7 | 77.7 | 1,244,902 | 8,666 | |
| 5 | S3A1 | 4.0 | 77.0 | 3,906,581 | 9,117 | 9,023 |
| | S4A1 | 4.6 | 87.0 | 2,660,796 | 8,645 | |
| | S4A2 | 4.2 | 87.1 | 1,645,025 | 9,306 | |
| | S1A1 | 4.3 | 110.3 | 513,837 | 8,524 | |
| | S1A2 | 4.4 | 116.1 | 275,645 | 9,938 | |
| 20 | S1A1 | 6.8 | 69.8 | 1,079,784 | 10,643 | 10,630 |
| | S2A1 | 6.7 | 87.8 | 916,558 | 10,643 | |
| | S3A2 | 6.8 | 105.9 | 131,250 | 10,605 | |
| | S1A2 | 6.5 | 78.1 | 501,856 | 10,587 | |
| | S2A2 | 6.5 | 86.8 | 557,981 | 10,657 | |
| | S4A1 | 6.6 | 97.8 | 307,502 | 10,194 | |
| | S4A2 | 6.6 | 98.4 | 109,173 | 10,723 | |

[A] The average value of $\lvert E_0^* \rvert$ is calculated based on only the values in black.

Figure-A III-1 shows the results (Wöhler curves) of the fatigue tests performed by using uniaxial tension-compression tests at 10 °C and 10 Hz for the unmodified and lignin-modified HMAs with different contents. The most important things to be looked at in these curves are

the position of the curve on the log $Nf_{50\%}$ axis and the slope of the curve. As can be seen, the ranking of the HMAs is similar to what was observed for the complex modulus (section 7.2.1.2). The modified HMA with 5 % lignin (first/upper trend line) shows the highest fatigue life since the strain level required to reach 1,000,000 cycles (6.0 on the log scale, y-axis) is the highest. The unmodified HMA (0 % lignin) is second (middle trend line) and followed by the modified HMA with 20 % lignin (third/lower trend line). In terms of the slope, the unmodified HMA shows steeper slope compared to the modified HMAs with 5 and 20 % lignin content. Therefore, the unmodified HMA is more sensitive to a change of strain. In the context of using lignin, the modified HMA with higher lignin content (20 %), ranked third, shows lower slope compared to the low lignin content (5 %), ranked first, leading to less sensitive HMA to a change of strain. In order to get out of this, the use of pavement design software (e.g. Alize), with the help of the complex modulus, can assist which lignin content is better among the studied contents. Regarding $R^2$ value for each lignin content, fatigue tests have higher intrinsic variability compared to the other tests presented here, so the dispersion of the data points around the trend lines is normal.

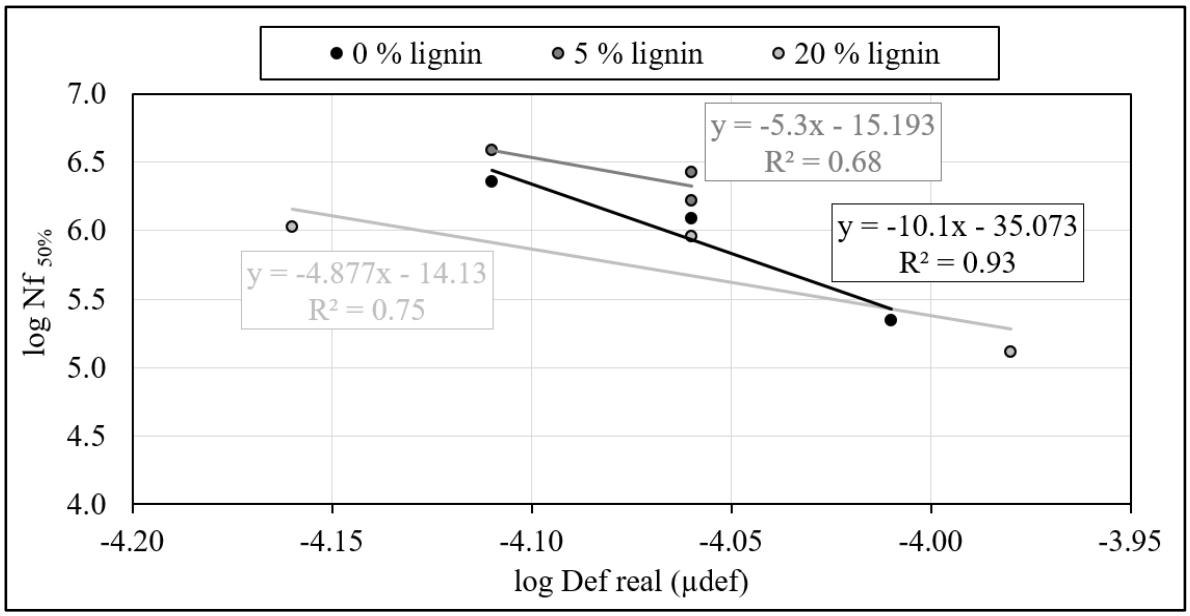


Figure-A III-1 Wöhler curves ($N_{f\,50\%}$ criterion) of the uniaxial tension-compression tests results of the unmodified and lignin-modified HMAs tested at 10 °C and 10 Hz and different strain levels

The fact that the specimens of the modified HMA with 20 % lignin have higher air voids (average of 6.8 %) compared to the reference HMA (average of 4.4 %) and 5 % lignin (average of 4.3 %) interprets most of the differences between the HMAs. In other words, higher air voids content means lower fatigue life. However, the differences observed here are important, but not unexpected for a high difference in the air voids content as it is the case here. To this end, the presented tests results (Wöhler curves, Figure-A III-1) are not only due to the lignin addition itself, but also the higher air voids content compared to the unmodified HMA.

In order to better evaluate the effects of the lignin itself, a correction of the fatigue tests results based on the air voids content within the tested specimen was done. More specifically, the effect of the air voids on the results is limited/reduced. This was done by using the equation presented in Moutier (1991). The correction was done only on the deformation (strain), and the number of cycles was kept as it is. By applying this principle, a new Wöhler curve for each lignin content can be obtained. Figure-A III-2 shows the new Wöhler curves obtained based on the corrected air voids content. As can be seen, the position of the curves is not affected (modified HMA with 5 % lignin is ranked first, unmodified HMA is second and the modified one with 20 % is third). As for the slope of the curve and the dispersion of the data points ($R^2$ value), slight effects can be observed and the main findings are not changed. To this end, the use of $Nf_{50\%}$ criterion does the job to evaluate the effect of lignin addition on the fatigue cracking of HMA. In this context, other criteria such as $Nf_{II-III}$ (fatigue life at the transition point from phase 2 to 3) can be used. In fact, although all tests were performed and $Nf_{II-III}$ criterion was discussed but it is not presented here due to some values of $Nf_{\Delta\varepsilon ax}$ and $Nf_{\Delta\phi}$ (section 2.2.2.2) that are out of the acceptable range (± 25 % for $Nf_{\Delta\varepsilon ax}$ and ± 5 % for $Nf_{\Delta\phi}$), including non-homogeneous test.

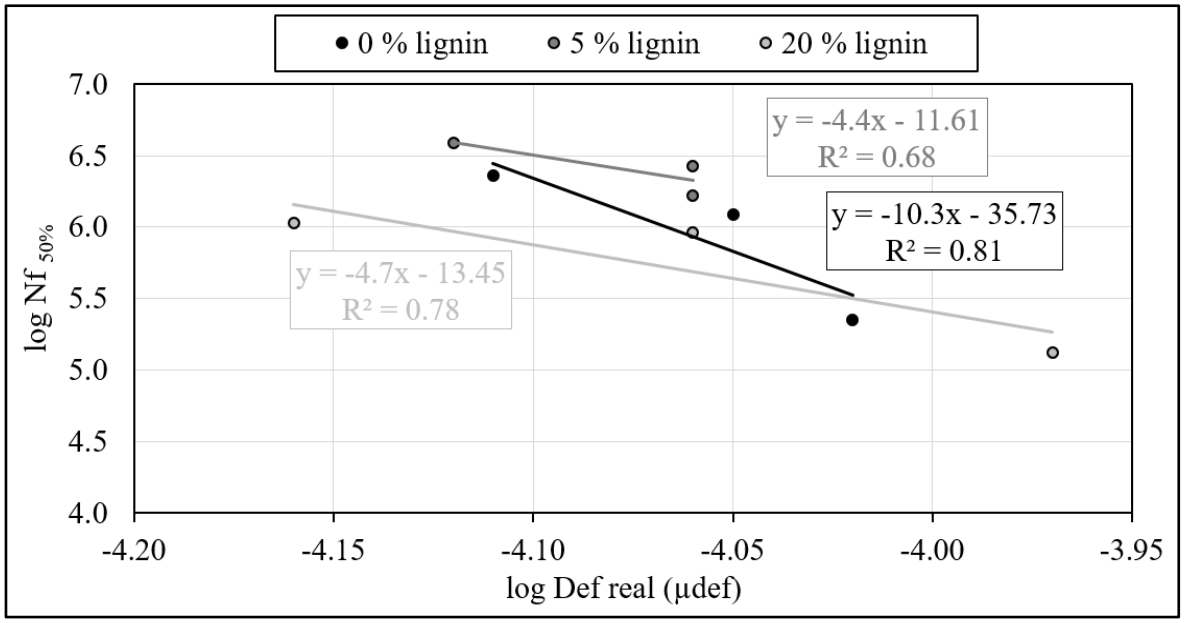


Figure-A III-2 Wöhler curves ($N_{f\,50\%}$ criterion) of the uniaxial tension-compression tests results based on the corrected air voids content of the unmodified and lignin-modified HMAs tested at 10 °C and 10 Hz and different strain levels

From the Wöhler curves shown in Figures A III-1 and A III-2, the corresponding strain value (on the log scale of x-axis) of 1,000,000 cycles (6.0 on the log scale of y-axis) can be determined. This value is called $\varepsilon_6$. Table-A III-2 shows the summary of $\varepsilon_6$ values determined before and after (Figures A III-1 and A III-2, respectively) the correction of the air voids content within the tested specimens of the unmodified and lignin-modified HMAs with different lignin contents. As can be seen, the use of 5 % lignin content within the HMA shows the highest $\varepsilon_6$ value, which is expected since it shows the highest fatigue life (ranked first) among the other HMAs. While the modified HMA with 20 % lignin shows the lowest $\varepsilon_6$ value, leading to shorter fatigue life compared to 5 % lignin. However, the determined values of $\varepsilon_6$ before and after the correction of the air voids content within the tested specimens for each lignin content are similar. This is expected since the correction of the air voids does not affect significantly the slope of the Wöhler curves of the HMAs and the position of these curves remains the same (Figure-A III-2).

Table-A III-2 Summary of $\varepsilon_6$ values obtained before and after the correction of the air voids for each lignin content

| Lignin content (%) | $\varepsilon_6$ (before/after the correction of the air voids content) | |
|---|---|---|
| | Before | After |
| 0 | 86.1 | 85.9 |
| 5 | 94.4 | 95.0 |
| 20 | 78.3 | 78.3 |

According to the presented findings of the fatigue tests, the lignin can be used to increase the fatigue cracking resistance of the HMA. More tests, including specimens at similar air voids, can be performed and many criteria can be discussed and involved in the analysis. Finally, for future studies, it is recommended to perform fatigue tests on the modified HMAs with different lignin contents maintaining the same bitumen content within the HMA (all lignin contents studied here are to replace part of the bitumen).

## LIST OF REFERENCES


Abas, F. O., & Abass, R. U. (2014). The Use of New Techniques in The Management of Waste Plastic by Reuse it in The Asphalt Mix. *Engineering and Technology Journal,32*(10 Part (A) Engineering), 25482567.

Abdullah, M. E., Abd Kader, S. A., Putra Jaya, R., Yaacob, H., Abdul Hassan, N., & Che Wan, C. N. (2017). Effect of Waste Plastic as Bitumen Modified in Asphalt Mixture. *MATEC Web of Conferences*, 103, 09018. doi:10.1051/matecconf/201710309018.

Abdulshafi A (1988). Rutting-review of existing models and some application to Saudi Arabia. *Proceed. 3rd IRF Middle East Regional Meet., 6*: 244-256.

Adwani, D., Sreeram, A., Pipintakos, G., Mirwald, J., Wang, Y., Hajj, R., Jing, R., & Bhasin, A. (2023). Interpreting the effectiveness of antioxidants to increase the resilience of asphalt binders: A global interlaboratory study. *Construction and Building Materials*, 366, 130231.

Airey, G. D., Rahimzadeh, B., & Collop, A. C. (2003). Viscoelastic limits for bituminous materials. *Materials and Structures, 36*, 643-647. DOI: 10.1007/BF02479495

Al-Azawee, E. T., & Qasim, Z. I. (2018). The influence of crumb rubber modifier (CRM) on the properties of asphalt concrete mixtures. *Int J Civil Eng Technol, 9*(10), 201-212.

Al-falahat, W., Lamothe, S., Carret, J. C., & Carter, A. (2023). Effects of kraft lignin on the performance grade of two bitumens used for cold climate. *International Journal of Pavement Research and Technology*, 1-14.

Almusawi, A., Sengoz, B., Topal, A., & Oner, J. (2019). Comparison between zero shear viscosity and steady shear flow methods to determine mixing and compaction temperatures of PMB. *Eurasian Journal of Civil Engineering and Architecture, 3*(2), 1-8.

Alossta, A., & Zeiada, W. A. (2011). Evaluation of Warm Mix Asphalt Versus Conventional Hot Mix Asphalt for Field and Laboratory-Compacted Specimens. *In Masters Abstracts International (Vol. 50*, No. 03).

Al-Qadi, I. L., & Nassar, W. N. (2003). Fatigue shift factors to predict HMA performance. *International Journal of Pavement Engineering, 4*(2), 69-76.

Al-Qadi, I. L., Wang, H., Baek, J., Leng, Z., Doyen, M., & Gillen, S. (2012). Effects of curing time and reheating on performance of warm stone-matrix asphalt. J. Mater. Civ. Eng, 24(11), 1422-1428.

Al Qudah, A., Rahim, M. A., Ghazaly, Z. M., Mashaan, N. S., Koting, S., Napiah, M., Omar, W. M., & Issa, Y. (2018). Effect of aged crumb rubber bitumen on performance dense graded mix in Malaysia. *International Journal of Civil Engineering and Technology, 9*(4), 1356-1369.

Antunes, V., Freire, A. C., Quaresma, L., & Micaelo, R. (2015). Influence of the geometrical and physical properties of filler in the filler–bitumen interaction. *Construction and Building Materials, 76*, 322-329.

Antunes, V., Freire, A. C., Quaresma, L., & Micaelo, R. (2016). Effect of the chemical composition of fillers in the filler–bitumen interaction. *Construction and Building Materials, 104*, 85-91.

Arafat, S., Kumar, N., Wasiuddin, N. M., Owhe, E. O., & Lynam, J. G. (2019). Sustainable lignin to enhance asphalt binder oxidative aging properties and mix properties. *Journal of cleaner production, 217*, 456-468.

Attaelmanan, M., Feng, C. P., & Al-Hadidy, A. I. (2011). Laboratory evaluation of HMA with high density polyethylene as a modifier. *Construction and Building Materials, 25*(5), 2764-2770.

Azam, A. M., El-Badawy, S. M., & Alabasse, R. M. (2019). Evaluation of asphalt mixtures modified with polymer and wax. *Innovative Infrastructure Solutions, 4*(1). doi:10.1007/s41062-019-0230-3

Babagoli, R., Ameli, A., & Shahriari, H. (2016). Laboratory evaluation of rutting performance of cold recycling asphalt mixtures containing SBS modified asphalt emulsion. *Petroleum Science and Technology, 34*(4), 309–313. doi:10.1080/10916466.2015.1135168

Badeli, S., Carter, A., Doré, G., & Saliani, S. (2018). Evaluation of the durability and the performance of an asphalt mix involving Aramid Pulp Fiber (APF): Complex modulus before and after freeze-thaw cycles, fatigue, and TSRST tests. *Construction and Building Materials, 174*, 60-71.

Badry, M. M., Dulaimi, A., Shanbara, H. K., Al-Busaltan, S., & Abdel-Wahed, T. (2021). Effect of Polymer on the Properties of Bitumen and Pavement Layers, Case Study: Expressway No. 1, Republic of Iraq. In IOP Conference Series: *Materials Science and Engineering (Vol. 1090*, No. 1, p. 012032). IOP Publishing.

Bairgi, B. K. (2015). Viability assessment of the use of ground tire rubber in asphalt pavements. *Arkansas State University*.

Bakheit, I., & Xiaoming, H. (2019). Modification of the dry method for mixing crumb rubber modifier with aggregate and asphalt based on the binder mix design. *Construction and Building Materials, 220*, 278-284.

Banaszek, C. (2009). ‘’Ultra High Shear Mixing Technology’’ (PDF). Retrieved 2009-12-27.

Barra, B., Momm, L., Guerrero, Y., & Bernucci, L. (2014). Characterization of granite and limestone powders for use as fillers in bituminous mastics dosage. *Anais da Academia Brasileira de Ciências, 86*, 995-1002.

Basueny, A. (2016). Complex modulus and fatigue baviour of recycled hot mix asphalt: laboratory investigation and modelling at the material levels (Doctoral dissertation, *École de technologie supérieure*).

Batista, K. B., Padilha, R. P. L., Castro, T. O., Silva, C. F. S. C., Araújo, M. F. A. S., Leite, L. F. M., Pasa, V. M. D., & Lins, V. F. C. (2018). High-temperature, low-temperature and weathering aging performance of lignin modified asphalt binders. *Industrial crops and products, 111*, 107-116.

Bausano, J., Kvasnak, A., & Williams, R. (2006). Development of Simple Performance Tests Using Laboratory Test Procedures to Illustrate the Effects of Moisture Damage on Hot Mix Asphalt.

Behnood, A., & Olek, J. (2017). Rheological properties of asphalt binders modified with styrene-butadiene-styrene (SBS), ground tire rubber (GTR), or polyphosphoric acid (PPA). *Construction and Building Materials, 151*, 464-478.

Bell, C. A., Hicks, R. G., & Wilson, J. E. (1984). Effect of percent compaction on asphalt mixture life. *ASTM International*.

Bernier, E., Lavigne, C., & Robidous, PY. (2013). “Life Cycle Assessment of Kraft Lignin for Polymer Applications”. *Int J Life Cycle Assess, 18* (2), 520-528.

Bodley, T., Andriescu, A., Hesp, S., & Tam, K. (2007). Comparison between binder and hot mix asphalt properties and early top-down wheel path cracking in a northern Ontario pavement trial. *Asphalt Paving Technology-Proceedings, 76*, 345.

Boltzmann, L. (1876). Zur Theorie der elastischen Nachwirkung. *Pogg. Ann. Phys. 7*, 624–654.fa.

Bradley, AH., & Thiam, P-M. (2021). “Development of Lignin-Modified Asphalt for Use in Canada”, *Proceedings, TAC-ATC Conference & Exhibition*, Innovations in Roadway/Embankment Materials and Geotechnical Engineering Session.

Caro, S., Masad, E., Bhasin, A., & Little, D. N. (2008). Moisture susceptibility of asphalt mixtures, Part 1: mechanisms. *International Journal of Pavement Engineering, 9*(2), 81–98. https://doi.org/10.1080/10298430701792128.

Carter, A., & Paradis, M. (2010). Laboratory Characterization of the Evolution of the Thermal Cracking Resistance with the Freeze-thaw Cycles. *Retrieved from data. abacus*. hr.

Chen, J. S., & Peng, C. H. (1998). Analyses of tensile failure properties of asphalt-mineral filler mastics. *Journal of Materials in Civil Engineering, 10*(4), 256-262.

Chen, X., & Huang, B. (2008). Evaluation of moisture damage in hot mix asphalt using simple performance and superpave indirect tensile tests. *Construction and Building Materials, 22*(9), 1950–1962. https://doi.org/10.1016/j.conbuildmat.2007.07.014.

Chen, M., Lin, J., & Wu, S. (2011a). Potential of recycled fine aggregates powder as filler in asphalt mixture. *Construction and building materials, 25*(10), 3909-3914.

Chen, M. Z., Lin, J. T., Wu, S. P., & Liu, C. H. (2011b). Utilization of recycled brick powder as alternative filler in asphalt mixture. *Construction and Building Materials, 25*(4), 1532-1536.

Cheriet, F., Carter, A., & Haddadi, S. (2021). Rheological and chemical properties of bitumen modified with crumb rubber in the dry process. *Canadian Journal of Civil Engineering, 48*(6), 616-627.

Consuegra, A. E., Little, D. N., Von Quintus, H., & Burati, J. (1988). Comparative evaluation of laboratory compaction devices based on their ability to produce mixtures with engineering properties similar to those produced in the field (Master's thesis, *Texas A&M University*).

Copeland, A. (2007). Influence of moisture on bond strength of asphalt-aggregate systems. *Zhurnal Eksperimental'noi I Teoreticheskoi Fiziki*.

Costa, L., Peralta, J., Oliveira, J., & Silva, H. (2017). A New Life for Cross-Linked Plastic Waste as Aggregates and Binder Modifier for Asphalt Mixtures. *Applied Sciences, 7*(6), 603.doi:10.3390/app7060603

Csanyi, L. H. (1962). Functions of fillers in bituminous mixes. *Highway Research Board Bulletin*, (329).

Czerwinski, F., & Birsan, G. (2017). Gas-enhanced ultra-high shear mixing: a concept and applications. *Metallurgical and Materials Transactions B, 48*, 983-992.

Delaporte, B., Di Benedetto, H., Chaverot, P., & Gauthier, G. (2007). « Linear viscoelastic properties of bituminous materials: from binders to mastics ». *Association of Asphalt Paving Technologists, vol. 76*, p. 488-494.

Di Benedetto, H., Ashayer Soltani, M. A., & Chaverot, P. (1996). Fatigue damage for bituminous mixtures: a pertinent approach. *Journal of the Association of Asphalt Paving Technologists*, *65*, 142-158.

Di Benedetto, H., & De La Roche, C. (1998). State of the art on stiffness modulus and fatigue of bituminous mixtures. *Rilem Rep. No. 17*, Bituminous Binders and Mixtures. L Francken, ed., E&FN Spon. London.

Di Benedetto, H., de la Roche, C., Baaj, H., Pronk, A., & Lundström, R. (2004). Fatigue of bituminous mixtures. *Materials and structures, 37*, 202-216. DOI: 10.1007/BF02481620

Di Benedetto H., & Corté, J.-F. (2005). Matériaux routiers bitumineux 2: Constitution et propriétés thermomécaniques des mélanges [Bituminous paving materials 2: Constitution and thermomechanical properties of mixtures]. *Paris: Hermes-Lavoisier*. [in French]

Di Benedetto, H., Delaporte, B., & Sauzéat, C. (2007a). Three-dimensional linear behaviour of bituminous materials: Experiments and modeling. *International Journal of Geomechanics, 7*, 149-157. DOI: 10.1061/(ASCE)1532-3641(2007)7:2(149)

Di Benedetto, H., Neifar, M., Sauzeat, C., & Olard, F. (2007b). Three-dimensional thermo-viscoplastic behaviour of bituminous materials: the DBN model. *Road Mater Pavement Des 8*(2):285–316.

Diebold, J. P. (1999). A review of the chemical and physical mechanisms of the storage stability of fast pyrolysis bio-oils.

Dong, F., Zhao, W., Zhang, Y., Wei, J., Fan, W., Yu, Y., & Wang, Z. (2014). Influence of SBS and asphalt on SBS dispersion and the performance of modified asphalt. *Construction and Building Materials, 62*, 1-7.

Dongmo-Engeland B. (2005). Caracte´risation des de´formations d'ornie´rage des chausse´es bitumineuses. The`se de Doctorat *ENTPE-INSA* [in French]

El-Hakim, M., & Tighe, S. (2014). Impact of freeze-thaw cycles on mechanical properties of asphalt mixes. Transportation Research Record: *Journal of the Transportation Research Board, (2444)*, 20–27.

El Mansouri, N. E., & Salvadó, J. (2006). Structural characterization of technical lignins for the production of adhesives: Application to lignosulfonate, kraft, soda-anthraquinone, organosolv and ethanol process lignins. *Industrial crops and products, 24*(1), 8-16.

Emery, J. (2005). Asphalt pavement rutting experience in Canada. In: Dunn L, Thompson E (eds) Compendium– paving rutting–lessons learned, *Canadian Technical Asphalt Assoc.*, pp 27–37. ISBN 0-921317-63-8

Erskine, J., Hesp, S. A. M., & Kaveh, F. (2012). Another look at accelerated aging of asphalt cements in the pressure aging vessel. *In Proceedings, Fifth Eurasphalt and Eurobitumen Congress*, Istanbul, Turkey.

Eskandarsefat, S., Dondi, G., & Sangiorgi, C. (2019). Recycled and rubberized SMA modified mixtures: A comparison between polymer modified bitumen and modified fibres. *Construction and Building Materials, 202*, 681 691.doi:10.1016/j.conbuildmat.2019.01.045

Evans, M., Marchildon, R., & Hesp, S. A. (2011). Effects of physical hardening on stress relaxation in asphalt cements: implications for pavement performance. *Transportation research record, 2207*(1), 34-42.

Fang, X. (2016). A fundamental research on cold mix asphalt modified with cementitious materials (Doctoral dissertation, *ETH Zurich*).

Fang, X., Garcia-Hernandez, A., & Lura, P. (2016). Overview on cold cement bitumen emulsion asphalt. *RILEM Technical Letters, 1*, 116-121.

Fayzrakhmanova, G. M., Zabelkin, S. A., Grachev, A. N., & Bashkirov, V. N. (2016). A study of the properties of a composite asphalt binder using liquid products of wood fast pyrolysis. *Polymer Science Series D, 9*(2), 181–184. doi:10.1134/s1995421216020052

Feng, P., Wang, H., Ding, H., Xiao, J., & Hassan, M. (2020). Effects of surface texture and its mineral composition on interfacial behavior between asphalt binder and coarse aggregate. *Construction and building materials, 262*, 120869.

Ferrotti, G., Pasquini, E., & Canestrari, F. (2014). Experimental characterization of high-performance fiber-reinforced cold mix asphalt mixtures. *Construction and Building Materials, 57*, 117-125.

Filbakk, T., Jirjis, R., Nurmi, J., & Hoibo, O. (2011) The effect of bark content on quality parameters of Scots pine (Pinus sylvestris L.) pellets. *Biomass Bioenergy, 35*, 3342–3349.

Fini, E.H., Yang, S. H., & Xiu, S. (2010). "Characterization and Application of ManureBased Bio-binder in Asphalt Industry", *Transportation Research Board 89th Annual Meeting*, Washington, DC, USA.

Fini, E.H., Oldham, D. J., & Abu-Lebdeh, T., (2013). " Synthesis and Characterization of Biomodified Rubber Asphalt: Sustainable Waste Management Solution for Scrap Tire and Swine Manure", *Journal of environmental engineering @ ASCE*. No. 139: 1454-1461.

Freeston, J. L., Gillespie, G., Hesp, S. A., Paliukaite, M., & Taylor, R. (2015). Physical hardening in asphalt. *In Proceedings of the Sixtieth Annual Conference of the Canadian Technical Asphalt Association (CTAA)*: Winnipeg, Manitoba.

Gao, J., Wang, H., Liu, C., Ge, D., You, Z., & Yu, M. (2020). High-temperature rheological behavior and fatigue performance of lignin modified asphalt binder. *Construction and Building Materials, 230*, 117063. doi:10.1016/j.conbuildmat.2019.117063

García, S. (2012). Centrales Termoeléctricas de Biomasa. *Editorial Renovetec*. Madrid, Spain.

Gaudenzi, E., Cardone, F., Lu, X., & Canestrari, F. (2023). The use of lignin for sustainable asphalt pavements: A literature review. *Construction and Building Materials, 362*, 129773.

Ghanoon, S. A., Tanzadeh, J., & Mirsepahi, M. (2020). Laboratory evaluation of the composition of nano-clay, nano-lime and SBS modifiers on rutting resistance of asphalt binder. *Construction and Building Materials, 238*, 117592.

Goh, S. W., & You, Z. (2012). Evaluation of hot-mix asphalt distress under rapid freeze-thaw cycles using image processing technique. *In CICTP 2012*: Multimodal Transportation Systems Convenient, Safe, Cost-Effective, Efficient (pp. 3305-3315).

Gómez-Meijide, B., Pérez, I., & Pasandín, A. R. (2016). Recycled construction and demolition waste in Cold Asphalt Mixtures: evolutionary properties. *Journal of Cleaner Production, 112*, 588–598. doi:10.1016/j.jclepro.2015.08.038

Gordobil, O., Delucis, R., Egüés, I., & Labidi, J. (2015). Kraft lignin as filler in PLA to improve ductility and thermal properties. *Industrial Crops and Products, 72*, 46-53.

Government of Canada, (2021). "Canadian Net-Zero Emissions Accountability Act", *Minister of Justice*, S.C. 2021, c. 22.

Guduru, G., Kumara, C., Gottumukkala, B., & Kuna, K. K. (2021). Effectiveness of different categories of rejuvenators in recycled asphalt mixtures. *Journal of Transportation Engineering*, Part B: Pavements, 147(2), 04021006.

Guler, M., Bahia, H. U., Bosscher, P. J., & Plesha, M. E. (2000). Device for measuring shear resistance of hot-mix asphalt in gyratory compactor. *Transportation Research Record, 1723*(1), 116-124.

Harrigan, E. T. (2002). Significance of" as-constructed" HMA Air Voids to Pavement Performance from an Analysis of LTPP Data. *NCHRP Research Results Digest*, (269).

Harris, ZM., Milner, S., & Taylor, G. (2018). "Greenhouse Gas Balances of Bioenergy Systems", *in Paul* (Editor), Chapter 5 - Biogenic Carbon - Capture and Sequestration, Academic Press.

Harvey, J., Sousa, J., Monismith, C., Eriksen, K., & Tayebali, A. (1994). Effect of laboratory compaction method on test results using SHRP A-003A type equipment. *In proceedings of the conference strategic highway research program (SHRP) and traffic safety on two continents*, hague, Netherlands, september 22-24 1993 (vti konferens NR 1A) (No. 1A: 3).

Hassan, H. F. (2005). Recycling of municipal solid waste incinerator ash in hot-mix asphalt concrete. *Construction and building materials, 19*(2), 91-98.

Head M. (2019). "Improvement of Biogenic Carbon Accounting in the Life Cycle of Wood Used in Construction in Canada", PhD Thesis, *Polytechnique Montreal*.

Hesp, S. A., Iliuta, S., & Shirokoff, J. W. (2007). Reversible aging in asphalt binders. *Energy & fuels, 21*(2), 1112-1121.

Hesp, S. A., Soleimani, A., Subramani, S., Phillips, T., Smith, D., Marks, P., & Tam, K. K. (2009a). Asphalt pavement cracking: analysis of extraordinary life cycle variability in eastern and northeastern Ontario. *International Journal of Pavement Engineering, 10*(3), 209-227.

Hesp, S. A. M., Genin, S. N., Scafe, D., Shurvell, H. F., & Subramani, S. (2009b). Five Year Performance Review of a Northern Ontario Pavement Trial: Validation of Ontario's Double Edge-Notched Tension (DENT) and Extended Bending Beam Rheometer (BBR) Test Methods. *In Proceedings of the Annual Conference-Canadian Technical Asphalt CTAA, 54*, 99–126.

Hesp, S. A., Kodrat, I., Scafe, D., Soleiman, A., & Subramani, S. (2009c). Rheological testing of asphalt cements recovered from an Ontario pavement trial. *In Proceedings of the sixth international conference on maintenance and rehabilitation of pavements and technological control (MAIREPAV6)*, Torino, Italy (pp. 8-10).

Hicks, R. G. (1991). Moisture damage in asphalt concrete (No. 175). *Transportation Research Board*.

Hobson, C. (2017). Evaluation of lignin as an antioxidant in asphalt binders and bituminous mixtures. Report FHWA-KS-16-17, *Federal Highway Administration*, Kansas. Dept. of Transportation, Bureau of Research.

Holt, A., Johnson, C., & Marks, P. (2015). Six-Year Performance of Ontario's Freeway Fibre and Polymer Modifier Trial Project. *In Proceedings of the Sixtieth Annual Conference*

*of the Canadian Technical Asphalt Association (CTAA)*: Winnipeg, Manitoba, 60, 379–394.

IKA laboratory equipment. (2009). ''Introduction to IKA's Three Stage Dispax Reactor'' (PDF). Retrieved 2009-06-05.

Iliuta, S., Andriescu, A., Hesp, S. A., & Tam, K. K. (2004). Improved approach to low-temperature and fatigue fracture performance grading of asphalt cements. *In Proceedings of the Annual Conference-Canadian Technical Asphalt CTAA* (pp. 123-158). Polyscience Publications; 1998.

Irfan, M., Ali, Y., Ahmed, S., & Hafeez, I. (2018). Performance evaluation of crumb rubber-modified asphalt mixtures based on laboratory and field investigations. *Arabian Journal for Science and Engineering, 43*(4), 1795-1806.

Iwański, M., & Chomicz-Kowalska, A. (2013). Laboratory Study on Mechanical Parameters of Foamed Bitumen Mixtures in the Cold Recycling Technology. *Procedia Engineering, 57*, 433–442. doi:10.1016/j.proeng.2013.04.056

Jamshidi, A., White, G., & Mohd Hasan, M. R. (2022). New Methodology to Characterize the Workability of Asphaltic Concrete Mixtures Based on Kinematic Compaction Energy. *Sustainability, 14*(11), 6550.

Jelčić, Ž., Ocelić Bulatović, V., Jurkaš Marković, K., & Rek, V. (2017). Multi-fractal morphology of un-aged and aged SBS polymer-modified bitumen. *Plastics, Rubber and Composites, 46*(2), 77-98.

Jenks, C. W., Jencks, C. F., Harrigan, E. T., Adcock, M., Delaney, E. P., & Freer, H. (2011). NCHRP Report 673: A manual for design of hot mix asphalt with commentary. *Transportation Research Board*, Washington, DC.

Jiang, J., Ni, F., Zheng, J., Han, Y., & Zhao, X. (2018). Improving the high-temperature performance of cold recycled mixtures by polymer-modified asphalt emulsion. *International Journal of Pavement Engineering*, 1–8. doi:10.1080/10298436.2018.1435882

Jung, D.H., & Vinson, T.S. (1994). Low-temperature cracking: test selection, *Strategic Highway Research Program*, SHRP-A-400.

Júnior, J. L. L., Babadopulos, L. F., & Soares, J. B. (2019). Moisture-induced damage resistance, stiffness and fatigue life of asphalt mixtures with different aggregate-binder adhesion properties. *Construction and building materials, 216*, 166-175.

Kassem, E., Masad, E., Lytton, R., & Chowdhury, A. (2011). Influence of air voids on mechanical properties of asphalt mixtures. *Road Materials and Pavement Design, 12*(3), 493-524.

Kavussi, A., & Hicks, R. G. (1997). Properties of bituminous mixtures containing different fillers. *Journal of the Association of Asphalt Paving Technologists, 66*.

Kennedy, T. W., Roberts, F. L., & Anagnos, J. N. (1984). Texas boiling test for evaluating moisture susceptibility of asphalt mixtures (No. FHWA-TX-85-63+ 253-5). *Austin, TX, USA: Center for Transportation Research, Bureau of Engineering Research, University of Texas at Austin*.

Khan, M. I., Sutanto, M. H., Sunarjono, S., Room, S., & Yusoff, N. I. M. (2019). Effect of Crumb Rubber, Epolene (EE-2), and Date Palm Ash as Modifiers on the Performance of Binders and Mixtures: A Sustainable Approach. *Sustainability, 11*(22), 6484.

Khandelwal M. (2019), "Carbon Footprint of Lignin Modified Asphalt Mix", A Tree to Gate LCA Assessment. Master Thesis, *Utrecht University*.

Koohmishi, M., & Palassi, M. (2017). Evaluation of morphological properties of railway ballast particles by image processing method. *Transportation Geotechnics, 12*, 15-25.

Kuang, D., Zhang, B., Jiao, Y., Fang, J., Chen, H., & Wang, L. (2017). Impact of particle morphology on aggregate-asphalt interface behavior. *Construction and Building Materials, 132*, 142-149.

Kuity, A., Jayaprakasan, S., & Das, A. (2014). Laboratory investigation on volume proportioning scheme of mineral fillers in asphalt mixture. *Construction and Building Materials, 68*, 637-643.

Kumar, K. R., & Mahendran, N. (2014). Experimental studies on modified bituminous mixes using waste HDPE and crumb rubber. *International Journal of Emerging Technology and Advanced Engineering, 4*(4), 587-597.

Kun, D., & Pukánszky, B. (2017). Polymer/lignin blends: Interactions, properties, applications. *European Polymer Journal, 93*, 618–641. doi:10.1016/j.eurpolymj.2017.04.035

Kütük-Sert, T., & Kütük, S. (2013). Physical and Marshall properties of borogypsum used as filler aggregate in asphalt concrete. *Journal of Materials in Civil Engineering, 25*(2), 266-273.

Lamothe, S. (2014). Endommagement d'un enrobé bitumineux partiellement saturé en eau ou en saumure soumis à des sollicitations cycliques de gel-dégel et mécaniques (Doctoral dissertation, *École Nationale des Travaux Publics de l'État [ENTPE*]). [in French]

Lamothe, S., Carret, J.-C., Al-Falahat, W., & Carter, A. (2022). Field Trial Sections of Kraft Lignin-Modified Hot Mix Asphalt. *In 67th annual conference of Canadian Technical Asphalt Association (CTAA)*, Nov. 6-9, 2022, Kelowna, British Columbia.

Leandro, R. P., Vasconcelos, K. L., & Bernucci, L. L. B. (2017). Evaluation of the laboratory compaction method on the air voids and the mechanical behavior of hot mix asphalt. *Construction and Building Materials, 156*, 424-434.

Leonardi, G. (2015). Finite element analysis for airfield asphalt pavements rutting prediction. *Bulletin of the Polish Academy of Sciences: Technical Sciences*, (2).

Lesueur, D., Petit, J., & Ritter, H. J. (2013). The mechanisms of hydrated lime modification of asphalt mixtures: a state-of-the-art review. *Road materials and pavement design, 14*(1), 1-16.

Li, R., Karki, P., & Hao, P. (2020a). Fatigue and self-healing characterization of asphalt composites containing rock asphalts. *Construction and Building Materials, 230*, 116835. doi:10.1016/j.conbuildmat.2019.116835

Li, R., Bahadori, A., Xin, J., Zhang, K., Muhunthan, B., & Zhang, J. (2020b). Characteristics of bioepoxy based on waste cooking oil and lignin and its effects on asphalt binder. *Construction and Building Materials, 251*, 118926. doi:10.1016/j.conbuildmat.2020.118926

Linden, R. N., Mahoney, J. P., & Jackson, N. C. (1989). Effect of compaction on asphalt concrete performance. *Transportation research record, (1217)*.

Little, D. N., & Petersen, J. C. (2005). Unique effects of hydrated lime filler on the performance-related properties of asphalt cements: Physical and chemical interactions revisited. *Journal of materials in civil engineering, 17*(2), 207-218.

Liu, M., Han, S., Han, X., Qi, X., & Dong, S. (2019). Microcapsule and polymer reinforcement techniques developed asphalt for use of pothole repairs in winter and rainy seasons. *Cold Regions Science and Technology, 167*, 102865. doi:10.1016/j.coldregions.2019.102865

Liu, Y., Huang, Y., Sun, W., Nair, H., Lane, D. S., & Wang, L. (2017). Effect of coarse aggregate morphology on the mechanical properties of stone matrix asphalt. *Construction and Building Materials, 152*, 48-56.

Lu, X., & Isacsson, U. (1997). Rheological characterization of styrene-butadiene-styrene copolymer modified bitumens. *Construction and building materials, 11*(1), 23-32.

Lu, X., & Isacsson, U. (2000). Modification of road bitumens with thermoplastic polymers. *Polymer testing, 20*(1), 77-86.

Lu, X., Gu, X., & Shi, Y. (2022). A review on lignin antioxidants: Their sources, isolations, antioxidant activities and various applications. *International Journal of Biological Macromolecules*.

Lundstrom, R. (2002). « Rheological and fatigue characterization of asphalt concrete mixtures using unaxial testing ». *Kungl Tekniska Hogskolan*.

Luo, D., Khater, A., Yue, Y., Abdelsalam, M., Zhang, Z., Li, Y., Li, J., & Iseley, D. T. (2019). The performance of asphalt mixtures modified with lignin fiber and glass fiber: A review. *Construction and Building Materials, 209*, 377-387.

Luz, P. M. S. G., Ziegler, C. R., Mendonça, A. M. G. D., & Rodrigues, J. K. G. (2021). Rheological evaluation of pg 64–22 asphalt binder modified with lignin of pinus and eucalyptus woods. *Materials and Structures, 54*(4), 166.

Lytton, R. L. (2004). Adhesive fracture in asphalt concrete mixtures. *Asphalt Technology Handbook*. Marcel Dekker, Monticello, New York.

Ma, J., Hesp, S. A., Chan, S., Li, J. Z., & Lee, S. (2022). Lessons learned from 60 years of pavement trials in continental climate regions of Canada. *Chemical Engineering Journal, 444*, 136389.

Mangiafico, S. (2014). Linear viscoelastic properties and fatigue of bituminous mixtures produced with Reclaimed Asphalt Pavement and corresponding binder blends. ENTPE, Lyon.

Maupin, G. W., & Diefenderfer, B. K. (2006). Design of a high-binder--high-modulus asphalt mixture. *Virginia Transportation Research Council*.

Michel, Q., Orozco, G., Carter, A., & Vaillancourt, M. (2023). Influences of type and concentration of recycled mineral construction, renovation and demolition waste on the linear viscoelastic behavior of bituminous mastics. *Construction and Building Materials, 371*, 130668.

Mills-Beale, J., You, Z., Fini, E., Zada, B., Lee, C. H., & Yap, Y. K., (2014), "Aging Influence on Rheology Properties of Petroleum-Based Asphalt Modified with Biobinder". *Journal of materials in civil engineering* © ASCE. No. 26: 358-366.

Mirabdolazimi, S. M., & Shafabakhsh, G. (2017). Rutting depth prediction of hot mix asphalts modified with forta fiber using artificial neural networks and genetic programming technique. *Construction and Building Materials, 148*, 666–674. https://doi.org/10.1016/j.conbuildmat.2017.05.088

Miranda, T., Montero, I., Sepúlveda, F. J., Arranz, J. I., Rojas, C. V., & Nogales, S. (2015). A review of pellets from different sources. *Materials, 8*(4), 1413-1427.

Moghaddam, T. B., Karim, M. R., & Abdelaziz, M. (2011). A review on fatigue and rutting performance of asphalt mixes. *Scientific Research and Essays, 6*(4), 670-682.

Monismith, C. L. (1992). Analytically based asphalt pavement design and rehabilitation: *Theory to practice*, 1962-1992 (No. 1354).

Moretti, C., Corona, B., Hoefnagels, R., Vural-Gursel, I., Gosselink, R., & Junginger, M. (2021). "Review of Life Cycle Assessments of Lignin and Derived Products: Lessons Learned", *Science of the Total Environment, 770*, 144656.

Moretti, C., Corona, B., Hoefnagels, R., Van Veen, M., Vural-Gursel, I., Strating, T., Gosselink, R., & Junginger, M. (2022). "Kraft Lignin as a Bio-Based Ingredient for Dutch Asphalts: An Attributional LCA". *Science of the Total Environment, 802*, 150316.

Mostafa, V., & Mahmoud, A. (2018). Rutting performance of road pavement asphalt binders modified by polymers. *Proceedings of the Institution of Civil Engineers - Construction Materials*, 1–19. doi:10.1680/jcoma.17.00073

Moutier, F. (1991). Étude statistique de l'effet de la composition des enrobés bitumineux sur leur comportement en fatigue et leur module complexe [Statistical study of the effect of bituminous mixture composition on their fatigue behavior and complex modulus]. *Bulletin de liaison des Laboratoires des Ponts et Chaussés*, *172*, 33-41. [in French]

Msallam, M., & Asi, I. (2018). Improvement of local asphalt concrete binders using crumb rubber. *Journal of Materials in Civil Engineering, 30*(4), 04018048.

MTMDET, (2017). Enrobés à chaud formulés selon la méthode de formulation du Laboratoire des chaussées. *Québec*.

MTQ. (2015). Les enrobés du MTQ et leurs usages en milieu municipal. *Congress Infra 2015 – CERIU*, December 1st, 2015 [In french].

Muniandy, R., Aburkaba, E., Yunus, R., Hamid, H., & Salihudin, H. (2012). Influence of mineral filler particle size and type on rheological and performance properties of SMA asphalt-filler mastics. *Asian J Appl Sci, 5*(8), 522-537.

Nasir, S., Ayoub, M., Zafarullah, S., Bilal, A., Amjad, B., & Kakar, E. (2014). Effective Use of Waste Plastic as Bitumen Strength Modifier. Retrieved from http://www.hrpub.org/journals/article_info.php?aid=2159.

Natural Resources Canada. (2005). Road Rehabilitation Energy Reduction, Guide for Canadian Road Builders, *In Collaboration with the Canadian Construction Association, Canadian Industry Program for Energy Conservation*, Electronic version, https://publications.gc.ca/collections/Collection/M144-67-2005E.pdf.

Norgbey, E., Huang, J., Hirsch, V., Liu, W. J., Wang, M., Ripke, O., Li, Y., Annan, G. E. T., Ewusi-Mensah, D., Wang, X., & Treib, G. (2020). Unravelling the efficient use of waste

lignin as a bitumen modifier for sustainable roads. *Construction and Building Materials, 230*, 116957.

Nunes, L.J.R., Matias, J.C.O., & Catalao, J.P.S. (2014). Mixed biomass pellets for thermal energy production: A review of combustion models. *Appl. Energy, 127*, 135–140.

Olard, F. (2012). GB5 mix design: high-performance and cost-effective asphalt concretes by use of gap-graded curves and SBS modified bitumens. *Road Materials and Pavement Design, 13*(sup1), 234–259.

Olard, F., & H. Di Benedetto. (2003). « General ‘‘2S2P1D’’ model and relation between the linear viscoelastic behaviours of bituminous binders and mixes ». *Road materials and pavement design, vol. 4*, no 2/2003, p. 1-40.

Olard, F., & Di Benedetto, H. (2005a). Experimental characterization and constitutive modeling of the thermo-viscoelasto-plastic behavior of bituminous mixes: the ‘‘DBN’’ law. *Presentation at the annual meeting of the Association of Asphalt Paving Technologists (AAPT)*, Long Beach, CA, March 2005. Publication in the J AAPT 74:791–827.

Olard, F., & Di Benedetto, H. (2005b). The" DBN" Model: A Thermo-Visco-Elasto-Plastic Approach for Pavement Behavior Modeling (With Discussion). *Journal of the Association of Asphalt Paving Technologists, 74*.

Olard, F., Di Benedetto, H., Dony, A., & Vaniscote, J.-C. (2005). Properties of bituminous mixtures at low temperatures and relations with binder characteristics. *Materials and Structures, 38*, 121-126. DOI: 10.1007/BF02480584

Olard, F., Le Noan, C., Bonneau, D., Duperiet, S., & Alvarez, C. (2008). Very high rate (50%) in hot mix and warm mix asphalts for sustainable road construction (may, 2008), 866. Paris: *Revue generale des routes (RGRA)*.

Oliviero Rossi, C., Caputo, P., Ashimova, S., Fabozzi, A., D’Errico, G., & Angelico, R. (2018). Effects of natural antioxidant agents on the bitumen aging process: An EPR and rheological investigation. *Applied Sciences, 8*(8), 1405.

Omar, H. A., Yusoff, N. I. M., Mubaraki, M., & Ceylan, H. (2020). Effects of moisture damage on asphalt mixtures. *Journal of Traffic and Transportation Engineering (English Edition), 7*(5), 600-628.

Ossa, A., & Collop, A. (2006). Dilation behavior of asphalt mixtures. *Road Mater Pavement Des 7*:93–109

Othman, A. M. (2010). Effect of Low-Density Polyethylene on Fracture Toughness of Asphalt Concrete Mixtures. *Journal of Materials in Civil Engineering, 22*(10), 1019–1024. doi:10.1061/(asce)mt.1943-5533.0000106

Ouyang, C., Wang, S., Zhang, Y., & Zhang, Y. (2006). Improving the aging resistance of styrene–butadiene–styrene tri-block copolymer modified asphalt by addition of antioxidants. *Polymer degradation and stability, 91*(4), 795-804.

Paul Togunde, O., & Hesp, S. A. M. (2012). Physical hardening in asphalt. *Int. J. Pavement Res. Technol. 5*, 46–53.

Pellinen, Terhi Kristiina. (2001). « Investigation of the use of dynamic modulus as an indicator of hot-mix asphalt peformance ». 3004132, United States -- Arizona. *Arizona State University*, 803 p. p. In ProQuest Dissertations & Theses (PQDT); ProQuest Dissertations & Theses A&I.

Pérez, I. P., Rodríguez Pasandín, A. M., Pais, J. C., & Alves Pereira, P. A. (2019). Use of lignin biopolymer from industrial waste as bitumen extender for asphalt mixtures. *Journal of Cleaner Production*. doi:10.1016/j.jclepro.2019.02.082

Pérez, I., Pasandín, A. R., Pais, J. C., & Pereira, P. A. A. (2020). Feasibility of Using a Lignin-Containing Waste in Asphalt Binders. *Waste and Biomass Valorization*. doi:10.1007/s12649-019-00590-4

Perraton, D., Di Benedetto, H., Sauzéat, C., De La Roche, C., Bankowski, W., Partl, M., & Grenfell, J. (2011). Rutting of bituminous mixtures: wheel tracking tests campaign analysis. *Materials and structures, 44*, 969-986.

Pinzón, E. C., & Such, C. (2004). Evaluation of moisture sensitivity of bituminous mixtures by a complex modulus approach. *Transportation research record, 1891*(1), 62-67.

Poddar, S., Kamruzzaman, M., Sujan, S.M.A., Hossain, M., Jamal, M.S., Gafur, M.A., & Khanam, M. (2014). Effect of compression pressure on lignocellulosic biomass pellet to improve fuel properties: Higher heating value. *Fuel, 131*, 43–48.

Prasad, K. S. B. (2012). Utilization of waste plastic as a strength modifier in surface course of flexible and rigid pavements.

Rajan, B., & Singh, D. (2017). Understanding influence of crushers on shape characteristics of fine aggregates based on digital image and conventional techniques. *Construction and Building Materials, 150*, 833-843.

Raschia, S., Perraton, D., Graziani, A., & Carter, A. (2020). Influence of low production temperatures on compactability and mechanical properties of cold recycled mixtures. *Construction and Building Materials, 232*, 117169.

Read, J., & Whiteoak, D. (2003). The Shell Bitumen Handbook, 5th ed.; Thomas Telford: London, UK, ISBN 10:072773220X.

Reinke, G. (2003). Determination of mixing and compaction temperature of PG binders using a steady shear flow test. *In presentation made to the Superpave Binder Expert Task Group*, https://engineering. purdue. edu/~ spave/old/Technical% 20Info/Meetings/Binder% 20ETG% 20Sept.

Rigg, A., Duff, A., Nie, Y., Somuah, M., Tetteh, N., & Hesp, S. A. (2017). Non-isothermal kinetic analysis of reversible ageing in asphalt cements. *Road Materials and Pavement Design, 18*(sup4), 185-210.

Robati, M., Carter, A., & Perraton, D. (2015). New conceptual model for filler stiffening effect on asphalt mastic of microsurfacing. *Journal of Materials in Civil Engineering, 27*(11), 04015033.

Robert, L.Y., & Suckhong, L. (1996). Short-term and Long-term aging behavior of rubber modified asphalt paving mixture. *Transportation Research Record, 1530*, pp.11-17.

Romero, P., & Stuart, K. (1998). Evaluating accelerated rut testers. *Public Roads, 62*(1), 50-54.

Roque, R., Dominguez, G., & Romero, P. (1995). Effect of asphalt mixture characteristics and design on frictional resistance of bituminous wearing course mixtures. *Transportation research record, 1507*, 39.

Salençon, J. (2009). Viscoélasticité pour le calcul des structures. Paris: Éditions de l'École Polytechnique.

Sefimazgi, N. R., Tashman, L., & Bahia, H. (2012). « Internal structure characterization of asphalt mixtures for rutting performance using imaging analysis ». *Journal of the Association of Asphalt Paving Technologists (AAPT)*.

Sengoz, B., & Topal, A. (2005). Use of asphalt roofing shingle waste in HMA. *Construction and Building Materials, 19*(5), 337-346.

Shamshuddin, M. K., Abdullah, M. E., & Shah, S. R. (2010). The development of moisture sensitivity test for compacted asphalt. *International Journal of Integrated Engineering, 2*(2), 17-25.

Shanbara, H. K., Ruddock, F., & Atherton, W. (2018). A laboratory study of high-performance cold mix asphalt mixtures reinforced with natural and synthetic fibres. *Construction and Building Materials, 172*, 166-175.

Sharma, V., Chandra, S., & Choudhary, R. (2010). Characterization of fly ash bituminous concrete mixes. *Journal of Materials in Civil Engineering, 22*(12), 1209-1216.

Shatnawi, S., Nagarajaiah, M., & Harvey, J. (1995). Moisture sensitivity evaluation of binder-aggregate mixtures. *Transportation research record, 1492*, 71-84.

Siroma, R. S., Nguyen, M. L., Hornych, P., Lorino, T., & Chailleux, E. (2021). Clustering aged bitumens through multivariate statistical analyses using phase angle master curve. *Road Materials and Pavement Design, 22*(sup1), S51-S68.

Soenen, H., Vansteenkiste, S., & Kara De Maeijer, P. (2020). Fundamental approaches to predict moisture damage in asphalt mixtures: state-of-the-art review. *Infrastructures, 5*(2), 20.

Solaimanian, M., Harvey, J., Tahmoressi, M., & Tandon, V. (2003). Test methods to predict moisture sensitivity of hot-mix asphalt pavements. *In Transportation research board national seminar*. San Diego, California (pp. 77-110).

Solaimanian, M., Bonaquist, R. F., & Tandon, V. (2006). Improved Conditioning Procedure for Predicting the Moisture Susceptibility of HMA Pavements.

Su, J., Li, P., Wei, X., Sun, S., Zhu, L., & Dong, C. (2020). Analysis of interface interaction of aggregate-asphalt system and its effect on shear-slip behavior of asphalt mixture. *Construction and Building Materials, 264*, 120680.

Su, Y., Tang, S., Cai, M., Nie, Y., Hu, B., Wu, S., & Cheng, C. (2023). Thermal oxidative aging mechanism of lignin modified bitumen. *Construction and Building Materials, 363*, 129863.

Tapkın, S. (2008). Mechanical evaluation of asphalt–aggregate mixtures prepared with fly ash as a filler replacement. *Canadian Journal of Civil Engineering, 35*(1), 27-40.

Tapsoba, N., Baaj, H., Sauzéat, C., Di Benedetto, H., & Ech, M. (2016). 3D analysis and modelling of Thermal Stress Restrained Specimen Test (TSRST) on asphalt mixes with RAP and roofing shingles. *Construction and Building Materials, 120*, 393-402.

Tayfur S., Ozen H., Aksoy, A. (2007). Investigation of rutting performance of asphalt mixtures containing polymer modifiers. *J. Constr. Build. Mater., 21*: 328-337.

Terrel, R. L., & Al-Swailmi, S. (1992). Final Report on Water Sensitivity of Asphalt-Aggregate Mixtures Test Development. Strategic Highway Research Program.

Theyse, H., De Beer, M., & Rust, F. (1996). Overview of South African mechanistic pavement design method. Transportation Research Record: *Journal of the Transportation Research Board, (1539)*, 6–17.

Topal, A. (2010). Evaluation of the properties and microstructure of plastomeric polymer modified bitumens. *Fuel Processing Technology, 91*(1), 45-51.

Uzun, İ., & Terzi, S. (2012). Evaluation of andesite waste as mineral filler in asphaltic concrete mixture. *Construction and Building Materials, 31*, 284-288.

Wang, H., & Derewecki, K. (2013). Rheological Properties of Asphalt Binder Partially Substituted with Wood Lignin. *Airfield and Highway Pavement 2013*. doi:10.1061/9780784413005.081

Wang, X., Shen, S., Huang, H., & Zhang, Z. (2019). Towards smart compaction: Particle movement characteristics from laboratory to the field. *Construction and Building Materials*, 218, 323-332.

Wang, Y. D., Ghanbari, A., Underwood, B. S., & Kim, Y. R. (2019). Development of a performance-volumetric relationship for asphalt mixtures. *Transportation Research Record*, 2673(6), 416-430.

Watkins, D., Nuruddin, M., Hosur, M., Tcherbi-Narteh, A., & Jeelani, S. (2015). Extraction and characterization of lignin from different biomass resources. *Journal of Materials Research and Technology, 4*(1), 26–32. doi:10.1016/j.jmrt.2014.10.009

White, T. D., Haddock, J. E., & Rismantojo, E. (2006). Aggregate tests for hot-mix asphalt mixtures used in pavements (Vol. 557). *Transportation Research Board*.

Wöhler, A. (1870). Über die Festigkeitsversuche mit Eisen und Stahl [On the strength tests with iron and steel]. *Zeitschrift für Bauwesen, 20*, 73-106.

Wong, Y. D., Sun, D. D., & Lai, D. (2007). Value-added utilisation of recycled concrete in hot-mix asphalt. *Waste Management, 27*(2), 294-301.

Wright, L., Kanabar, A., Moult, E., Rubab, S., & Hesp, S. (2011). Oxidative Aging of Asphalt Cements from an Ontario Pavement Trial. *International Journal of Pavement Research & Technology, 4*(5).

Xie, J., Yang, Y., Lv, S., Peng, X., & Zhang, Y. (2019). Investigation on preparation process and storage stability of modified asphalt binder by grafting activated crumb rubber. *Materials, 12*(12), 2014.

Xie, S., Li, Q., Karki, P., Zhou, F., & Yuan, J. S. (2017). Lignin as renewable and superior asphalt binder modifier. *ACS Sustainable Chemistry & Engineering, 5*(4), 2817-2823.

Xie, X., Lu, G., Liu, P., Wang, D., Fan, Q., & Oeser, M. (2017). Evaluation of morphological characteristics of fine aggregate in asphalt pavement. *Construction and Building Materials, 139*, 1-8.

Xing, B., Du, Y., Fang, C., Sun, H., Lyu, Y., & Fan, W. (2022). Particle morphology of mineral filler and its effects on the asphalt binder-filler interfacial interaction. *Construction and Building Materials, 321*, 126292.

Xu, C., Wang, D., Zhang, S., Guo, E., Luo, H., Zhang, Z., & Yu, H. (2021). Effect of lignin modifier on engineering performance of bituminous binder and mixture. *Polymers, 13*(7), 1083.

Xu, G., Wang, H., & Zhu, H. (2017). Rheological properties and anti-aging performance of asphalt binder modified with wood lignin. *Construction and Building Materials, 151*, 801-808.

Xue, Y., Hou, H., Zhu, S., & Zha, J. (2009). Utilization of municipal solid waste incineration ash in stone mastic asphalt mixture: Pavement performance and environmental impact. *Construction and Building Materials, 23*(2), 989-996.

Yao, H., You, Z., Li, L., Goh, S. W., Lee, C. H., Yap, Y. K., & Shi, X. (2013). Rheological properties and chemical analysis of nanoclay and carbon microfiber modified asphalt with Fourier transform infrared spectroscopy. *Construction and Building Materials, 38*, 327-337.

Yoon, H. H., & Tarrer, A. R. (1988). Effect of aggregate properties on stripping (No. 1171).

You, Z., J. M. Beale, H. E. Fini, S. W. Goh, & B. Colbert. (2011) "Evaluation of Low Temperature Binder Properties of Warm Mix Asphalt, Extracted and Recovery RAP and RAS, and Bioasphalt." *Journal of Materials in Civil Engineering*.

Young, J. Francis. (1998). The Science and technology of civil engineering materials. Coll. « *Prentice-Hall international series in civil engineering and engineering mechanics* ». Upper Saddle River, N.J.: Prentice-Hall, xiv, 384 p.

Yue, Y., Abdelsalam, M., Luo, D., Khater, A., Musanyufu, J., & Chen, T. (2019). Evaluation of the Properties of Asphalt Mixes Modified with Diatomite and Lignin Fiber: A Review. *Materials, 12*(3), 400. doi:10.3390/ma12030400

Yue, Z. Q., Bekking, W., & Morin, I. (1995). Application of digital image processing to quantitative study of asphalt concrete microstructure. *Transportation Research Record, 1492*, 53-60.

Zarei, A., Zarei, M., & Janmohammadi, O. (2018). Evaluation of the Effect of Lignin and Glass Fiber on the Technical Properties of Asphalt Mixtures. *Arabian Journal for Science and Engineering*. doi:10.1007/s13369-018-3273-4

Zhang, G., Zhang, H., Bu, X., & Yang, H. (2018). Laboratory study on performances of bimaleimide/unsaturated polyester resin modified asphalt. *Construction and Building Materials, 179*, 576-586.

Zhang, Y., Liu, X., Apostolidis, P., Gard, W., van de Ven, M., Erkens, S., & Jing, R. (2019). Chemical and Rheological Evaluation of Aged Lignin-Modified Bitumen. *Materials, 12*(24), 4176.

Zhang, Y., Wang, X., Ji, G., Fan, Z., Guo, Y., Gao, W., & Xin, L. (2020). Mechanical Performance Characterization of Lignin-Modified Asphalt Mixture. *Applied Sciences, 10*(9), 3324. doi:10.3390/app10093324

Zhang, Y., Liu, X., Ren, S., Jing, R., Lin, P., Apostolidis, P., Erkens, S., Wang, X., & Scarpas, A. (2022). Effect of Bio-oil on Rheology and Chemistry of Organosolv Lignin–Modified Bitumen. *Journal of Materials in Civil Engineering, 34*(4), 1-16.

Zhu, J., Birgisson, B., & Kringos, N. (2014). Polymer modification of bitumen: Advances and challenges. *European Polymer Journal, 54*, 18-38.

Ziari, H., Goli, A., & Amini, A. (2016). Effect of Crumb Rubber Modifier on the Performance Properties of Rubberized Binders. *Journal of Materials in Civil Engineering, 28*(12), 04016156. doi:10.1061/(asce)mt.1943-5533.0001661

Zoorob, S. E., Al-Bahar, S. K., & Al-Otaibi, S. F. (2018). Design and optimization of a rubber-bitumen blend in preparation for a rubberized-asphalt road trial in the state of Kuwait. *MATEC Web of Conferences, 195*, 04001.doi:10.1051/matecconf/201819504001

Zulkati, A., Diew, W. Y., & Delai, D. S. (2012). Effects of fillers on properties of asphalt-concrete mixture. *Journal of transportation engineering, 138*(7), 902-910.